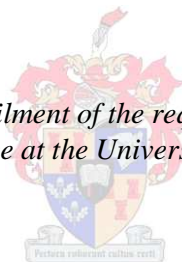


**GEOLOGY OF THE KRANZBERG SYNCLINE AND
EMPLACEMENT CONTROLS OF THE USAKOS
PEGMATITE FIELD, DAMARA BELT, CENTRAL
NAMIBIA**

by
Geoffrey J. Owen

*Thesis presented in fulfilment of the requirements for the degree
Master of Science at the University of Stellenbosch*



Supervisor: Prof. Alex Kisters

Faculty of Science
Department of Earth Sciences

March 2011

DECLARATION

By submitting this thesis electronically, I declare that the entirety of the work contained therein is my own, original work, that I am the sole author thereof (save to the extent explicitly otherwise stated), that reproduction and publication thereof by Stellenbosch University will not infringe any third party rights and that I have not previously in its entirety or in part submitted it for obtaining any qualification.

Signature:

A handwritten signature in black ink, appearing to be 'C. du Toit', written in a cursive style.

Date: 15. February 2011

ABSTRACT

The Central Zone (CZ) of the Damara belt in central Namibia is underlain by voluminous Pan-African granites and is host to numerous pegmatite occurrences, some of which have economic importance and have been mined extensively. This study discusses the occurrence, geometry, relative timing and emplacement mechanisms for the Usakos pegmatite field, located between the towns of Karibib and Usakos and within the core of the regional-scale Kranzberg syncline.

Lithological mapping of the Kuiseb Formation in the core of the Kranzberg syncline identified four litho-units that form an up to 800 m thick succession of metaturbidites describing an overall coarsening upward trend. This coarsening upwards trend suggests sedimentation of the formation's upper parts may have occurred during crustal convergence and basin closure between the Kalahari and Congo Cratons, rather than during continued spreading as previously thought.

The Kranzberg syncline is a regional-scale NW verging, NE-SW trending, strongly non-cylindrical structure that consists of a moderately SE dipping, normal NW limb and a steep- to overturned SE limb. First- and lower-order folds show relatively consistent E - SE plunges at moderate angles and stretching lineations and boudinage of competent layers point to a fold-parallel stretch during folding. Folding is associated with a moderate- to steep SE dipping transecting foliation that shows a consistent anticlockwise rotation with respect to the axial plane of the fold. The transecting cleavage and a component of non-coaxial shear along the overturned limb suggest that folding was accompanied by a dextral component of shear thought to be related to the SW-directed extrusion of the adjacent Usakos dome during regional NW-SE directed shortening. It is further suggested that the Kranzberg syncline evolved within the overall regional pattern of regional dome and

syncline structures in the sCZ, and not as a forced fold in response to the formation of neighbouring dome structures.

Based on cross-cutting relationships and deformation, four main generations of bedding-concordant sills and bedding-discordant pegmatite dykes were identified. Along the normal limb, shallowly-dipping sills dominate, highlighting the significance of bedding anisotropies for sheet propagation. Along the overturned limb, interconnected dyke and sill geometries co-exist. Here, pegmatite emplacement appears to have been influenced by (1) the regional strain, (2) differing wall rock rheologies; (3) the orientation of pre-existing anisotropies; and (4) driving melt pressures.

Dykes within the Usakos pegmatite field formed within dilational sites, at high angles to the regional stretch, whereas sills formed at high angles to the regional shortening strain and in contractional sites. Where driving pressures for melt ascent were high enough, an interconnectivity of dykes and sills and subsequent melt transfer from contractional into dilational sites is developed. Where melt pressures dropped below a critical value pegmatites were arrested, thus preserving the ascent pathways of the melts. These complex intersecting melt pathways are developed throughout the Kranzberg syncline. This suggests the existence of fairly stable melt networks in the continental crust. This geometrical complexity also accounts for the stockwork-like structures observed in pegmatite fields.

Uittreksel

Die Sentrale Sone (CZ) van die Damara gordel in sentrale Namibië is onder lê deur volumineuse Pan-Afrikaanse graniete en speel gasheer vir talle pegmatiet voorkomste, waarvan party van ekonomiese belang is en is ekstensief ontgin. Hierdie studie bespreek die voorkoms, geometrie, relatiewe tydsberekening en inplasing meganismes vir die Usakos pegmatiet gebied, wat tussen die stede van Karibib en Usakos en wat binne die kern van die regionale-skaal Kranzberg sinklien geleë is.

Litologiese kartering van die Kuiseb Formasie in die kern van die Kranzberg sinklien het vier lito-eenhede geïdentifiseer. Hierdie eenhede, wat saam tot 'n 800 m dik opeenvolging van metaturbidiete vorm, beskryf 'n algemene opwaartse vergroeiing neiging. Hierdie tendens dui aan dat sedimentasie van die Formasie se boonste dele tydens die aardkorst konvergensie en kom sluiting tussen die Kalahari en die Kongo kratons voorgekom het, eerder as in 'n oseaanvloerverbreiding omgewing soos voorheen gedink was.

Die Kranzberg sinklien is 'n regionale-skaal struktuur met 'n NW vergensie, 'n NO-SW koersing, wat sterk nie-silindries is en wat uit 'n matige SO helling, normale NW flank en 'n steil-tot omgeslaande SO flank bestaan. Eerste- en laer-orde plooie vertoon relatief konsekwent matige O - SO duikings en strek lineasies en boudinage van kompetent lae dui 'n plooi parallel strek tydens plooiing aan. Plooiing is geassosieer met 'n ongeveer aksiale planêre, matig- tot steil SO helling foliasie wat omstandig waargeneem word om 'n konsekwente antikloksgewyse rotasie met betrekking tot die aksiale vlak van die plooi te hê. Hierdie antikloksgewyse rotasie is 'n bewyse vir 'n komponent van nie-koaksiale regse skuifskuur deur die omgekeerde flank en dui dit ook aan dat 'n regse komponent van skeur gedurende of na plooiing plaasgevind het. Daar is gedink dat die regse komponent van skeur in verband met die laterale, SW-gerig extrusie van die aangrensende Usakos koepel gedurende plaaslike NW-SO verkorting ontwikkel het. Dit is verder voorgestel dat

die Kranzberg sinklien binne die totale patroon van plaaslike koepel en sinklien strukture in die sCZ geontwikkel het, en nie as 'n gedwonge plooi in reaksie op die formasie van die naburige koepel strukture (bv. Usakos koepel).

Gebaseer op kruis-sny verhoudings en deformasie, was vier generasies van gelaagdheid-konkordant plate en gelaagdheid-diskordant pegmatiet dyke geïdentifiseer. In die normale flank, vlak-helling plate oorheers, wat die belangrikheid van die laagvlak-anisotropiese op plaat voortplanting beklemtoon. In die steil, omgekeerde flank, bestaan onderlinge verbindende dyke en plaat geometrië gelyktydig. Hier is pegmatiet inplasing blykbaar beïnvloed deur (1) die regionaal span; (2) verskillende wandgesteentes reologie; (3) die oriëntasies van anisotropie (ie. gelaagdheid); en (4) smeltsel druk.

Dyke in die Usakos pegmatiet gebied het binne dilatationele liggings, teen hoë hoeke aan die regionaal strek gevorm, terwyl plate teen hoë hoeke aan die plaaslike verkorting span en in kontraksionele liggings gevorm het. Waar smeltsel druk hoog genoeg was, is 'n onderlinge verbinding van dyke en plate, en die daaropvolgende smeltsel oordrag van kontraksionele liggings na dilatationele liggings behou. In teenstelling, waar smeltsel druk onder 'n kritieke waarde geval het, word die pegmatiet geblokeer, en dus kan die behoude smeltsel styging paaie waargeneem word. Hierdie snyende smeltsel geometrië, in beide kontraksionele en dilatationele liggings dui aan dat redelik stabiele smeltsel netwerke in die kontinentale kors kan bestaan en verder kan en verklaar die algemene stokwerk-agtige strukture wat in pegmatiet velde van ander mid-korstige omgewings waargeneem word.

ACKNOWLEDGEMENTS

- Professor Alex Kisters for his enthusiasm, encouragement, appreciation for ‘sexy geology’, laughs, beers, and possibly one day, the acceptance for gumboot mapping! I couldn’t have asked for a better supervisor.
- My family and wife, Paula for never-ending love and support in all that I do.
- Navachab Gold Mine, for financially supporting and facilitating this research.
- Frik Badenhorst for his hospitality and the excellent braais.
- Nick Steven, for the geological discussions and support.
- Friends, new and old for the great times along the way.

CONTENTS

DECLARATION	ii
ABSTRACT.....	iii
ACKNOWLEDGEMENTS	v
CONTENTS	viii
Chapter 1 - INTRODUCTION.....	1
1.1 BACKGROUND	1
1.2 AIMS	4
1.3 LOCATION AND ACCESS.....	5
1.4 METHODOLOGY.....	7
Chapter 2 - REGIONAL GEOLOGICAL SETTING.....	8
2.1 THE DAMARA OROGEN	8
2.2 TECTONOSTRATIGRAPHIC EVOLUTION OF THE DAMARA BELT AND LITHOSTRATIGRAPHY OF THE sCZ	10
2.3 GRANITOIDS IN THE DAMARA BELT.....	18
2.4 PEGMATITES IN THE CZ.....	21
Chapter 3 - LITHOSTRATIGRAPHY OF THE STUDY AREA.....	25
3.1 ETUSIS FORMATION: NW LIMB.....	25
3.2 RÖSSING FORMATION: NW LIMB.....	25
3.3 CHUOS FORMATION: NW LIMB.....	27
3.4 ARANDIS FORMATION.....	29
3.5 GHAUB FORMATION.....	31
3.6 KARIBIB FORMATION	32
3.7 KUISEB FORMATION	34
Chapter 4 - STRUCTURAL GEOLOGY.....	41
4.1 INTRODUCTION.....	41
4.2 MAPPING APPROACH.....	50
4.3 FIRST- AND SECOND- ORDER STRUCTURES.....	52
4.4 THIRD- ORDER AND OUTCROP-SCALE STRUCTURES.....	52
4.5 STRUCTURAL DOMAINS OF THE KRANZBERG SYNCLINE	56
4.6 DEVIATIONS FROM D2 TRENDS.....	67
4.7 STRAIN	75
Chapter 5 - PEGMATITES OF THE USAKOS PEGMATITE FIELD	78
5.1 INTRODUCTION.....	78
5.2 PEGMATITE ORIENTATIONS AND GEOMETRIES.....	92
5.3 EMPLACEMENT STYLE AND PEGMATITE GEOMETRIES	106
5.4 DEFORMATION OF PEGMATITES.....	118
5.5 SUMMARY	123

Chapter 6 - DISCUSSION	124
6.1 LITHOSTRATIGRAPHY OF THE KUISEB FORMATION	124
6.2 STRUCTURE OF THE KRANZBERG SYNCLINE IN THE USAKOS TOWN AREA	127
6.3 PEGMATITE EMPLACEMENT.....	137
Chapter 7 - CONCLUSION	154
REFERENCES	158

Chapter 1 - INTRODUCTION

1.1 BACKGROUND

Granitic pegmatites form a volumetrically minor, but almost ubiquitous component of most deeply-eroded sections of the continental crust. The majority of pegmatites are interpreted to be associated with the late-stage crystallization of granite plutons. They form the residual fraction of a silicic melt and a vapour phase, and concentrate elements that are otherwise difficult to incorporate into the common granite mineralogy. As such, the two hallmarks of pegmatites are their coarse grain size and their often unusual, but broadly granitic mineralogy. Both the textural development of pegmatites as well as their mineralogical variations have been the focus of a large body of research for many decades (e.g. Jahns and Burnham, 1969; Jahns and Tuttle, 1963; Černý, 1991, Dingwell et al., 1996; London, 1996). Moreover, pegmatites in many terrains worldwide also host economically important deposits, forming a major source for e.g. Rare Earth Elements, lithium, niobium and tantalum, industrial minerals (e.g. micas, feldspar, piezometric quartz, etc.) and, of course, gemstones. The economic aspects of pegmatites have been studied equally well (e.g. Trueman and Černý, 1982; London, 1986; Černý, 1991; Novak et al., 1999; Thomas et al., 2000).

Despite this, the actual emplacement mechanisms and controls of pegmatites have received very little attention in the literature (e.g. Brisbin, 1986; Klemens and Schwerdtner, 1997; Henderson and Ihlen, 2004). Pegmatites are described occurring in a variety of tectonic settings including collisional and extensional settings as well as around granite plutons without the presence of a regional deviatoric stress field (eg. Brisbin, 1986; Rogers et al., 1998; Wang et al., 2007; Küster et al., 2009). Granitic pegmatites commonly intrude as sheets, i.e. as intrusive bodies of narrow width, but, depending on their orientation, relatively large strike-

and down-dip extents. They may occur as dyke swarms with consistent or systematically varying orientation, sheeted sills, but also as irregular plugs or pods. The sheet-like geometry is commonly explained to reflect the propagation of the melt-vapour mixture in fractures. As such, the emplacement of pegmatite swarms can be expected to follow regional and/or local stress and strain fields and/or pre-existing anisotropies (Anderson, 1936, 1951; Brisbin, 1986). Pegmatite stockworks describe rather irregular masses of intersecting sheet geometries, often developed within or close to the cupolas of granite plutons. The resulting wall-rock brecciation and the seemingly random orientation of pegmatite sheets are thought to have occurred as a result of melt and/or volatile overpressures. In this case, fracture propagation is driven by the melt/volatile pressure that may negate regional stresses (e.g. Brisbin, 1986).

The Central Zone (CZ) of the Damara belt in central Namibia is underlain by voluminous Pan-African granites and is host to numerous pegmatite occurrences ranging from thin dykes and sills to large, regionally mappable masses (Miller, 2008) (Fig. 1.1). Pegmatites of the Damara belt have been investigated by a number of workers (eg. de Kock, 1932; Von Knorring, 1985; Diehl, 1986; Baldwin, 1993), but these studies focused mainly on the mineralogy and economic geology of individual pegmatite dykes and pegmatite fields. Some of these pegmatites are of economic importance and have been studied and/or mined extensively for Sn, Li, Nb, Ta, Cs, mica, feldspar, and gem tourmaline and gem beryl (eg. Frommurze et al., 1942; Keller et al., 1999). In contrast, there has been, to date, no study that comprehensively documents and discusses the geometry, spatial and temporal relationships and structural controls of pegmatites as well as their regional setting and controls. This study focuses on the prominent Usakos pegmatite field between the towns of Karibib and Usakos, some 170 km NW of Windhoek (Fig. 1.2). The pegmatites are intrusive into metasediments of the Kuiseb Formation that occur in the core of the regional-scale F2 structure of the Kranzberg syncline.

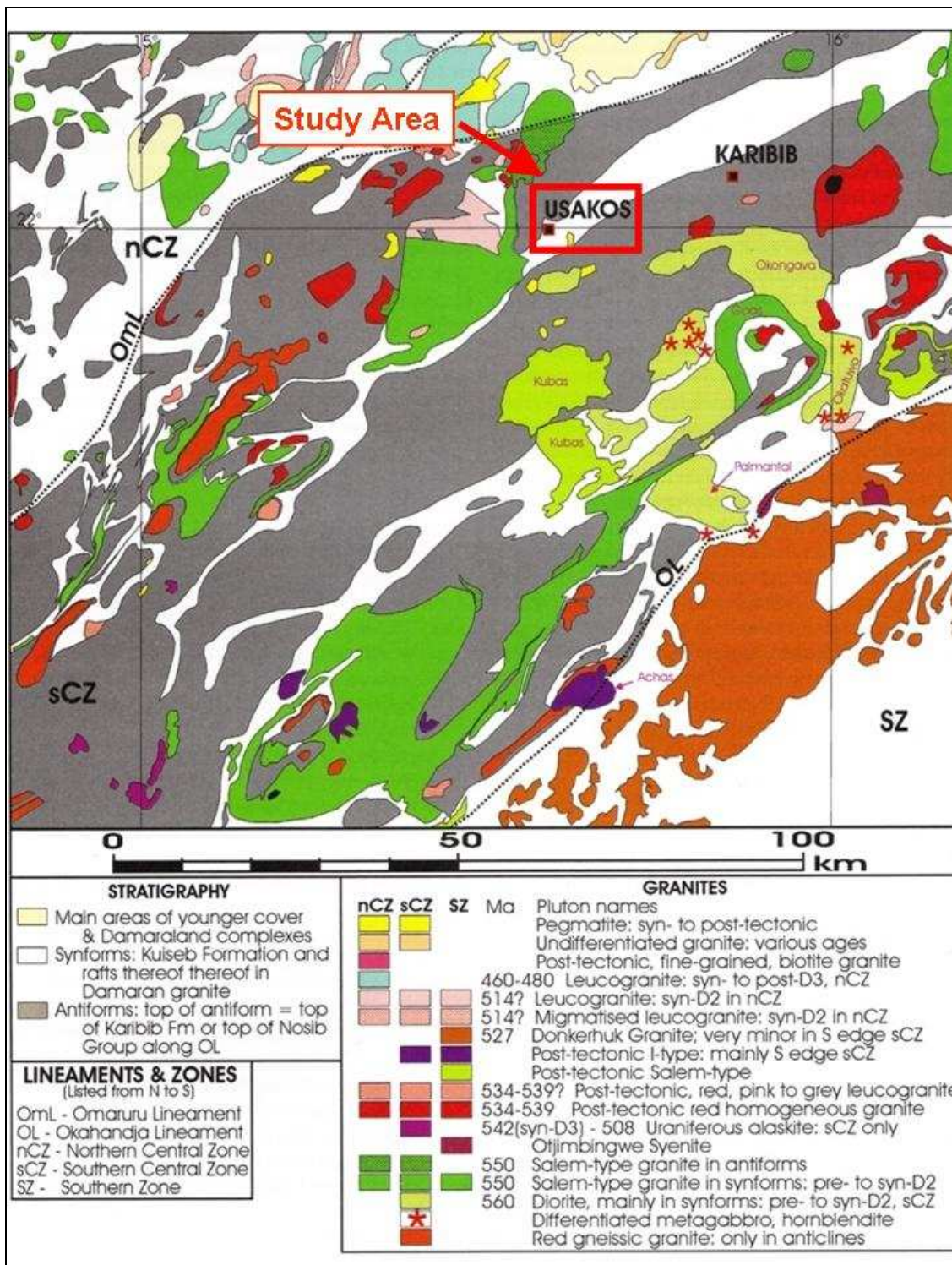


Figure 1.1: Granites and pegmatites of the sCZ and around Usakos, also showing the location of the Usakos pegmatite field (red box). Modified from Miller (2008).

Throughout the syncline, the pegmatites are and have been mined for, gem-quality tourmaline, including pink tourmaline, zoned watermelon tourmaline and black tourmaline (schorl) as well as beryl and lepidolite. Even at first glance and on a regional scale, the systematic occurrence and orientation of pegmatites in the Kranzberg syncline suggest an either structural and/or lithological control, or combination thereof, on pegmatite emplacement. The documentation of the lithological succession and variations as well as the structural geology of the Kranzberg syncline is, hence, of paramount importance for an understanding of the controls of pegmatite emplacement.

1.2 AIMS

The aims of this study are the following;

1. To document the lithological inventory of the Kranzberg syncline. The syncline is cored by the regionally very monotonous, metaturbiditic, quartz-biotite schist-dominated sequence of the Kuiseb Formation for which, in this part of the Damara Belt, no existing stratigraphic subdivision has been established (e.g. Badenhorst, 1992; Miller, 2008). Special attention will be paid to understanding how stratigraphy and lithological heterogeneities influence pegmatite emplacement. In the process, this study will also aim to provide a lithostratigraphic layout of the Kuiseb Formation within the sCZ.

2. To document and discuss the geometry and kinematics of the regional-scale Kranzberg syncline within the framework of the Damara Belt. Previous structural work in the region have almost exclusively focused on the prominent D2 antiformal dome structures of the south Central Zone (e.g. Coward, 1983; Kröner, 1984; Oliver, 1994; Poli and Oliver, 2001; Kisters et al., 2004; Johnson, 2005), for which a number of different origins have been proposed. The intervening synformal structures, in contrast, have not been dealt with in any detail. This is also a result of the monotonous nature of the Kuiseb Formation in the core of the synforms, which complicates detailed structural mapping.

3. To document and discuss the occurrence, geometries, relative timing and emplacement mechanisms of pegmatites of the Usakos pegmatite field. To date, the emplacement mechanisms and controls of pegmatite intrusions have not been investigated for any of the, in places, gemstone-bearing pegmatite fields. This study focuses on the emplacement controls of pegmatites.

1.3 LOCATION AND ACCESS

The town of Usakos is located in the south Central Zone (sCZ) of the Damara belt in central Namibia, approximately 150 km NE of Swakopmund and 170 km NW of Windhoek (Fig. 1.2).

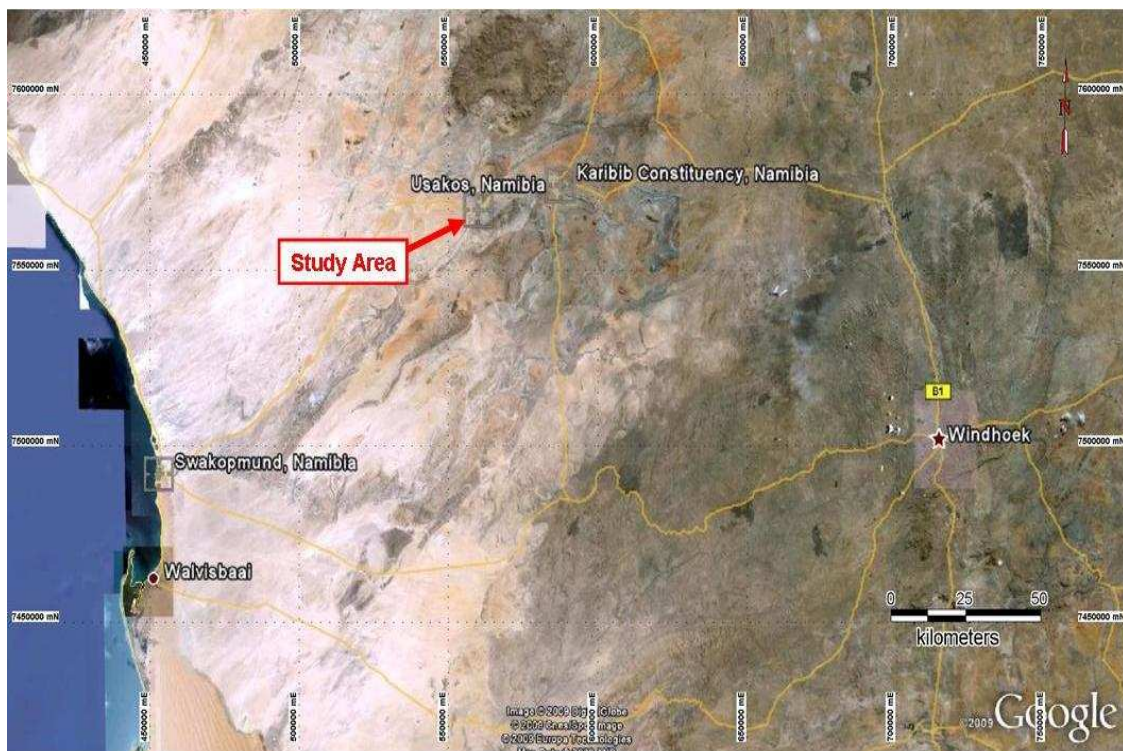


Figure 1.2: Google Earth image showing the location of the study area, approximately 150 km NE of Swakopmund and 170 km NW of Windhoek.

The study area is located some three kilometres to the E and S of town and is centred at UTM coordinates 565000E and 7567000N (WGS 84) (Fig. 1.3), covering an area of approximately 80 km². For the most part, the area is well exposed,

providing good three-dimensional outcrop for structural and lithological analysis. The boundaries of the study area are as follows:

Western boundary: This is marked by the NE - SW trending Khan River. The drainage typically follows the contact between rocks of the lower Swakop and the underlying Nosib Group.

Eastern boundary: The Ghaub Formation along the NW limb of the adjoining Usakos dome was used for this boundary.

Northern boundary: A prominent drainage at coordinates UTM 566113E; 7569017S (WGS 84) marks the northern boundary. The area to the North is almost entirely covered by alluvium and provides very little exposure.

Southern boundary: The closure of the first-order hinge (UTM 557445E; 7560724S WGS 84) marks the southern boundary.

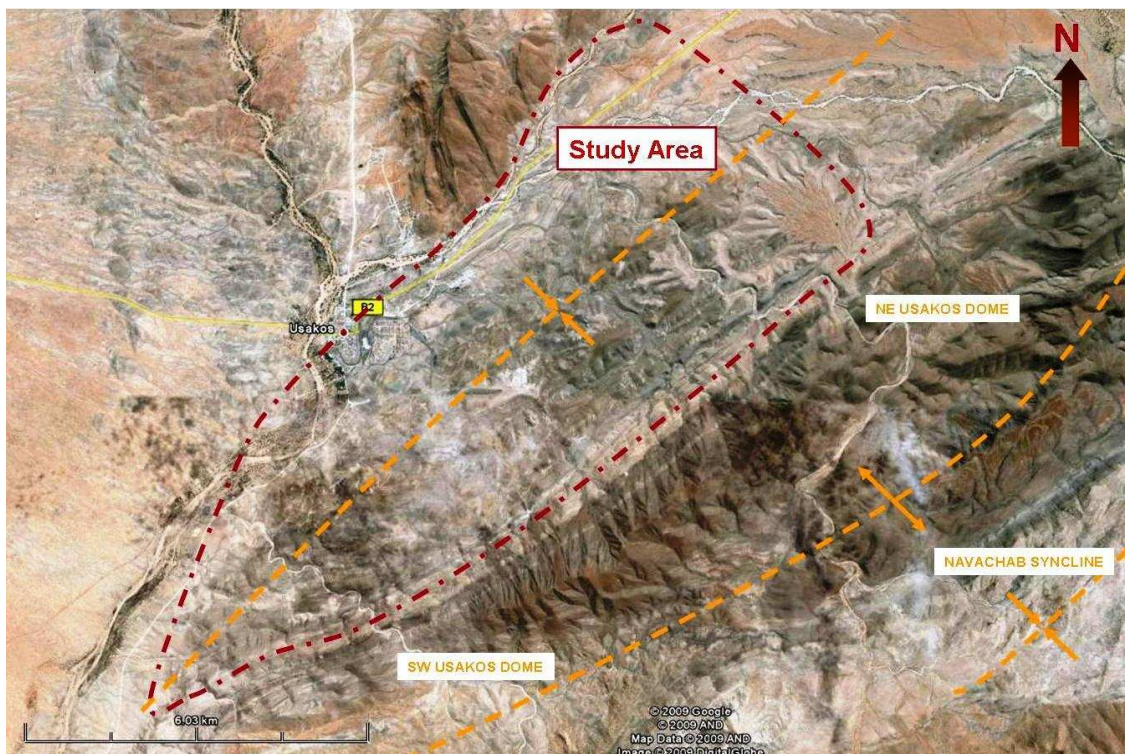


Figure 1.3: Location of study area, centred approximately three kilometres E of Usakos, adjacent to the NW limb of the Usakos dome.

1.4 METHODOLOGY

Field work was undertaken over a period of two and a half months from June 15 to Aug 8, 2009 and from October 22 to November 8, 2009. Access was mainly on foot with occasional use of a 4wd vehicle on dirt roads and river beds. Permission was received from local land owners prior to accessing the properties.

Base maps were generated and digitized using Google Earth and Mapinfo GIS software. These base maps were printed and later used for ground truthing. Final geological and structural maps were produced using Microsoft Office PowerPoint 2003, MapInfo Professional 8.5.1B and ArcView 3.1. Petrographic studies and use of the Scanning Electron Microscope (SEM) at Stellenbosch University were used to identify mineral compositions and lithological units listed in the thesis. Structural readings were taken with the Brunton conventional structural compass. Planar readings were recorded as strike azimuth and dip angles using the right-hand rule, while linear readings were recorded as trend direction and plunge angles. All stereographic projections are equal area and into the lower hemisphere.

Chapter 2 - REGIONAL GEOLOGICAL SETTING

This chapter gives a brief outline of the tectonostratigraphic evolution and geodynamic environment of the Damara belt and provides geochronological constraints on the temporal evolution of the belt. Before this background, the lithological inventory, structural geology and the intrusive history of the Kranzberg syncline will be presented and discussed in subsequent chapters.

2.1 THE DAMARA OROGEN

The Damara Orogen (Fig. 2.1) formed as a result of the amalgamation of the Gondwana supercontinent during the Proterozoic and early Phanerozoic (Prave, 1996; Trompette, 1997). It comprises three collisional belts, namely the Gariiep belt, Kaoko belt and the Damara belt. The Gariiep and Kaoko belts are the N-S trending belts straddling the Atlantic seaboard, whereas the Damara belt is the SW-NE trending so-called inland branch of the Damara Orogen (Miller, 1983).

The Damara belt marks the collisional suture between the Congo and Kalahari Cratons. It is approximately 400 km in width, over 1,000 km in length and its lithological inventory records nearly 300 Ma of rifting, marine transgression, convergence and final collision (Miller, 1983, 2008; Porada, 1989; Gray et al., 2006). The belt has been subdivided into distinct tectonostratigraphic zones based on lithology, structure, metamorphic grade, plutonic rocks, geochronology and aeromagnetic expression (Martin, 1965; Martin and Porada, 1977; Miller and Hoffman, 1981; Corner, 1982, 2000; Anderson and Nash, 1997). From north to south, these zones are the Northern Platform (NP), Northern Zone (NZ), Central Zone (CZ), Okahandja Lineament Zone (OLZ), Southern Zone (SZ), Southern Marginal Zone (SMZ), and the Southern Foreland (SF) (Fig. 2.1).

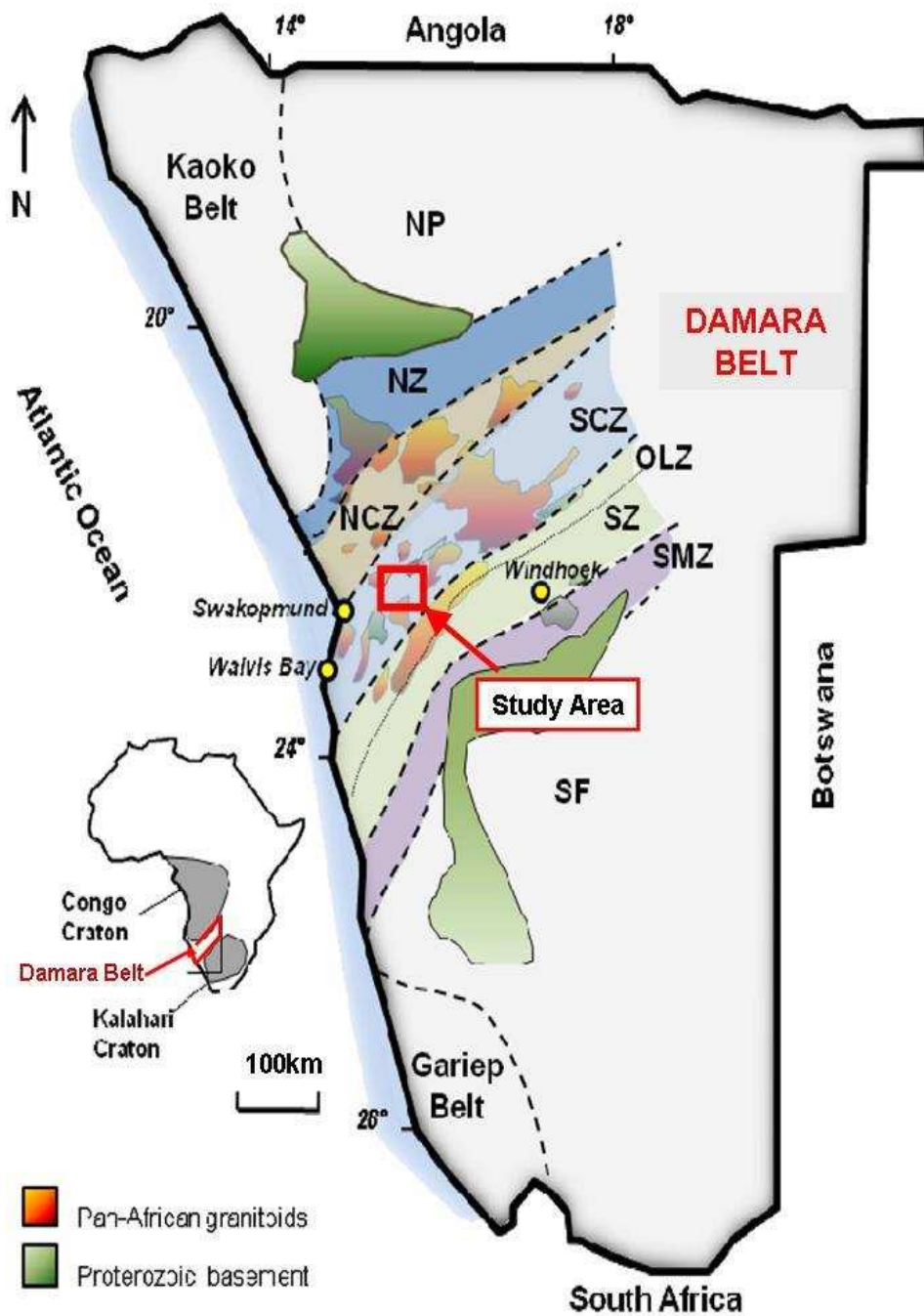


Figure 2.1: The Damara Orogen and Damara belt in Central Namibia (after Miller, 1983). NP: Northern Platform; NZ: Northern Zone; NCZ: Northern Central Zone; SCZ: Southern Central Zone; OLZ: Okahanja Lineament Zone; SZ: Southern Zone; SMZ: Southern Margin Zone; SF: Southern Foreland (after Miller, 1983 and modified from Kitt, 2008).

The CZ is known as the magmatic axis of the Damara belt characterized by high-T, low-P metamorphism and an abundance of pre-, syn-, late- and post-tectonic granites (Jacob, 1974; Miller, 1983; Masberg et al., 1992; Jung et al., 1995; Tack and Bowden, 1999; Johnson et al., 2006). The CZ is divided into a northern (nCZ) and a southern (sCZ) Central Zone by the NE-SW trending, mainly geophysically defined Omaruru Lineament (Corner, 1982). The study area is located within the sCZ near the small town of Usakos and is centred at UTM 565000E and 7567000N (WGS 84) (Fig. 2.1).

2.2 TECTONOSTRATIGRAPHIC EVOLUTION OF THE DAMARA BELT AND LITHOSTRATIGRAPHY OF THE sCZ.

Detailed summaries of the tectonostratigraphic evolution of the Damara belt have been compiled by Miller (1983, 2008), Porada (1989), Stanistreet et al. (1991) and Gray et al. (2006). The following section is a brief overview, focusing on the evolution of the CZ within the Damara belt. A stratigraphic overview of the CZ is provided in Table 2.1. The sCZ comprises pre-Damara gneisses and overlying Nosib to Swakop Group rocks of the Neoproterozoic Damara Supergroup (Miller, 2008). The depositional environment of the Damara Supergroup in the sCZ is interpreted as being part of an extensive continental slope, locally segmented by basement highs, developed along the leading edge of the Congo Craton (Stanistreet et al., 1991; Badenhorst, 1992; Miller, 2008).

2.2.1 RIFTING AND MARINE TRANSGRESSION

The tectonic and lithostratigraphic evolution of the CZ in the Damara Belt originated with Neoproterozoic intracontinental rifting between the Congo and Kalahari Cratons. Deposition of rift-type sediments and metavolcanic rocks of the lower Nosib Group, the Etusis Formation, has been constrained to between 746 ± 2 and 756 ± 2 Ma by Hoffman et al. (1996) corresponding to the age of 752 ± 7 Ma obtained by de Kock et al. (2000) for volcanic rocks in the Etusis Formation.

Table 2.1: Stratigraphy of the Damara Supergroup within the sCZ (modified from Badenhorst, 1992; Miller, 2008).

	Group	Formation	Description	Thickness	Age
DAMARA SEQUENCE	Swakop	Kuiseb	Quartz-biotite-cordierite schist and turbiditic metapsammites	40 to >3300 m (Smith, 1965; Badenhorst, 1987).	
		Karibib	Grey and white calcitic and dolomitic marbles with intermittent calc-silicate felses and marble breccias	Up to 1000 m	
		Ghaub	Daheim Member- Amphibolites- occasionally within a carbonate matrix	0 to 120 m (Badenhorst, 1992).	635.5±1.2 Ma (Hoffmann et al., 2004)
			Glaciomarine pelites, psammites and dropstone units	0 to tens of metres	
		Arandis	Oberwasser Member- Grey quartz-biotite-tremolite-cordierite schist and calc-silicate felses	50 to 700 m (Badenhorst, 1987).	
			Okawayo Member- Blue-grey dolomitic and calcitic marbles and calc-silicate felses, intercalated calc-silicates	ca. 100 m thick	
			Spes Bona Member- Quartz-biotite schists and meta-psammites.	20 to >600 m (Badenhorst, 1992; Steven, 1993).	
	Chuos	Glaciomarine diamictite.	0 to 700 m (Henry et al., 1986)	746±2Ma (Hoffman et al., 1996)	
		Rössing	Interbedded marbles, calc-silicates and siliciclastic rocks	Possibly 0 to 150 m. Highly variable	
	Nosib	Etusis	Quartz-arenites.	0 to 3500 m (Smith, 1965; Miller, 1983; Lehtonen et al., 1996).	756±2 Ma to 746±2 Ma (Hoffman et al., 1996)
Abbas Basament			Pink and grey quartzo-felspathic augengneisses, schists, amphibolites and pegmatites		1925±330Ma (Jacob et al., 1978)

NOSIB GROUP

Etusis Formation

Within the Nosib Group, the Etusis Formation forms the lowermost part of the Damara Supergroup, resting unconformably on mainly Palaeoproterozoic gneisses of the Abbas Metamorphic Complex (Miller, 1983). The rocks are characterized by reddish brown, fine- to medium-grained feldspathic quartzites with less abundant arkose layers and, locally, intercalated volcanic and volcanoclastic horizons (Hawkesworth et al., 1983; Miller, 1974, 1979, 1980). Decimetre- to metre-scale cross-bedding is common, together with channel-fill conglomerates (Henry, 1992; Miller, 2008). The Etusis Formation displays dramatic variations in thickness,

reaching up to several thousand metres in the CZ. These variations likely reflect deposition in half-graben structures, while areas of little or no deposition are indicative of paleohighs such as graben shoulders. Within the CZ, U-Pb zircon ages from volcanic horizons in the Etusis Formation indicate sedimentation and volcanism occurred ca. 752 ± 7 Ma (de Kock et al., 2000).

The Khan Formation that forms the upper part of the Nosib Group, is not developed in the study area.

SWAKOP GROUP

Rössing Formation

Thermal subsidence during continued crustal extension between the Kalahari and Congo Cratons led to the opening of the Khomas Sea and subsequent shelf-sequence deposition of the lower Swakop Group (Hartnady et al., 1985; Henry et al., 1988; Stanistreet et al., 1991; Hoffmann, 1990). The earliest marine units of the lower Swakop Group in the study area are those of the Rössing Formation, a lithologically heterogeneous marble-dominated unit also containing quartzites and biotite schists representing shallow-marine conditions of sedimentation (Smith, 1965; Nash, 1971; Jacob 1974; Brandt, 1985; Henry, 1992; Miller, 1983, 2008). Deposition of the Rössing Formation is believed to have been initially siliciclastic-dominated, particularly close to the Okahandja Lineament (Miller, 2008), and later dominated by carbonates (Henry, 1992).

Chuosi Formation

Overlying the Rössing Formation is the glacio-marine Chuosi Formation with associated dropstones, turbidites and minor volcanics (Henry et al., 1986; Hoffmann et al., 2004). The Chuosi Formation is associated with the late Neoproterozoic Sturtian glaciation, with the underlying volcanics in the NZ providing an age

constraint of ca 746 ± 2 Ma (Hoffman et al., 1996). It forms an important marker horizon in the NZ and sCZ of the Damara Belt (e.g. Badenhorst, 1992) and varies lithologically from massive tillites with or without iron formations to heterogeneous clast-supported diamictites (Martin, 1965; Smith, 1965; Miller, 1980, 1983).

The Chuos Formation varies in thickness from 600 m south of the Khan Mine in the SW of the sCZ to 120 m in the NE at the Navachab mine (Miller, 2008). The Chuos Formation is only developed as a thin, strongly schistose unit on the western edge of the field area.

Arandis Formation

Rifting and continental breakup were followed by large-scale marine transgressions and basin deepening. The southern margin of the Congo Craton developed into a carbonate-dominated epicontinental shelf while the northern Kalahari Craton margin produced terrigenous sediments (Stanistreet et al., 1991). During this time, a thick succession of mixed siliciclastics and chemogenic sediments were deposited in the sCZ, comprising biotite schists, metapsammites, marbles and calc-silicate felsels of the Arandis and Ghaub Formations.

The Arandis Formation (Lehtonen et al., 1995) consists of three main members, namely the Spes Bona Member at the base, and the Okawayo and Oberwasser Members higher up in the stratigraphy. Its exposure is limited within the sCZ, but thickens to almost 4,000 m in the nCZ (Miller, 2008).

Spes Bona Member

The Spes Bona Member overlies the Chuos Formation and was first given its name by Badenhorst (1988) to describe intercalated biotite schists and calc-silicate felsels below the Okawayo Member. It has limited exposure in the sCZ (Steven, 1993), but north of Omaruru it exceeds 2,500 m in thickness (Miller, 2008). The sequence is commonly interpreted as being a turbidite sequence, and Badenhorst (1988)

suggested a subtidal to intertidal depositional environment on a siliciclastic-rich shelf. The Spes Bona Member is exposed in the core and the steep- to overturned NW limb of the Usakos dome with a minimum estimated thickness of 600 m (Johnson, 2005).

Okawayo Member

A distinctive unit with highly variable thickness, the Okawayo Member occurs in both the nCZ and sCZ and consists of interbedded marbles, marble breccias, biotite schists and calc-silicate horizons (Badenhorst, 1987, 1992; Miller, 2008). The extensiveness of the Okawayo signifies considerable crustal stability and likely a warm, shallow-water depositional environment in the CZ. At the nearby Navachab mine, the gold skarn-quartz mineralization is located within the calcitic and dolomitic marbles of the Okawayo Member.

Oberwasser Member

The Oberwasser overlies the Okawayo Member and is composed largely of feldspathic biotite schists and quartz-biotite schists with lesser calc-silicate units (Klein, 1980). A felsic volcanic unit dated by Hoffmann et al. (2004) provides an age constraint of $635 \pm 1\text{Ma}$. Closer to the contacts with the overlying Karibib Formation, 1-10 m thick sedimentary breccias, containing mica-rich clasts and rare carbonate lenses are locally developed. Hoffmann et al. (2004) correlated these, and the thin marble horizons, to the Ghaub glacial diamictite and associated Daheim mafic volcanics.

Ghaub Formation

Daheim Member

Hoffmann et al. (2004) recognized the upper Oberwasser and Daheim Members to be part of the Ghaub Formation. The Daheim Member overlies the Oberwasser Member. It comprises metamorphosed basic pillow lavas and pyroclastic rocks in the sCZ (Miller, 1983, 2008; Badenhorst, 1992). U-Pb zircon ages of $635 \pm 1\text{Ma}$ from

volcanic horizons constrain the age of deposition (Hoffmann et al., 2004). The Daheim Member has the composition of continental alkali basalts suggesting they were likely deposited on the margin of a deep, submerged basin near the Congo Cratons' southern passive continental margin (Miller, 1983, 2008). On the NW limb of the Usakos dome, Daheim volcanics form up to 80 m thick and a few hundred metres long lens-shaped intrusions with the thickest central areas being correlated with volcanic feeder zones (Badenhorst, 1992).

Karibib Formation

The sCZ remained a relatively shallow-marine environment and was subsequently 'swamped' by a thick succession of carbonates of the Karibib Formation, indicative of warmer climatic conditions (Stanistreet et al., 1991; Badenhorst et al., 1992) and signifying a period of large-scale marine transgression between ca. 625 Ma to ca. 600 Ma (Miller, 2008). This carbonate unit is substantially thicker than the earlier deposited Okawayo Member marbles, and probably indicates the submergence of the rift edges (grabens) forming a larger platform for carbonate deposition and/or a decrease in the rate of basin spreading (Miller, 2008). The Karibib Formation in the sCZ typically consists of light- and dark-grey calcitic marbles, grey- to beige dolomitic marbles, marble breccias and calc-silicate felses. It reaches a thickness of up to 700 m at the Navachab mine (Badenhorst, 1992) and is up to 1,000 m thick SE of Walvis Bay (Sawyer, 1981).

Kuiseb Formation

A deepening of the basin following carbonate sedimentation is indicated by the deposition of the Kuiseb Formation, a thick, metaturbiditic sequence that forms the uppermost unit of the Damara Supergroup. The thickness of the Kuiseb Formation ranges from approx. 1,000 m in the CZ to 8-10,000 m in the SZ (Miller, 2008). The Kuiseb Formation forms the highest stratigraphic unit of the Damara Supergroup and is widely distributed throughout the CZ. The regionally widespread distribution

of the Kuiseb Formation suggests the formation of a large depositional basin covering much of the originally strongly segmented basin of the Khomas Sea and adjacent second-order basins. It conformably overlies the marble units of the Karibib Formation and typically cores synforms of variable shapes within the CZ (eg. Miller, 1983). Within the Karibib area, basal layers of the Kuiseb schist are seen to interfinger with the marbles of the Karibib Formation. This interlayered schist-marble succession was termed the Onguati Member (Badenhorst, 1992).

The Kuiseb Formation is typically composed of fine- to coarse-grained, biotite-rich quartzo-feldspathic schists with cordierite, amphibole or sillimanite porphyroblasts that increase in abundance west of Karibib (Miller, 2008). Closer to Swakopmund and at higher metamorphic grades, the schists become more migmatitic (Miller, 2008). The transition from carbonate-dominated sedimentation to a turbidite succession suggests an increase in sea basin subsidence within the sCZ (Steven, 1993). Higher up in the stratigraphy, competent, up to 20 m thick psammitic units are developed. Bedding is often destroyed by regional fabric development and recrystallization of the rocks. A top contact of the Kuiseb Formation is not exposed so that a complete inventory of the formation is not available.

2.2.2 CRUSTAL CONVERGENCE AND EMPLACEMENT OF PLUTONS

The timing at which spreading reversed and the onset of convergence in the Damara belt began is not well constrained, but is thought to have commenced at 600-580 Ma (e.g. Miller, 2008). Gray et al. (2006) proposed northward subduction of the Kalahari underneath the Congo Craton to have originated at ca. 580 Ma. Within the CZ, S1 bedding-parallel fabrics and D1 large-scale recumbent folding developed (Miller, 1983). The truncation of marker units and thickness variations within the Damara Supergroup were also interpreted to be the result of low-angle, bedding-subparallel D1 thrusts (e.g. Kisters et al., 2004). Crustal convergence and the early collisional stages (D1) were associated with or immediately followed by the emplacement of numerous gabbroic, dioritic and syenitic plutons between 565 and

550 Ma (e.g. Jacob et al., 2000; de Kock, 2000). Individual plutons are relatively small, but rocks of the Goas Dioritic Suite are distributed throughout the sCZ.

Collisional tectonics and final closure of the Khomas Sea ensued at ca. 550-540 Ma and probably lasted until ca. 510 Ma (Miller, 1983, 2008; Jacob et al., 2000; Jung et al., 2001), leading to the formation of regional-scale D2/3 structures. The D2/3 deformation resulted in the main (E)NE-trending structural grain of the Damara belt, consisting of regional-scale (>10 – 100 km strike length), NE trending anti- and synclinoria and associated thrust zones. In the sCZ, the D2/3 tectonism resulted in the formation of kilometre-scale, doubly-plunging dome structures and intervening synclines, as well as thrusts recording mainly top-to-the-NW kinematics. Regionally pervasive NE-SW trending, mainly ductile fabrics are associated with the large-scale structures. SW-verging sheath folds (Coward, 1983; Poli and Oliver, 2001; Kisters et al., 2004; Johnson, 2005) seem to record the orogen-parallel (SW-directed) extrusion of the rocks, at high angles to the NW-SE directed shortening strains. Deformation was associated with the syn- and late-kinematic emplacement of a number of different granite suites (Table 2.2). Metamorphic conditions during the D2/3 deformation reached amphibolite-facies grades around the Usakos region attaining peak P-T conditions of ca. 3 ± 1 Kbar and 600-650°C (e.g. Puhon, 1983; Steven, 1993). Granulite-grade conditions resulting in pervasive partial melting and migmatization of both basement and cover rocks were reached some 150 km to the SW closer to the Atlantic coast (Jung and Mezger, 2003; Ward et al., 2008).

The late- and post-tectonic evolution of the Damara belt is characterized by the intrusion of large post-tectonic granitoids and a complex and long lived thermal evolution between ca. 510 and 465 Ma that probably reflects this episodic advective heat transfer (Kröner, 1982; Haack et al., 1983; Miller, 1983; Jung et al., 1998; Tack and Bowden, 1999; Jung et al., 2000; Jacob et al., 2000) and granite emplacement. Cooling of the belt below temperatures of ca. 300°C by ca. 460 Ma is indicated in the Ar-Ar ages of micas (e.g. Gray et al., 2006).

2.3 GRANITOIDS IN THE DAMARA BELT

Ever since the first regional reconnaissance mapping (e.g. Gürich, 1891; Gevers, 1931), the Damara belt and the CZ, in particular, have been recognized as one of the world's best-preserved granite and pegmatite terrains. Since then, the granites and pegmatites of the Damara belt have been the subject of numerous studies (eg., Smith, 1965; Jacob, 1974; Miller, 1983; Haack et al., 1980, 1982, 1988; Hawkesworth et al., 1983; McDermott et al., 1996; Jung et al, 2000, 2001, 2005; amongst many others) and both field as well as geochronological relationships were used to establish a broad sequence of intrusive events. This sequence describes, from oldest to youngest, a broadly compositional trend from older I-type gabbros, diorites, syenites and tonalite, via coarse-grained porphyritic biotite-rich granites and minor granodiorites (mainly the broad group of Salem-type granites), to S-type leucogranites, uraniferous leucogranites and pegmatites (Miller, 2008). Table 2.2 summarizes the stratigraphic position and timing of granite emplacement in the CZ (after Miller, 2008).

The two large granite plutons of the Stinkbank and Klein Aukas Granites occur closest to the study area (Fig. 2.2). The Salem-type Stinkbank granite is located less than 10 km SW of Usakos and occupies a similar stratigraphic and structural position compared to the Usakos pegmatite field, namely within the core of the Kranzberg syncline and in rocks of the Kuiseb Formation, immediately above marbles of the Karibib Formation. As a typical member of the Salem-type granites, it consists of mineralogically and texturally two main and very distinct phases. An earlier biotite-rich, K-feldspar megacrystic granite is intruded by a later, more voluminous leucogranite consisting of quartz, K- feldspar, and plagioclase with accessory biotite, tourmaline, muscovite, garnet and monazite. Recent U-Pb zircon dating of the megacrystic variety indicates an emplacement at 549 ± 11 Ma (Johnson et al., 2006). The Klein Aukas leucogranite is located within the southern hinge of

the Usakos dome, only a few hundred metres to the SE of the study area at its closest point.

Table 2.2: Stratigraphic position and timing of granitoids in the CZ

Type/Name	Stratigraphic position and timing of granitoids
Stanniferous pegmatites and balloon shaped granites	Stratigraphically highest intrusions in the CZ, intrusive into the Kuiseb Formation, intrusive mainly between 510-465 Ma
Leucogranites in the Kuiseb Formation	Located above the Salem granites, intrusive between 540-465 Ma
Salem-type granites	Located very close to the base of the Kuiseb Formation and preferably in D2/3 synforms (syn- to post D2/3 emplacement, ca. 550-540 Ma)
Early diorites and gabbros	Only in synforms below the Salem granites and above the Karibib Formation (late D1, pre- to syn, D2/3; ca. 565-550 Ma)
Red homogenous granites	Located in D2/3 antiforms. Sometimes seen in higher stratigraphic levels as dykes and plugs
Uraniferous alaskites	Concentrate in the Khan Formation and occasionally in the Chuos Formation, mainly in high-grade SW parts of the CZ, SW of Usakos (post D3, 520-465 Ma)
Red gneissic granite	D2/3 anticlines, commonly within the Nosib Group or pre-Damaran basement
Unfoliated post-tectonic migmatites	Nosib Group and pre-Damaran basement in the high-grade SW parts of the CZ

The granite is typically a very coarse-grained, garnet-bearing two-mica granite that is stratigraphically situated below the Karibib marbles and in the hinge zone of the D2 Usakos dome (Johnson, 2005). Recent structural studies by Johnson (2005) on the Klein Aukas granite and Vietze (2009) on the Stinkbank granite suggest that both granites are relatively thin, composite sheets showing largely concordant wall-rock contact relationships and, thus, sill-like or laccolithic geometries. Both studies suggest a syn-D2 timing of the two granites, during F2 folding and regional NW-SE subhorizontal shortening and associated orogen-parallel, NE-SW directed stretch (Kisters et al., 2004; Johnson, 2005; Vietze, 2009).

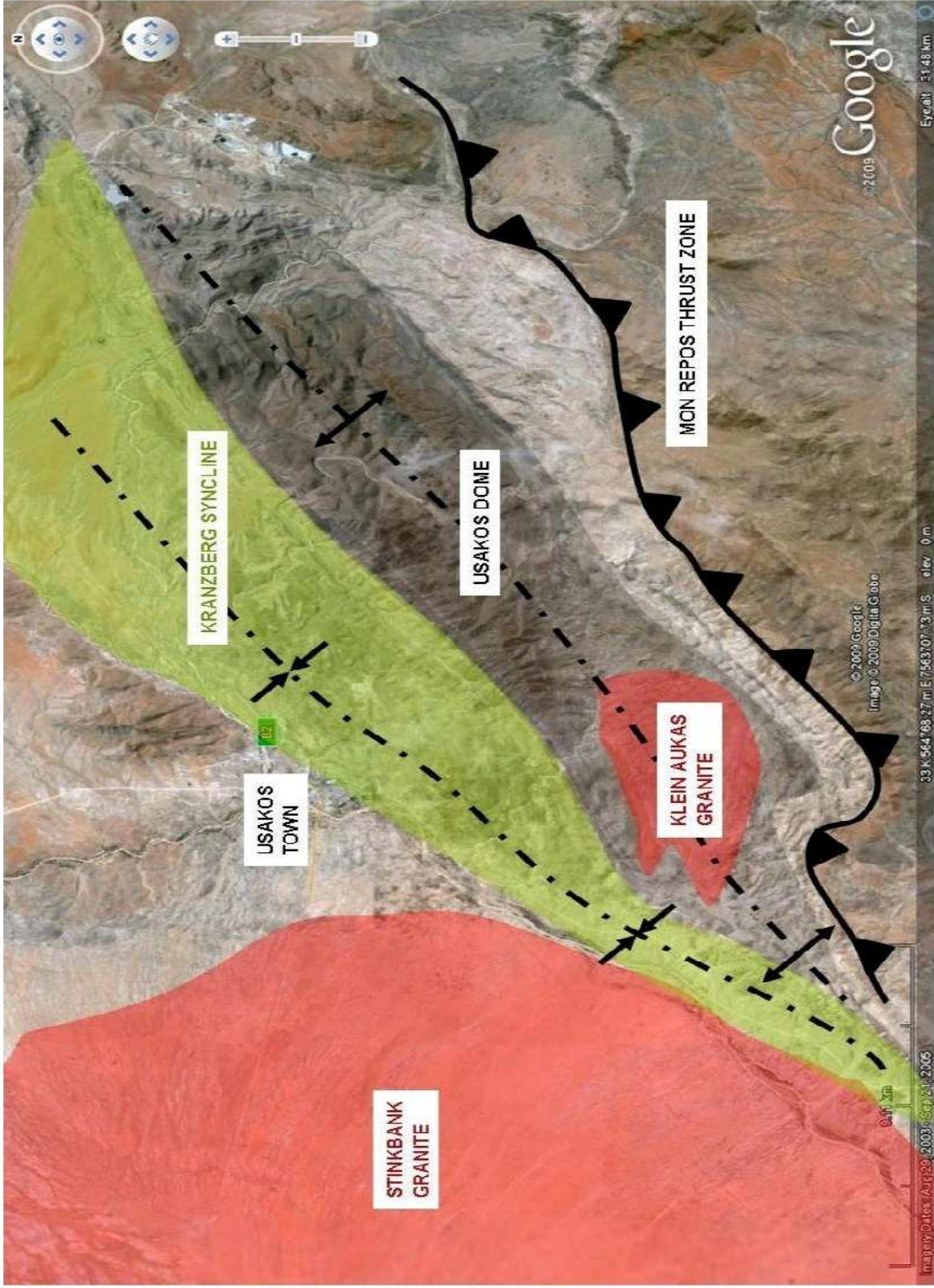


Figure 2.2: Annotated Google Earth image showing the regional relationships between first-order structures and granite intrusions. Usakos dome (black), Kranzberg syncline (green), Mon Repos Thrust Zone (from middle right to bottom left of image), and Stinkbank and Klein Aukas granites (red).

2.4 PEGMATITES IN THE CZ

The Central Zone (CZ) of the Damara Belt is host to numerous pegmatite occurrences ranging from thin dykes and sills to large, regionally mappable masses (Miller, 2008). A common definition of a pegmatite is “*a very coarse-grained rock, typically found in veins or lenticular or podlike bodies around the margins of large, deep-seated plutons, usually extending from the pluton itself into the surrounding country rocks*” (e.g. MacDonald et al., 2003). Pegmatites are further classified as being either simple or complex based on internal structures (e.g. Landes, 1933). Simple pegmatites are mineralogically equivalent to granites and are either found in high-grade metamorphic terrains, or as coarse-grained pods within finer-grained granitoids. Complex pegmatites, in comparison, are typically zoned, with a quartz-rich core and structures and textures such as graphic intergrowths and, in places, extremely coarse crystal sizes that indicate the crystallization kinetics of the melt-vapour rich pegmatites. In addition, complex pegmatites contain variable amounts of rare minerals as a result of the incorporation of otherwise incompatible elements into the late-stage crystallization products of the host granites (Raymond, 2002; MacDonald et al., 2003).

Since the late 1800s, German prospectors began to understand the economic importance of pegmatites in the CZ and, more specifically, in the Karibib District. Early records show that the pegmatites were recognized to host a variety of minerals, both rare and precious, ranging from massive accumulations to large isolated crystals of e.g. tourmaline, beryl or lepidolite. By the 1920s, most mineral occurrences had been located and were being prospected for cassiterite, tantalite, wolframite, lithium-bearing minerals and a number of precious and semi-precious gems. Petrologists and mineralogists soon followed and a number of both academic and economic studies were conducted on the stanniferous and lithium pegmatites during the 1920s and 1930s (e.g. Gevers and Frommurze, 1929; de Kock, 1932; Gevers, 1936). De Kock (1932) stated that “*the deposits [of the Karibib District] are*

probably the most extensive of their kind in the world”, and that there “should be a good future for these S.W.A lithium ore deposits.”

Interest in the regions' pegmatites continued through the 1950s and 1960s. Structural and textural characteristics were compared with similar pegmatites in e.g. Brazil, the U.S.A and Canada (eg. Cameron, 1955). A research group from the University of Witswatersrand performed an intensive study from 1959 to 1963 on the origin and regional setting of economically mineralized pegmatites in the vicinity of Karibib. Within the CZ, Roering (1961) was the first worker to record a relationship between the emplacement of Li- and Be- bearing pegmatites and regional structures. Eleven pegmatites, ten of which were within 20 miles of Karibib, were mapped in detail with the aim to develop an exploration model for economically viable bodies. Roering (1961) recognized three main types of pegmatites ranging in timing from syn- to post-tectonic, with simpler types being the earliest and most abundant, and the complex types being late and less common. He described the close correlation between complex pegmatites and tension-gash type structures that most likely developed during wrench-faulting in the area. However, at this stage, no comprehensive lithostratigraphy of rocks of the Damara Supergroup had been established making a correlation between pegmatites and the broader geological and structural framework impossible (Roering, 1961). This regional approach was adopted by Smith (1965, 1966) and his 1:125,000 scale map of the Karibib and Usakos region represented a milestone in Damaran geology. His research and regional mapping provided the first comprehensive overview of the geology around the Khan and Swakop Rivers, an understanding of the granitic and igneous rock types of the area and their relationships to the wall-rocks, as well as an account of mining centres and locations of prospects at that time. His study and map have since become one of the most widely referenced works in literature regarding the geology of the Damara belt.

From the 1970s to the present day, a number of studies have dealt with, at least partly, the structure and mineralogy of pegmatites in the CZ (eg. Jacob, 1974; Behr et

al., 1983; von Knorring and Condliffe, 1985; Diehl, 1986; Wagener, 1989; Baldwin, 1993; Steven, 1993; Keller et al., 1999). Most of these studies have focused on the complex and typically zoned, economically important pegmatites which have been and are mined for Sn, Li, Nb, Ta, Cs, mica, feldspar, and gem tourmaline and gem beryl. Most economic-grade pegmatites are emplaced into tightly folded supracrustals of the Damara Supergroup (Keller et al., 1999) whereas simple pegmatites, lacking economic-grade mineralization, are commonly found in pre-Damaran igneous and metamorphic basement rocks (Haack and Gohn, 1988; Diehl, 1993).

A number of studies have attempted to group pegmatites according to characteristics such as stratigraphic level of emplacement, genetic relationship with granite plutons and/or geographical distribution (eg. Frommurze et al., 1942; Diehl, 1993; Keller et al., 1999). For example, Keller et al. (1999) have categorized the pegmatite fields of the CZ into five main zones, including (I) The Northern Tin Belt which includes the Strathmore, Karlowa and Uis pegmatite swarms, (II) the Central Tin Belt located west of Omaruru, (III) the Southern Tin Belt including the Rössing pegmatite belt, (IV) the Karibib pegmatite belt comprising pegmatites of the Karibib and Usakos area, and (V) the Okahandja pegmatite belt (Fig. 2.3).

To date, no study has focused on the geometry, spatial and temporal relationships and structural controls of pegmatites in relation to the regional settings and controls, except for the aspect of pegmatite emplacements briefly mentioned by Roering (1961). This thesis attempts to provide a detailed analysis of the above relationships, which are further discussed in Chapters 4 and 5.

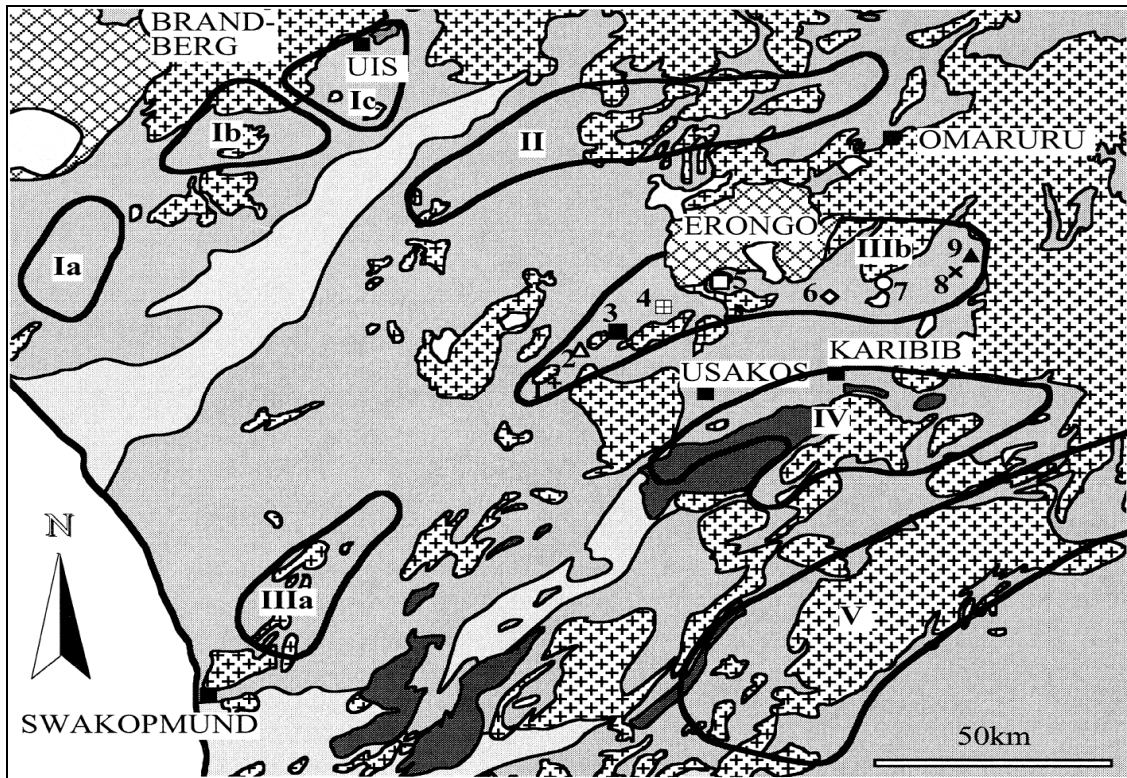


Figure 2.3: Grouping of Pegmatites in the CZ (after Keller et al., 1999).

Chapter 3 - LITHOSTRATIGRAPHY OF THE STUDY AREA

The Kranzberg syncline is cored by the thick succession of the Kuiseb Formation. The syncline shows a steeply-dipping to overturned SE limb and a normal, shallowly dipping NW limb (Chapter 4). Different formations show considerable variations in thickness and stratigraphic succession on both limbs, and are therefore briefly discussed below. Due to poor exposure along the NW limb, stratigraphic columns for the Etusis Formation up to the Oberwasser Member and a subsequent correlation of these units within the study area are not provided. This study follows the recently revised lithostratigraphic subdivision of rocks of the sCZ suggested by Miller (2008).

3.1 ETUSIS FORMATION: NW LIMB

The Etusis Formation is only developed along the NW limb of the Kranzberg syncline. Here, it underlies much of the Rooiberg structure, a topographic high composed of heavily jointed, positively weathered, fine- to medium- grained arkosic metasediments and quartzites (Fig. 3.1). Weathered surfaces are reddish-pink in colour, while fresh surfaces are generally light grey. Cross bedding is often preserved and the formation hosts a number of dark-reddish-brown Pan-African pegmatites trending, on average, between 290 ° and 010 °.

3.2 RÖSSING FORMATION: NW LIMB

Within the sCZ, the Rössing Formation has not been recorded to extend this far to the E (e.g. Brandt, 1985), but a ca. 50 m thick section of what is here interpreted as Rössing Formation is exposed in sections along the Khan River, NW of Usakos.



Figure 3.1: (a) Exposures of well-bedded and jointed Etusis Formation in the Khan River bed, southern edge of the Rooiberg Mountains, looking NE; (b) Close-up of the typical medium-grained, reddish-pink weathered surface colour of the Etusis Formation.

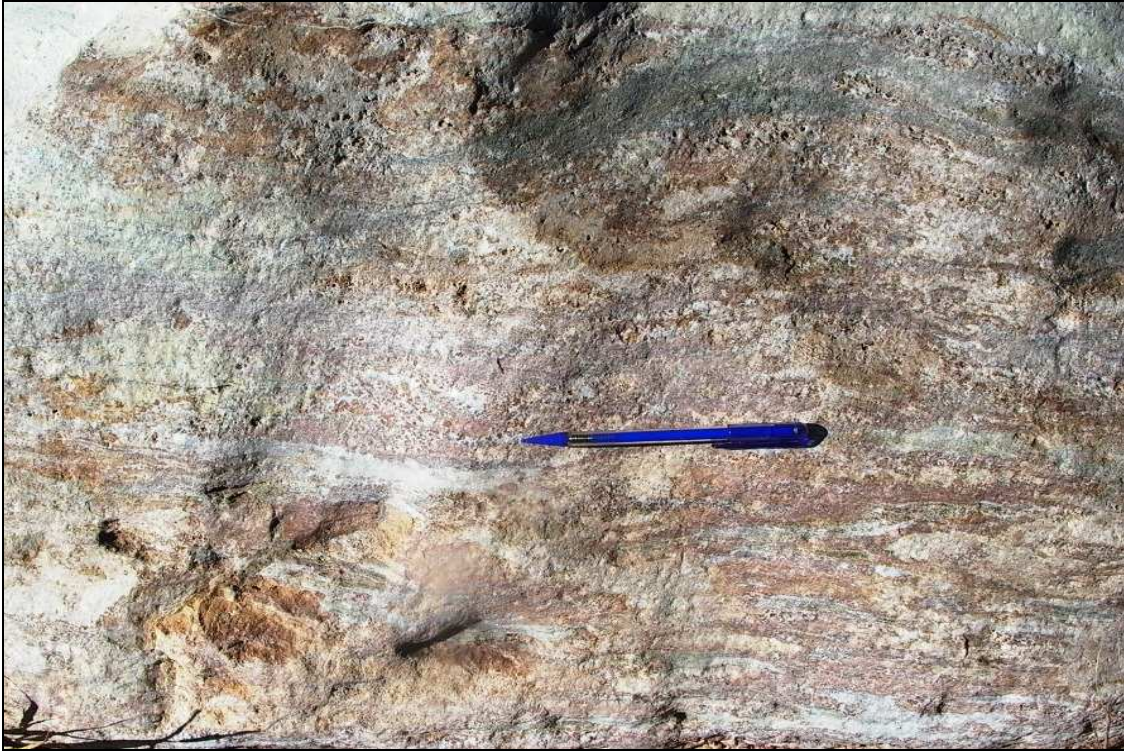


Figure 3.2: Rössing Formation along the NW limb with black, grey and green calc-silicate layers, and interlayered quartzites (pink).

The formation is composed of interbedded marbles and calc-silicate felses with interlayered pink quartzites. The dolomitic marbles are typically white with grey, green and black calc-silicate layers. Locally, tremolite-rich patches occur (Fig. 3.2).

3.3 CHUOS FORMATION: NW LIMB

Badenhorst (1992) regarded the Chuos Formation as a good marker horizon as it is developed from the NZ through to the sCZ. Along the NW limb of the syncline, rocks of the Chuos Formation are exposed in up to 15 m thick sections. The rocks are typically schistose containing a lithologically heterogeneous clast suite of granite, gneiss and quartzite, reaching up to 20 cm in length, as well as smaller, angular feldspar fragments. This diamictite formation has a fine-grained siliceous matrix, giving it a slight greenish hue due to the presence of calc-silicate minerals such as diopside and retrograde chlorite (Fig. 3.3a, b).

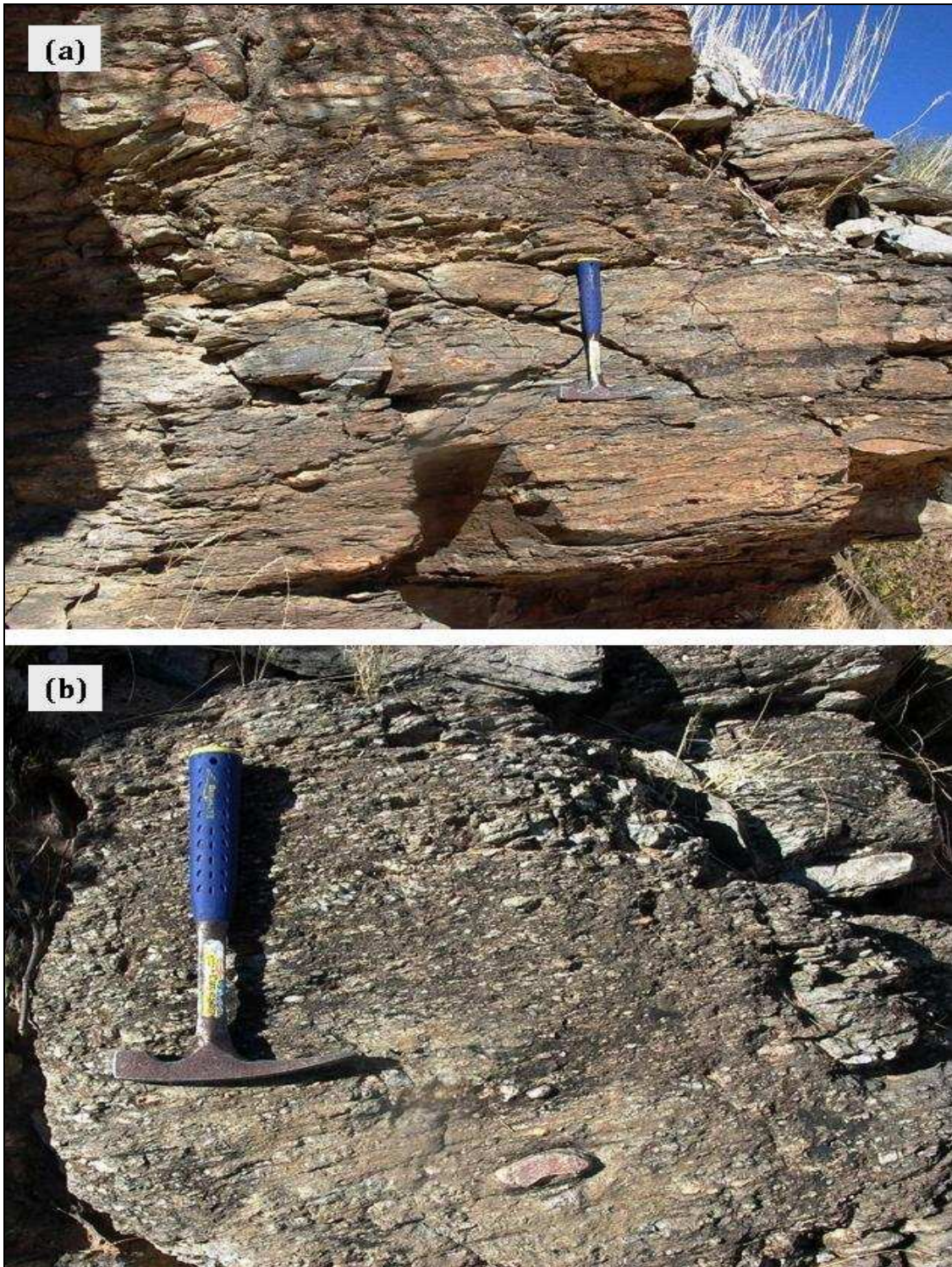


Figure 3.3: (a) Exposure of well-foliated and compositionally layered Chuos Formation along the banks of the Khan River; (b) Close-up of the Chuos Formation diamictite, showing cm-sized clasts, flattened in the plane of bedding-parallel foliation.

3.4 ARANDIS FORMATION

3.4.1 Spes Bona Member

On the SE limb of the syncline and in the adjoining Usakos Dome, the Spes Bona Member is the lowermost exposed unit of the Damara Supergroup. The Spes Bona Member shows lithological variations from quartz-biotite-cordierite schists at lower stratigraphic levels to banded metapsammities and calc-silicate felses higher in the formation. The lowermost portion is not exposed in the Usakos Dome, but the entire formation is estimated to have a minimum thickness of 600 m (Johnson, 2005; Kitt, 2008). The metapelitic schists are fine grained, contain no relict bedding, and mainly consist of quartz and biotite with variable amounts of feldspar, cordierite and hornblende. The metapsammities higher in the stratigraphy weather positively and commonly preserve cross-bedding on scales of a few centimetres. Fresh samples generally show a light-grey to greenish colour, but oxidize to a reddish-brown on outer surfaces.

Along the NW limb of the syncline, the formation is considerably thinner, ranging in thickness between 20 m and 100 m. Towards the northern end of the NW limb, the Spes Bona is developed as a 20 m wide package that is finely laminated and predominantly composed of quartz-biotite-cordierite schist. These units may correlate with the lowermost basal unit of the Spes Bona Formation. The formation here is highly strained, evidenced by the boudinage of more competent calc-silicate felses and the complete obliteration of primary sedimentary features by a pervasively developed bedding-parallel S1 foliation. Closer to Usakos town, up to 100 m wide sections of the Spes Bona Member are developed. Here, the formation predominantly comprises up to 2 m wide metapsammitic units, interbedded with medium-grained biotite schists and felses.

3.4.2 Okawayo Member

Along the SE limb of the syncline, the Okawayo Member is ca. 100 m wide and varies from light-grey marble in the lower stratigraphic levels to a more weathering-resistant light-blue marble in its central part. The upper stratigraphic levels are pale-grey in appearance and show abundant interbedding with rusty brown calc-silicate felses. Fresh surfaces show the marble to be completely recrystallized, obliterating any primary textures such as intraformational breccias and/or laminations that are present elsewhere in the area.

On the NW limb, only sporadic and poor exposures of a light-grey coloured marble with calc-silicate felses can be mapped, so that the stratigraphic position of these marbles must remain uncertain and these units cannot unequivocally be correlated with the Okawayo Member.

3.4.3 Oberwasser Member

The Oberwasser Member is only developed on the SE limb of the syncline where it stratigraphically overlies the Okawayo Member. It is composed of mainly feldspathic biotite- and quartz-biotite schists with lesser calc-silicate units. These one-to-five-metre thick calc-silicate horizons are mostly observed at the base of the Oberwasser Member. They are grey-green in colour on fresh surfaces and light-brown to reddish on weathered surfaces. The schists, composed primarily of quartz, biotite and feldspar ± cordierite, are light- to dark-grey in colour with greyish-brown weathered surfaces. Cordierite porphyroblasts may reach 1.5 cm in size, giving a spotted texture to the rock. Bedding is poorly preserved due to a pervasive, bedding-parallel (S1/S2) schistosity, but is occasionally evident in colour, texture and compositional differences.

Numerous garnet-bearing, two-mica leucogranite sheets related to the Klein Aukas granite to the immediate south preferentially intrude the Oberwasser Member. Johnson (2005) noted that granite sheets may constitute > 75 % of the rock volume within siliciclastic-rich host rocks, but quickly blunt and terminate once they reach

the overlying marble-rich Karibib Formation. The Oberwasser Member was not observed along the NW limb.

3.5 GHAUB FORMATION

Only the Daheim Member of the Ghaub Formation was observed along the SE limb of the syncline. The Daheim Member overlies the Oberwasser Member and consists of metamorphosed pillow lavas and pyroclastic rocks (Miller, 2008). In the study area, it is composed of intercalated amphibolite breccias set in a massive, coarsely recrystallized marble matrix. Its thickness ranges between 1 and 80 m. The amphibolites are dark- green to black in colour with occasional white plagioclase phenocrysts. Being weathering resistant, the Daheim Member forms a topographic high on the SE limb of the Kranzberg syncline along the Karibib marble contact. On a regional scale, the amphibolites are lens-like in shape, pinching out along strike to the NE and SW (Fig. 3.4).

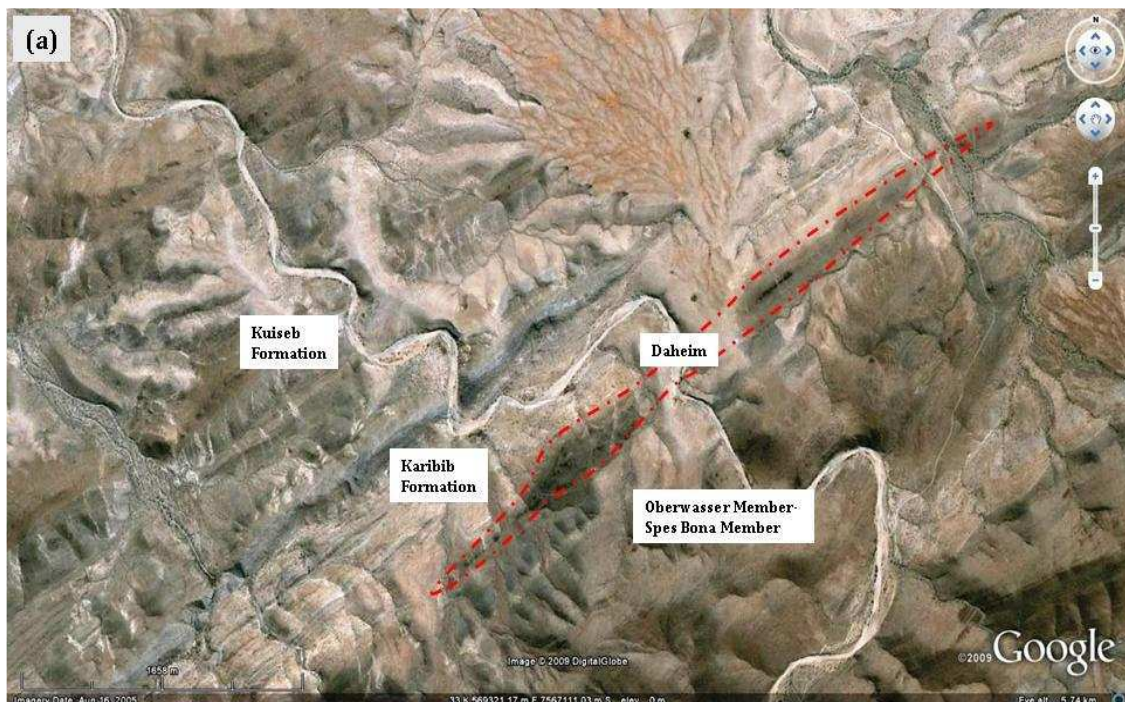


Figure 3.4: Aerial image from Google Earth showing the black amphibolites of the Daheim Member along the SE limb of the Kranzberg syncline (NW limb of Usakos dome). The red dashed line outlines the lens-like shape of the amphibolites. Badenhorst (1992) interpreted these as volcanic centres and feeders, laterally grading into thinner flows.

3.6 KARIBIB FORMATION

Along the synclines SE limb, the Karibib Formation forms a between 540 m and 880 m thick heterogeneous sequence of bluish-grey-white calcitic marbles, dark-grey graphitic marbles with intercalated calc-silicate felses (Fig. 3.5), cream-coloured to white dolomitic marble horizons and intraformational marble breccias. This thickness is variable and is unlikely to represent the true stratigraphic thickness of the unit due to intrafolial folding and bedding transposition (Chapter 4).

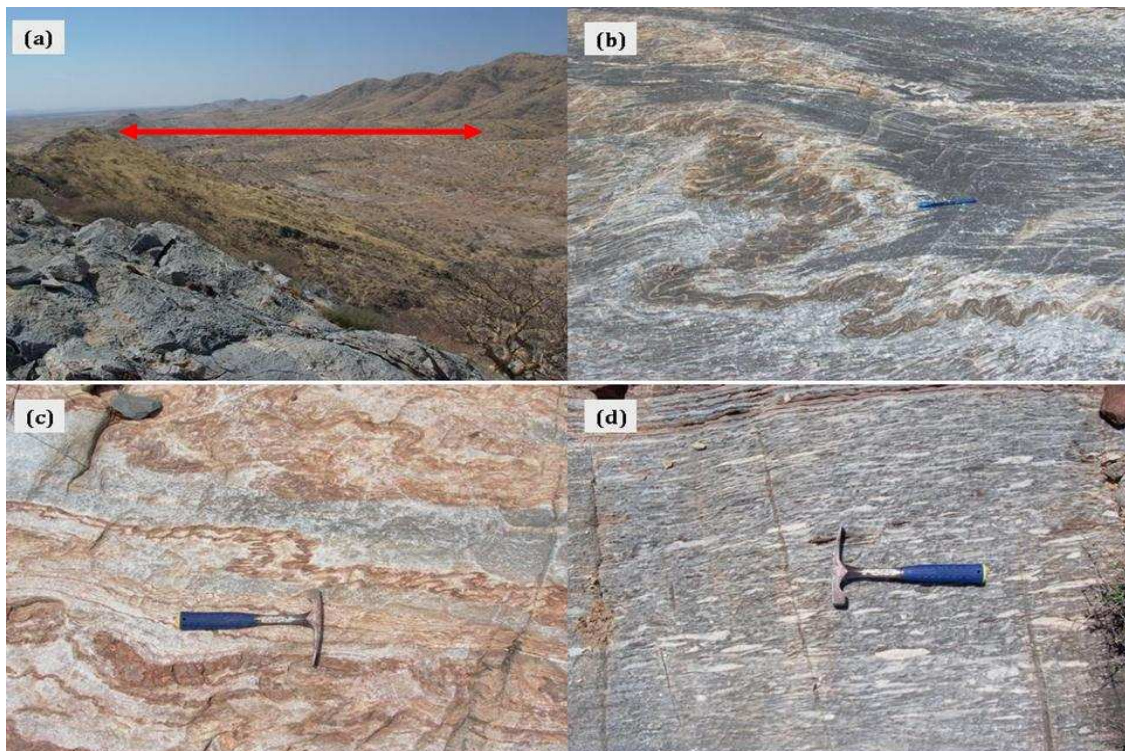


Figure 3.5: Karibib Formation along the SE limb: (a) Photo taken from Karibib graphitic marbles (base of formation) looking NE with thick units of the Spes Bona Member making up the NW limb of the Usakos dome in background and at the right (SW) side of photo. The Karibib Formation extends from the point at which this photo was taken to the base of the Usakos dome, some 800 m in width at this location (indicated by double arrowed red line); (b) Tightly folded interlayered marble, with pencil indicating S₂, and reddish-brown calc-silicate felses indicating bedding; (c) Cream coloured marbles with intercalated calc-silicate felses (red-brown); (d) Intraformational marble breccia with white and dark-grey marble fragments. Typically, breccia fragments are oriented at an angle to bedding, tracking the S₂ foliation (Chapter 4).

The calc-silicate bands are brownish-red on weathered surfaces and pale-green or light- to medium-grey on fresh surfaces and typically comprise quartz, K-feldspar,

calcite, diopside, hornblende, actinolite, titanite, biotite and minor garnet. The rusty brown calc-silicate bands range from a few millimetres to tens of centimetres in width and often contain varying quantities of sulphides. The cream-coloured and grey calcitic marbles are medium- to coarse-grained, commonly recrystallized, and moderately to highly strained. The sedimentary marble breccias form good marker horizons. The horizons are up to five metres thick and consist of white- to light-grey marble clasts embedded within a dark-grey marble matrix. The breccia clasts are commonly elongated, showing aspect ratios from 1:1 to 10:1.

Dolomitic marbles in the Karibib Formation are distinguished by their beige-coloured surfaces and weathering resistance, forming < 1 m and up to 10 m high ridges. They are medium- to coarse-grained and more competent than the calcitic and cream-coloured marbles, often displaying boudinage in higher strained parts of the Karibib Formation. Fresh surfaces are typically medium- to coarse-grained, white, and with a recrystallized sugary texture. The uppermost unit is an 80 m thick, dark, nearly black marble with intercalated, polymict marble breccias. This unit is clearly visible on aerial photographs, forming a very good marker horizon along the SE limb of the syncline. The dark-grey colour of the marble is attributed to microscopic grains of graphite within the matrix. The marble is medium- to coarsely recrystallized and intrafolial folds testify to the pervasively developed bedding transposition in this unit. The depositional environment of this unit was likely a deep water one, in which oxidation of organic material was inhibited (Badenhorst, 1992).

The Karibib Formation is much thinner along the NW limb compared to the SE limb, with an estimated maximum thickness of < ca. 150 m. Moreover, units within the Karibib Formation along this limb are highly variable and seem discontinuous along strike, rendering actual thickness determinations difficult. A tentative lithostratigraphy of the Karibib Formation on the NW limb is provided below.

The base of Karibib Formation is made up of mainly coarsely-recrystallized dolomitic marbles, ranging in width between 10 and 20 m. Unlike the SE limb, the dolomitic marbles do not appear to form topographic highs. Overlying this basal unit is a 15 to 70 m wide unit of calcitic and dolomitic marbles with intercalated calc-silicate bands. The calcitic marbles generally form ≤ 25 cm wide bands that are light-blue to white in colour on weathered surfaces. Fresh surfaces typically display a recrystallized, medium- to coarse-grained sugary texture. Oval- to rectangular-shaped boudins of more competent dolomitic marbles and calc-silicates are common in this unit. Higher up in the stratigraphy, the calc-silicate felses progressively thicken, reaching up to 0.5 m in width, with occasional interbedded calcitic and dolomitic marbles no wider than a few centimetres. The uppermost dark grey-black unit of the Karibib Formation is only intermittently observed along this limb. It ranges from being absent near Usakos town to 30 m in thickness two kilometres further NE. The unit is very often transposed and recrystallized with a light-blue to grey colour and sugary texture on fresh surfaces. The overall thickness of the Karibib Formation on the NW limb is highly variable and ranges from ca. 25 m to 130 m.

3.7 KUISEB FORMATION

The Kuiseb Formation is the youngest formation of the Damara Supergroup and typically cores F2 (F3 after Miller, 1983) synclines in the CZ of the Damara belt. Rocks of the Kuiseb Formation also occupy the core of the Kranzberg syncline and host the Usakos pegmatite field that is, in places, mined for gem-quality tourmaline, beryl, mica and quartz crystals. In the study area, the Kuiseb Formation can be subdivided, from bottom to top, into four lithologically distinct subunits, henceforth termed Units 1 to 4 (Fig. 3.6). The overall thickness of the Kuiseb Formation in the Kranzberg syncline is approximately 750-800 m, although tight- to isoclinal folding and localized bedding transposition complicate a more accurate thickness estimation.

Stratigraphy Kuseib Formation

- Top is not exposed
- Coarsening upwards sequence
- Lowermost units have similarities to Onguati 20km away

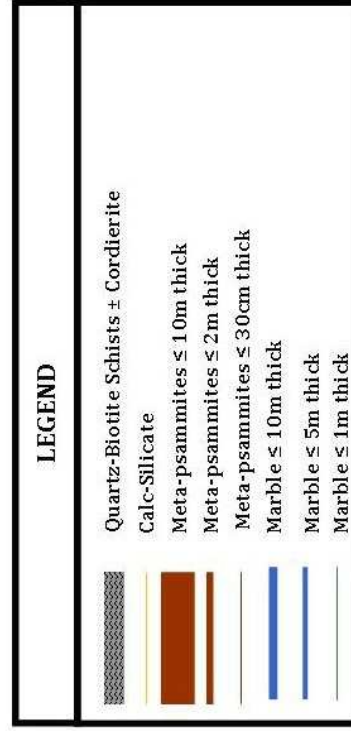
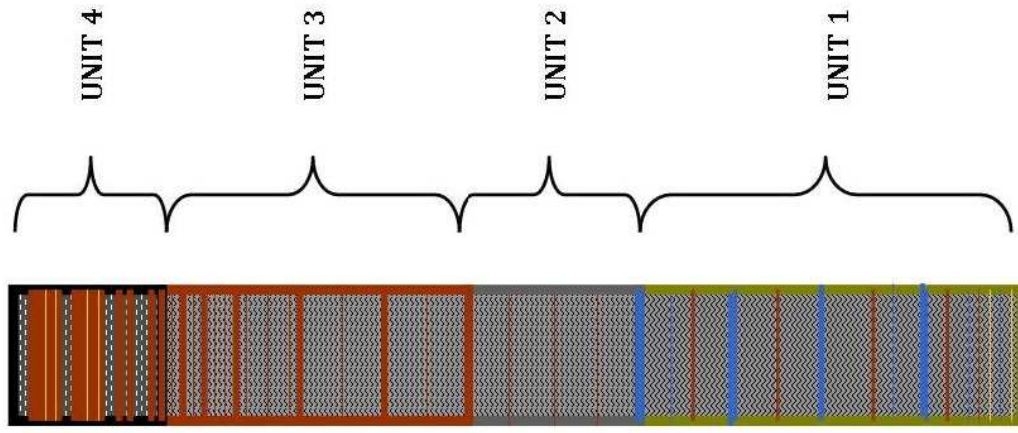
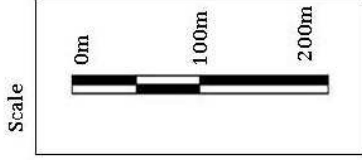


Figure 3.6: Detailed lithostratigraphic column of the Kuseib Formation in the study area.

As described below, the sequence shows an overall coarsening upwards trend, from basal interlayered marble and schist horizons, via metapelitic schists and interlayered metapsammites to thickly-bedded arkosic metapsammites and only minor metapelites.

Unit 1:

Unit 1 has a thickness of ca. 300 m. The contact against the stratigraphically lower Karibib Formation is drawn where the first metapelitic biotite- and biotite-cordierite schists occur in the succession. The lowermost ca. 60 m of Unit 1 consist of intercalated light blue-grey marbles, \leq one metre wide brownish-purple calc-silicate felses, minor metapsammitic and metapelitic units (Fig. 3.7). The calc-silicate felses are the first to disappear from this unit as metapelitic quartz-biotite schists become more abundant towards the top of Unit 1. The schists often contain up to three centimetre large cordierite \pm sillimanite porphyroblasts.



Figure 3.7: Vertical cliff section of marbles (light- to medium grey, right-hand side of the photo), \leq 1 m wide calc-silicate felses (brown) and minor metapsammitic and schistose metapelitic units (both dark grey) within Unit 1 of the Kuiseb Formation (coordinates UTM WGS 84 566952E, 7567560S), looking SW. Younging direction in photo is from left to right.

This basal horizon has a sharp contact with the overlying, positively weathering, up to two metre thick metapsammitic units, light blue-grey 0.2 m to 10 m wide marble horizons, and medium- to coarse-grained metapelitic schists that form the remainder of Unit 1. Unit 1 may correspond to the Onguati Member identified by Badenhorst (1992) as a transitional unit between the marble-dominated Karibib Formation and the overlying schist-dominated Kuiseb Formation as the uppermost formation of the Damara Supergroup.

Unit 2:

Unit 2 is a ca. 150 m thick unit of predominantly fine- to coarse-grained quartz-biotite-muscovite schists with variable amounts of cordierite porphyroblasts that may, in places, reach 2.5 cm in diameter (Fig. 3.8a,b). The schists are dark-grey to reddish-black in colour on weathered surfaces. Bedding, often preserved by variations in cordierite content and occasional laminated turbiditic units, ranges from a few millimetres to tens of metres in thickness, although primary features are often overprinted by a pervasive (S₂) foliation. Minor amounts of quartz-biotite felses and intercalated < 1 m wide metapsammitic units are developed throughout Unit 2.

Unit 3:

The predominantly metapelitic succession of Unit 2 is overlain by the ca. 220 -250 m thick Unit 3. Unit 3 is dominated by up to two metre thick, positively weathering metapsammites that often form prominent ridges. The metapsammites are fine- to medium- grained, greyish in colour on fresh surfaces and often preserve primary bedding features such as ripple marks and cross-bedding. The deposition and introduction of these psammitic units indicates the beginning of a coarsening up sequence in which more terrigenous sediments were deposited. A strong colour contrast to the metapelites aids in locating fold structures (discussed in Chapter 4) within the unit.

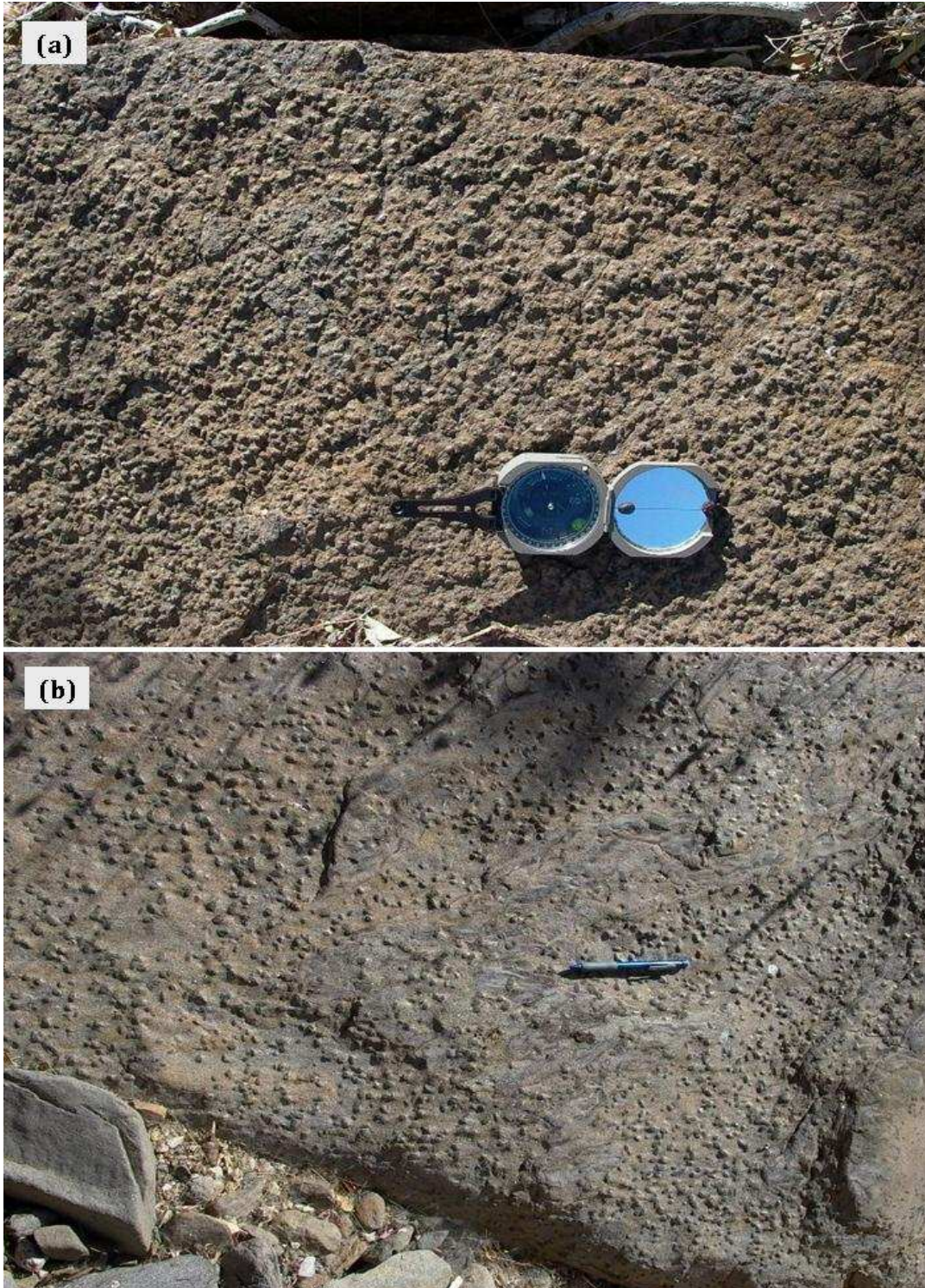


Figure 3.8: Unit 2 of the Kuiseb Formation: (a) Example of coarse-grained, positively weathering cordierite porphyroblasts that are common in metapelites of Unit 2; (b) Tightly-folded bedding in cordierite-rich biotite-quartz schists (plan view) in Unit 2. The pencil is parallel to the axial surface of the fold.

Unit 4:

Unit 4 is the uppermost stratigraphic unit of the Kuiseb Formation in the Kranzberg syncline. It is composed of up to 10 m thick and massive metapsammitic units (Fig. 3.9a). The metapsammites are intercalated with metapelitic biotite schists, containing up to two centimetre large cordierite porphyroblasts, and thin calc-silicate felses.



Figure 3.9: Unit 4 of the Kuiseb Formation: (a) Example of a thick sequence of 1 - 5 m wide metapsammitic horizons that form a topographic high within the study area; (b) Bedding in Unit 4 is often characterized by Bouma-type sequences, showing coarse and massively developed metapsammites at the base of each unit, grading into finely laminated schists towards the top.

The metapsammites form prominent marker horizons and topographic highs due to their resistance to weathering. They are nearly arkosic in composition with 65-75% quartz, 20-30% feldspar and 5 % mica and, in places, contain garnet porphyroblasts. They are dark reddish-brown in colour on weathered surfaces, and light grey on freshly exposed faces. Low fabric intensities in the metapsammites commonly preserve primary sedimentary features such as cross-bedding and laminations typical of turbiditic depositional environments. Bouma-type sequences showing

gradational bedding from metapsammities through to pelitic tops are common (Fig. 3.9b). The uppermost contact of the Kuiseb has been eroded, and therefore a complete stratigraphic section and total thickness of the formation could not be established.

Chapter 4 - STRUCTURAL GEOLOGY

4.1 INTRODUCTION

For easier analysis and understanding, the NE-trending syncline has been divided into three structural domains (Fig. 4.1);

Domain 1: a normal, shallow SE-dipping NW limb,

Domain 2: an overturned, steeply SE-dipping SE limb, and

Domain 3: a first-order hinge zone in the SW parts of the study area.

Terminology and conventions used are described as the following;

- D: deformation event
- F: folding of planar and linear fabrics
- L: linear penetrative fabrics
- S: planar penetrative fabrics

Lower numerical values indicate earlier formed structural elements identified and described in the study area. A summary is provided in Table 4.1.

Recent studies around the Karibib and Usakos domes have recognized two main deformation events, D1 and D2 (Kisters et. al., 2004; Johnson, 2005). Johnson (2005) further proposed a later D2b event involving a late-stage, orogen-parallel, SW-directed extrusion of rocks around the Usakos dome. The earlier D1 event in the study area is evident by a bedding subparallel foliation (S1). The second deformation phase, D2 (D3, after Miller, 1983, 2008) involves the formation of kilometre-scale folds and associated planar and linear fabrics that determine the NE-trending structural grain of the Damara belt as a whole.

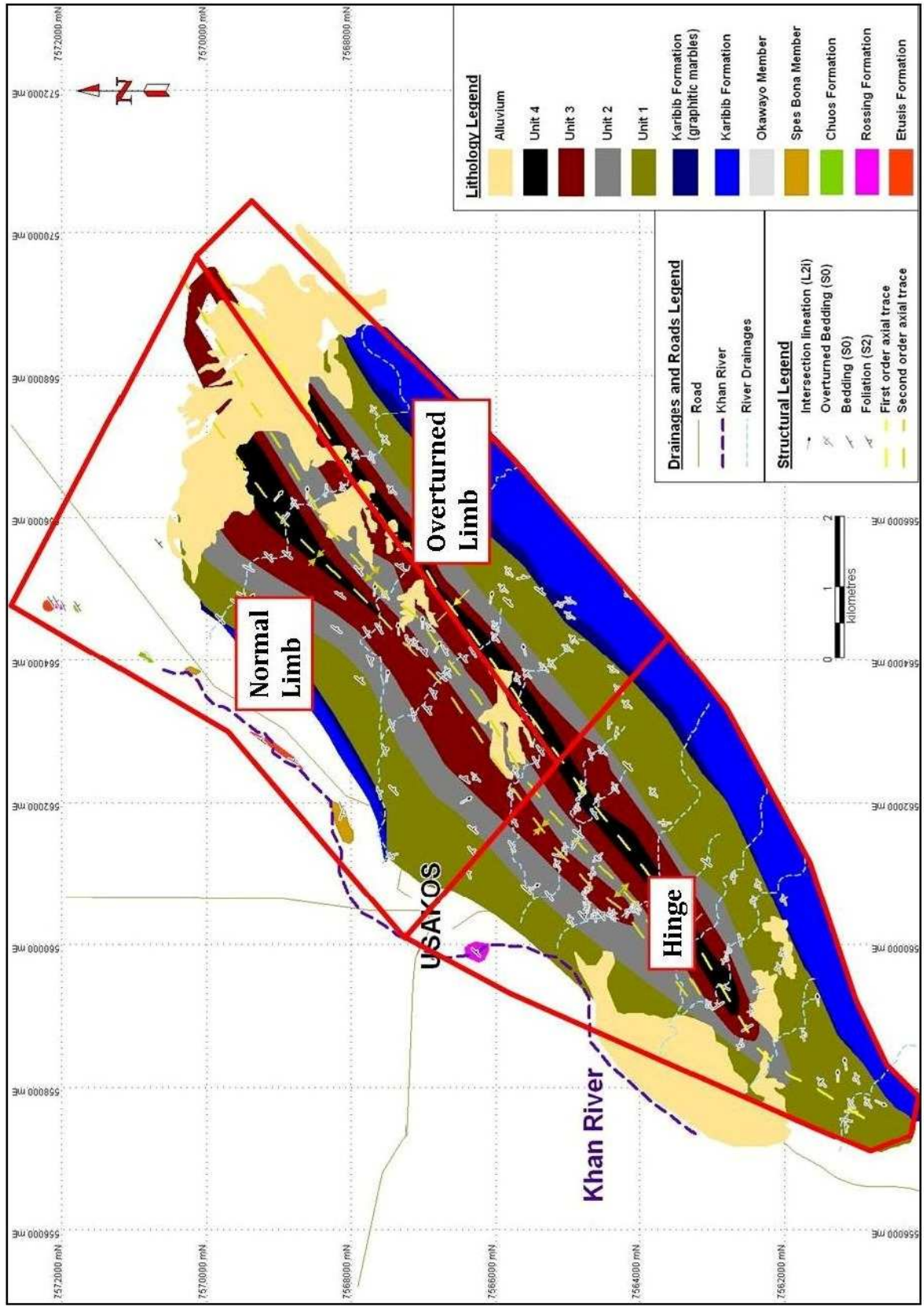


Figure 4.1: Geological map outlining the boundaries of structural domains (hashed red lines).

Table 4.1: Structural elements in the study area

DEFORMATION PHASE	STRAIN REGIME	FABRIC ELEMENT	FABRICS
			Field Expression, Orientation and Occurrence
Primary		S0	Primary bedding. Primary compositional layering and cross-bedding with variable orientations.
D1	Low Angle Shearing	S1	Subparallel to bedding-parallel schistosity. Most commonly observed within fold hinges cored by metapelitic units.
D2	Top to the NW thrusting and associated NW verging folds	S2	Moderate -to steep SE-dipping, NE-striking axial-planar to transecting foliation observed in metapelitic units.
		F2a	First-order syncline; kilometre scale, NW verging, NE trending Kranzberg syncline
		F2b	Second- and lower-order folds, hundreds of metres to centimetres in wavelength
		Late F2	Late fold structures ie asymmetrical folding of calc-silicates in marbles, later strike-parallel shortening of e.g. boudin trains
		L2m	Mineral and mineral stretching lineation, moderate- to steep, variably plunging, stretched cordierite porphyroblasts, sillimanite and elongated quartz and biotite.
		L2i	Moderate to steep, E - S plunging intersection lineation between S0/S1 and S2
		L2f	Moderate to steep, E and S plunging fold-hinge crenulations on lower-order parasitic folds.

This deformation was in response to the main collisional event between the Kalahari and Congo Cratons at approx. 550-510 Ma (Miller, 2008). F2 folding is commonly associated with a well-developed, moderate- to steeply-dipping, NE-SW-trending schistosity (S2) and NE-trending, composite lineations (L2, Table 4.1).

4.1.1 Bedding (S0)

Lithological variations between formations of the Damara Supergroup are easily identified, even on aerial photographs and satellite images. For example, contacts between the compositionally distinct Okawayo and Oberwasser Members as well as the Karibib Formation can be followed for kilometres along the NE strike of the units, particularly on the steep SE limb of the syncline. In the central hinge and normal NW limb, laterally continuous marker horizons are more difficult to identify, but bedding is well preserved on a scale of centimetres to even tens of metres in the metaturbiditic sequence. Structural mapping in the rather monotonous Kuiseb Formation has traditionally been considered to be problematic, but the identification of the four main lithounits described in Chapter 3 allows for the definition of second- and third-order folds that delineate the underlying structure of the first-order Kranzberg syncline. The preservation of primary structures varies

due to fabric and strain intensities in different rock types and location with respect to the first-order syncline. For example, primary structures such as ripple marks and cross-bedding are particularly well preserved in metapsammities and calc-silicate felses of e.g. the Oberwasser Member on the steep SE limb or the Kuiseb Formation in the core of the Kranzberg syncline (Fig. 4.2.a-d). The marble-dominated units of the Okawayo Member and Karibib Formation also preserve compositional banding, intraformational breccias or intercalated calc-silicate felses. However, marble units are, in many places, strongly recrystallized and bedding transposition is common. Strain in the Kuiseb Formation is often localized into the marble and metapelitic units, highlighting competence contrasts between lithologies and rheological heterogeneities.

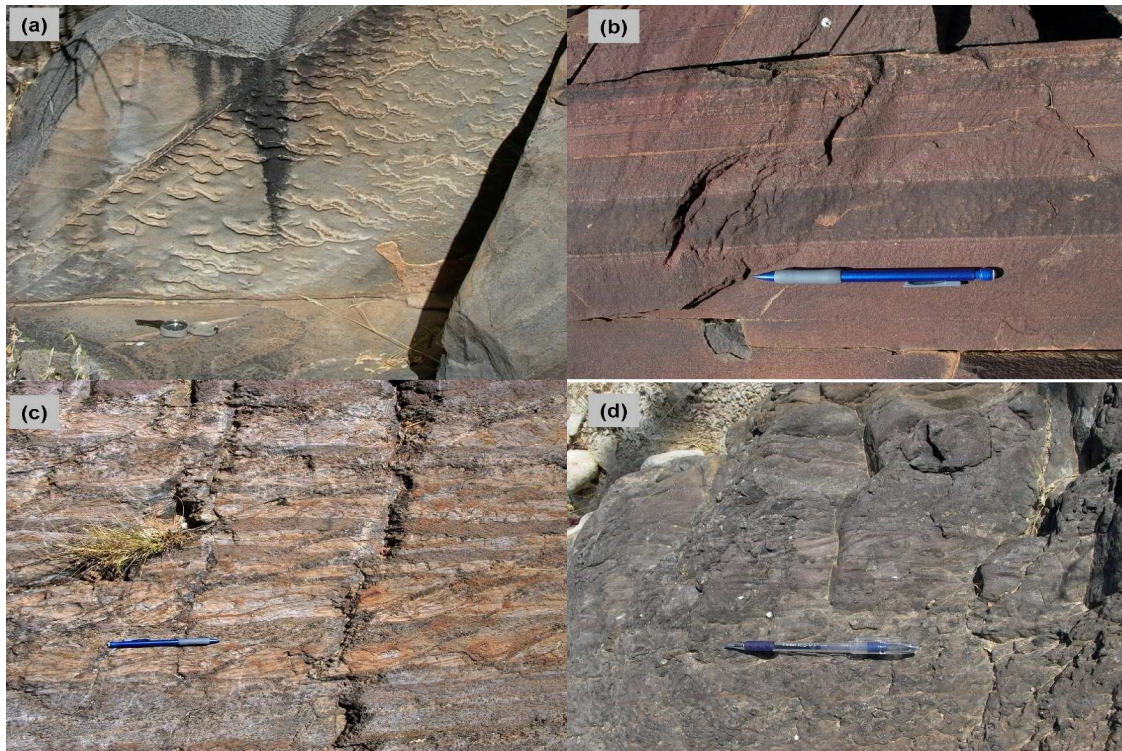


Figure 4.2: (a) Ripple marks in metapsammitic rocks of the Kuiseb Formation; view is towards the base of a bedding plane; (b) bedding in a calc-silicate felse, consisting of alternating hornblende-rich layers (dark) and diopside-plagioclase-rich layers (chocolate-brownish weathering); (c) cross-bedding in sandy units (beige-brown) alternating with planar laminations in more pelitic horizons (biotite-quartz-cordierite schists, medium grey) of the Kuiseb Formation. Younging direction is towards the top of the photo; (d) cross-bedding in grey metapelitic units of the Kuiseb Formation; younging direction is towards the bottom of the photo.

4.1.2 Secondary Tectonic Fabrics: S1

An S1 foliation is commonly defined by the bedding-parallel, preferred orientation of biotite and muscovite in metapelitic units of the Kuiseb Formation and the Oberwasser Member. Given that S1 and S2 (see below) are commonly parallel or subparallel on the limbs of F2 folds, the two foliations may only be discernable in the hinges of F2 folds where they are at high angles to each other. Marble units may contain the S1 foliation, but the lack of e.g. mica and the pervasive recrystallization of marbles render an identification of the early foliation difficult. Competent units such as calc-silicate felses or metapsammities are commonly devoid of the S1 foliation.

4.1.3 Tectonic Fabrics: S2

Particularly the metapelitic units of the Oberwasser Member and Kuiseb Formation commonly contain a penetrative S2 foliation. S2 is defined by the preferred orientation of mica, particularly biotite, and, in many places, millimetre- to centimetre-spaced pressure solution seams (Fig. 4.3 a-b). In marble breccias, S2 is defined by flattened clasts. The long axes of clasts are commonly at an angle to bedding, and track the S2 foliation. The S2 foliation shows consistent moderate- to steep (35-60°) SE dips throughout the folded sequence of the Kranzberg syncline. In mesoscale folds, S2 can be seen to have an axial planar orientation with respect to F2 folds. A fanning and refraction of the S2 foliation is observed in compositionally heterogeneous successions, e.g. interlayered calc-silicate felses and biotite-cordierite schists (Fig. 4.3 c-d). F2 fold hinges represent locations where S2 is most easily distinguished from S0/S1 fabrics (e.g. Fig. 4.3c-d), due to the high angles they enclose in the hinges. Although S2 is axial planar to folds on an outcrop scale, the regional compilation of orientation data indicates that S2 is, in fact, a transecting cleavage. In this orientation, S2 shows a consistent anticlockwise sense of rotation in its angle with respect to an ideally axial planar cleavage to the first- and/or second-order F2 folds (see Chapter 4.7).

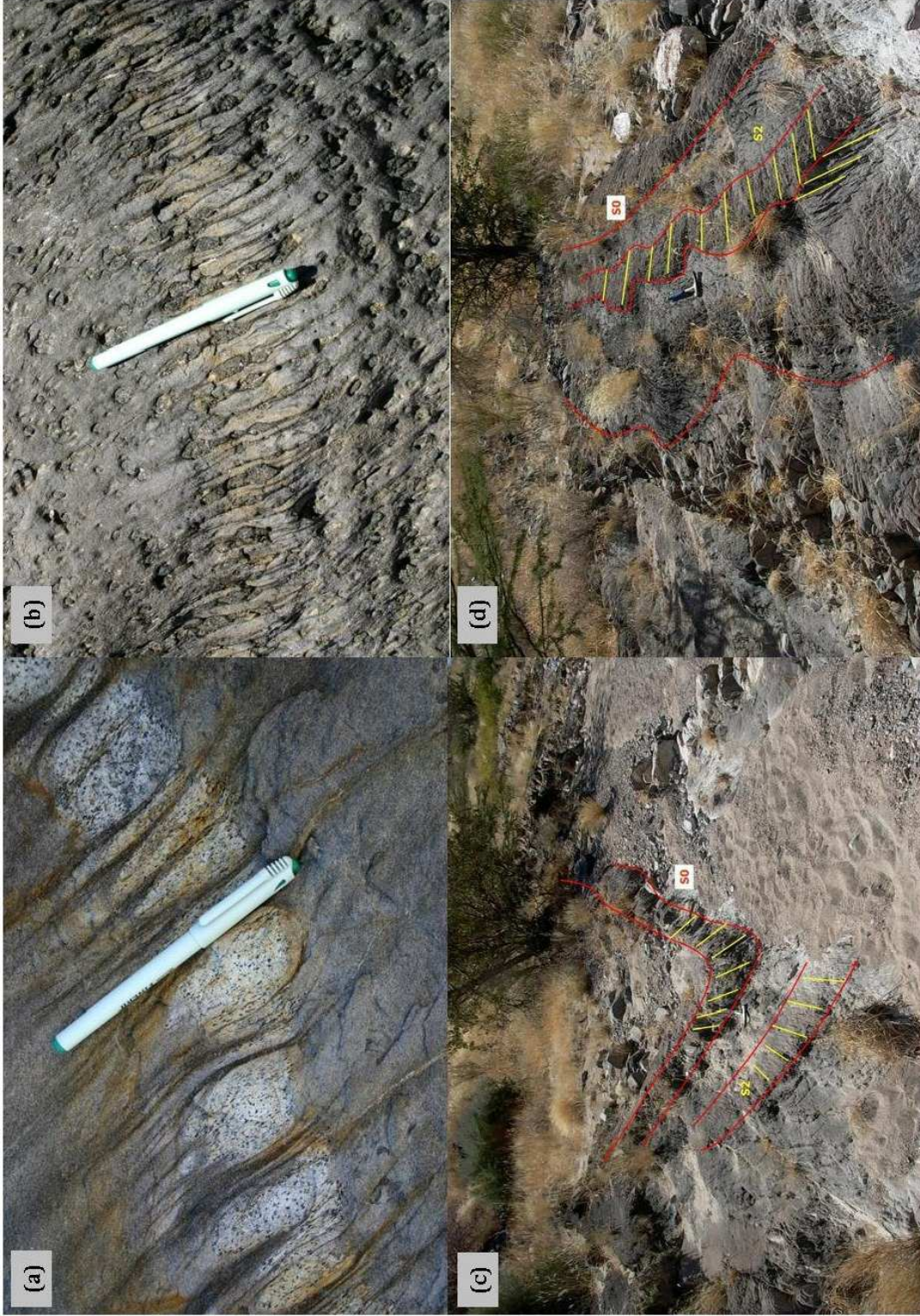


Figure 4.3: S2 developed as pressure solution seams in F2 fold hinge zones in the Kuiseb Formation. Pressure solution is evidenced by the darker, commonly biotite-rich foliation domains that separate more quartz-feldspathic domains or lithons. (a) Alternating metapsammite (white) and metapelite layers (grey) with strong pressure solution seams evident in metapsammite layer; (b) Pressure solution seams and gentle refraction of the seams; porphyroblasts are cordierite; (c) and (d) (Coordinates UTM 564802E; 7567668S WGS 84) S0 is perpendicular (red lines) to S2 (yellow lines) representing a fold hinge. Note also the strong cleavage refraction displayed by S2 in the different units; here, alternating metapelites and more psammitic layers.

4.1.4 Linear Fabrics (L2)

The majority of lineations in the study area are associated with the second deformational event, and therefore are labelled as L2. Three different types of lineations occur in the study area. Mineral and mineral stretching lineations (L2m) are defined by the preferred orientation of sillimanite and/or cordierite porphyroblasts (Fig. 4.4) or the stretching and/or rodding of particularly quartz-feldspar aggregates and quartz or the elongation of e.g. cordierite porphyroblasts.

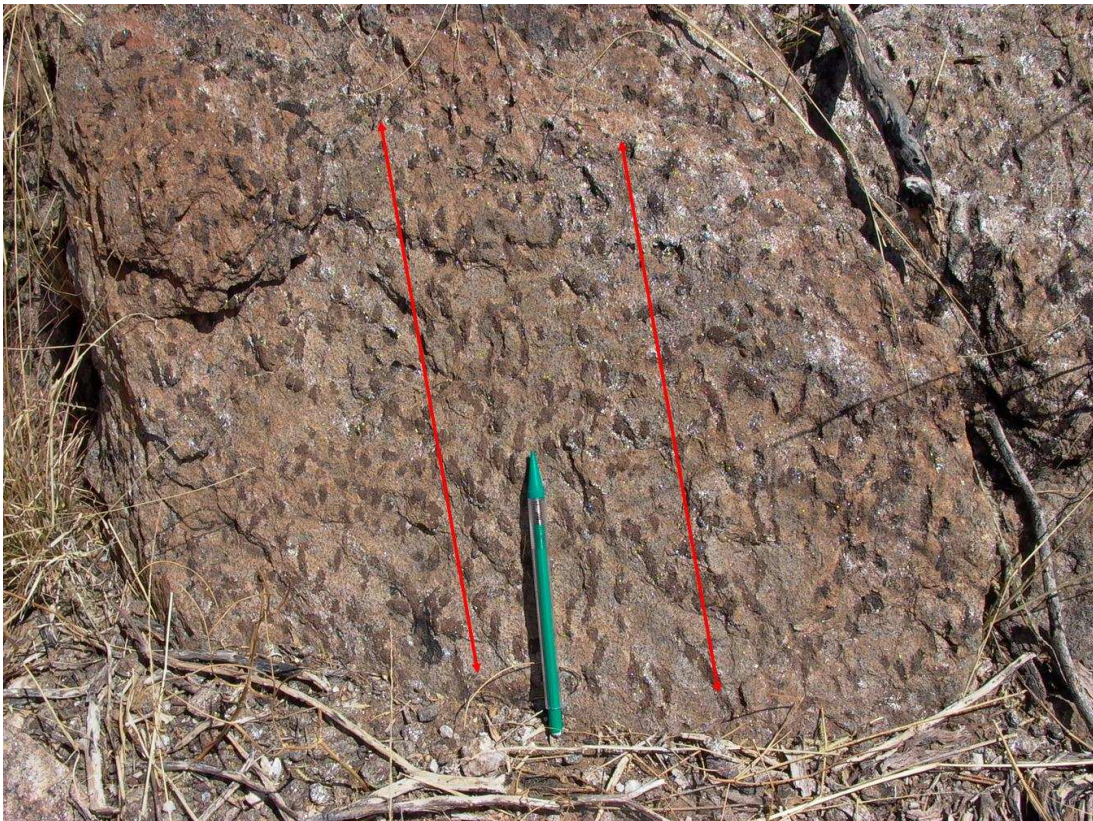


Figure 4.4: Mineral lineation defined by centimetre-sized cordierite (dark porphyroblasts on biotite-rich foliation plane (S2) showing a preferred orientation, here trending from bottom right to top left of photo and at slight angles to the pencil (indicated with red lines).

Quartz rodding lineations are also developed along the contacts between pegmatites and wall rocks (Chapter 5.1.3). Intersection lineations (L2i) are defined by the intersection of bedding (S0) and the S2 foliation (Fig. 4.5). These lineations are best developed on the S0 planes of more competent psammitic units, and form the majority of L2 lineations measured in the study area. Intersection lineations plunge to the E-ENE, subparallel to second- and lower-order fold (F2) plunges.



Figure 4.5: Example of intersection lineations observed on a bedding plane (S0) of a metapsammitic unit trending from top left to bottom right of photo.

The intersection lineations have been used to determine the plunge of F2 folds, although the lineations are not, strictly speaking, δ -lineations, i.e. the intersection lineation between folded bedding and a truly axial planar foliation (S2). Crenulation lineations (L2f) are small-scale (mm- to cm- wavelength) folds, refolding bedding laminations or the S1 foliation, and are typically observed in lower-order fold (F2) hinges with moderate to steep E- to ENE- plunges. In most parts of the Kranzberg syncline, mineral, mineral stretching, intersection and crenulation lineations are subparallel to each other. Deviations from the commonly E plunges are largely confined to a NE-trending corridor along the NW margin of the study area between Usakos town and the river bed of the Khan River (see below).

4.1.5 F2 Folds

Folding is observed on all scales and is likely the most prominent mesoscale manifestation of deformation in the Kranzberg syncline. The study area is characterized by NW-verging, NE-trending, E-plunging, non-cylindrical folds that

range from millimetres to kilometres in wavelength and amplitude. Centimetre- to metre- scale folds are best observed in the marbles and intercalated calc-silicate bands of the Karibib Formation and in metapsammitic and metapelitic horizons of the Kuiseb Formation. Large-scale second- and third-order folding is delineated by the outcrop pattern of regionally traceable lithounits in the Kuiseb Formation, whereas fourth-order and smaller-scale folds are most readily observed in outcrop. The folds show commonly similar geometries with thickened fold hinges and thinned limbs. Early, intrafolial F1 folds that are regionally described (e.g. Jacob, 1974; Miller, 1983; Kisters et al., 2004) cannot be identified with certainty given the D2 fabric intensities and, in places, D2 bedding transposition.

4.1.6 Other fabric elements

There are two main fold types and orientations that cannot directly be related to the regionally-developed NE-trending F2 folds. Around Usakos (centred at UTM 561635; 7566805 WGS 84), a number of upright to nearly recumbent, close- to isoclinal folds with N-S trends and plunges are developed from the Karibib Formation and into the Spes Bona Member. This corridor of N-trending folds coincides with the rotation of mineral lineations (Chapter 4.1.4), an aspect that is further discussed in Chapter 4.6.2. Along the SE limb of the Kranzberg syncline, the Karibib Formation and Unit 1 of the Kuiseb Formation often contain asymmetrically folded marbles and calc-silicate felses (Chapter 4.6.3). This fold generation seems rather to be associated with a later and more localized folding event. Moreover, along the NW limb of the syncline, calc-silicate felses in marbles of the Karibib Formation seem to have undergone an early phase of layer-parallel stretch and boudinage, followed by a later phase of layer-parallel shortening. These folds and the shortening of boudin trains have also been described by Johnson (2005) from the interior and margins of the immediately adjacent Usakos Dome, which she termed the late F2 event. As the Kranzberg syncline shares this limb with the Usakos dome, this fold phase will be referred to as late F2, following Johnson (op cit.). A N- to NE-trending, locally developed fracture cleavage was also evident in the study area. This cleavage is distinct from S1 and S2 and is mainly found adjacent (within

ca. 10-15 m) to pegmatite dykes that cross-cut the lithological layering and S2 foliation. Hence, the foliation is not considered to be of regional significance, but rather to the emplacement of pegmatite dykes and will be discussed in conjunction with aspects of pegmatite emplacement in Chapter 5.

4.2 MAPPING APPROACH

Bedding/cleavage relationships, younging relationships deduced from primary sedimentary features and the overall lithological subdivision into Units 1-4 outlined in Chapter 3 were used to delineate first- and second- order fold structures. Bedding (S0) and cleavage (S2) angular relationships proved to be very important during regional mapping (Fig. 4.6). In areas where S0 is steeper than S2, the strata is overturned. In contrast, where S0 is shallower than S2, the strata is younging upwards, pointing to the presence of a normal limb in a fold. Larger angles (up to 90°) between S0 and S2 indicate the proximity of a fold hinge, whereas S0 and S2 enclose smaller angles on the limbs of folds, where they may, in fact, be parallel to each other. This relationship always assumes that S2 is axial planar to F2 folds. As mentioned above and illustrated below, this is not exactly the case as S2 is, on a regional scale, a transecting cleavage. However, the close association between the S2 foliation and F2 folds (1) suggest their contemporaneous formation, and (2) angular relationships between S2 and folded S0 surfaces in individual outcrops only deviated by a few degrees from ideal axial planar relationships.

Primary bedding features, such as graded bedding, load casts or the presence of rip-up clasts in the turbidite sequence were used to determine younging directions in areas of lower fabric intensity. Subtle compositional layering in e.g. metapelitic units is also evidenced by variations in e.g. the abundance of cordierite porphyroblasts, also aiding the determination of S0.

(a) Relationship between S0 and S2

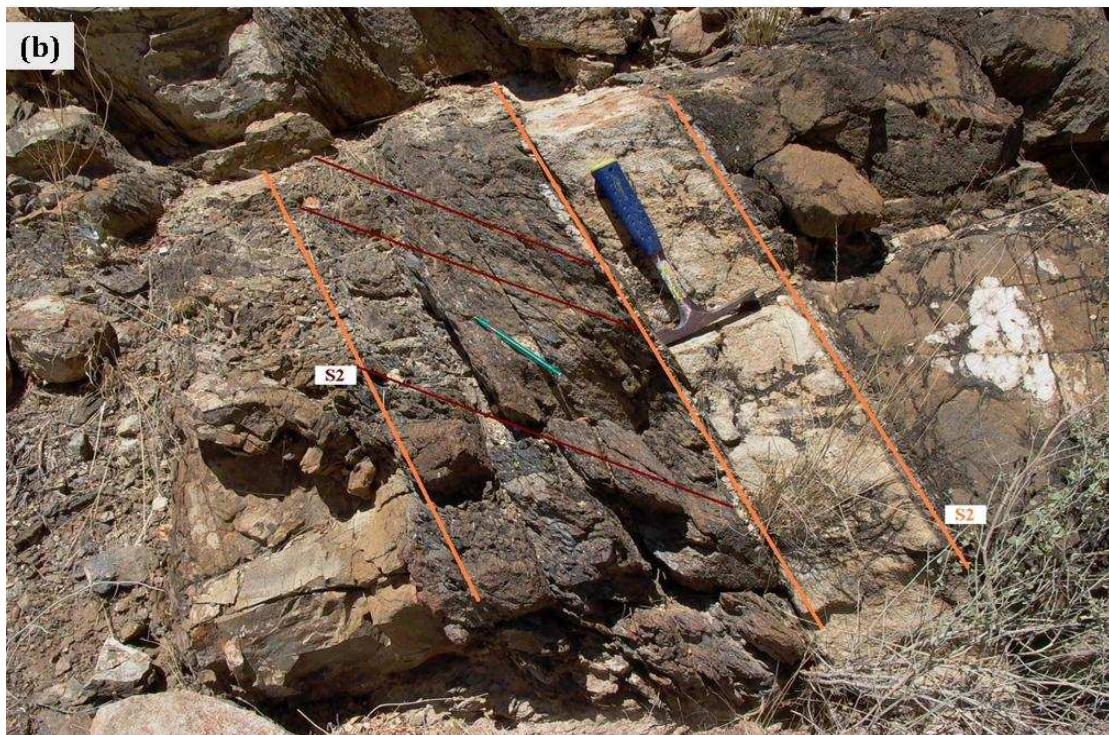
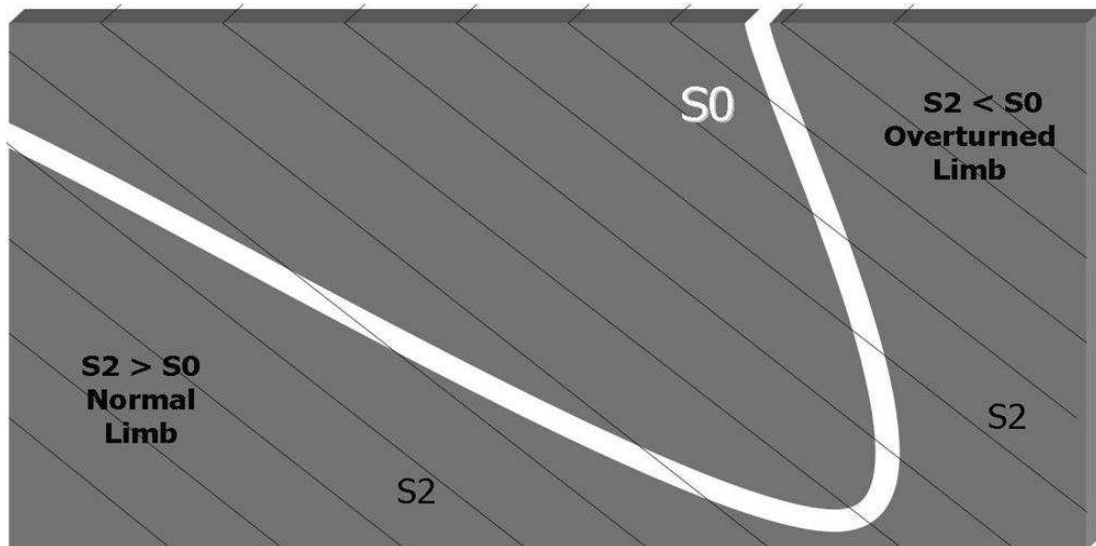


Figure 4.6: (a) Relationship between S0 and S2; (b) S2 outlined in red and S0 outlined in orange. S0 dips steeper than S2 and therefore represents strata on an overturned limb of an F2 fold.

The location of the first-, and second- order folds was determined through the correlation of the main lithological subdivisions (ie. Units 1-4). Third- and lower-order fold closures are best identified within the river drainages that cross-cut the Kranzberg syncline from E-W. These river beds were subsequently used to establish the detailed structural geology that was then followed and extrapolated between individual drainages to achieve complete coverage (Figure 4.7).

4.3 FIRST- AND SECOND- ORDER STRUCTURES.

Moderate SE dips on the normal NW limb and steep SE dips on the overturned SE limb result in the tight- to near- isoclinal geometry and overall NW vergence of the F2 Kranzberg syncline (Fig. 4.7). The half wavelength of the syncline is between three and five kilometres. Second-order anticlines and synclines also show a NW vergence and have wavelengths of between 250 and 650 m with tight- to isoclinal interlimb angles. The first-order hinge closes in the SW part of the study area and is evident by (1) the rotation of bedding (S0) from the regional NE trends to E-W trends over a few hundred metres; (2) the apparent thickening of units; and (3) the stratigraphic younging of units towards the NE, i.e. older Units (Units 1 and 2) are exposed in the SW of the study area, grading into Units 3 and 4 towards the NE. Two vertical cross-sections across the Kranzberg syncline are provided in figure 4.8.

4.4 THIRD- ORDER AND OUTCROP-SCALE STRUCTURES

The regional geological map and cross-sections are based on detailed outcrop analysis and the correlation of marker units or prominent structures between river drainages. Third- and higher-order folds have wavelengths of ≥ 150 -250 m. These can only be shown in part, or on the geological map and regional sections (Fig. 4.9) and, as such, fourth- and lower-order structures (≤ 250 m) provide the best scales for detailed illustrations.

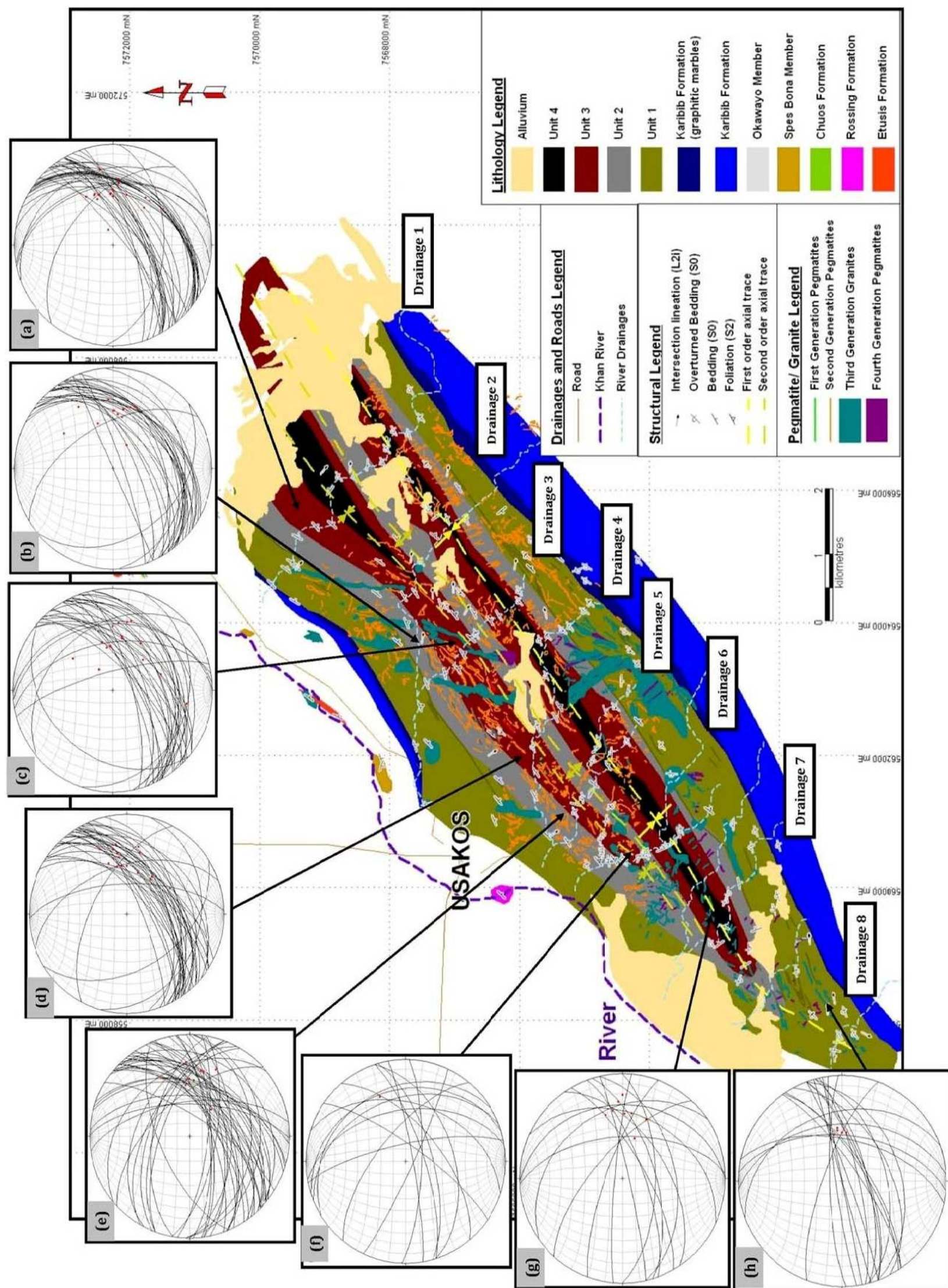


Figure 4.7: Geological map of the Kranzberg syncline showing the location of the main river drainages that were followed for detailed structural mapping, orientation diagrams for bedding (great circles) and intersection lineations (Li): (a) Drainage 1 S0 (n=38) and Li (n=18); (b) Drainage 2 S0 (n=28) and Li (n=12); (c) Drainage 3 S0 (n=32) and Li (n=15); (d) Drainage 4 S0 (n=37) and Li (n=16); (e) Drainage 5 S0 (n=58) and Li (n=9); (f) Drainage 6 S0 (n=15) and Li (n=2); (g) Drainage 7 S0 (n=14) and Li (n=14); (g) Drainage 8 S0 (n=20) and Li (n=5).

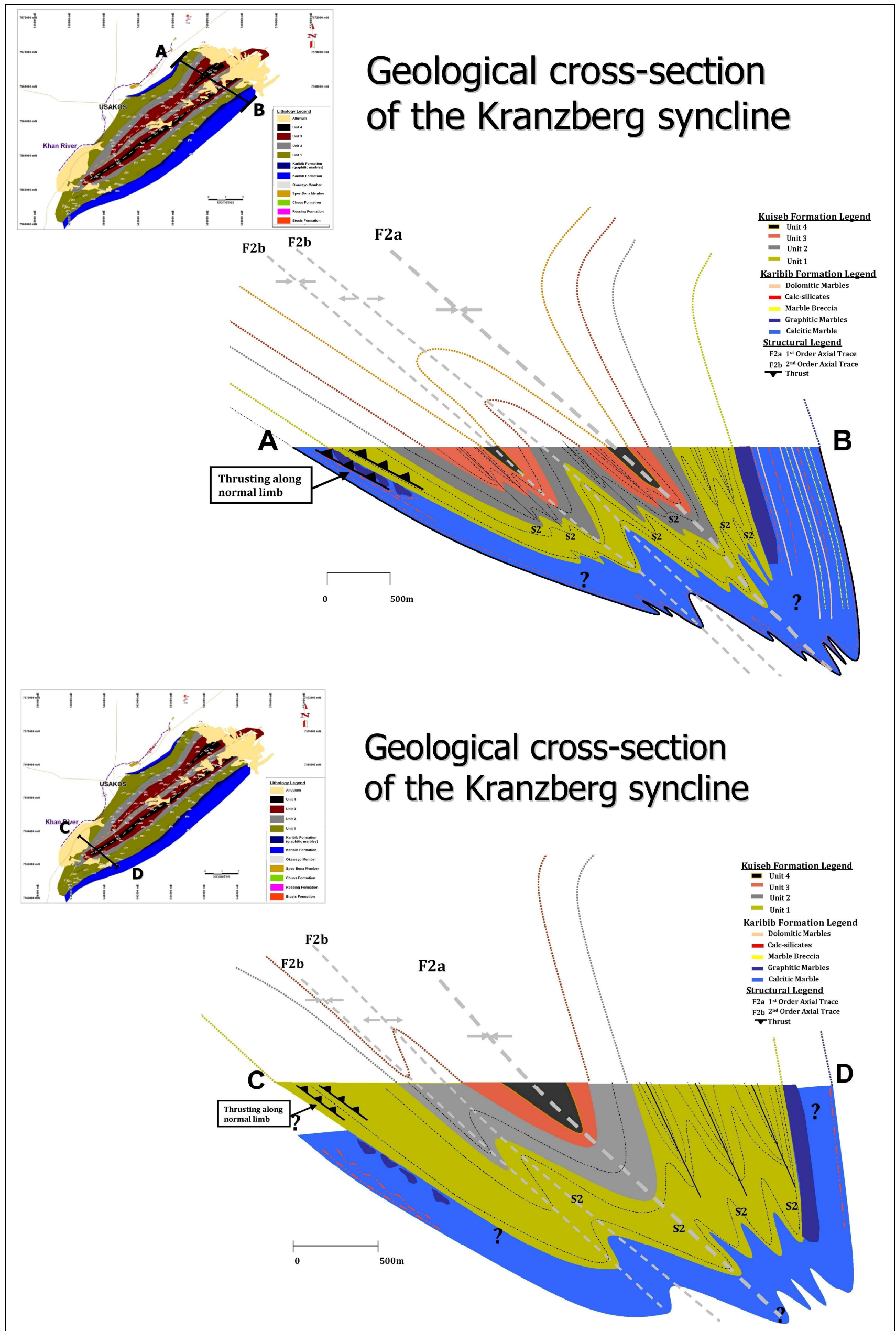


Figure 4.8: Vertical cross-sections A-B and C-D across the Kranzberg syncline: (a) across Drainage 1 where both second-order folds are evident; (b) across the first-order hinge domain, with Unit 1 on the overturned limb being much thicker than on the normal limb, testifying to the structural duplication that has taken place. Second-order synclinal and anticlinal structures are indicated by the duplication of the lower stratigraphic units (ie. Units 1 and 2).

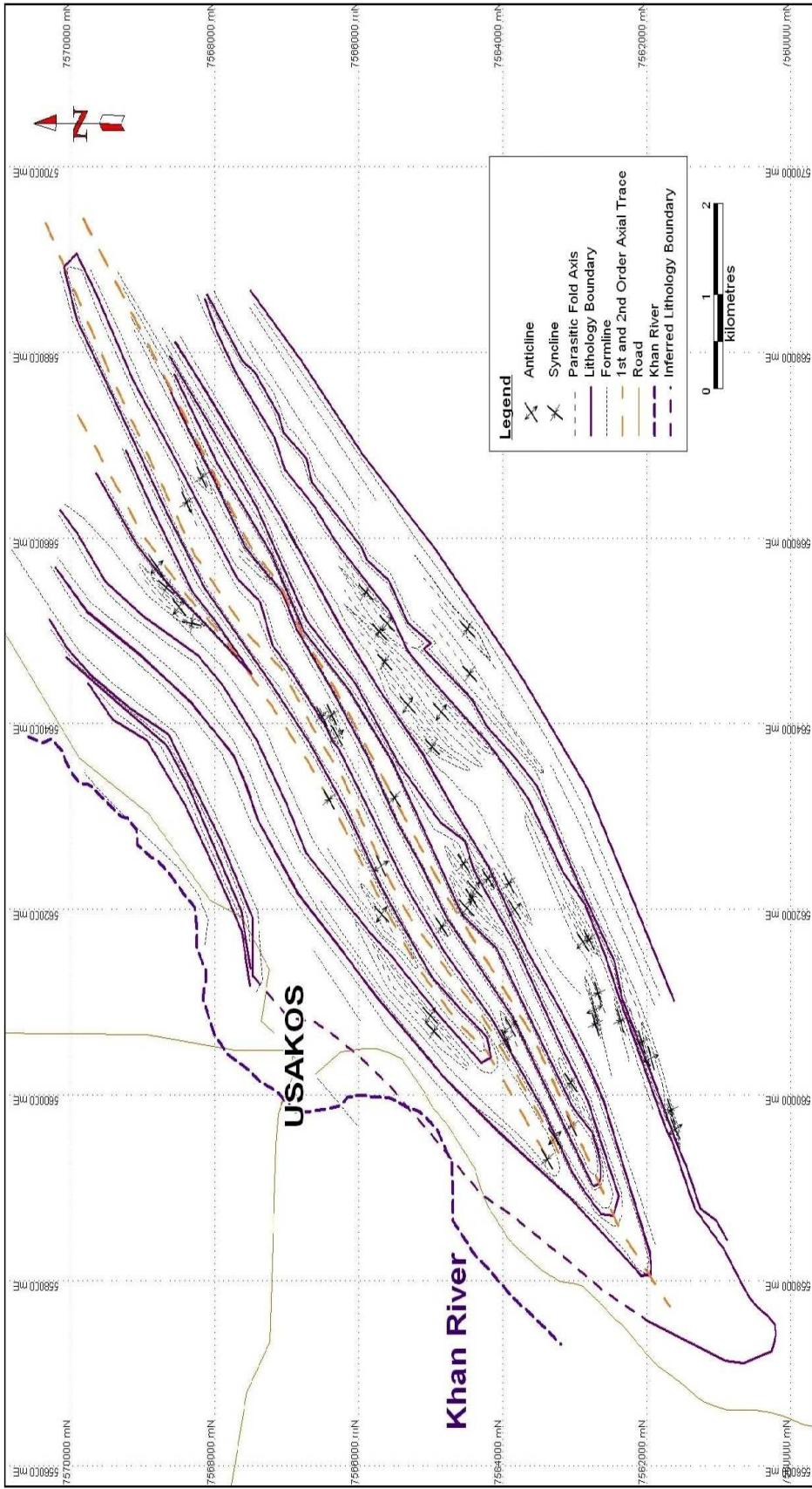


Figure 4-9: Structural formline map of the Kranzberg syncline in the study area indicating axial trace locations of first- and second- order fold structures (orange hashed line) and parasitic folds (blue hashed line). Lithological contacts between Units 1 to 4 are indicated by solid purple line.

4.5 STRUCTURAL DOMAINS OF THE KRANZBERG SYNCLINE

4.5.1 Domain 1: the normal NW limb

Figure 4.10 illustrates the distribution of lithologies as well as orientation diagrams for bedding (S0), cleavage (S2) and intersection lineations (L2i) along the normal limb. Bedding shows an average orientation of 059°/39° SE. Primary sedimentary features such as cross bedding and laminations within the more competent metapsammitic and calc-silicate units are commonly well preserved. S2 along the normal limb trends, on average, 045° with an average dip of 46°. This coincides with S0/S2 relationships as S2 has a steeper dip than S0 (Fig. 4.10a and d), indicating the normal nature of the NW limb. The regionally compiled average values for S0 and S2 indicate the anticlockwise transection of the fold limb by S2 by ca. 14° (compare Figs. 4.10 a and d). Mineral and mineral stretching lineations (L2m) are commonly defined by the preferred alignment of cordierite porphyroblasts and stretched quartz-feldspar aggregates, showing an overall E to ESE trend at moderate plunges (25-50°), parallel to intersection lineations (L2i) between bedding (S0) and cleavage (S2) (Fig. 4.10b, c).

Two major F2b folds can be delineated on the NW limb of the Kranzberg syncline. The axial trace of the F2b syncline can be traced by outcrops of Unit 3 and, further along strike (NE), the uppermost Unit 4 of the Kuiseb Formation that forms the core of the F2b fold. Similarly, the axial trace of the F2b antiform is delineated by outcrops of Unit 2 in the core of the fold, surrounded by younger Units 3 and 4 (Figs 4.7 - 4.10). Third- and fourth- order folds with wavelengths of several tens of metres are the most common folds that can be mapped in river section outcrops and followed between drainages. These folds tend to be tight, plunging at 40- 50° to the E. An exception to this is around the town of Usakos where fold hinge crenulations (L2f) show more southerly plunges. This is discussed in more detail in Chapter 4.6.2.

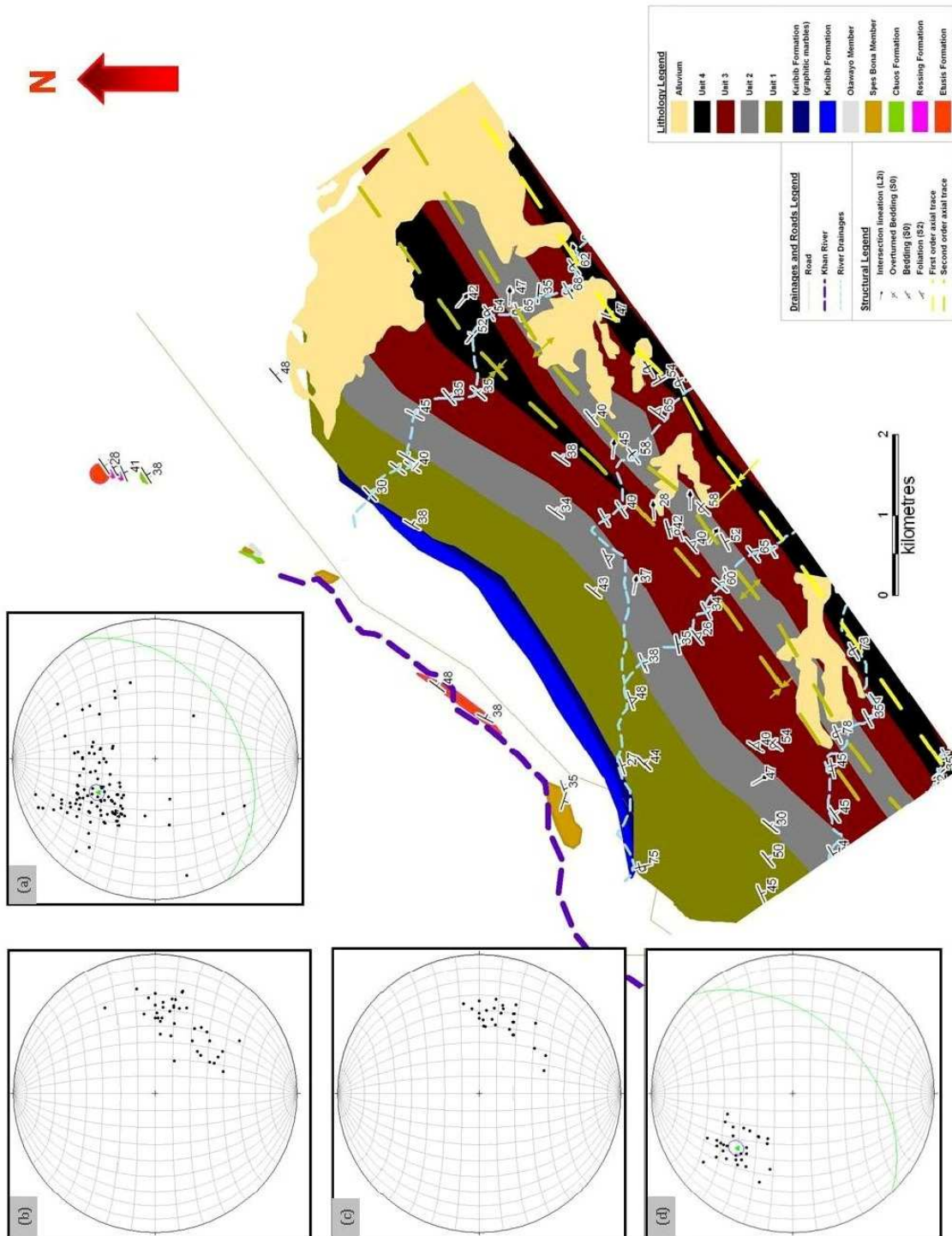


Figure 4.10: Geological map and orientation diagrams for the NW limb of the Kranzberg syncline: (a) Poles to bedding with mean vector plotted. Great circle to mean vector represents average strike (39°) and dip (0.59°); (b) Intersection lineations along the normal limb with a mean trend and plunge of 110/44° (n=41); (c) Mineral lineations along the normal limb with a mean trend and plunge of 111/45° (n=23); (d) Poles to S2 and mean vector plotted. Great circle to mean vector indicates the regional orientation of S2 along the normal limb (n=23) and the, on a regional scale, transecting geometry of S2 showing an anticlockwise rotation of 14° with respect to F2 axial traces.

Drainage 1 (Fig. 4.7), located at the northern part of the study area, provides well exposed sections through Units 1 to 4 of the Kuiseb Formation also demonstrating the abundance of lower-order folds that determine the distribution of units throughout the Kranzberg syncline (Fig. 4.11). Figure 4.11, illustrates thick, folded units of interlayered metapsammites and metapelites. Folds show wavelengths of 90-100 m, amplitudes of ca. 60 m and close- to tight interlimb angles. Intersection (L2i) and mineral stretching (L2m) lineations typically show trends between 090-095° and plunges between 40 and 45°, parallel to the plunge of the folds.

Compositional variations and rock types within Units 3 and 4 typically make folds easier to identify, whereas folding is, in many places, only indicated by changes in the relative angles between S0 and S2 in metapelite-dominated units (eg. Unit 2). The S2 foliation (eg. Fig. 4.3), is commonly closely spaced and pervasively developed in metapelitic units. In cases like this, bedding is often only discernable where the rocks show prominent compositional banding or laminations. A refraction of the S2 cleavage is also common and, on both local and regional scales, accounts for the scatter in foliation readings (eg. Fig. 4.10d), fanning in places by up to 30° in metapsammitic units.

4.5.2 Domain 2: SE Overtured Limb

The overturned limb of the syncline consists of, from SE to NW, the Oberwasser and Daheim Members and the Karibib and Kuiseb Formations. Bedding is, for the most part, overturned, NE-striking, showing steep- to subvertical dips. It has an average strike and dip of 054/55° respectively. The S2 foliation, in turn, shows an average strike of 028° and a dip of 50° (Fig. 4.12a and d). This is indicative of (1) the regionally overturned nature of Kranzberg synclines SE limb, and (2) the transecting nature of S2 with respect to F2 folds, showing an anticlockwise rotation, similar to that recorded on the NW limb, of ca. 25°. The Karibib marbles vary from low strain (ie. graphitic marbles) to high strain (ie. cream coloured marbles) and bedding is, locally, transposed into S2 (Fig. 4.13).

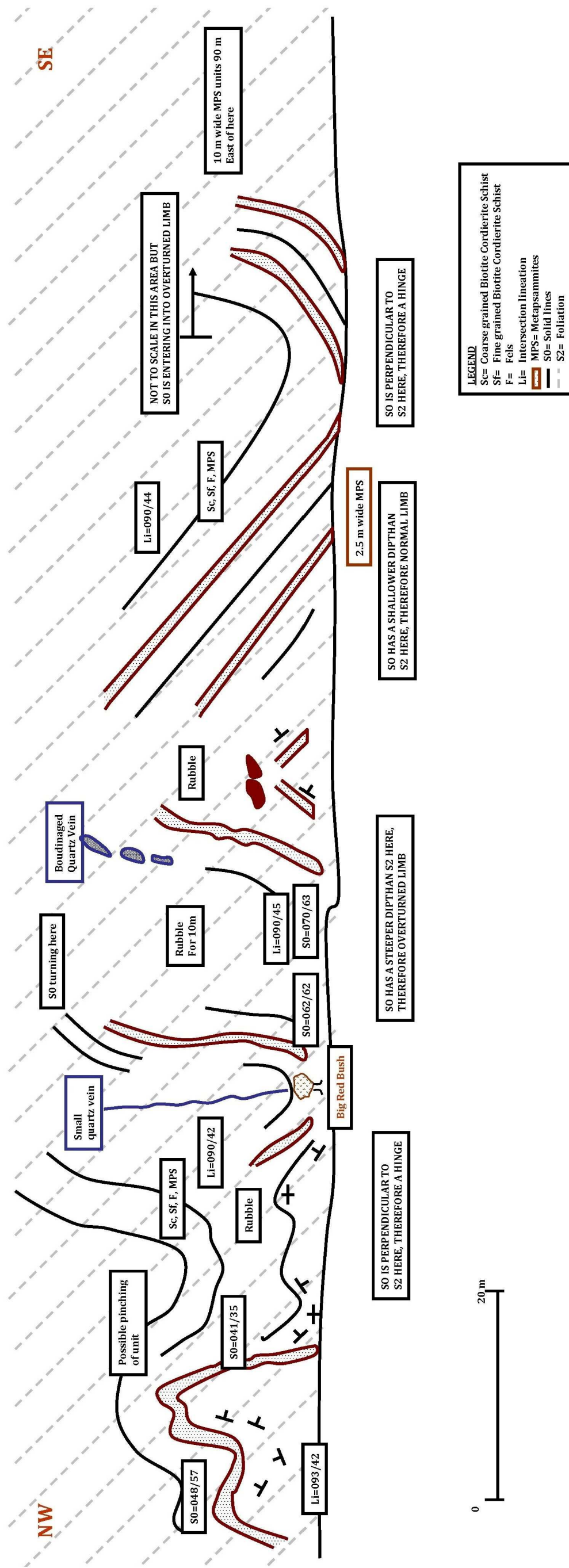


Figure 4.11: (Coordinates UTM 566183E; 7568812S WGS 84) Detailed section of fourth- and lower- order anticline and syncline overfolds with close- to tight- inter-limb angles and with 45-50 m half wavelengths, within Unit 4 of the Kuiseb Formation; cross-sectional view. Mineral and intersection lineations typically gave trends between 090-095° and plunges between 40 and 45°. S2 for the area is marked on sketch as hashed grey line. When compared with S0, the angles between the two give the location of the fold (ie. normal or overturned limb) and the approximate location of the fold hinge.

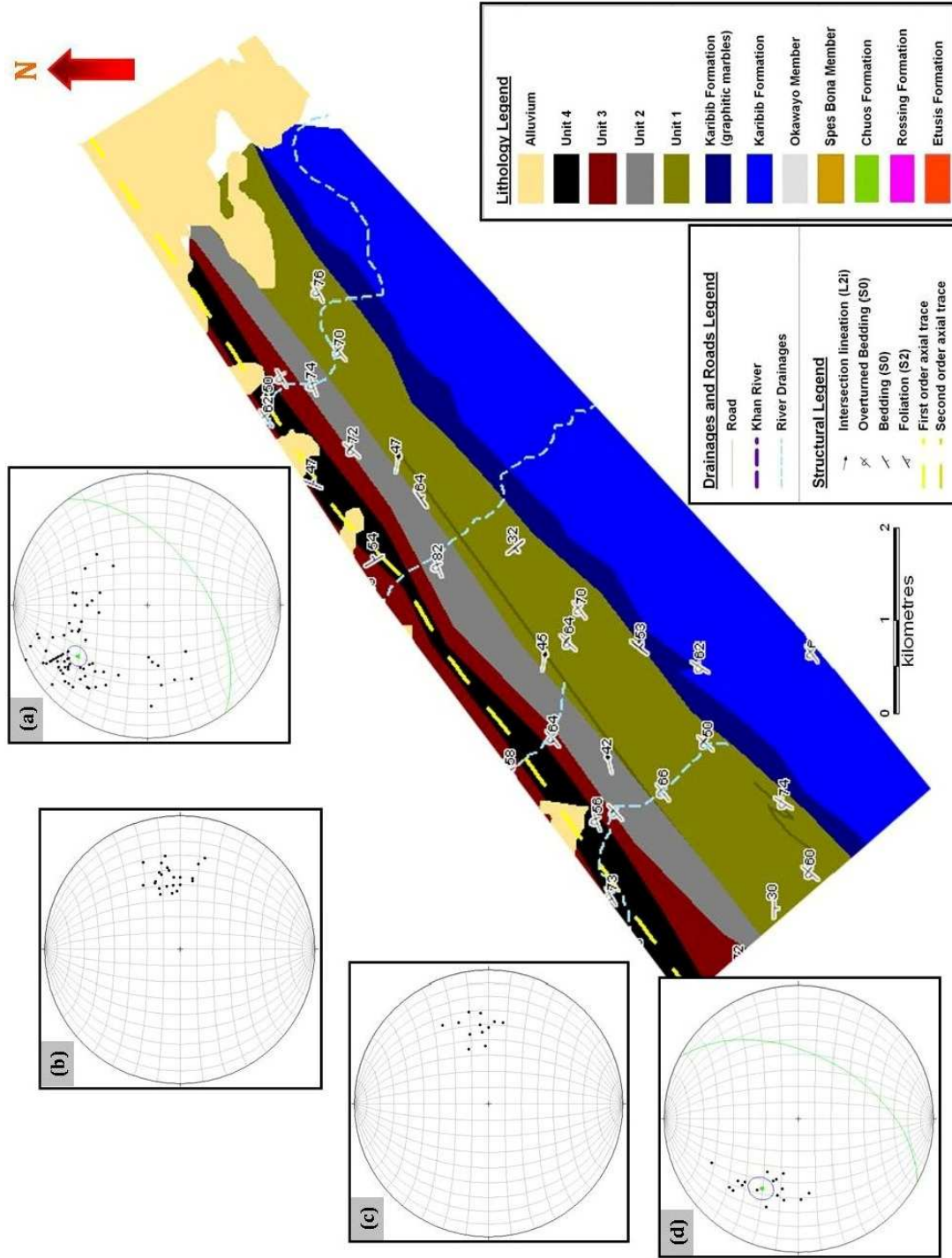


Figure 4.12: Geological map and orientation diagrams for the SE limb of the KS: (a) Poles to bedding with mean vector plotted. Great circle to mean vector represents average strike (054°) and dip (55°) of bedding along the overturned limb (n=71); (b) Intersection lineations along the overturned limb with a mean trend and plunge of 083/45° (n=26); (c) Mineral lineations along the overturned limb with a mean trend and plunge of 081/41° (n=12) (d) Poles to S2 and mean vector plotted. Great circle to mean vector indicates the regional mean strike of 028° and a dip of 50° along the overturned limb (n=18). Note again, the anticlockwise rotation of S2 against S0 and F2 fold axial trace.

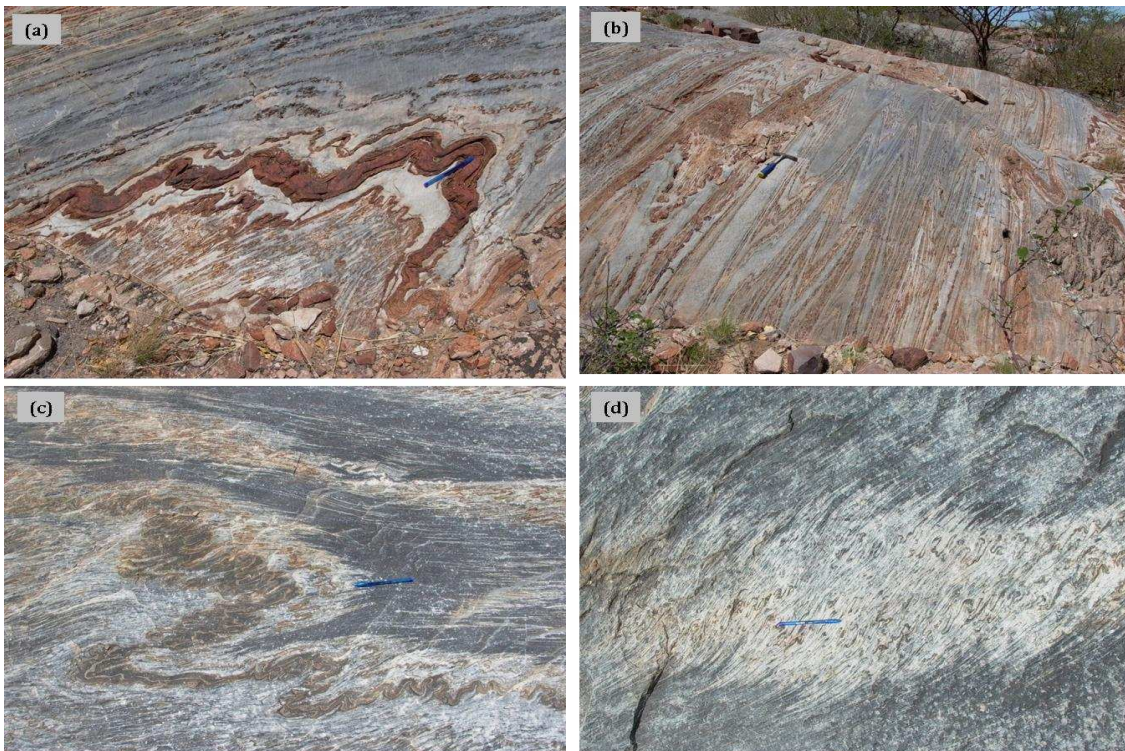


Figure 4.13: Folding observed within the Karibib Formation along the overturned limb. Folding is most prominently displayed by alternating marble and calc-silicate sequences (Fig. 4.13a, b) or in alternating dolomitic and calcitic marble layers (Fig. 4.13c, d). In places, folding leads to the progressive transposition of bedding into the S2 foliation (e.g. 4.13b, d). Bedding transposition is characteristic for large parts of the overturned SE limb of the Kranzberg syncline.

Bedding in marble units of the Karibib Formation is often preserved as alternating layers of dolomitic, calcitic, and graphitic marbles intercalated with calc-silicates. Marble-breccia horizons are also common throughout the formation, with carbonate clasts often oriented at moderate angles to bedding, tracking the S2 foliation in the rocks (Fig. 4.14). In high-strain zones, clasts in marble breccias are highly flattened resulting in an almost banded-like appearance of the marbles.

Within the Kuiseb Formation, primary features such as cross-bedding and laminations are best preserved in the more competent calc-silicate and metapsammitic units. In metapelitic units, S1 fabrics and S0 primary features are often overprinted by a pervasive, steeply-dipping S2 foliation, particularly on the limbs of F2b and lower-order parasitic folds.



Figure 4.14: Marble breccia (left side of photo) of the Karibib Formation. Note that flattened marble clasts define a fabric that is at an oblique angle of 10° to bedding. The long axis of the marble clasts traces the S2 foliation.

In contrast to rocks developed on the NW limb of the syncline, fabric and strain intensities on the SE limb are invariably higher and primary features are, in places, no longer preserved with many units displaying evidence of bedding transposition. Mineral and mineral stretching lineations (L2m) consistently show a subparallel plunge to intersection lineations (L2i) and crenulation lineations (L2f). Trends range from 070 - 100° and plunges between 40 - 50° (Fig. 4.12b, c). Crenulation lineations are best developed in calc- silicate horizons at fold hinges within marble horizons of Unit 1 in the lower Kuiseb Formation. Fold plunges in the Karibib Formation are steep and to the E and ENE, with lower-order folds in the transposed zones sometimes displaying rootless, centimetre- to tens of metre- sized fold hinges. Within the Kuiseb Formation, fold limbs and hinge zones are most easily determined by following marble marker horizons, whereas the pronounced bedding transposition render the use of S0/S2 angular relationships difficult (Fig. 4.15).

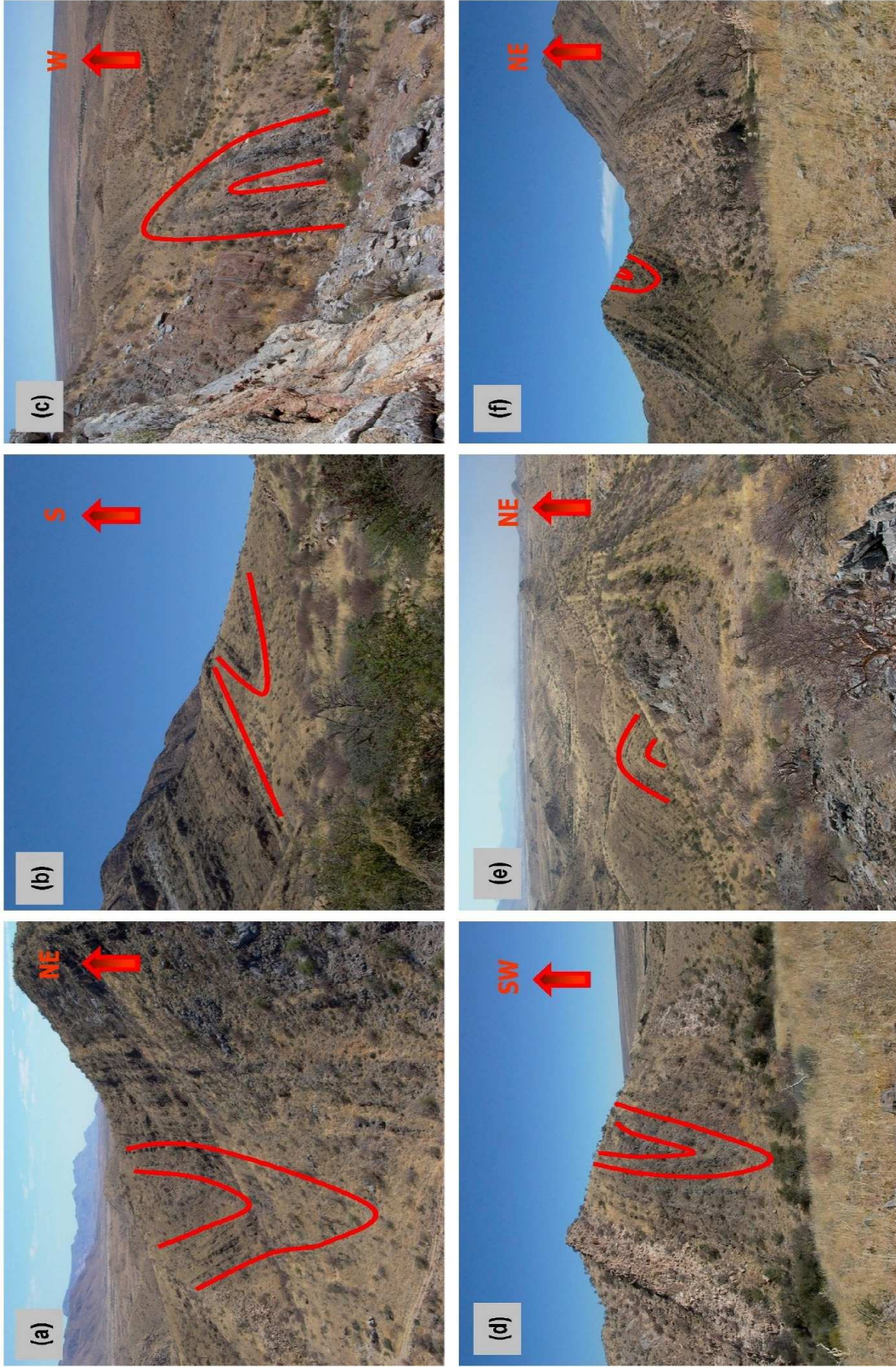


Figure 4.15: Regional photos (a - e) illustrating the pervasive folding (F2) of e.g. Unit 1 of the Kuseib Formation along the overturned limb of the Kranzberg syncline. F: F2 folding also affects the Karibib Formation, near the contact of dolomitic (beige) and graphitic (dark blue) marbles. Red lines outline the marble marker horizons and fold closures.

Unit 1 of the Kuiseb Formation has incurred a large amount of duplication evidenced by abundant, closely-spaced F2b fold structures. F2b folds are often tight-to isoclinal, showing half wavelengths of up to 65 m in length. They are parallel to the F2a syncline structure, and have hinge trends of 070-100° and plunges of 40-60°.

4.5.3 Domain 3: First-Order Hinge

The first-order hinge zone of the Kranzberg syncline is located to the immediate south of Usakos. Here, the fold is cored by Units 1 and 2 of the Kuiseb Formation, hosting abundant and voluminous granitic and pegmatite intrusions (Fig. 4.7). In the hinge, bedding rotates from the regional NE trends on the limbs of the syncline to NW strikes and NE dips. This rotation occurs over a width of ca. 200 m. The π -diagram (Fig. 4.16a) indicates a plunge of the first-order hinge of 094°/38°, subparallel to lower-order parasitic folds on the limbs (Chapters 4.3 and 4.4). In the hinge of the Kranzberg syncline, S1 is commonly at high angles to S2 and the two foliations are more readily distinguished compared to the fold limbs. The S2 foliation shows, on average, an orientation of 045°/46° (Fig. 4.16d). Intersection lineations (L2i) scatter around easterly plunge directions (70-110°) at moderate plunges (35-45°) with an average of 092°/41° (Fig. 4.16b, c), corresponding very well with the plunge of the first-order syncline determined from the π -diagram for poles to bedding (Fig. 4.16a).

F2b synclines and anticlines are tight- to isoclinal with half wavelengths of ≤ 70 m and plunges of 30-40° to the E. Parasitic folding observed near the contact of Unit 3 and Unit 4 of the Kuiseb Formation, and near the axial trace of the first-order hinge is illustrated in figure 4.17. In this example, a bedding-parallel granitic sill allows for easier observation of the folding. The asymmetrically folded anticline and syncline here mimic higher-order folds, with a shallowly-dipping normal limb and a steeply-dipping overturned limb. The fold plunge is also consistent with higher-order folds, having a trend of 073° and a plunge of 37°.

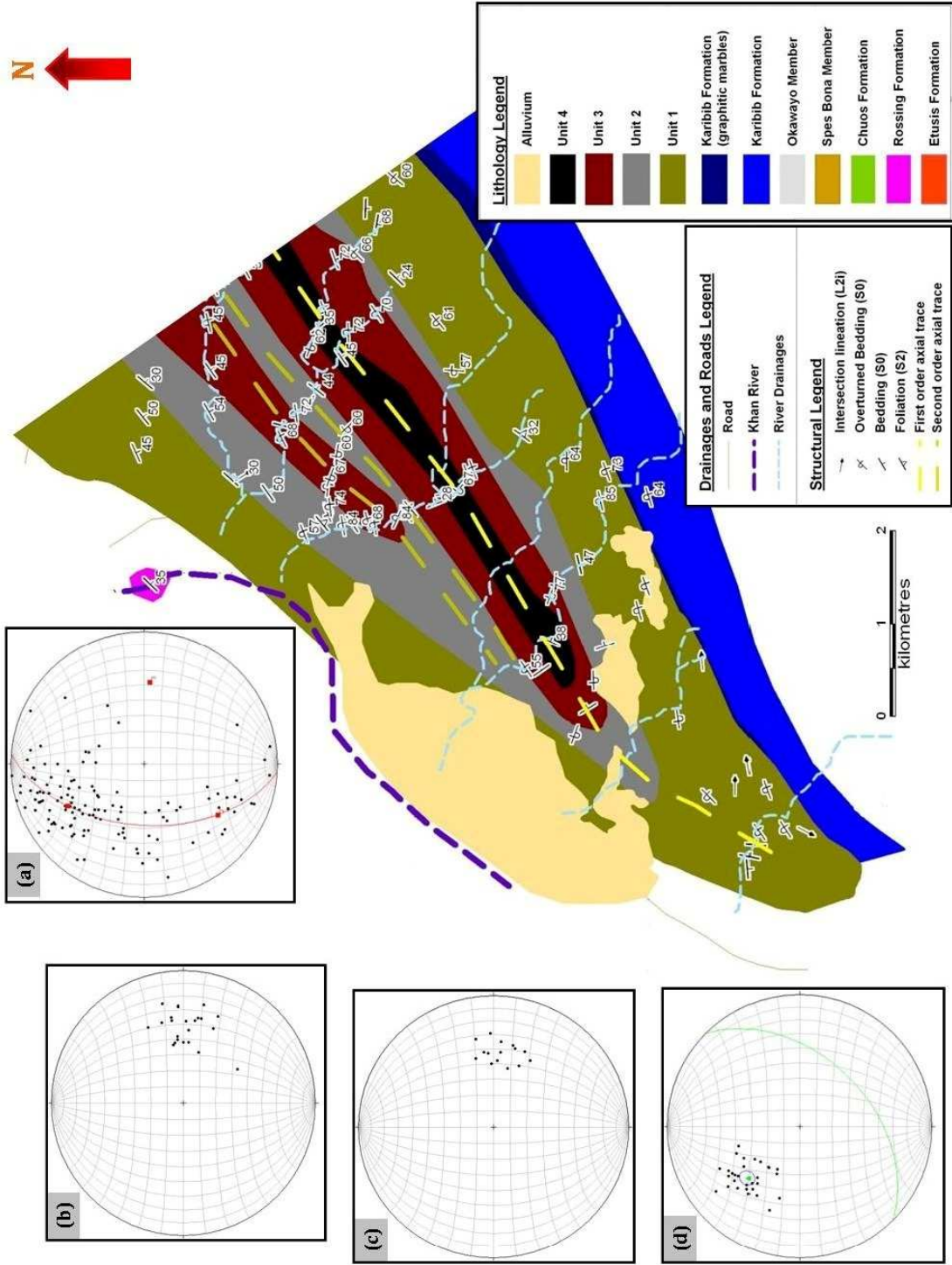


Figure 4.16: Geological map and orientation diagrams for the hinge domain: (a) Poles to bedding with great (n-) circle indicating cylindrical best fit. The pole to this great circle gives an average fold axis trend and plunge of 094° and 38° (indicated by red square in eastern part of the orientation diagram) (n=132); (b) Intersection lineations within the hinge domain with mean vector having a trend and plunge of 092° and 41° (n=25); (c) Mineral lineations within the hinge domain with mean vector having a trend and plunge of 096° and 42° (n=15); (d) Poles to S2 and mean vector plotted. Great circle to mean vector indicates the regional mean strike of 045° and a dip of 46° (n=30).

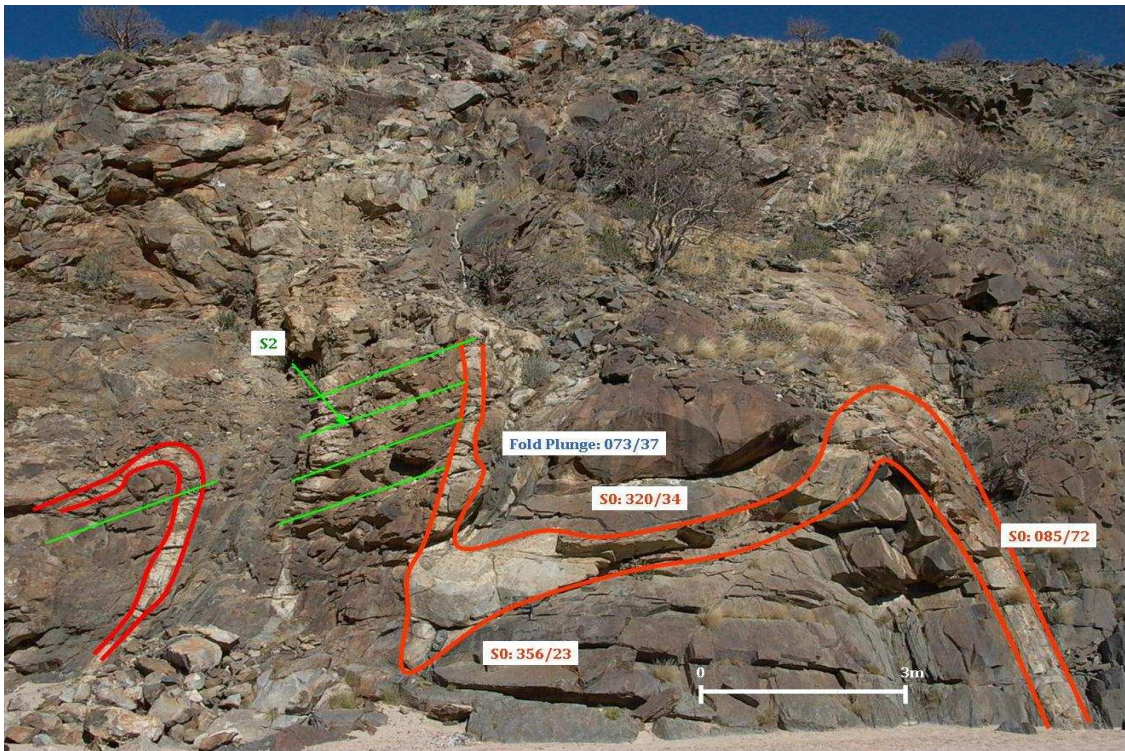


Figure 4.17: (Coordinates UTM 559160E; 7562928S WGS 84) Looking SW. Lower-order syncline - anticline pair along Drainage 8 near the first-order hinge, developed near the contact of Units 3 and 4, characterized by interlayered quartz-biotite felses and metapsammities (rusty-brown weathering surfaces) and a granitic sill (light-grey). S2 is indicated by green line.

The combined lineations (L2) for the entire study area (normal, overturned and hinge domains) show a regional trend towards the E at 097° and a plunge of 42° (Fig. 4.18). For comparison, a cylindrical best fit for bedding (S0) was also plotted (same as Fig. 4.16a). Its pole, indicating the average regional fold axis orientation coincides very well to the above lineations (L2) giving an average trend of 098° and a plunge of 36° (Fig. 4.19).

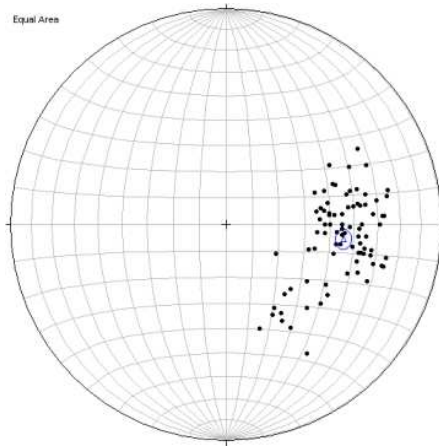


Figure 4.18: Intersection lineations for the entire study area. Mean vector of intersection lineations has a trend and plunge of 097° and 42° respectively (n=92).

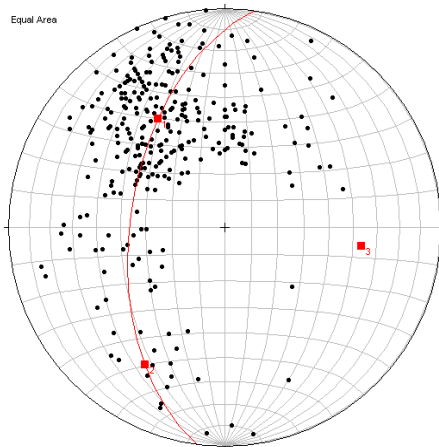


Figure 4.19: Poles to bedding with a cylindrical best fit (red great circle). The pole to this great circle indicates a regional fold axis orientation of 098° and a plunge of 36° (indicated by red square in eastern part of orientation diagram) (n=317).

4.6 DEVIATIONS FROM D2 TRENDS.

Regional mapping in this study has identified a corridor (Figs. 4.20 and 4.22) within the Kranzberg syncline, where particularly D2 linear elements (e.g. fold (F2) and lineation (L2) plunges) as well as bedding orientations deviate from the commonly recorded D2 trend. This zone coincides with significant and abrupt changes in the

width of lithological packages and the somewhat sporadic occurrence of units (Fig. 4.20). These changes are discussed in more detail below.

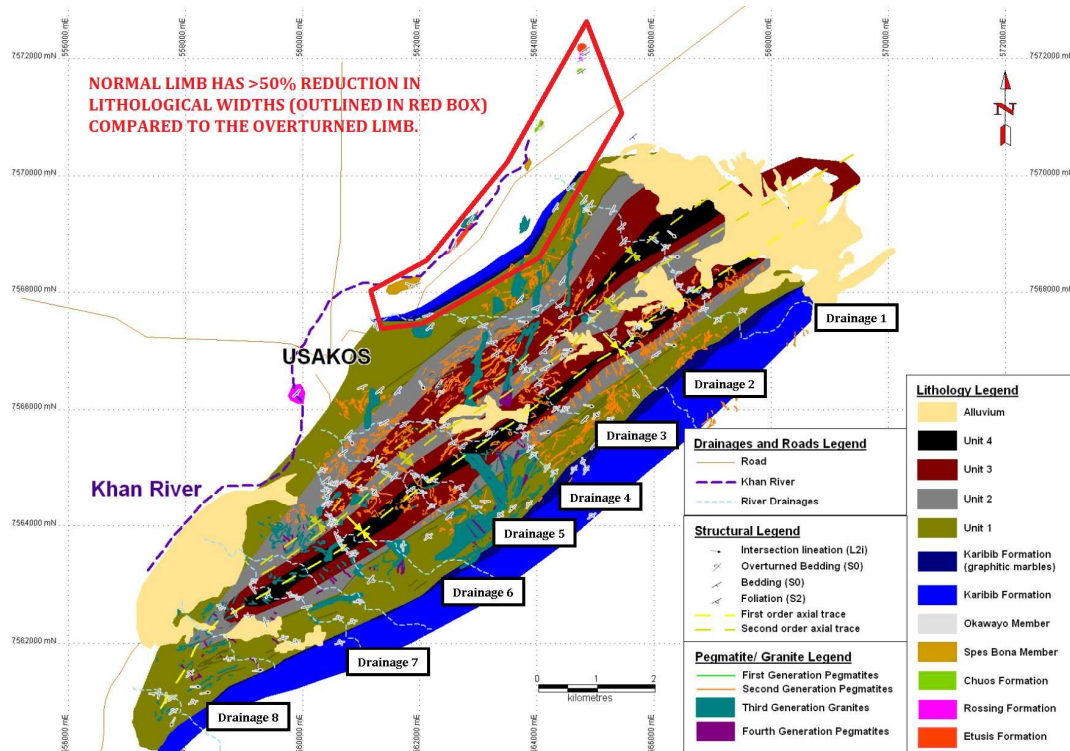


Figure 4:20: Map outlining area where a > 50% reduction in lithological thickness along the normal limb is recorded (red box).

4.6.1 Lithological variations between the SE and NW limb

Marble units of the Karibib Formation on the normal limb are, though highly variable, on average, only 180 m thick, which is less than a quarter of the thickness of the Karibib Formation on the overturned SE limb. Between the Etusis and the Karibib Formations, the Rössing and Chuosi Formations as well as the Spes Bona, Okawayo, and Oberwasser Members are developed, but thicknesses are highly variable and overall greatly reduced. The Spes Bona Member, has an estimated minimum thickness of 600 m on the overturned limb of the Kranzberg syncline (Johnson, 2005), yet is no more than 100 m wide on the normal limb (Chapter 3). Structural readings of bedding (S0) indicate generally NE trends of units at moderate SE dips, similar to bedding orientations on much of the normal limb. Figure 4.21 shows a mean strike of 055° and a dip of 40° for bedding in the area.

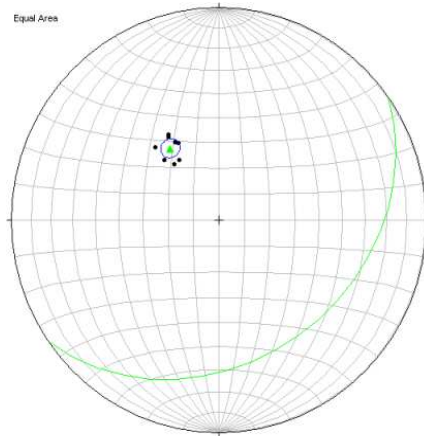


Figure 4.21: (a) Poles to bedding for the area NE of the study area, along the Khan River, with the mean vector plotted. Stratigraphic levels observed are the Etusis Formation to the Karibib Formation. Great circle to mean vector gives mean strike and dip for area 055°/40° (n=8).

Primary features are often completely overprinted by a pervasively developed S2 fabric in the more pelitic units and through complete recrystallization of marble units.

4.6.2 Usakos Town Area

In the immediate vicinity of Usakos town, the distribution of lithologies and orientation of structural elements such as lineations, fold plunges and bedding orientations change considerably (centred at UTM 561635; 7566805 WGS 84). While marker horizons of e.g. marble horizons of Unit 1 of the Kuiseb Formation and the dark graphitic marbles of the Karibib Formation, are well-developed on the SE limb, these units are absent around Usakos. (Fig. 4.22). First- to 3rd- generation pegmatites/granites in the area show highly-sheared contacts, with NE strikes and SE dips between 35-40°. These pegmatite orientations and sheared contacts are unique to this area and not observed elsewhere in the Kranzberg syncline. Bedding (S0) orientations are still consistent with the regional bedding, but, significantly, mineral stretching and intersection lineations show a clockwise rotation to more southerly plunges, assuming down-dip orientations.

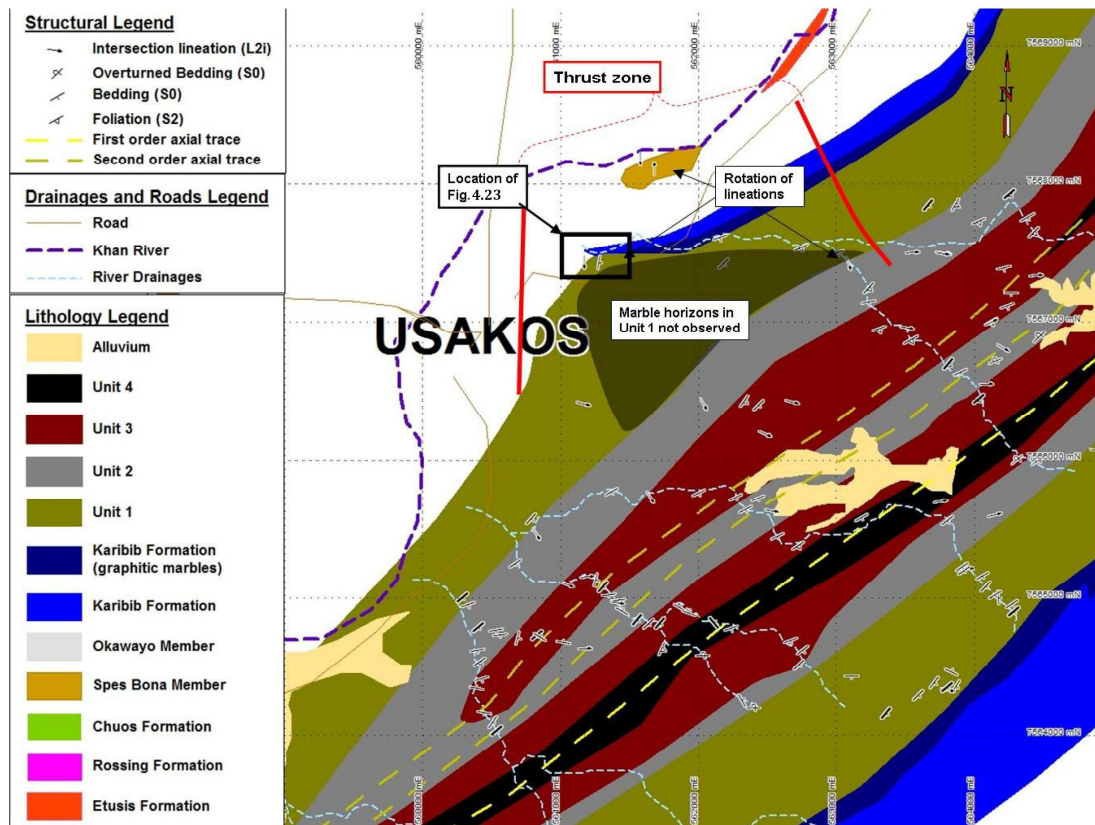


Figure 4.22: Geological map and structure around the Usakos town area showing area of missing marble horizons within Unit 1 (dark shading) and a rotation of intersection, mineral stretching and fold hinge crenulation lineations to S plunges. Fold axis orientations in the Spes Bona Member have very shallow fold plunges to the N and S. Proposed thrust zone in the Usakos area located between solid red lines (see text for further explanation).

This rotation of lineations coincides with the rotation of fold plunges to SE and S plunges, particularly along the contacts between the Kuiseb and Karibib Formations, being at high angles to the regional F2 fold plunges. Fold hinge crenulations (L2f) show plunge directions of 130° to 170°, with plunges between 10° and 40°. Figure 4.23 shows a well exposed river section that illustrates these relationships. Folding in these outcrops is characterized by reclined to nearly recumbent, parallel, tight- to isoclinal anticlines and synclines, with half-wavelengths and amplitudes of ca. five metres or less (Fig. 4.24). Bedding is, in places, rotated to E and ESE trends. This structural disruption from the overall D2 trend is also recorded in stratigraphically lower sections in e.g. the Spes Bona Member in exposures along the Khan River bed (Fig. 4.22 coordinates UTM 561867E; 7568258S WGS 84).



CASE STUDY NEAR THE TOWN OF USAKOS

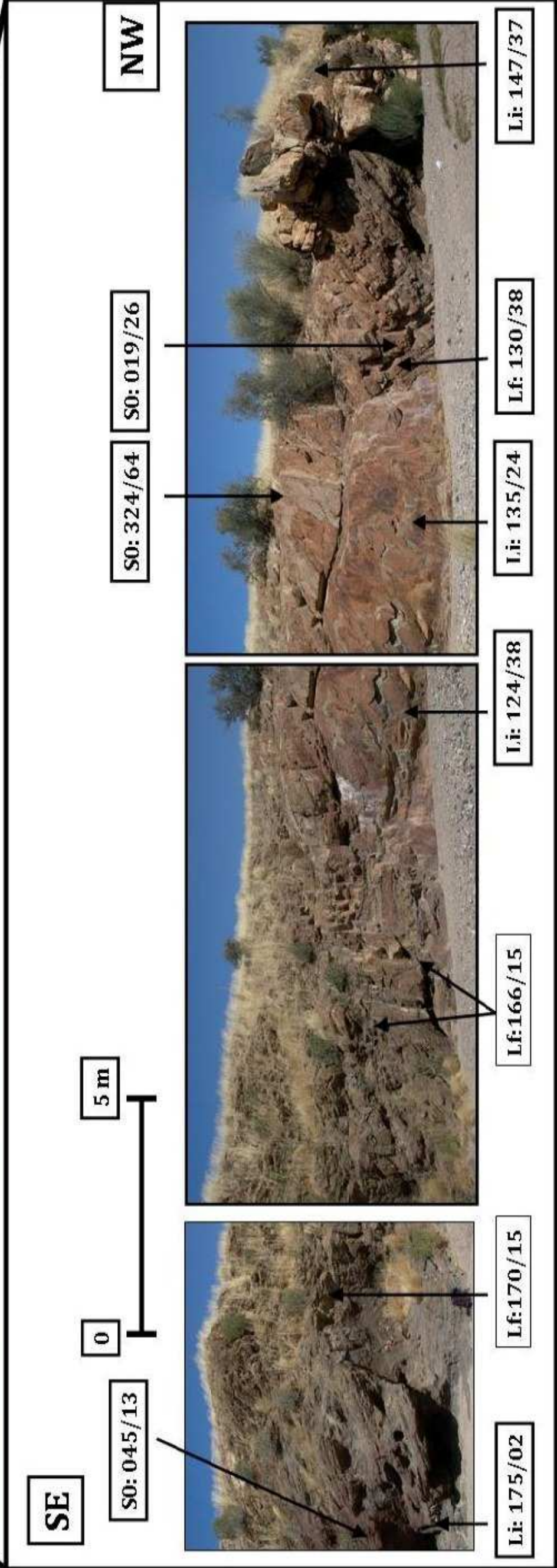


Figure 4.23: (Coordinates UTM 561226E; 7567463S WGS 84) Case study of the Kuiseb/Karibib Formation contact near the town of Usakos with crenulation lineations (L2f), intersection lineations (L2i), and bedding (S0) measurements taken from the SE (left side of photo) towards the NW (right side of the photo), and indicating fold axis orientations towards the SE and S, a strong deviation from regional D2. The Karibib Formation is located 5 m to the NW of the photo.



Figure 4.24: Oblique section of figure 4.23, illustrating tight to isoclinal and overturned to nearly recumbent anticline and synclines at the Karibib and Kuiseb Formation contact.

Here, the Spes Bona Member dips shallowly (05° - 45°) to the S, and in contrast to folds along the Karibib/Kuiseb contact, folds are upright, parallel, close- to tight antiforms and synforms, showing N-S trends and shallow plunges of $< 15^{\circ}$ N (Fig. 4.25).

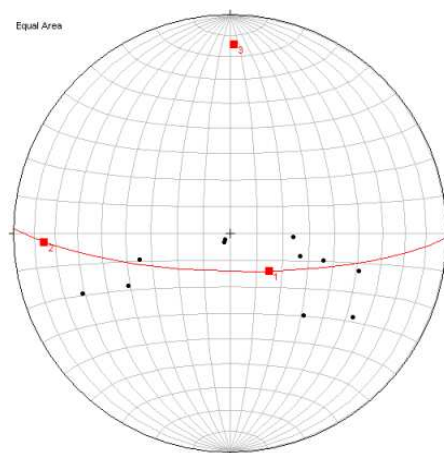


Figure 4.25: Poles to bedding for the Spes Bona located near the town of Usakos. The best fit great circle (red line) indicates a northerly fold plunge (indicated by red square in northern part of the orientation diagram) ($001/14$). ($n=11$) of the folded sequence.

Taken in conjunction, the only intermittently developed units along this part of the NW limb, the seemingly complete disappearance of marble horizons of the Kuiseb Formation, the presence of high-strain fabrics and sheared pegmatites, and the deviation of linear elements such as fold hinges and mineral lineations from the common NE-SW trends, suggest the presence of an underlying structure. The fact that fold hinges and lineations are rotated into a down-dip orientation and the local development of high-strain fabrics in e.g. the Chuos Formation and Spes Bona Member may point to the presence of a thrust that has developed with the NW-vergent F2 folds, recording a top-to-the-NW thrust sense of movement (see Chapter 6 for a detailed discussion).

4.6.3 Late F2 folds and refolded boudins

Steep- to subvertical, mainly NE plunging, asymmetric folds (late F2) in calc-silicate bands of the Karibib marbles and, in some areas, of the Kuiseb Unit 1 marbles, are ubiquitous along the overturned limb. The folds typically show wavelengths of only several centimetres to a maximum of one metre. They are characterized by close-to tight interlimb angles and almost always show a Z-shaped asymmetry. Neither their steep NE plunge nor the Z-shaped asymmetry of the folds can be reconciled with an origin as F2b parasitic folds to flexural slip or flow along the fold limbs of the first-order fold structures of the Usakos dome or the Kranzberg syncline (Fig. 4.26).

Along the normal limb, similar fold patterns are only locally observed. More commonly, however, calc-silicate bands in marbles appear to have undergone an early phase of layer-parallel stretch and boudinage, followed by layer-parallel shortening. This is evidenced by the presence of shortened and, in places, imbricated boudins (Fig. 4.27).



Figure 4.26: Asymmetric, Z-shaped folds developed in finely-banded, alternating calc-silicate bands (rusty, brown) and marbles (grey). The folds show consistently steep plunges, both to the NE and SW and a Z-shaped asymmetry. The steep fold plunges and fold asymmetry indicate that the folds do not merely represent parasitic F2 folds to e.g. the Kranzberg syncline or the adjoining Usakos dome;

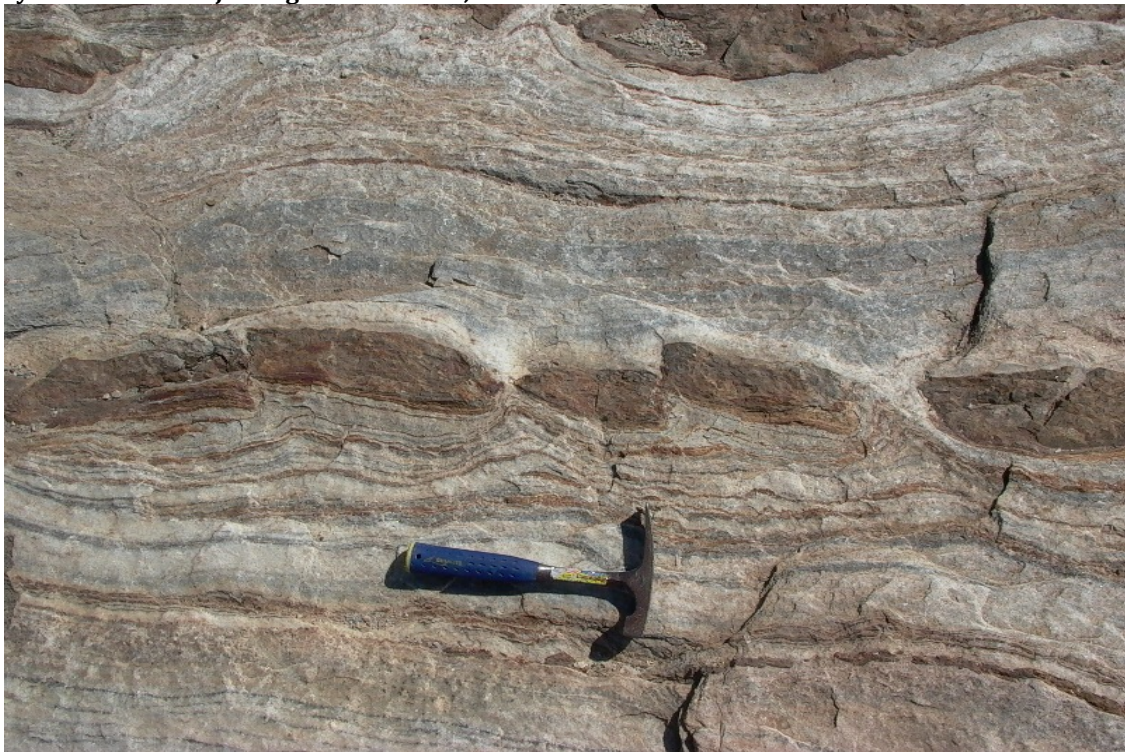


Figure 4.27: Boudinaged calc-silicate felses (brown) in marbles (grey), (plan view). Boudinage is contained in S₀, indicating initial layer-parallel stretch (i.e. separation and boudinage of calc-silicate layers) followed by layer-parallel shortening of boudins. Rock hammer handle is directed towards the NE.

The refolding of layering around late F2 folds and layer-parallel shortening of boudin trains seems related to a later, localized deformation event that involved NE-SW shortening. The localization of these structures to the interlayered marble-calc-silicate bands emphasizes the sensitivity of the highly contrasting rheologies for these later strains that are not recorded in e.g. siliciclastic units. Late F2 folding is also far more widespread on the SE overturned limb than the Kranzberg syncline shares with the Usakos Dome. The possible origin of late F2 folds shall be discussed in Chapter 6.

4.7 STRAIN

The fabric and, therefore, strain intensities are heterogeneous not only in different lithologies, but also show systematic variations in different parts of the Kranzberg syncline. Since regional strains most likely exert an important control on the emplacement of the sheet-like intrusions such as pegmatites, this section intends to delineate and qualitatively characterize (1) the general strain state in different parts of the Kranzberg syncline, and (2) variations in strain intensity.

Folding and boudinage of competent layers and the orientation of stretching lineations and foliations can all be used to qualitatively constrain the general strain in the Kranzberg syncline. For the most part, boudinage seems to be of the three-dimensional type displaying three near-orthogonal axes of unequal length (with $X > Y > Z$) (Fig. 4.28a-d). The orientation of boudins of e.g. calc-silicate felses in marbles and/or schists, as well as pegmatites in schists consistently points to a NE-SW directed stretch during NW-SE directed shortening. Where boudins were exposed in 3-D and could be mapped in their entirety, the maximum stretch is not horizontal, but shows a NE to E plunge (Fig. 4.28d). Mineral-stretching lineations ideally provide direct information about the regional stretch (X). In the Kranzberg syncline, stretching lineations show E plunges, parallel to crenulation and intersection lineations and, thus, the plunge of F2 folds.

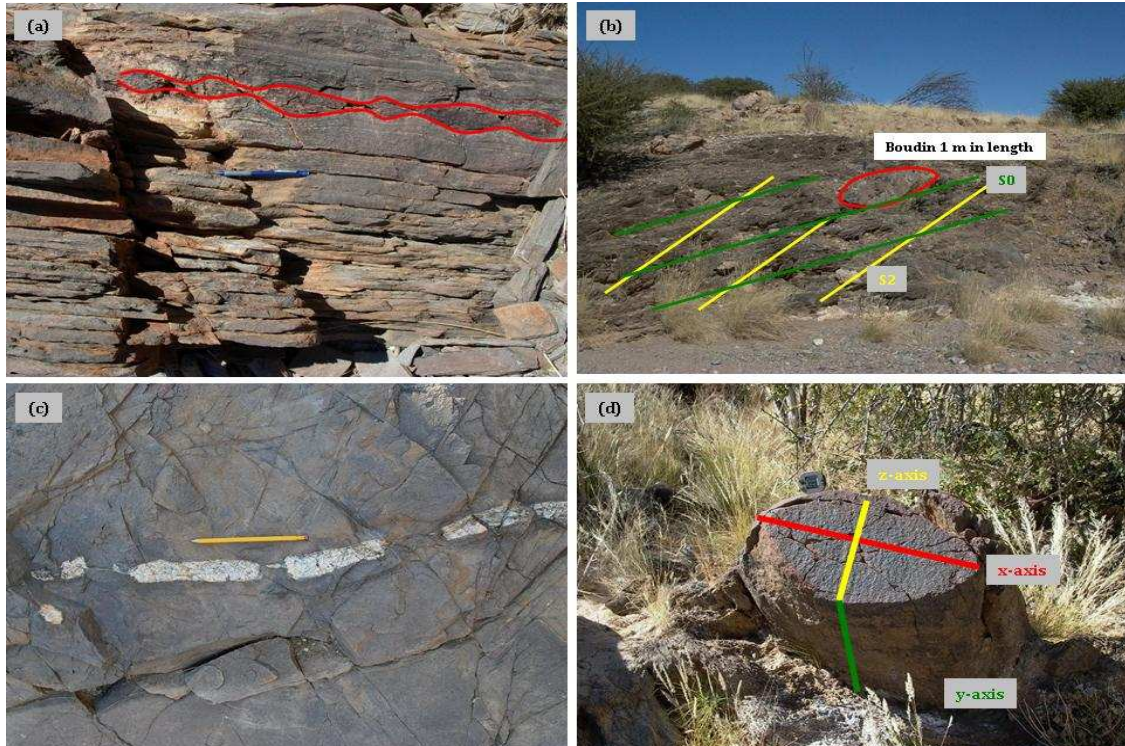


Figure 4.28: (a) Pinch and swell deformation of calc-silicates (outlined in red) in metapsammites. S0 is parallel to the calc-silicates, from bottom right to top left of photo; (b) Two metre wide isolated metapsammite boudin. S2 (yellow lines) runs from top right to bottom left of photo, and dips shallower than S0 (green lines) indicating boudin is located along a normal limb; (c) Rectangular boudinage of small pegmatite in psammitic host rock; (d) Well developed boudin in metapelitic host rocks with x (red), y (green) and z (yellow) axes defined; The stretch direction(X) plunges at moderate angles to the E.

The regional compilation of fabric data suggest an anticlockwise rotation of S2 by as much as 15°-25° against S0 and the axial trace of F2 folds so that S2 is not exactly axial planar to F2 folds. Figures 4.10a, d and 4.12a, d illustrate this angular relationship between S2 and the F2 axial traces for both fold limbs. Hence S2 is, strictly speaking, a transecting cleavage. The SE limb shows a larger transection angle compared to the NW limb. The occurrence of fold-transecting cleavages has been described from folds of many low-grade metamorphic belts (e.g. Blewett and Pickering, 1988). The origin of transecting cleavages has been interpreted through e.g. multiple fold and fold superimposition events (e.g. Van Oer Pluijm, 1990) or, more commonly, folding during transpression, where deformation involves a non-coaxial component (Treagus and Treagus, 1992). The consistently anticlockwise rotation of S2 with respect to the F2 axial trace suggest a dextral component of non-coaxial shear during folding (e.g. Blewett and Pickering, 1988). Notably, the dextral

sense of shear is consistent with the uniformly Z-shaped asymmetry and steep plunge of late F2 folds particularly developed on the steep SE limb of the syncline. This aspect will be discussed in more detail in Chapter 6.

In summary, strain in the Kranzberg syncline records a component of NW-SE directed shortening and associated E stretch, parallel to F2 fold axes. The anticlockwise rotation of S2 with respect to F2 folds suggests the presence of a non-coaxial component during folding. In general, fabric intensities on the steep and overturned SE limb of the Kranzberg syncline are considerably higher compared to the normal NW limb, where primary sedimentary features are commonly well preserved despite the presence of a well-developed S2 foliation and, particularly in metapelitic units, a bedding-parallel S1 foliation. Higher strain intensities on the SE limb are also indicated by the intense transposition folding, also resulting in the dramatic structural thickening of units, particularly Units 1 and 2 of the Kuiseb Formation and the Karibib Formation. This structural thickening due to bedding transposition is clearly illustrated in the cross-sections of [figure 4.8](#). Pervasive fabrics along the NW normal limb of the syncline where lithologies are discontinuous and/or completely non-existent are likely due to the presence of an underlying discrete structure, eg. a thrust.

Chapter 5 - PEGMATITES OF THE USAKOS PEGMATITE FIELD

5.1 INTRODUCTION

Pegmatites of the Usakos pegmatite field are typically composed of quartz, K-feldspar, plagioclase, muscovite, biotite and accessory tourmaline, garnet, beryl and lepidolite in variable amounts. Grain sizes vary from medium-grained (ca. 0.5 cm), equigranular and rather granitic textures to coarsely-pegmatitic, with crystal lengths of up to 60 cm. Colours of the pegmatites vary from bright-white on fresh surfaces to reddish-brown, particularly on weathered surfaces. The mineralogy, grain size and particularly colour of the leucocratic pegmatites contrast greatly to the fine-grained, grey to dark-grey host rocks of the Kuiseb Formation. This prominent colour contrast, the sharp wall-rock contacts and the often positively weathering nature of pegmatites greatly aid the identification of pegmatite intrusions, even on a regional scale and with the use of areal photography (Fig. 5.1).



Figure 5.1: Google Earth image, centred at coordinates UTM 563768E; 7566211S WGS 84. Pegmatites and granites are easily distinguished from the wall rocks by their different colour, commonly positive weathering and blocky joint pattern. Fourth-generation pegmatites are outlined in purple and 3rd-generation granites are outlined in green. Most other pegmatites observed are 2nd-generation pegmatites. First-generation pegmatites are typically too small to be viewed from Google Earth images.

This following chapter describes the characteristics of pegmatites in the core of the Kranzberg syncline, focusing on their occurrence and distribution, relative timing, geometry and orientation, and their structural and/or lithological controls of emplacement. Here and throughout the thesis, the term 'sill' is used to describe bedding-parallel sheet-like granitoids. The term 'dyke' refers to cross-cutting sheets, irrespective of their orientation, i.e. whether vertical or inclined.

5.1.1 Overprinting relationships – pegmatite generations

Based on (1) cross-cutting relationships, and (2) the deformation of pegmatites, four generations of pegmatites can be distinguished, henceforth referred to as 1st - to 4th-generation pegmatites (Figs. 5.2 and 5.3). Pegmatite emplacement was early- to late-tectonic (D2) and no truly post-tectonic pegmatites can be identified. Earlier pegmatites appear tightly folded and/or boudinaged, whereas later pegmatites cross-cut regional fold structures and regional fabrics, but still display marginal fabrics or gentle folding and/or boudinage (Chapter 5.4).

All four pegmatite generations are mineralogically similar, and therefore, a classification based entirely on their mineralogical and textural characteristics cannot be adopted to distinguish them. However, pegmatites exhibit systematic variations in orientation, emplacement style and deformation, depending on their structural position in the Kranzberg syncline and on the stratigraphic level and host rocks they intrude. The general characteristics of the four generations are provided in Table 5.1.

First-generation pegmatites are the least common of the four generations. The folding and boudinage of the pegmatites indicate their emplacement prior or during regional deformation (D1/D2) (Chapter 5.4.1).



Figure 5.2: Field examples of 1st- to 4th- generation pegmatites/granites in the study area: (a) Steeply dipping, NE-trending, 1st-generation pegmatite (looking NE); (b) Steeply-dipping, parallel-sided 2nd-generation pegmatite (looking NE). Both photos (a and b) also illustrate the typically positive weathering of pegmatite dykes in the Kranzberg syncline; (c) Large, ca. 30 m wide 3rd-generation pegmatite forming a prominent topographic high along the normal limb of the Kranzberg syncline (coordinates UTM 561820E; 7564820S WGS 84, looking N); and (d) Late-stage, leucocratic 4th-generation pegmatite sharply cross-cutting marbles and interlayered calc-silicate felses of Unit 1 of the Kuiseb Formation; overturned limb of the Kranzberg syncline. Rusty colouration is from weathering and run-off of surface waters.

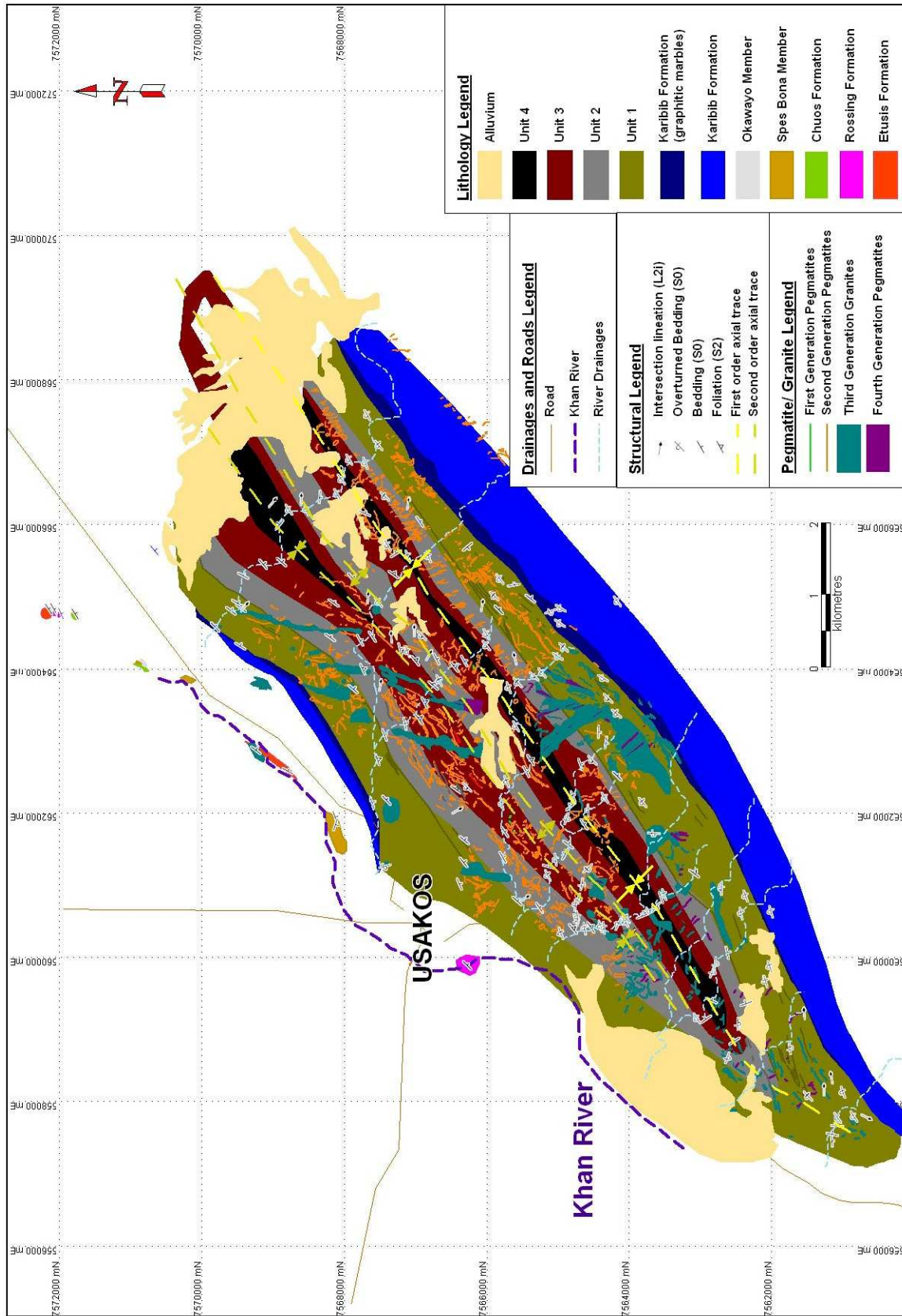


Figure 5.3: Pegmatite occurrences in the Kranzberg syncline.

Table 5.1: General characteristics of the four generations of pegmatites/granites observed in the study area. In this study, the occurrence and orientation of some 350 pegmatite sills and dykes have been considered.

Generation	Mineralogy Main Constituents	Texture	Size of Pegmatites	Abundance	Occurrence
First	Quartz, feldspar, muscovite, tourmaline	Coarse grained, but relatively equigranular	Generally <1m wide and <100m in length	Subordinate, mainly in Unit 2 and 3 of the Kuiseb Formation	Mainly along normal and overturned limb, occasionally in hinge domain
Second	Quartz, feldspar, muscovite, tourmaline, locally garnet	Fine- to very coarse grained	Sills up to 3 m wide and 100 m's in length. Dykes up to 15 m in width and < 100 m in length	Very common, all units of the Kuiseb Formation	Mostly observed along the normal and overturned Limb
Third	Quartz, feldspar, muscovite, tourmaline	Fine- to medium-grained and equigranular	Lensoid sills, up to 300m wide and 1,300m in length Dykes <50m wide and up to 3 kilometres in length	Not abundant, but very prominent, forming the largest granitic intrusives, mainly Units 1 and 2	Normal, overturned and hinge domains
Fourth	Quartz, feldspar, muscovite, tourmaline, locally lepidolite and beryl	Coarsely pegmatitic, i.e. locally large crystals of tourmaline up to 30 cm in length, up to 60 cm large feldspar	Dykes and sills up to 10 m's in width and 100 m's in length	Subordinate, in proximity to 3 rd generation pegmatites, mainly Units 1-3	Hinge domain and, in places, where the overturned limb grades into the hinge domain

Despite the deformation, they are commonly devoid of macroscopic fabrics, likely signifying the competence contrasts between the coarse-grained feldspathic pegmatites and the surrounding mainly metapelitic schists. The pegmatites are commonly reddish in colour and often, but not always, coarser grained towards their centres (Fig. 5.4a, b). Dykes occur preferentially within more metapelitic rock types of the Kuiseb Formation (Units 2 and 3).

Second-generation pegmatites are the most abundant of the four generations. They cross-cut 1st-generation pegmatites, but are cross-cut by 3rd- and 4th- generations. Second-generation pegmatites range from light-brown to brown in colour (Table 5.1) and textures range from fine-grained to coarsely pegmatitic with varying amounts of quartz, K-feldspar, plagioclase, muscovite, tourmaline and accessory garnet (Fig. 5.4 c, d). Locally, they are rich in mica, both muscovite and biotite, and tourmaline.



Figure 5-4: Textural characteristics and varieties of 1st to 4th- generation pegmatites/granites in the study area; (a) Zoned 1st-generation pegmatite, consisting of a coarser-grained, quartz-rich core; (b) Homogeneous 1st-generation pegmatite showing no zoning or textural variation; (c) Clusters of muscovite books developed in 2nd-generation pegmatite; (d) Equigranular, homogeneous 2nd-generation pegmatite; (e) Close-up and typical example of fine- to medium-grained 3rd-generation granite (f) Rare example of a 3rd-generation granite with very large tourmaline crystals (black spots around rock hammer); (g) Rubellite crystals in a 4th-generation pegmatite. The crystal in the centre of the photo is ca. 30 cm long; (h) Schorl in 4th-generation pegmatite (the blue pen for scale is 14 cm in length); (i) Tourmaline rosette, showing radial growth pattern in 4th-generation pegmatite; note up to 10 cm large euhedral K-feldspar (white-beige) while quartz (dark brown surface staining) is interstitial.

Tourmalines are very abundant (> 5 vol. %) and occasionally display centimetre-scale comb structures, growing from the margins to the interior of individual pegmatite sheets. First- and 2nd-generation pegmatites are mineralogically similar and, in places, difficult to differentiate in the field.

Third-generation pegmatites are texturally distinct from all other generations in the Kranzberg syncline (Fig. 5.4e, f). Compositionally and texturally, they resemble the more leucocratic varieties of the Salem-type Stinkbank granite, located some 10-15 km SW of the study area in the SW hinge of the Kranzberg syncline (e.g. Vietze, 2009). They have been subsequently termed 'granites' throughout the remainder of this thesis. A large sill-like sheet, and three main dyke-like bodies can be distinguished in the study area, cross-cutting 1st- and 2nd- generation pegmatites and the entire Kranzberg syncline at high angles (Figs. 5.1 and 5.3). Third-generation pegmatites mainly occur in Units 1-3 of the Kuiseb Formation.

Fourth-generation pegmatites are very leucocratic and the most coarse-grained pegmatites of all pegmatite generations in the Kranzberg syncline. Large microcline crystals may reach up to 60 cm in length and tourmalines (schorl and rubellite) of up to 30 cm length have been observed (Fig. 5.4g-i).

5.1.2 Dimensions

Pegmatites in the Kranzberg syncline range from large tabular bodies, tens of metres wide and over a kilometre long, to less than one metre wide and ≤ 50 m long (Table 5.1). In places, interconnected dykes and sills may resemble stockworks. Smaller pegmatites (< 20 cm width, < 10 m strike length) are common, but have not been considered in this study. For the most part, the terminations of dykes and sills can be established in the field or on areal photographs, so that the full extent of pegmatites, and therefore their aspect ratios, can be recorded in plan view.

First-generation pegmatites are consistently between 30 cm and one metre in width and are less than 100 m in strike length. There are no systematic variations in

length-to-width ratios between dykes and sills. Second-generation pegmatites range from two to 10 m in width and up to 300 m in length. Aspect ratios of 2nd-generation sills typically range from 75:1 to 20:1. Dykes, in contrast, show much lower aspect ratios ranging from 20:1 to 5:1, resulting in shorter and rather lensoid shapes. Third-generation granites are, by far, the largest intrusives with dykes reaching strike lengths of three kilometres and widths of 50 m. Third- and 4th-generation sills show aspect ratios ranging from 100:1 (in the southern part of the first-order fold hinge) to 10:1 while dykes vary from 70:1 to 10:1. Fourth-generation pegmatites are generally less than three metres in width and ≤ 200 m in length.

5.1.3 Pegmatite-wall rock contacts, xenoliths, and internal features

a. Contacts

Intrusive features, wall-rock contacts and textural characteristics vary for the different generations of pegmatites. Typically, but not always, pegmatite sills and dykes of 1st-, 2nd- and 4th- generations are parallel-sided with smooth, sharp wall-rock contacts (Fig. 5.5 a) while 3rd-generation granites show variable widths along strike and undulating contacts. First- and 2nd-generation pegmatites often contain thin biotite-rich rinds on their contacts. In places, these rinds contain a quartz stretching lineation developed at the very contact between pegmatites and wall rocks (Fig. 5.5b). This quartz-stretching lineation plunges parallel to intersection (L2i) and mineral lineations (L2m) (Figs. 4.11, 4.13, 4.17) and, therefore, also parallel to the regional fold plunge. Reaction zones such as narrow contact metamorphic aureoles around pegmatites, even within presumably highly reactive marble units, are largely absent. In places, marble units may be coarsely recrystallized and bleached over a zone rarely exceeding five centimetres from the pegmatite contact.

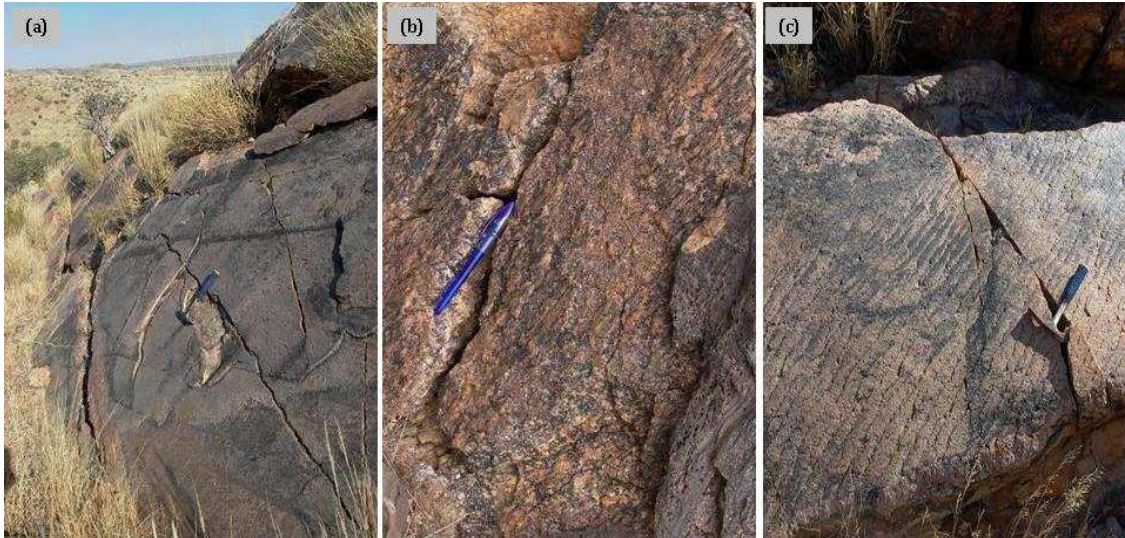


Figure 5.5: (a) Second-generation pegmatite with smooth, sharp wall-rock contact; (b) Quartz-stretching lineation, parallel to pen, on 2nd-generation pegmatite-wall rock contact. Quartz stretching lineation is parallel to the regional fold plunge; (c) Second-generation pegmatite with well defined intersection lineation between S2 and the pegmatite along the pegmatite contact, parallel to hammer handle.

Instead of the commonly observed sharp wall-rock contacts, the pegmatite walls may also show a somewhat serrated surface. This type of contact results from the intersection of the regional S2 foliation with the pegmatite walls, forming a sawtooth-type surface consisting of centimetre-wide steps developed all along the contact surface (Fig. 5.5c). In places, horn structures are also developed at the contacts between the pegmatites and wall rocks, indicating en-échelon or stepping propagation paths of the pegmatite sheets. The geometry of these horn-and-bridge structures provide information related to dyke dilation directions, which is further illustrated in Chapter 5.1.4.

The terminations of dykes and/or sills can be mapped in a number of places. Both dykes and sills commonly taper and are pointed at their lateral termination accounting for the generally lensoid geometry of the pegmatite sheets. The clockwise and anticlockwise rotation of, in particular, 2nd- generation dykes into the bedding plane within 5 - 20 m of their lateral termination is also common and often results in overall sigmoidal shapes (Chapter 5.3).

Once the dykes have rotated into parallelism with the bedding, and assume a sill-like geometry, they either become boudinaged and terminate with 2 - 10 m or may continue as bedding-parallel sills for tens of metres. This relationship between dykes and sills is critical for an understanding of the emplacement characteristics of the pegmatite sheets and will be illustrated and discussed in more detail in Chapter 5.3.

The interface between marble units of e.g. Unit 1 of the Kuiseb Formation or marbles of the Karibib Formation with siliciclastic units (e.g. biotite schists, metapsammites, etc.) represents an evidently sharp rheological boundary. Often dykes, even prominent ones that are several metres wide, have undergone tight folding and then terminated only a few metres into the marble units.

b. Xenoliths

Pegmatite sills and dykes contain only a few wall-rock xenoliths (Fig. 5.6a,b). Where present, the xenoliths are derived from the immediate wall rocks and mostly of the Kuiseb Formation. Xenoliths are recorded primarily in 2nd-generation pegmatite sills, and in 3rd- and 4th-generation dykes (Fig. 5.6).

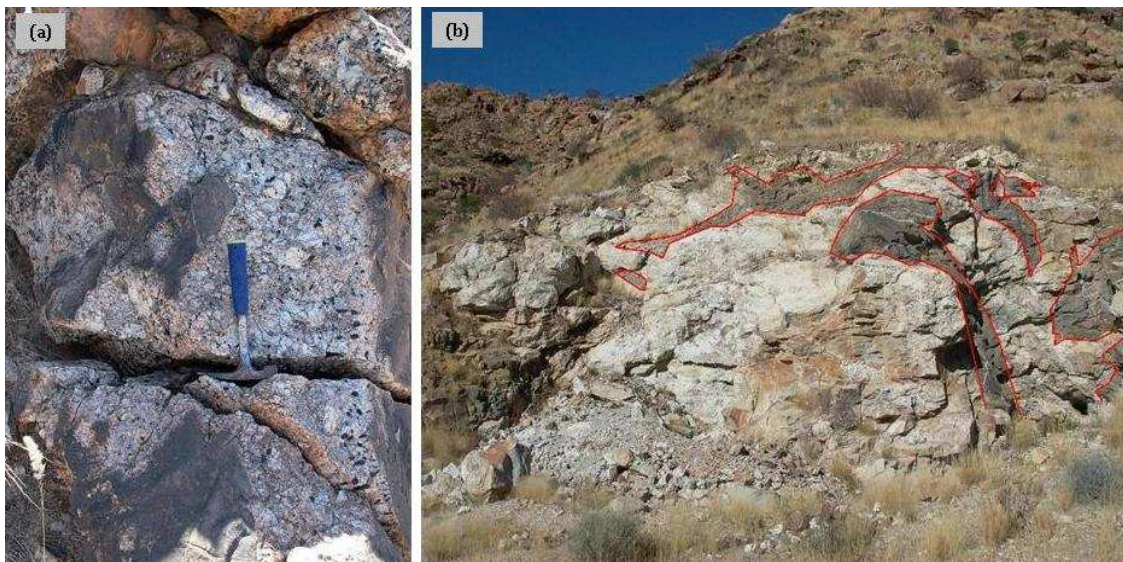


Figure 5.6: (a) Second-generation pegmatite sill with country rock fragments, here, biotite schists of the Kuiseb Formation (dark grey). Note that tourmaline at wall-rock contact is growing perpendicular to the contact; (b) Fourth-generation pegmatite with large, metre-wide/-long country-rock screens (annotated by red line).

The fragments are either angular and rather equidimensional, or elongated parallel to the pegmatite margins, rather resembling wall-rock screens. The narrow and elongated wall-rock screens seem to have been pried off the wall rocks by either apophysis of the main pegmatite intrusion, or, in places, multiple pegmatite sheets. Angular fragments can, in places, be seen to represent broken off wall-rock bridges between two adjacent *en-echelon* segments of pegmatite sills and/or dykes. For the most part, xenoliths do not seem to have undergone any rotation within the pegmatites, given that the internal banding (S0) and fabrics (S1 and S2) in xenoliths are parallel to that in the wall rocks. The presence of tectonic fabrics in xenoliths also highlights the relative timing of pegmatite intrusion. In places, xenoliths of Kuiseb Formation show characteristic cusp-like shapes and contacts against the surrounding pegmatites. This suggests the deformation of the less competent wall-rock xenoliths within the coarse-grained pegmatites, although the latter may be devoid of any fabrics.

c. Internal textures and zoning

Pegmatites of the Kranzberg syncline are either massive, layered or zoned (Fig. 5.7a-h). Layering is particularly common in 1st- and 2nd-generation pegmatites, while 3rd-generation pegmatites show mainly massive and homogeneous textures. Layering in the 1st- and 2nd-generation pegmatites is expressed as subtle variations in grain size and composition, mainly through differing amounts of biotite and/or tourmaline (Fig. 5.7b, c, d).

The internal layering is commonly parallel to the sides of pegmatites, and can be traced for several metres along strike. The contacts between individual layers are generally sharp, and display either planar and straight, or slightly undulating geometries. The origin of this layering is not clear. Comb structures are best observed in 2nd-generation pegmatites, where tourmaline crystals commonly grow inwards and normal to the pegmatite walls (Fig. 5.7e, f). Locally, multiple comb structures are developed within a single pegmatite, indicating multiple sheeting has taken place.



Figure 5.7: (a) Compositional and textural variations in 2nd-generation pegmatite, expressed by alternating coarse- and fine grained layers subparallel to the pegmatite margin. Differential weathering gives a stepped appearance to the right of the pencil; (b) Finer grained, granitic core, bordered by coarser grained, pegmatitic margins in a 2nd-generation pegmatite; (c) Compositional and textural layering in 4th-generation pegmatite defined by variable amounts of garnet (centre) and tourmaline (margin), as well as grain-size variations; (d) Subtle variations in biotite content leading to layering-type structures in 3rd-generation granite, note that boundaries between individual layers are sharp; (e and f) Tourmaline defining comb textures along the margin of 2nd-generation pegmatites, with tourmaline growth oriented normal to wall-rock contacts; (g) Zoning in 1st-generation pegmatite, showing a quartz- and tourmaline- rich miarolitic cavity in the core of the pegmatite; (h) Third-generation granite with sigmoidally shaped miarolitic cavity, showing the intergrowth of quartz (grey), K-feldspar (pink-beige) and tourmaline (black).

Miarolitic cavities are locally developed in 1st- and 2nd- generation pegmatites and are characterized by roundish- to elongate, coarse-grained, quartz-filled pockets, parallel to the margins and internal zoning of the pegmatites (Fig. 5.7g). Graphic intergrowths of quartz and tourmaline or quartz and feldspar are common in these pockets. Miarolitic cavities in 3rd-generation granites form, in places, late-stage ellipsoidal and often slightly sigmoidal fracture fillings enclosing angles of 15° up to 90° to the wall-rock contacts (Fig. 5.7h). With the exception of occasional quartz ribbons and muscovite books forming a margin-parallel foliation, structural fabrics are rarely observed in the pegmatites.

In summary, textural and mineralogical variations in pegmatites of the Kranzberg syncline can be ascribed to mainly (1) the crystallization and *in situ* differentiation of pegmatites, mainly expressed by a systematic zonation in the pegmatite sheets, and (2) multiple intrusive relationships.

5.1.4 Opening mode of pegmatite sheets

The propagation of sheet-like intrusives, e.g. mafic dykes and sills, or, in the present case, pegmatite dykes and sills, is commonly interpreted to have occurred as extensional (Mode I) and, to a lesser extent, shear (combined Mode II and III) fractures (e.g. Anderson, 1936, 1951; Morris et. al., 2008). In order to demonstrate the nature and origin of the fracture propagation, it is important to establish the opening mode of wall rocks adjacent to the pegmatite dyke and/or sill. Wherever possible, the opening vector across pegmatites was established by the relative displacement of matching lithologies and/or marker horizons across the pegmatite. While primary bedding is, for the most part, well preserved in the Kuiseb Formation, the relatively monotonous composition of particularly Units 2 and 3 make an unambiguous correlation of lithologies across the dykes often difficult, whereas marble- and calc-silicate horizons in e.g. Unit 1 provide good marker horizons. In case of larger dykes, the high-resolution Google Earth Imagery gives a good indication of relative displacements of units across the dykes (Fig. 5.8).

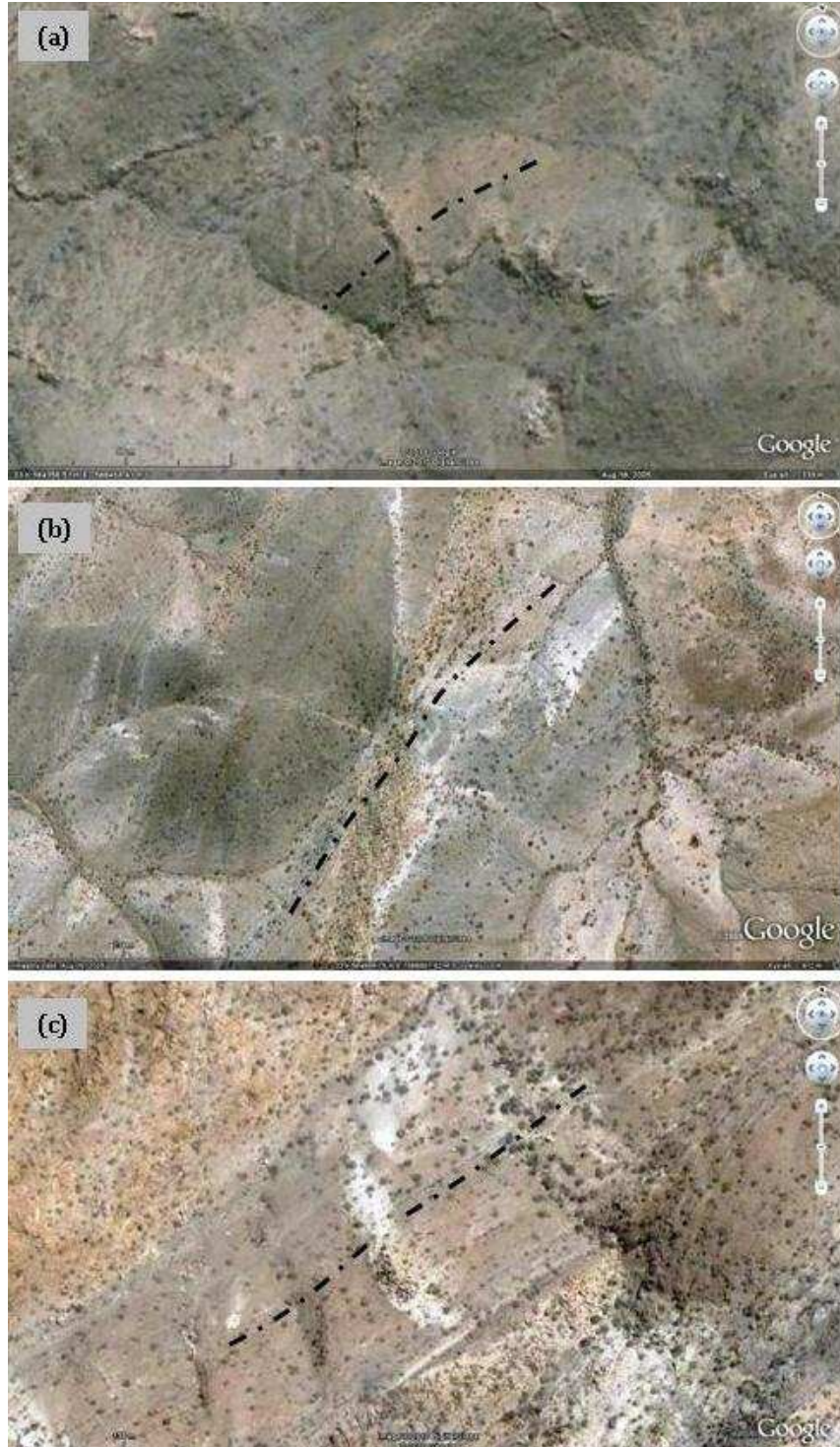


Figure 5.8: Google Earth images illustrating relative wall-rock displacements across 2nd- (a), 3rd- (b), and 4th- (c) generation pegmatite dykes. Bedding is annotated by black dash-dotted lines parallel to metapsammitic, marble and calc-silicate horizons, respectively. The lack of any lateral displacement of the mainly steep strata across the subvertical dyke walls suggest a Mode I opening of the pegmatite-filled fractures.

Comb structures along the margins of the pegmatites were also taken as an indication of the opening vector as crystal growth typically follows the cooling gradient of the pegmatite and tracking the opening vector of the intrusive sheet. Therefore, with tourmaline crystals regularly oriented normal to the pegmatite/wall-rock margin, an extensional (Mode I) opening is suggested. Moreover, where developed, horn-and-bridge structures (Fig 5.9-5.11) were used to establish dyke propagation and dilation directions (illustrated by rose diagram inserts in Fig. 5.9-5.11). Based on these criteria, both pegmatite sills and dykes in the Kranzberg syncline can overwhelmingly be regarded as having filled dilatational (Mode I) fractures, recording opening directions normal to their walls.

5.2 PEGMATITE ORIENTATIONS AND GEOMETRIES

A synopsis of dyke and sill orientations for each pegmatite generation in the respective structural domains of the Kranzberg syncline is provided in figure 5.12.

5.2.1 Orientation and Geometries of 1st-generation pegmatites

First-generation pegmatites are volumetrically minor and occur mostly along the normal limb. Sills show NE trends and shallow- to moderate SE dips, parallel to bedding. Dykes along the limbs have NW or S strikes with shallow to moderate dips to the NE and W respectively. The intersection lineation between the dykes and sills along the normal limb shows a shallow, SSW plunge (Fig. 5.12a). Towards the hinge, the dykes seem to undergo a rotation together with the bedding, showing W trends (Fig. 5.12d).

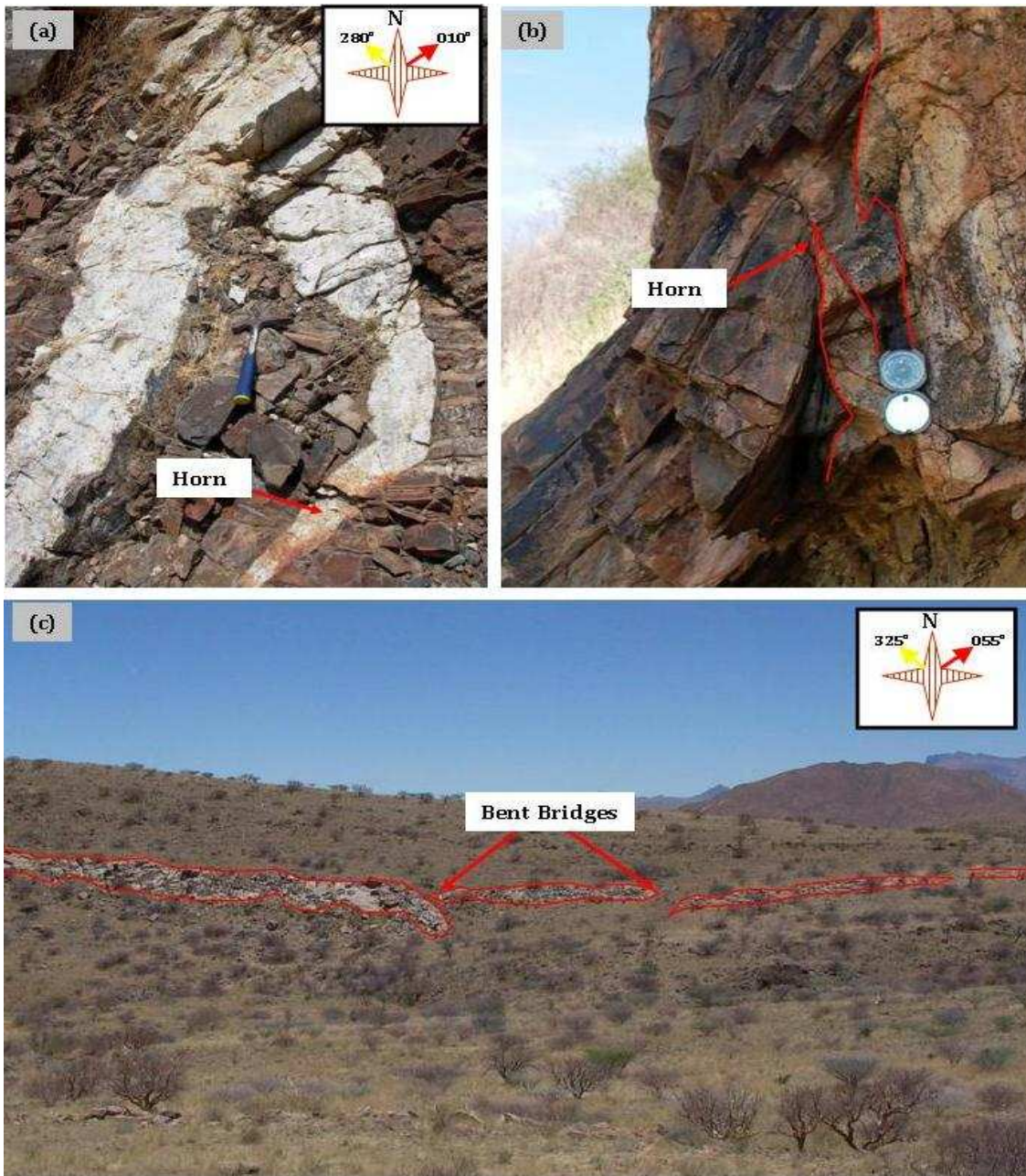


Figure 5.9: (a) Horn-and-bridge structure developed in a 4th-generation pegmatite; (b) Small-scale horn structure in a 3rd-generation granite on a vertical section, viewed along strike. Note also a slight upward rotation (drag?) of wall rocks adjacent to the granite sheet; (c) Coordinates UTM 564508E; 7565655S WGS 84. Composite 2nd-generation sills showing curling of tips along the termination of individual en-échelon segments. The en-échelon sills are not connected on surface and preserve bent wall-rock bridges between them. Inserts: on the compass, the red arrow indicates the orientation of the pegmatite while the yellow arrow shows the direction of fracture dilation.

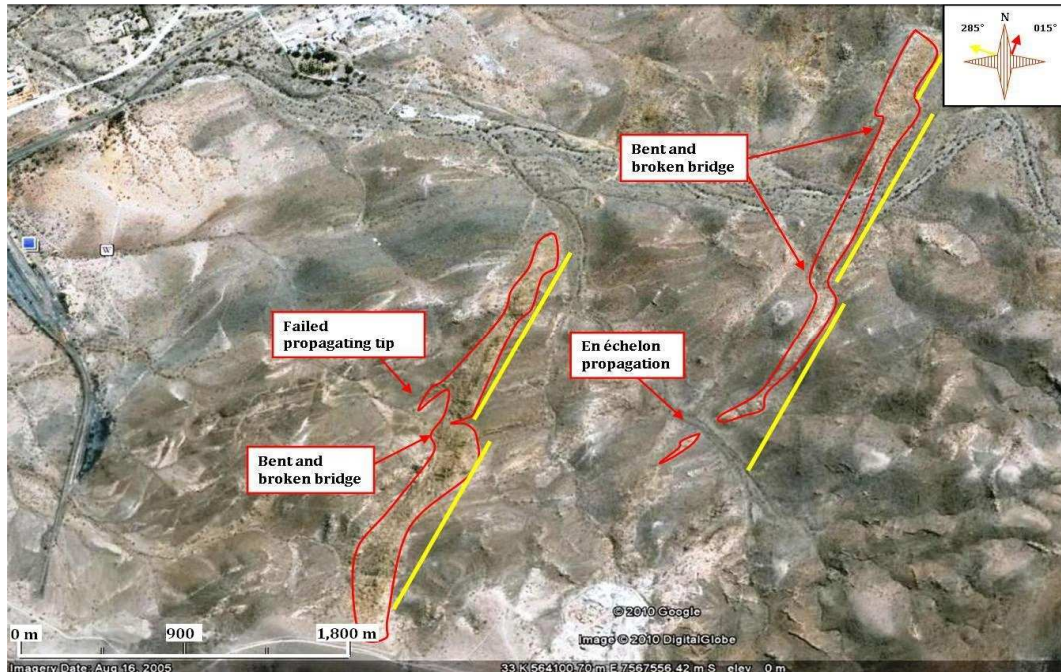


Figure 5.10: Third-generation granite dykes illustrating slightly curved (western dyke) and linear (eastern dyke) propagation paths. Yellow lines in image are equidistant and parallel to each other, used to illustrate the left-stepping *en-echelon* emplacement of the dykes cross-cutting the syncline. Location and scale are given at the bottom of the Google Earth image. Rose diagram in insert showing dyke propagation (red arrow) and dyke dilation (yellow arrow) directions.

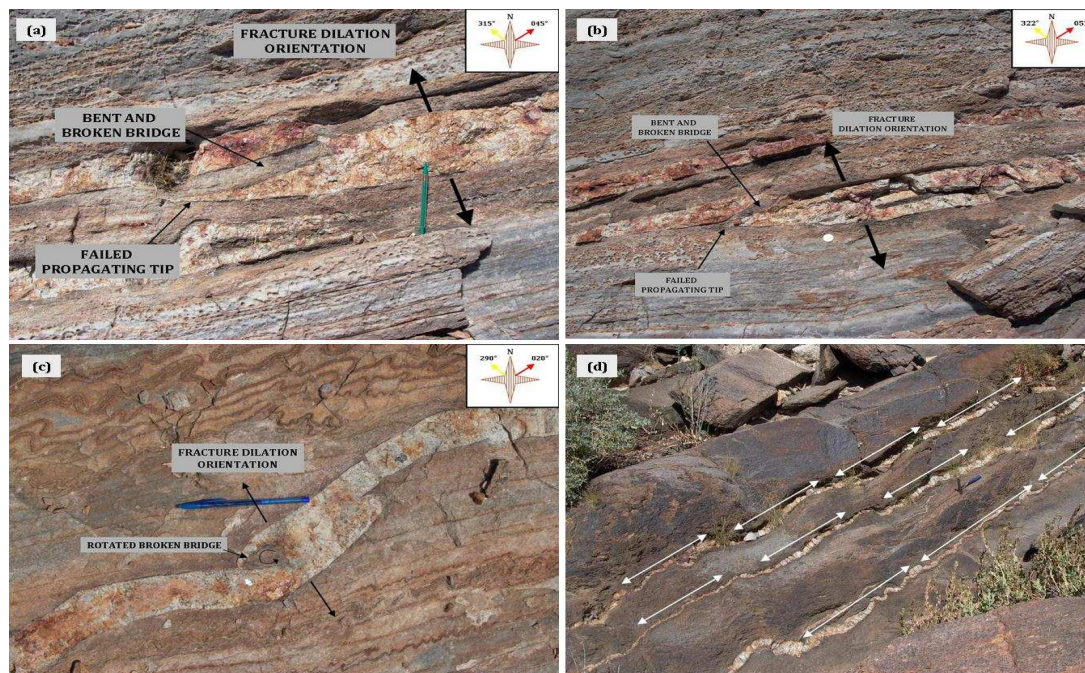


Figure 5.11: Examples of thin, 4th-generation pegmatites showing a stepping, *en-echelon* emplacement, indicating that fracture formation was determined by both near-field and far-field stresses. Inserts: on the compass, the red arrow indicates the orientation of the pegmatite while the yellow arrow shows the direction of fracture dilation. (a) and (b) illustrate linear propagation paths in marbles, suggesting that emplacement was controlled by regional (far field) stresses; (c) and (d) illustrate curved propagation paths employed in (c) marbles and (d) cordierite schists. The curved propagation paths and interacting dyke tips indicate near-field dominant stresses at the time of emplacement. Double ended arrows in (d) illustrate how the *en-echelon* fracture formed nearly equidistant steps.

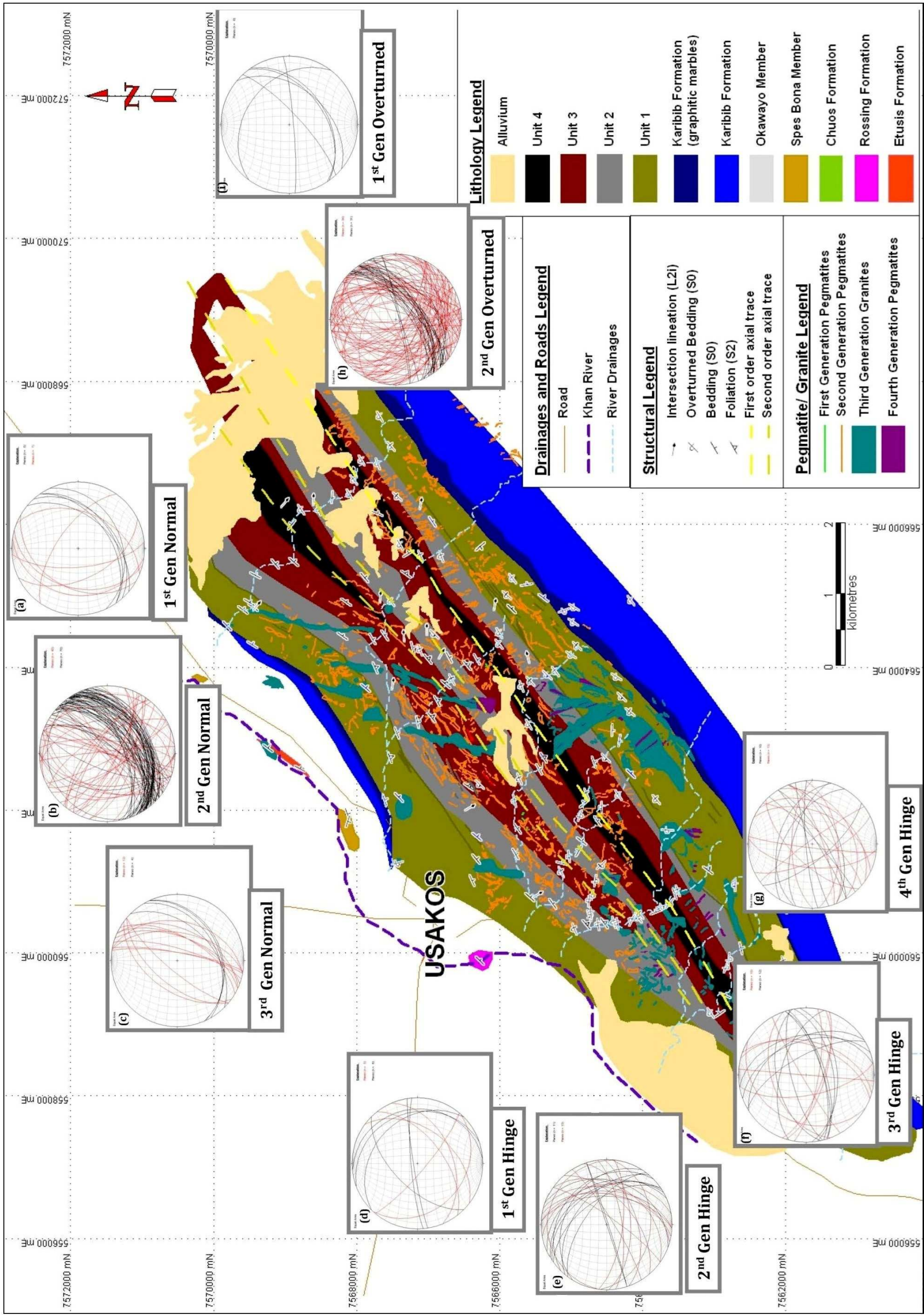
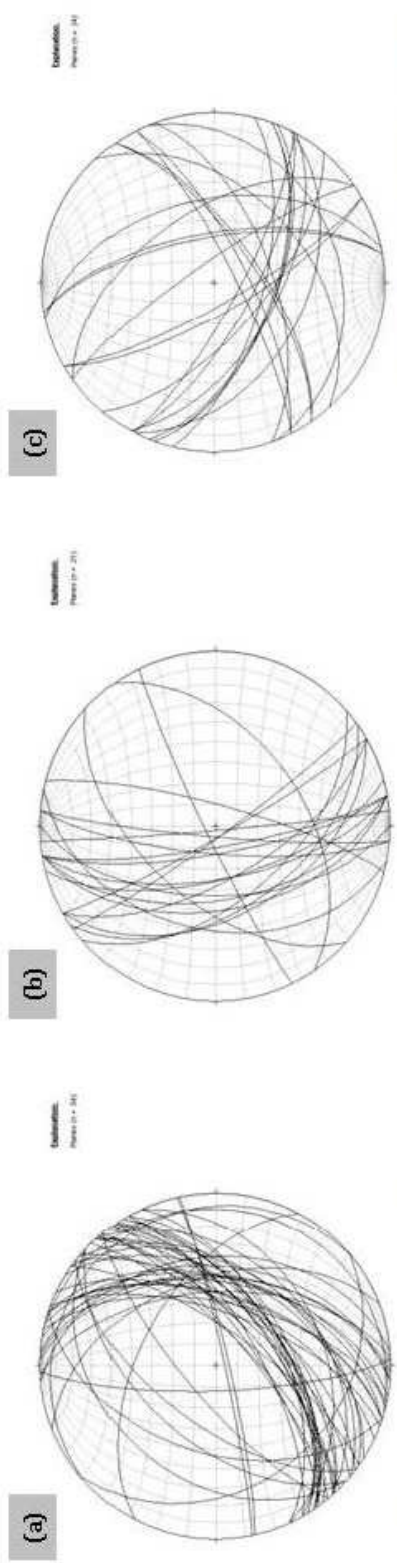


Figure 5.12: Map showing stereonet for pegmatite dykes (red great circles) and sills (black great circles) and 1st- to 3rd- generation stereonet domains are provided for the normal limb (a-c), 1st- and 2nd- generation stereonet for the overturned limb (d-g), and 1st- to 4th- generation for the hinge (h-1), and 1st- to 4th- generation for the hinge (d-g). (a) n=12 (b) n=110 (c) n=16 (d) n=11 (e) n=26 (f) n=22 (g) n=23 (h) n=125 (i) n=6.

5.2.2 Orientation and Geometries of 2nd-generation pegmatites

Second-generation pegmatites are by far the most widespread of the four pegmatite generations. Despite their occurrence throughout the stratigraphic sequence exposed in the Kranzberg syncline, they appear to be more abundant along the normal and overturned limbs, showing lower abundances towards the southwesternmost area of the first-order hinge. They are invariably deformed, but, for the most part, it is assumed that they largely preserve their original emplacement geometries and orientations without having undergone significant passive rotation. Exceptions to this occur in the hinge of the syncline as well as possibly on the SE limb (see below). Orientations of 2nd-generation dykes appear to be scattered at first, but, upon closer inspection, reveal well developed sets, with slight variations in their trends. Along the normal and overturned limbs, dykes and sills describe three main orientations (Fig. 5.12b, e and h): (1) NE-trending, moderate- to steeply-dipping, bedding-parallel sills; (2) NW-trending, moderate- to steeply-, mainly SW-dipping dykes. The strike of these dykes is parallel to the regional D2 (NW-SE) bulk shortening strain (Chapter 4) and; (3) N- to NNE-trending, moderate- to steeply dipping dykes that are perpendicular or at high angles to the E-ESE plunging F2 fold hinges of the Kranzberg syncline and lower-order folds.

Second-generation pegmatites in the first-order hinge show two dominant trends, namely to the E and to the NW (Fig. 5.12e). The different lithologies of the Kuiseb Formation appear to have had a significant influence on pegmatite geometries and emplacement. This is particularly pronounced in 2nd-generation pegmatites along the overturned limb, where pegmatites are predominantly sills in the lithologically heterogeneous Unit 1, but occur as mainly cross-cutting dykes at higher stratigraphic levels. Pegmatite geometries and orientations for a section along the overturned limb, and containing the different units of the Kuiseb Formation are shown in figure 5.13a-d.



Pegmatite Orientations in Unit 3-4

Pegmatite Orientations in Unit 2

Pegmatite Orientations in Unit 1



Figure 5.1.3: Second-generation pegmatite orientations within specific lithological units of the overturned limb. Unit 1 consisting of calc-silicate felses, marbles, metapsammites and metapelites, shows NNE striking dykes, but the majority of pegmatites are steep SE-dipping, bedding-parallel sills. Unit 2 consists of mostly metapelites and shows predominantly dykes with consistently S-SSE strikes. This pattern of short, highly cross-cutting dykes is developed in Unit 2 over a distance of, at least, 5 km. Sills are very subordinate in Unit 2. Units 3-4 consist of thick metapsammites and interlayered metapelites containing a prominent dyke set striking SE, with only subordinate sills. (a) n = 54 (b) n = 21 (c) n = 24.

Unit 1: metapsammites, biotite schists, marbles and calc-silicate felses

In Unit 1, pegmatite sills clearly dominate over cross-cutting dykes. The NE-striking sills are preferentially emplaced at contacts between metapelitic units and marbles or calc-silicate units, commonly extending for hundreds of metres along strike. Pegmatite sills here are much wider compared to sills elsewhere in the Kranzberg syncline, reaching thicknesses of up to 10 m.

Dykes show relatively consistent NNE trends and steep ESE dips (Fig. 5.13a). Systematic variations in trend point to a refraction of dykes between different units of the lithologically heterogeneous Unit 1. The majority of dykes along the overturned limb occurs near the hinge of a third-order fold, close to and just above the contact between marbles of the Karibib Formation and Unit 1 of the Kuiseb Formation.

Unit 2: Metapelitic quartz-biotite schists

In contrast to Unit 1, Unit 2 contains predominantly S-SSE striking and moderate- to steep W dipping dykes. These dyke trends in Unit 2 record an anticlockwise rotation of 20°-30° compared to dykes in Unit 1 (Fig. 5.13 a and b). In this orientation, dykes within Unit 2 are approximately normal to mineral stretching lineations (Lm2) and the regional fold plunge (F2a, b). Their lengths rarely exceed the width of Unit 2 (ca. 100 to 200 m) and the dykes terminate sharply against the stratigraphically overlying metapsammitic horizons of Units 3 and 4 and the underlying marble-dominated succession of Unit 1 highlighting the controls of lithology on their emplacement. The dykes show lensoid shapes in plan view, reaching the largest widths in the centre and gradually tapering towards their lateral terminations. The dykes show multiple intrusive relationships, made up of closely-spaced (ca. 1-5 m) dyke segments. These dyke clusters are spaced on average by 100 m with intervening areas showing very few thin dykes, or no dykes at all. This contrasts to

units 3 and 4, where dykes have a much wider spacing, occurring every 100 to 500 m (see Chapter 6.3.2). Sills are conspicuous by their absence in this unit.

Units 3-4: Metapelites and interlayered metapsammities

With the introduction of prominent metapsammitic horizons into Unit 3 and 4, pegmatite dykes show a re-orientation to two main sets, namely (1) a dominant SE-striking and steep SW-dipping set, and (2) a less common NNW-striking, steep ENE-dipping set (Fig. 5.13c). These two orientations possibly form a conjugate set, with the regional NW-SE directed shortening strain forming the bisectrix of the acute angle between the two sets. Sills are present, though subordinate and are largely confined to the contact between Units 2 and 3, again indicating that pronounced lithological variations exert a control on pegmatite emplacement.

In summary, the occurrence of wide, laterally continuous sills at prominent bedding contacts and the slight variations in dyke orientations within different stratigraphic levels in Unit 1 are likely due to the lithological heterogeneities in the alternating marble and schist succession of the lowermost unit of the Kuiseb Formation. In the metapelite-dominated Unit 2, dykes are the preferred style of emplacement. These dykes either terminate along the contacts with the stratigraphically higher Units 3 and 4 or they may undergo a slight rotation in the metapsammite-dominated higher units. Importantly, as some of the dyke orientations (ie. between Units 2 and 3-4) merely change by 20°-30°, this may reflect a strain refraction between the lithologically different Units 2 and 3/4 (Fig 5.14). An attempt to relate stereographic projections to a 3D model of pegmatite orientations has been made in figure 5.15.

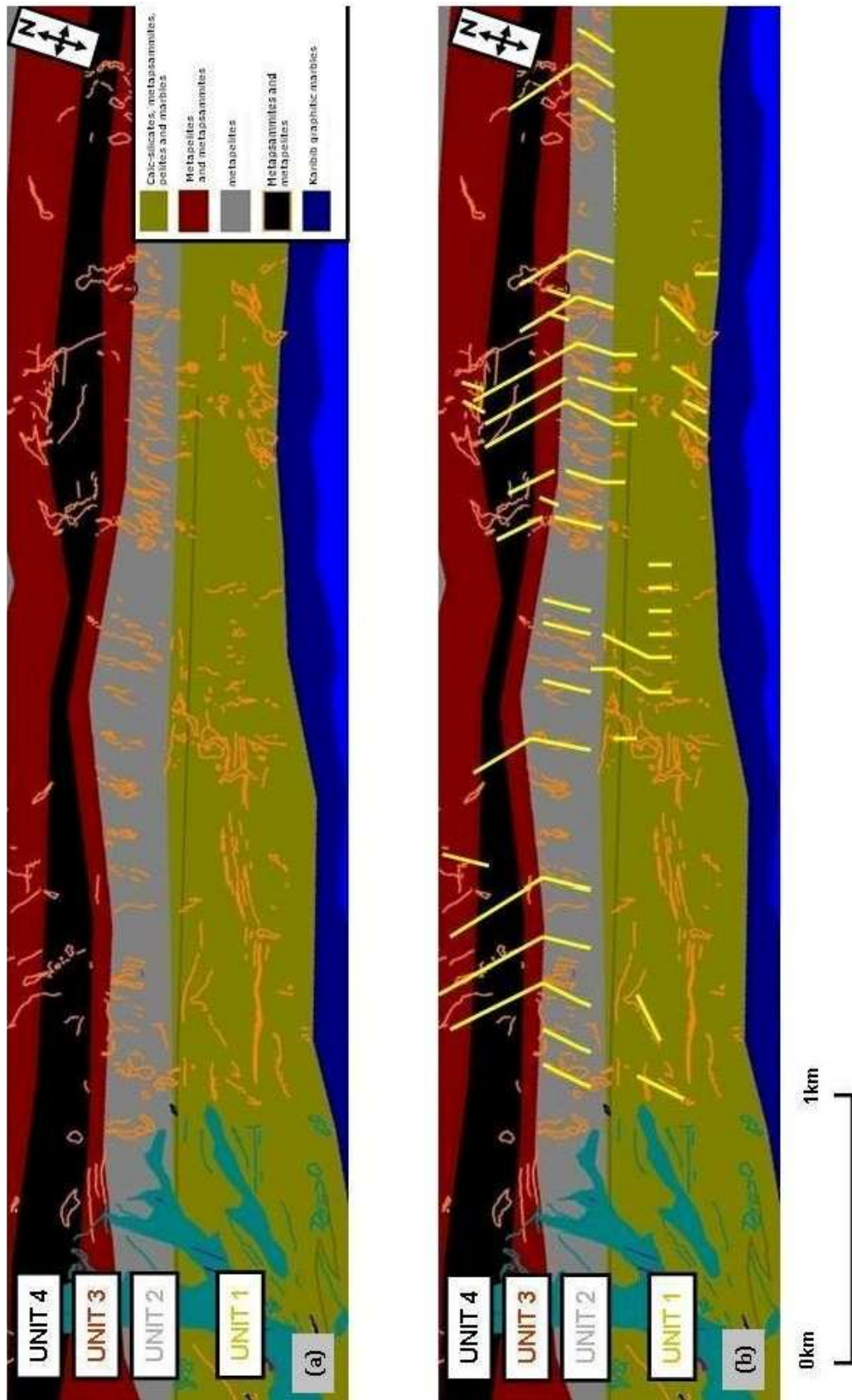


Figure 5.14: (Top) Lithological map of the overturned limb of the Kranzberg syncline with 2nd-generation pegmatites marked in orange. The geological maps shown here cover the area shown in Fig. 5.13.; (Bottom) Yellow lines illustrate the general trend of dykes and the seemingly systematic refraction of pegmatites in different lithologies in different units. Note that Unit 1 is dominated by sills (NE trending pegmatites) in comparison to Unit 2 and Unit 3-4.

Second-Generation Pegmatite Orientations within Lithological Units of the Kuiseb Formation along the Overturned Limb

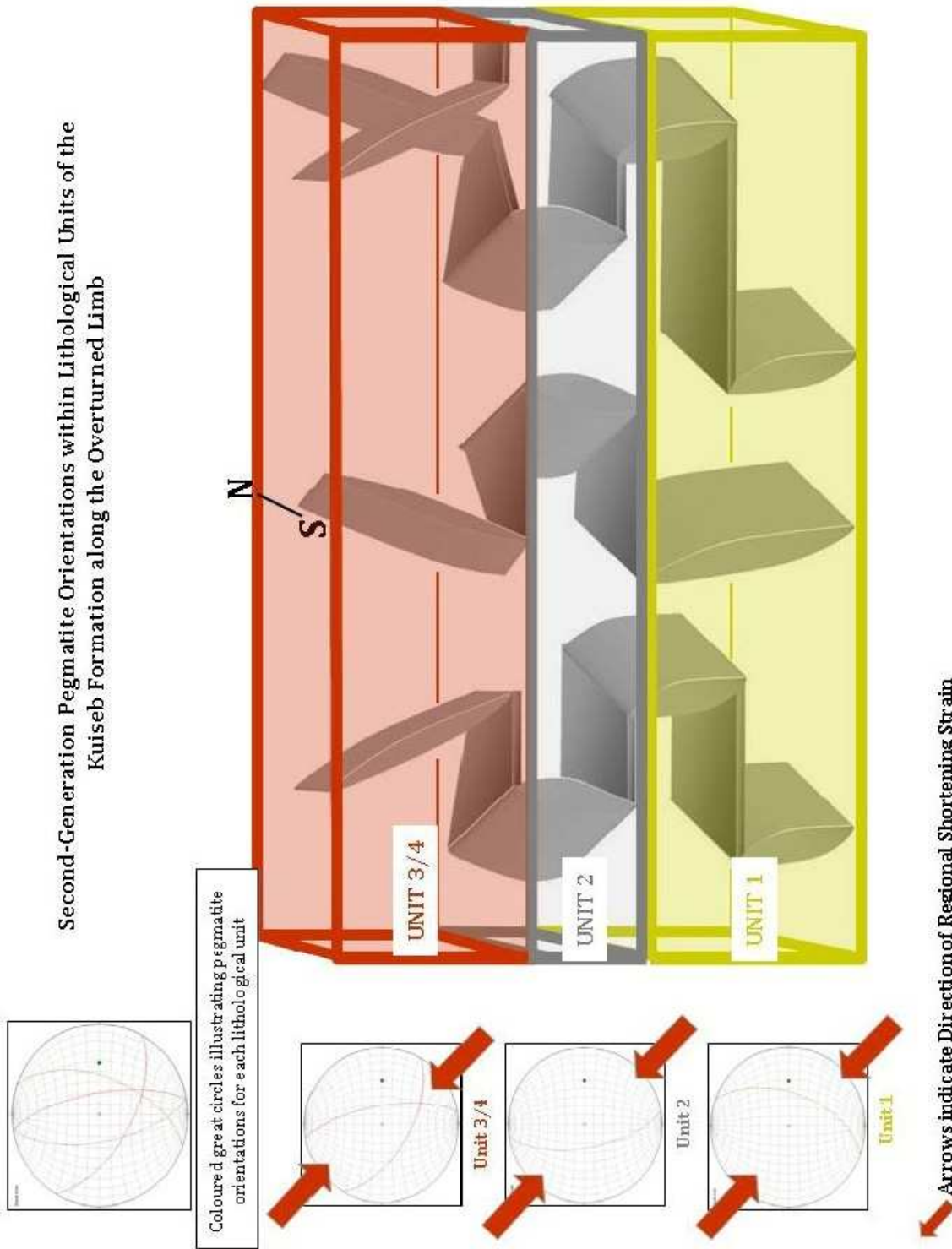


Figure 5.1.5: Schematic sketch illustrating the general geometry (dyke or sill) and orientation of 2nd-generation pegmatites in lithological units of the Kuiseb Formation along the overturned limb. Stereonets illustrate the average pegmatite orientation for each lithological unit and its relationship to the regional shortening strain. Green dots on stereonets represent the regional fold plunge for the study area. Bedding is dipping steeply towards the reader (NE).

5.2.3 Orientation and Geometries of 3rd-generation Granites

Mainly developed in Units 1-3, 3rd-generation granites are regionally the most voluminous intrusives in the Kuiseb Formation. The granites occur as three distinct geometries; (1) three voluminous dykes cross-cutting part of the overturned and all of the normal limb of the first-order fold, (2) voluminous, sill-like sheet(s) along the southern end of the overturned limb, and (3) a network of interconnected dykes and sills in the first-order hinge (Fig. 5.12). Granite dykes cross-cut the entire syncline, but terminate abruptly, where they intersect the second-order synclines that expose the stratigraphically highest Unit 4, characterized by massive metapsammitic horizons. Here the dykes pinch and form up to 600 m wide gaps, but they are developed on both sides of Unit 4. The effect of lithological controls on the emplacement of 3rd-generation dykes on the normal limb is furthermore suggested by the pronounced pinching of the dykes particularly where they cross-cut marble horizons of e.g. Unit 1. At these contacts, up to 50 m wide pegmatites narrow to less than 5 m before ballooning within metres of crossing the marble horizons (Fig. 5.16).

The marble units at these contacts, along with metapelites and metapsammites, often display, in plan view, a type of drag effect (Fig. 5.17). However, it is not clear whether this is an emplacement-related effect, i.e. wall-rock deformation and drag in response to dyke emplacement, or a post-emplacement drag along the pegmatite dykes as recorded in e.g. flanking structures (e.g. Passchier, 1998). Exposures of 3rd-generation granite host-rock contacts are rare so that orientation data are somewhat limited to the strike of the granite dykes. The dominant trend of the granites along the normal limb is approx. 010° with dip directions both to the ESE and WNW (Fig. 5.12c). Locally, less than three metre wide offshoots from larger dykes show trends between 010° and 070°.

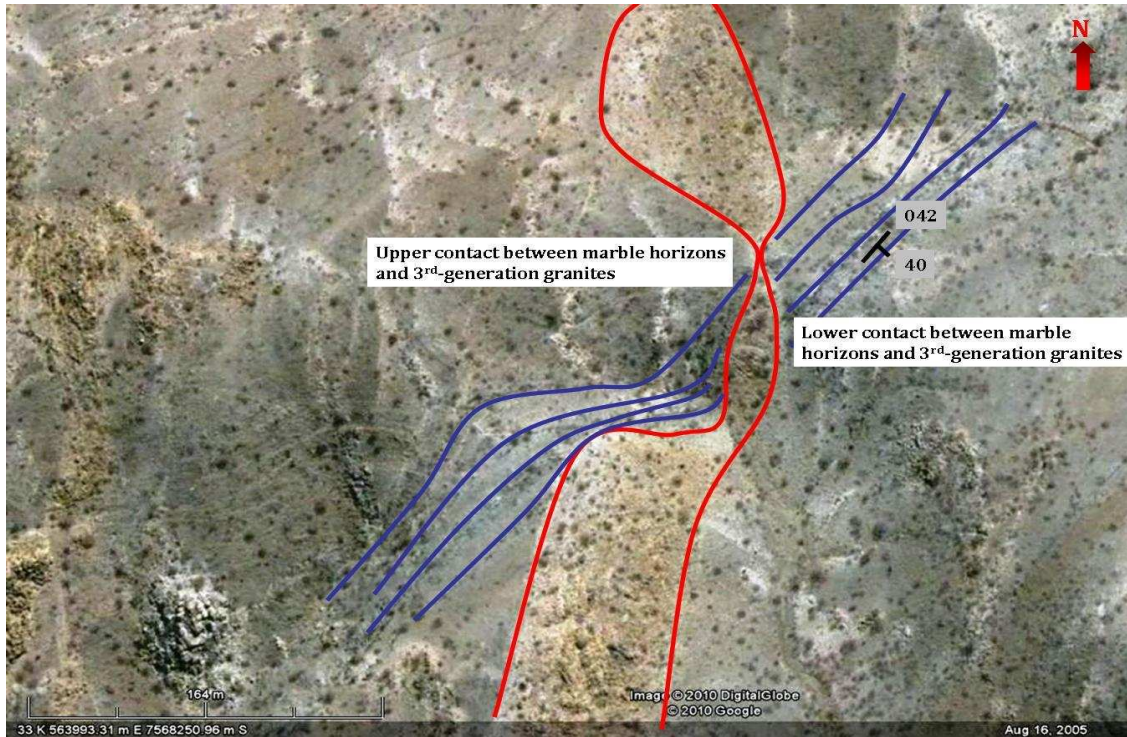


Figure 5.16: Third-generation granite dyke (outlined in red) pinching upon cross-cutting a prominent marble horizons (trend indicated by blue lines) in Unit 1 of the Kuiseb Formation. Bedding strikes at 042° and dips at only 40° , which causes the V-shaped deflection of the outcrop into the valley. The granite dyke is ± 50 m in width, but is reduced to only a few metres and down to 1 m in width as it intersects the topmost marble horizon, and ballooning to its original width within only 30 m of leaving the marbles. Coordinates UTM 563993E; 7568251S WGS 84.

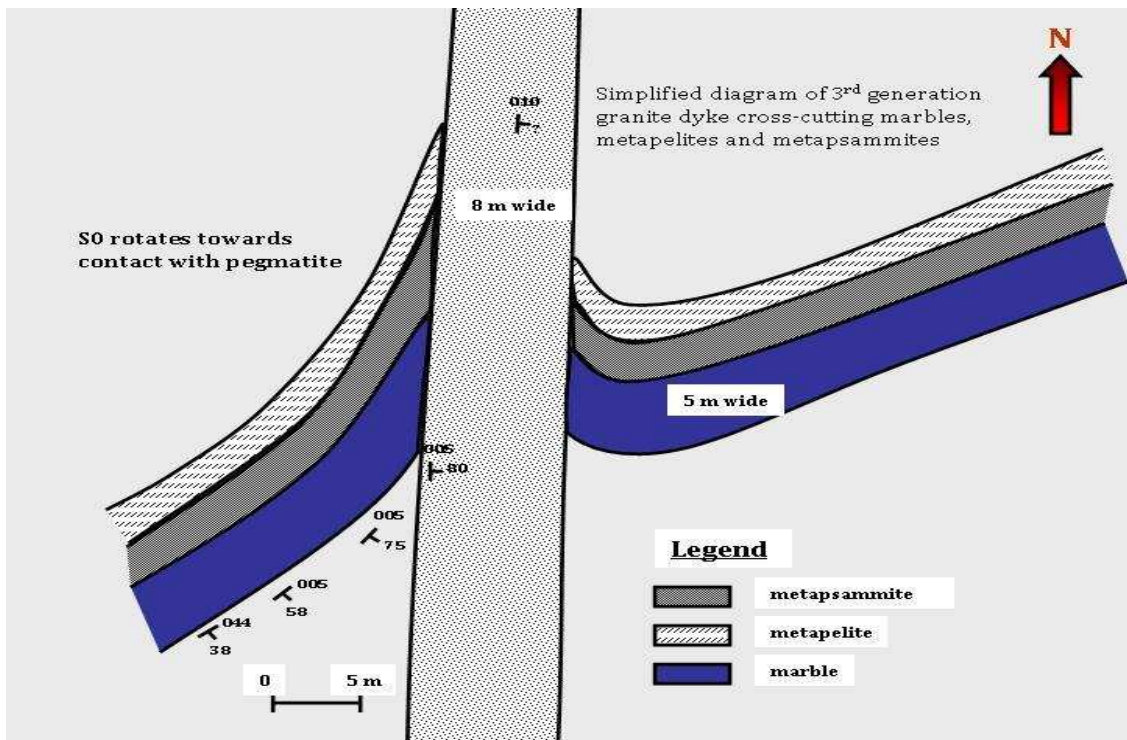


Figure 5.17: Simplified sketch of 3rd-generation granite dyke cutting through five metre wide marble horizon, plan view.

Along Unit 1 of the overturned limb, 3rd-generation granites form large sill-like masses. They also commonly occupy the closures of third-order anticlinal folds, forming elongate, up to 30 m wide and 100 m long granite blows. The upper and lower boundaries of these granites are commonly marked by prominent, up to 8 m wide marble horizons. The largest of the intrusions is located near the southern end of the overturned limb, where an elongate, up to 300 m wide and 1.3 km long sill-like granite is readily evident on remote imagery. This sill-like granite stock branches out into a network of interconnected dykes and sills of varying widths and lengths towards the N and NW and the adjoining hinge domain (Fig. 5.18).

Orientations of 3rd-generation granites in the hinge are summarized in figure 5.12f, with two general trends apparent; (1) a N-S trending, moderately E-dipping set at high angles to F2 fold hinges, and (2) an E-W trending, moderate- to steeply N- and S-dipping set. Although cross-cutting, third-generation granites are subparallel to bedding in the first-order hinge, they are not to the same extent as the 2nd-generation pegmatites, suggesting that the granites have not been affected by folding to the same extent.

5.2.4 Orientation and Geometries of 4th-generation Pegmatites

Fourth-generation pegmatites are almost only observed along the southern part of the overturned limb and in the first-order hinge, with isolated occurrences near the axial trace of the Kranzberg syncline, the Usakos pegmatite mine being an example of this (Fig. 5.12). Field observations suggest this generation to be preferentially emplaced into Units 1 and 2 of the Kuiseb Formation and locally within graphitic marbles of the Karibib Formation. In the first-order hinge, they show two dominant trends, namely to the E and the NW (Fig. 5.12g).

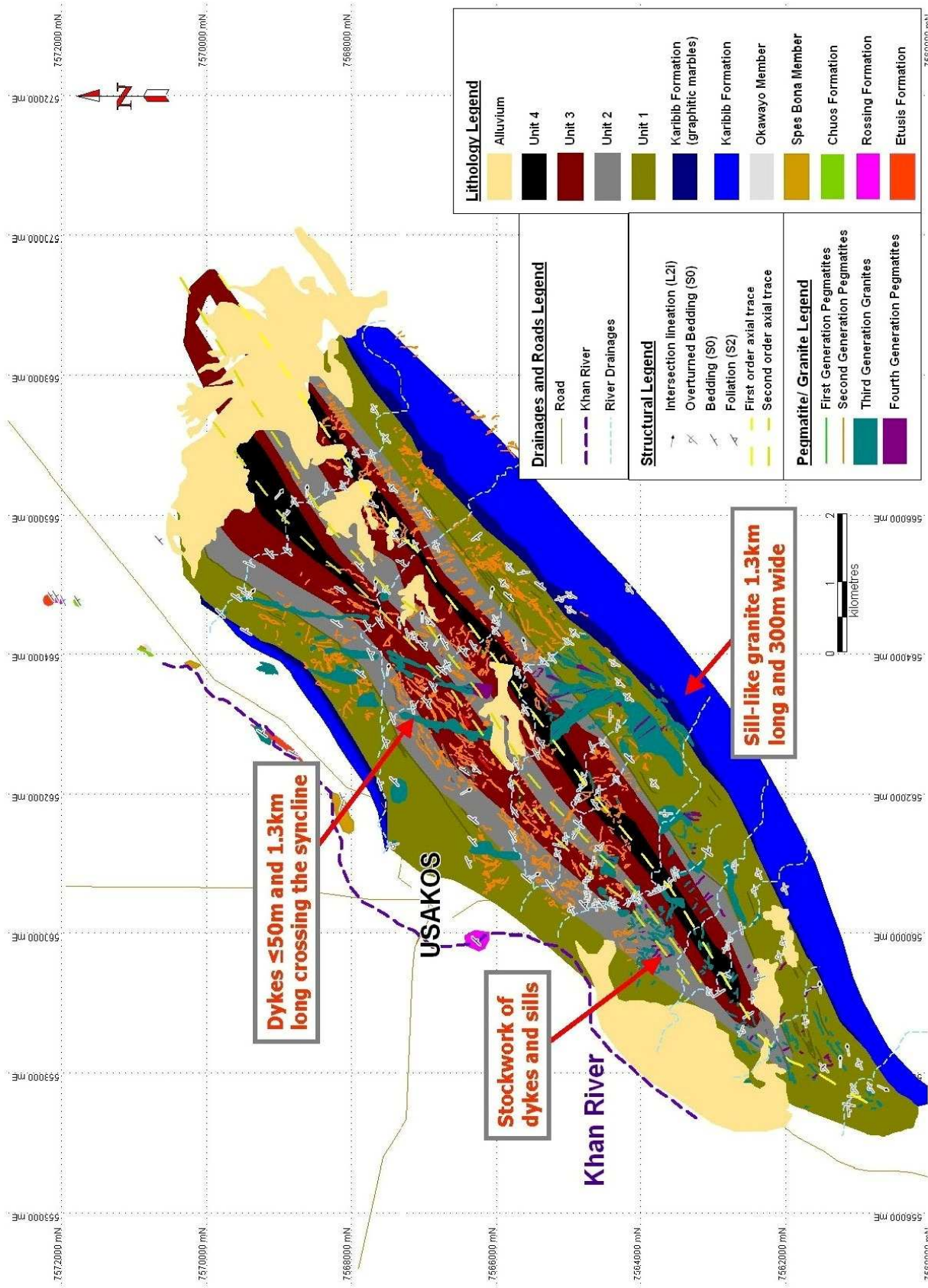


Figure 5.18: Geological map illustrating locations of pegmatites and granites in the syncline. Third-generation granites form dykes cross-cutting the entire syncline to the NE, a large sill-like mass at the southern end of the overturned limb towards the SE, and a stockwork of dykes and sills further into the hinge domain to the SW.

5.3 EMPLACEMENT STYLE AND PEGMATITE GEOMETRIES

All four generations of pegmatites exhibit systematic variations in emplacement styles and geometries depending on (1) the structural domain, and (2) the lithological unit in which they occur. In the following section, emplacement geometries are described for a number of well-exposed examples.

5.3.1 First-Generation Pegmatites

Cross-cutting relationships between these early dykes and sills are only rarely exposed and it remains unclear whether they are contemporaneous or have been emplaced successively. They are, however, clearly cross-cut by later generation pegmatites, testifying to their early emplacement.

5.3.2 Second-Generation Pegmatites Emplacement

As outlined in Chapter 5.2, 2nd-generation pegmatites show both dyke and sill geometries that form an intersecting network. However, the differently orientated sheets do not merely form cross-cutting sets, but gradational contacts between different pegmatite geometries are common. During field work, two main lines of evidence have been used to indicate the relative timing of dykes and sills with respect to each other:

(1) Obvious cross-cutting relationships and mineralogical and/or textural changes across intersecting pegmatites that indicate the successive emplacement of pegmatites. Based on this, the main subdivision into 1st- to 4th- generation pegmatites has been established.

(2) Truncating relationships and/or the displacement of pegmatite sheets across each other have been taken as a further indication of their relative timing. In cases, where there are no clear truncating relationships and where mineralogical and textural continuity is maintained between intersecting sheets, differently orientated

pegmatite geometries are interpreted to have intruded at the same time. Moreover, the termination of dykes into sills and vice versa, is interpreted to indicate the contemporaneous emplacement of the two different geometries rather than representing merely cross-cutting sheets.

Wherever possible, criteria (1) and (2) were used in conjunction to establish the relative timing of pegmatite sheets. For a better understanding of the controls of pegmatite emplacement, and for ease of geographical referencing, case studies of well-exposed pegmatite wall-rock relationships and geometries will be described in the following. These case studies have been selected in relation to the structural domain in which they occur also typifying the emplacement geometries and relationships that are common and seem to be characteristic for the area. All strike and dip measurements in black refer to pegmatite contacts.

Normal Limb

Figure 5.19 illustrates the relationship between a set of four bedding-parallel sills and a cross-cutting dyke. The sills show an even spacing of ca. 15 m (in plan view). They are relatively thin (<2 m) and can be traced along strike for > 100 m. All four sills gradually taper towards the SW, where they terminate at approximately the same location. Towards the NE, the sills terminate into a thick, up to 8 m wide dyke that crosscuts the bedding and foliation (S1) at right angles.

The sills do not continue past the dyke and, vice versa, the dyke does not continue beyond the NW and SE sill. There are no abrupt mineralogical and/or textural changes at dyke-sill contacts. Moreover, close to the dyke-sill-contacts, the sills tend to curve into parallelism with the dyke, indicating the connectivity between the two sheet geometries. The two NW sills show a clockwise rotation into the dyke, whereas the two SE sills rotate counter-clockwise into the dyke. Furthermore, the SE-most sill records a gradual thickening as it grades into the cross-cutting dyke. A short dyke segment linking and curving into the bounding sills is observed some 30 metres to the SW.

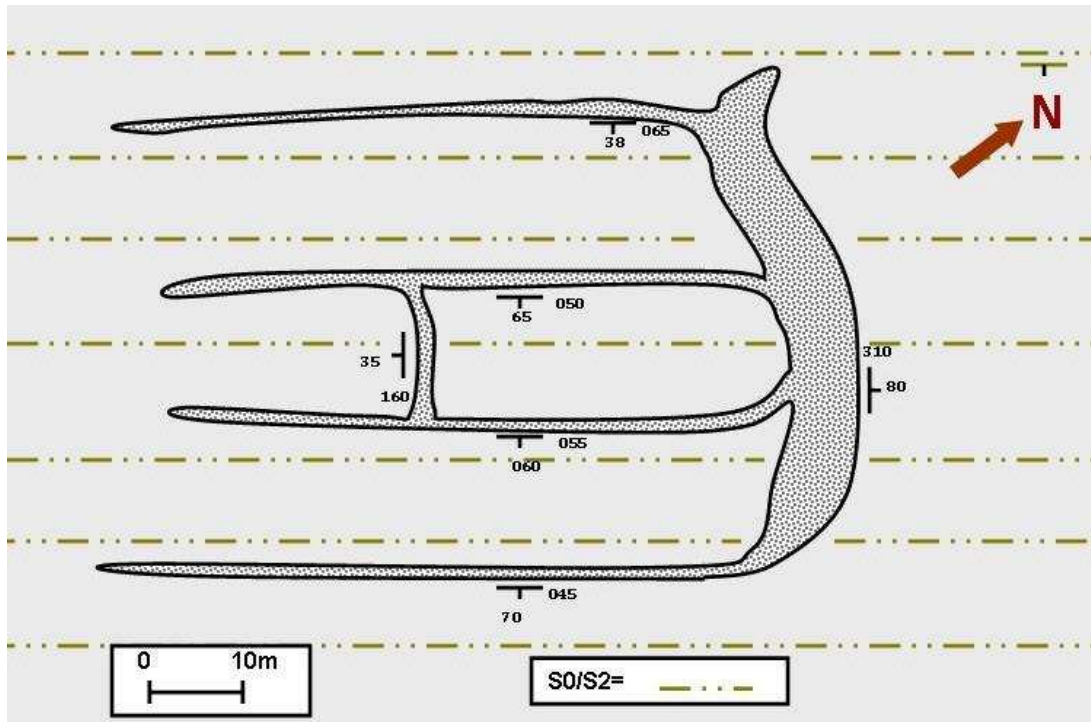


Figure 5.19: Detailed sketch map showing the relationships between a 2nd-generation dyke and four sills (coordinates UTM 563430E; 7566858S WGS 84).

Taken in conjunction, these features indicate the largely contemporaneous emplacement and connectivity between dykes and sills, where the two different sheet geometries have affected each other and, thus, melt transfer.

Figure 5.20 (coordinates UTM 563467E; 7567134S WGS 84) illustrates a somewhat different relationship between dykes and sills. In this case, two high-angle cross-cutting dyke segments display a sigmoidal geometry and an en-échelon arrangement. The dyke terminations are characterized by the lateral tapering of the dykes as the tips are re-orientated into a bedding-parallel orientation. Notably, dyke tips rotate away from, and not towards each other as might be expected from overlapping en-échelon segments, indicating the interaction of extensional stresses around the propagating fracture tips (e.g. Nicholson and Pollard, 1986). The northern dyke is connected to a two metre wide sill and the textural and mineralogical continuity between the two pegmatite geometries suggest their contemporaneous emplacement.

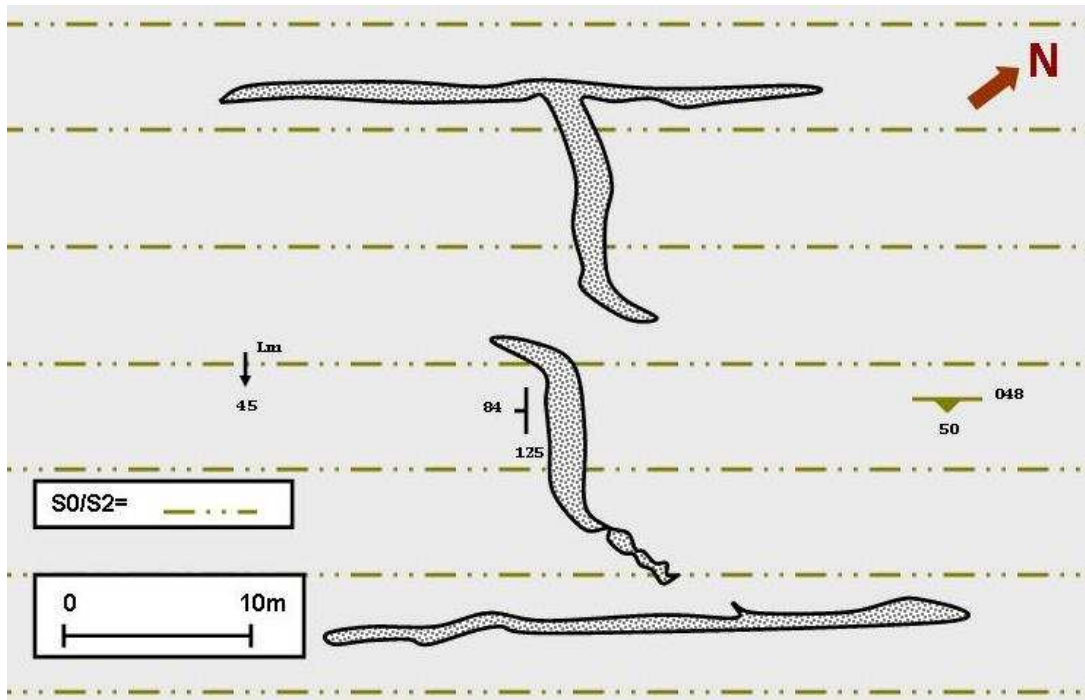


Figure 5.20: Dyke-sill relationships along the normal limb showing two sigmoidal and en-échelon dykes interacting with two bedding parallel sills.

The southern dyke displays a tapering and thinning as the tip rotates anticlockwise towards the NE and to lower angles to bedding. A small-scale spur in the sill points to the dyke, but the two geometries are physically not connected.

Dyke-sill relationships in which dykes are the dominant geometry are illustrated in figure 5.21, mapped at coordinates UTM 561855E; 7565420S WGS 84. Here, sills originate as thin and short sheets that rotate from their bedding-parallel orientation into cross-cutting dykes and then significantly widen over a distance of merely two to five metres. The sills may join individual dyke geometries, but, in places, they seem to be merely forming the termination of the dyke segment, in which the dyke tip is rotated into the bedding plane and S1 foliation before it tapers within 5-10 m. Together, interconnected dykes and sills form a systematic right-stepping pattern. Dyke orientations are almost perpendicular or at high angles to the regional F2 fold plunge.

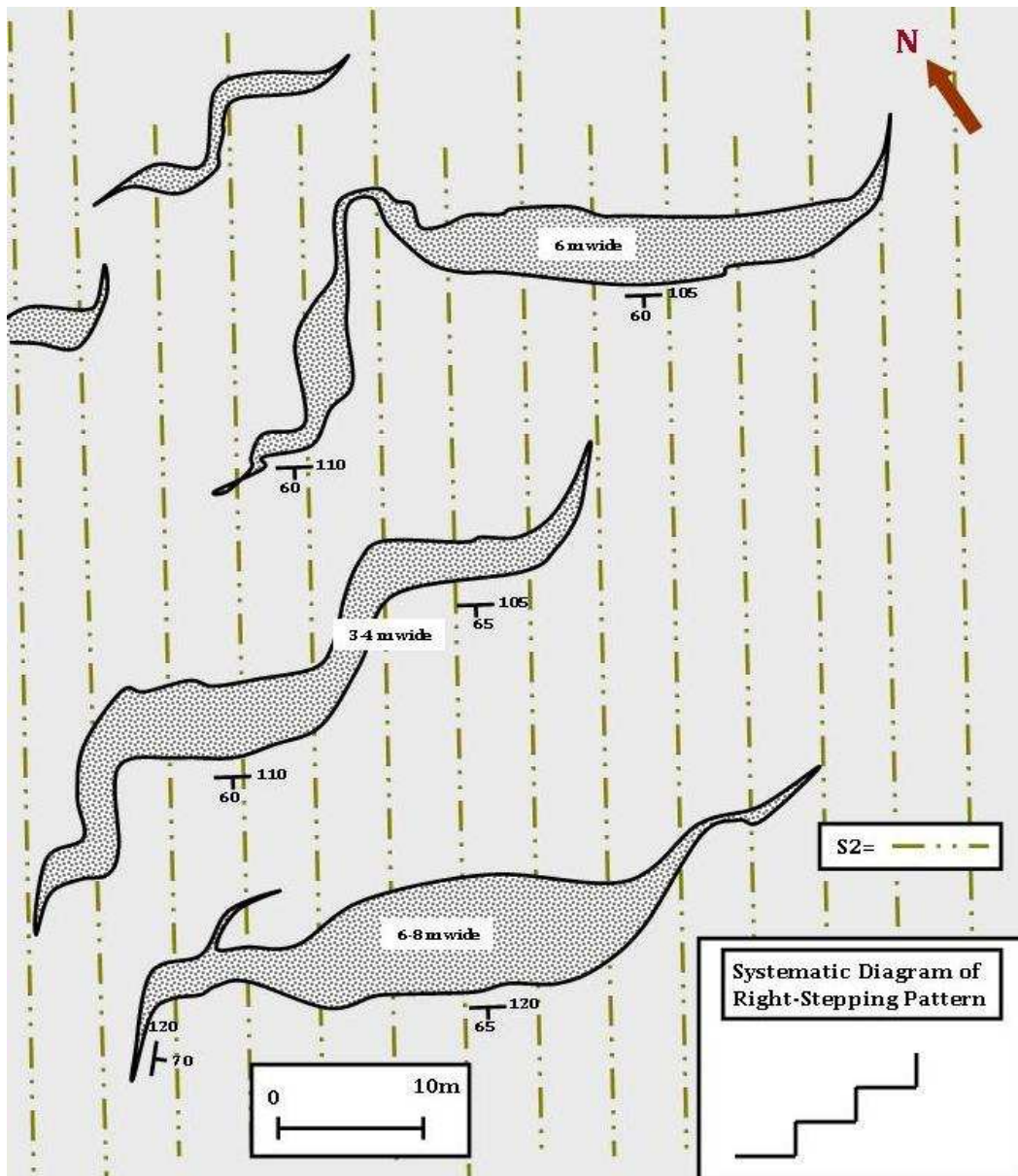


Figure 5.21: Second-generation dyke and sill interaction at southern end of the normal limb. Sills are considerably thinner than dykes, and together they form a right-stepping pattern seen in the systematic diagram at bottom right of illustration.

While there are obvious differences in the three selected field examples (Figs 5.19-5.21), a number of important commonalities exist that suggest these merely represent variations of a similar emplacement pattern. In all cases, the NW trending dykes are thicker than the bedding-parallel sills and sills show consistently higher aspect ratios compared to dykes. Dykes typically display sigmoidal geometries caused by the both clockwise and anticlockwise rotation of dyke tips into sills. This

is a common feature of dykes throughout the Kranzberg syncline. Dyke- and sill geometries show no clear cross-cutting relationships that would indicate the successive emplacement of dykes and/or sills. In fact, the thickening of e.g. sills at the intersections with dykes points to the fact that they were hydraulically connected. While it is common for dykes to terminate within a few meters after rotating into an S0/S2 parallel orientation (Figs. 5.20 and 5.21), sills may also continue along strike, which accounts for their commonly larger aspect ratios (Fig. 5.19). As such, there are areas in which dykes dominate over sills and where sills may or may not connect dykes, as well as areas where dykes are subordinate, only connecting between laterally more continuous sills. In the shallowly-dipping strata of the normal limb, it is important to note that dykes connect otherwise unconnected sills in a vertical direction, which would have allowed for a buoyancy-assisted melt transfer.

Overtured Limb

The overtured limb shows steeply dipping bedding/foliation compared to the normal limb of the Kranzberg syncline and exposes the entire lithological succession of the Kuiseb Formation over a width of some 800-1000 m. This cross-section through much of the Kuiseb Formation illustrates how lithological variations affect pegmatite emplacement.

Unit 1

Two well-exposed and representative field examples have been selected to illustrate the geometries and emplacement styles of pegmatites in Unit 1 of the overtured limb. The first case study (Fig; 5.22) shows a set of slightly sigmoidal, right-stepping en-échelon dyke segments, between two prominent sills that are situated adjacent to ≤ 10 m wide marble horizons. At the base of the map (Fig. 5.22), an S-shaped sigmoidal pegmatite sheet with dips to both the N and S, cross-cuts a biotite-schist dominated section and then terminates as metapsammite and marble horizons are introduced. Adjacent to these horizons, ≤ 10 m wide sills that can extend for over a kilometre in length are observed.

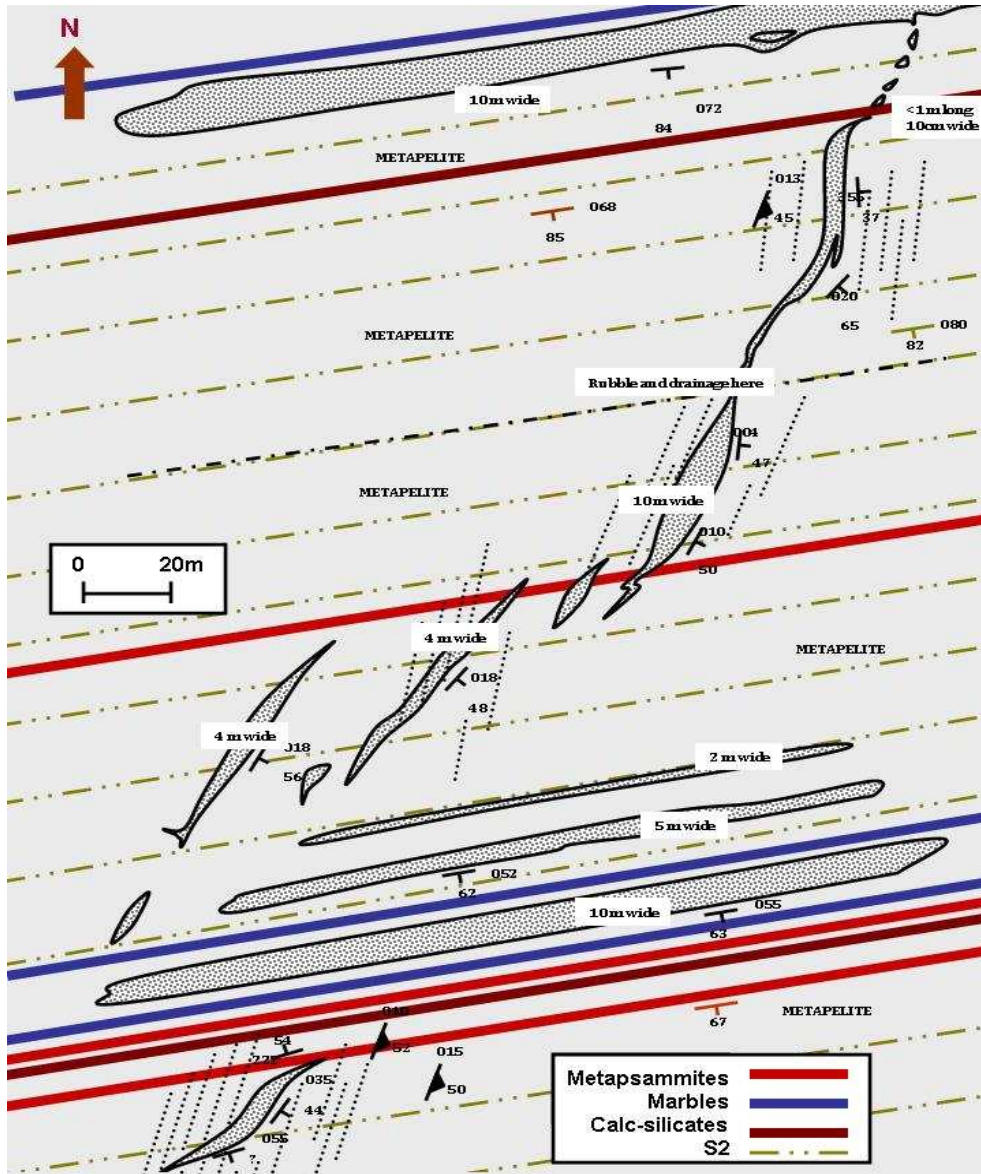


Figure 5.22: Coordinates UTM 564295E; 7565400S WGS 84. Sketch map showing the spatial relationship between dyke- and sill-geometries in the layered Unit 1 located on the overturned limb of the Kranzberg syncline. Up to 10 m wide sills seem to be confined to prominent lithological contacts, particularly between marble horizons and quartz-biotite schists. In this case, sills are stratigraphically situated in contact with marble horizons at, or close to, the interface with biotite schists. The thick schist package in between the marble units is cross-cut by short en-echelon dyke segments; at least the upper dykes seem to connect with the upper sill, whereas the lower dyke-sill contact is not exposed. (Black dotted lines represent a pegmatite parallel fabric and is discussed below, see figure 5.26).

Stratigraphically above the marbles (base of the map, Fig. 5.22), sills are no longer developed. Instead a set of right-stepping, SE-dipping en-échelon dykes is developed in the ca. 200 m wide package dominated by biotite schists. Individual dykes are, on

average, four metres wide and up to 70 m long. The dyke set terminates into a 10 m wide, 350 m long sill that is again located at the interface between schists and a prominent marble horizon. Dyke-sill relationships shown in figure 5.22 are typical for the SE limb of the Kranzberg syncline. They illustrate the influence of (1) lithological heterogeneities on the formation of a bedding-concordant albeit steeply dipping set of sills, particularly in interlayered schist-marble sequences, and (2) the predominance of dykes in lithologically more homogenous packages.

The second example, (Fig. 5.23) shows thin, one metre wide sills that are connected with two short, irregularly-shaped and rather stubby dykes. The highly irregular wall-rock contacts of dykes are related to thickness variations of the dykes.

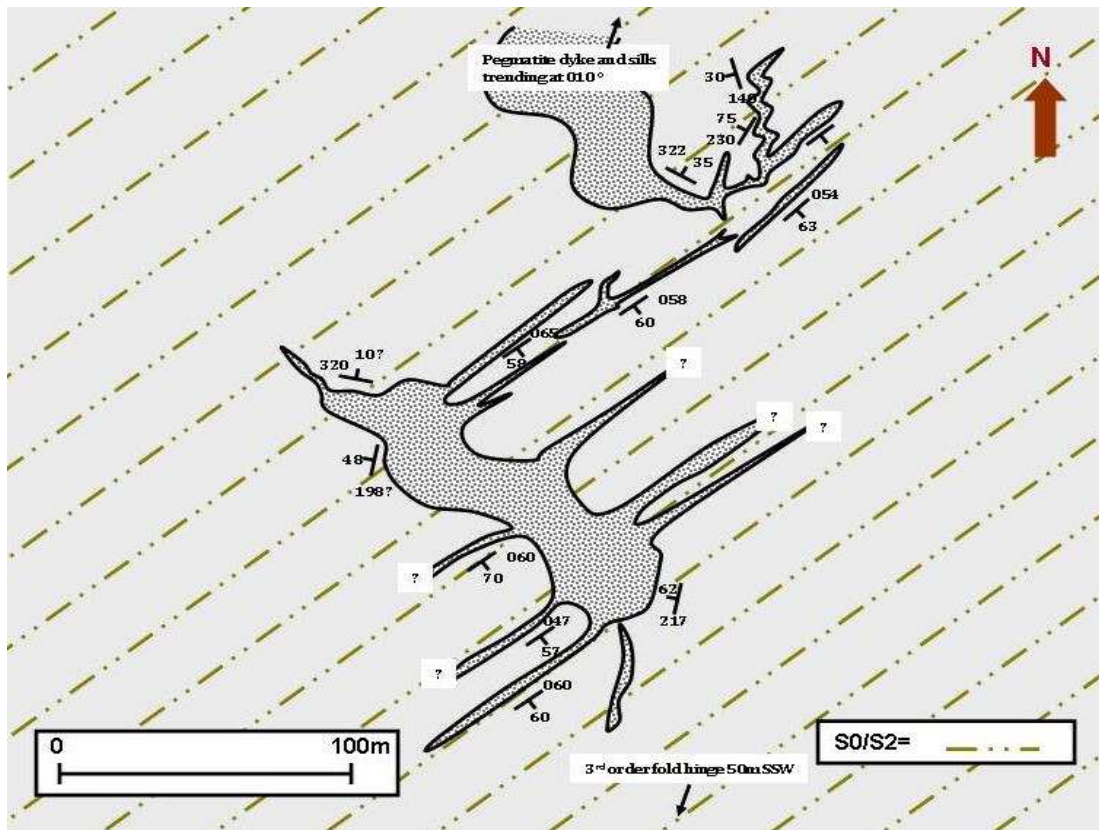


Figure 5.23: Coordinates UTM 565248E; 7566066S WGS 84. Connectivity between narrow sills and stubby, cross-cutting dykes. Note the protrusion along dyke margins where they intersect with sills.

At dyke-sill intersections, dykes form metre-wide protrusions and show a thickening, which, together with the textural and mineralogical continuity between sills and dykes indicates their contemporaneous emplacement and the connectivity between the two geometries. The cross-cutting dykes are prominent in this area and are up to 150 m long and 30 m wide. However, dykes are far less common than sills, although sills are thin and laterally discontinuous. Together, dykes and sills describe a systematic NNE (approx. 010-015°), stepping trend with the map of figure 5.23 illustrating only the lowermost part of this pattern.

Unit 2

Pegmatite geometries in Unit 2 are somewhat unique in that dykes commonly form isolated lenses, whereas connecting sills are not developed. The dykes may branch and coalesce, describing a more complex internal geometry and often enclose wall-rock slivers (Fig. 5.24).

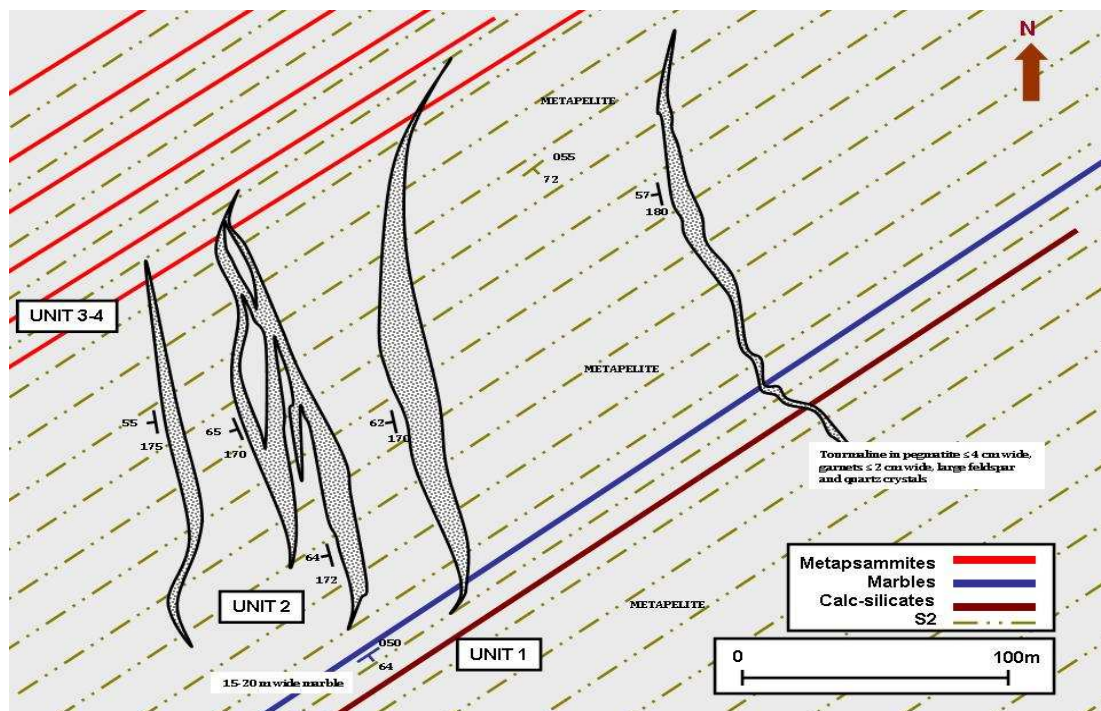


Figure 5.24: Coordinates UTM 565967E; 7567010S WGS 84. Pegmatites on a traverse along the overturned limb between Units 1 and 2 and the contact with Unit 3-4. Note the abrupt termination of the dykes along the contacts between different units as well as the clockwise rotation of dyke tips along the contact of Unit 1 and Unit 2 and the clockwise rotation of tips at the contact with Unit 3-4, resulting in the overall sigmoidal shape of dykes (as discussed in Chapter 5.2.2 and illustrated in Fig. 5.13).

Wall rocks, for the most part, maintain their NE trends (S0/S2), but, in places, wall rock bridges are rotated leading to the presence of rotated wall-rock fragments in the dykes. Figure 5.24 shows a series of less than eight metre wide, ≤ 200 m long, $160\text{-}180^\circ$ striking and moderate- to steep W-dipping dykes. The dykes are confined to Unit 2, gradually tapering against the over- and underlying Units 3/4 and 2, respectively. Against both contacts, the dykes show a slight clockwise rotation of their dyke tips before terminating. The dykes show the largest width in their central parts, resulting in a lensoid geometry.

Units 3-4

Figure 5.25 illustrates pegmatite emplacement patterns at the transition from Unit 4 on the overturned limb, across the first-order axial trace and into the normal limb.

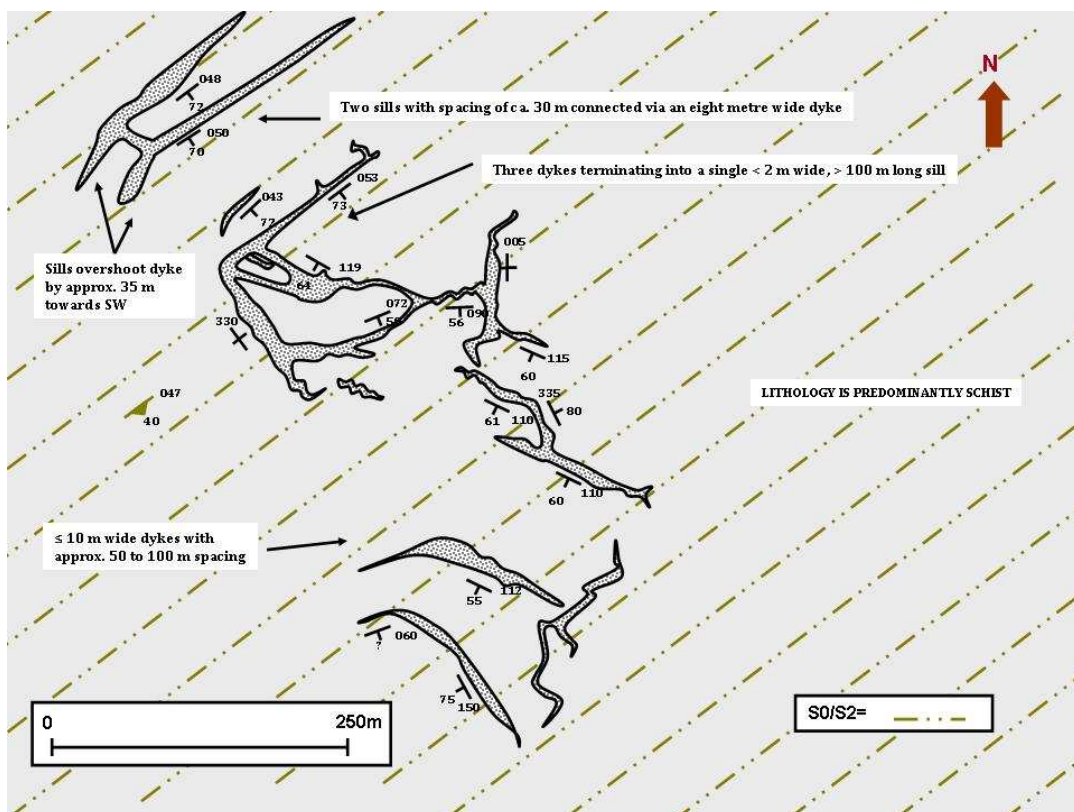


Figure 5.25: Coordinates UTM 563891; 7566349S WGS 84. Case study of pegmatites along the transition from the overturned limb at the bottom of figure to the normal limb at the top of figure. Sills become more prominent on the normal limb, whereas dykes are dominant on the overturned limb. Approximate location of the Kranzberg synclines axial trace is indicated by a solid black line.

Both dyke- and sill-like geometries are developed, showing similar intersecting geometries to those described above. Fig. 5.25, in particular, illustrates the effect of the general attitude of the wall-rock strata on the emplacement mode of pegmatites. The lower part of the map illustrates the emplacement of pegmatites on the steep, overturned limb, showing similar intersecting dyke-sill relationships compared to figures 5.22 – 5.24. The top part of the map covers the normal limb of the Kranzberg synform. Here, thin, only 2-5 m wide, but laterally relatively continuous sills (> 200 m) sills are developed. The two sills show a spacing of ca. 30 m and are connected via an eight metre wide SE-striking dyke. The sills do not merely curl into the connecting dyke, but overshoot the dyke by some 35 m towards the SW.

First Order Hinge

Figure 5.26 shows a detailed map of a 2nd-generation pegmatite complex in the 1st-order hinge of the Kranzberg syncline, centred at UTM coordinates: 560500E, 7563524S WGS 84. The pegmatites are developed as short, lensoid, N-trending and anastomosing dykes, linked by narrower, NE- and/or E-trending dykes. As such, emplacement geometries of pegmatites and dyke-sill relationships are similar to what is observed elsewhere in the Kranzberg syncline.

The most remarkable feature of this complex is a new, N trending fabric to the immediate E of the dyke complex. This fabric is observed in schist along the overturned limb as well as the hinge domain (eg. Figs. 5.22 and 5.26). It typically accompanies and runs subparallel to pegmatite dykes, and has a N-NNE strike and a moderate (40-50°) SE dip. The fabric is not defined by the growth of new minerals (eg. biotite etc for S1 and S2), but rather by a closely-spaced parting in the rock (Fig. 5.27). It is macroscopically observable within ca. 10 m from the dyke margins and progressively decreases in intensity away from the dyke margins.

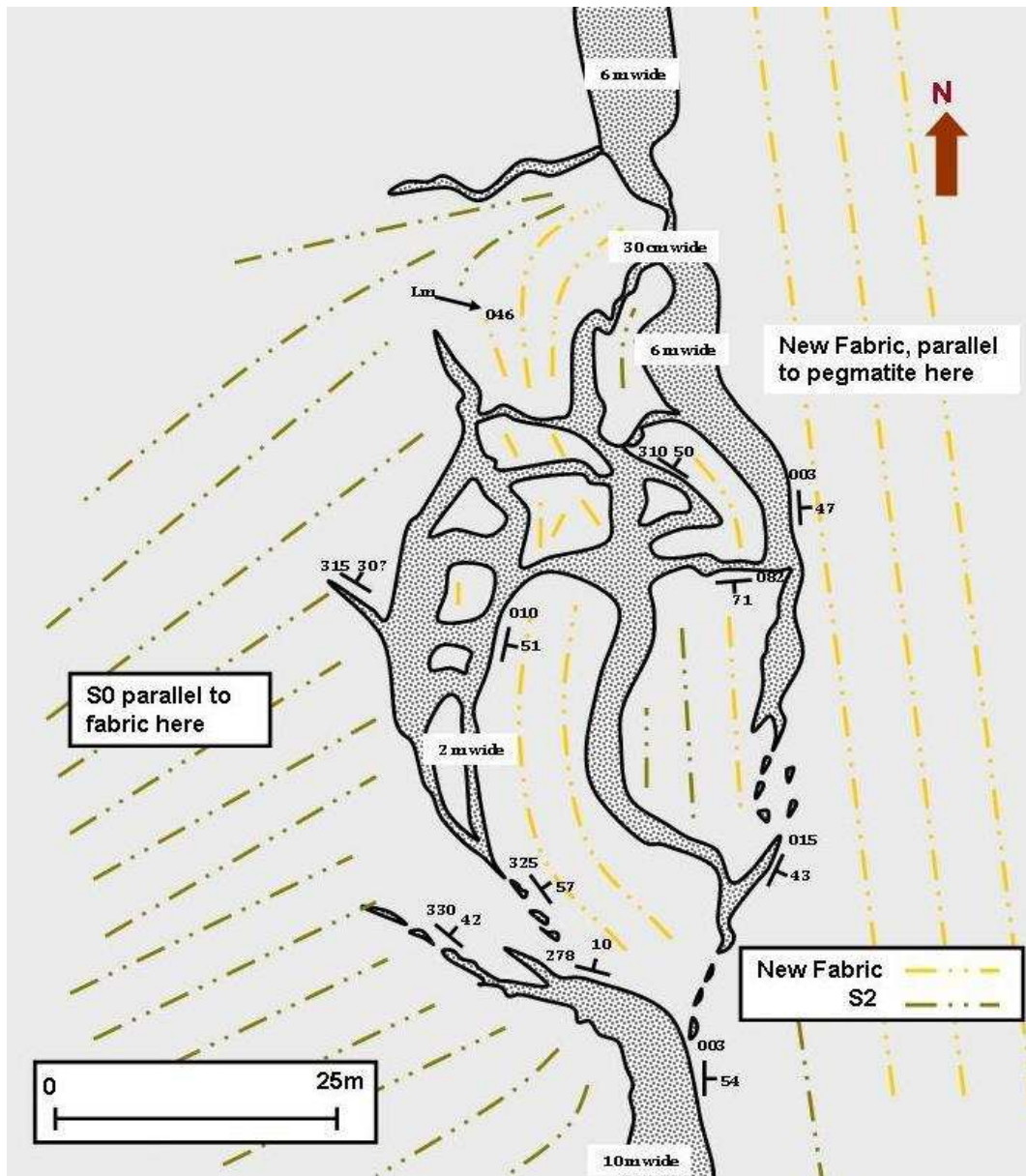


Figure 5.26: Case Study in first-order hinge shows a geometrically complex, stockwork like emplacement of pegmatite sheets. This stockwork marks the location of an abrupt change of foliation trends from NE trends in the W to N trends E of the pegmatite complex. The same fabric, located within metapelitic schists was also observed and illustrated in figure 5.22 (black dotted lines).

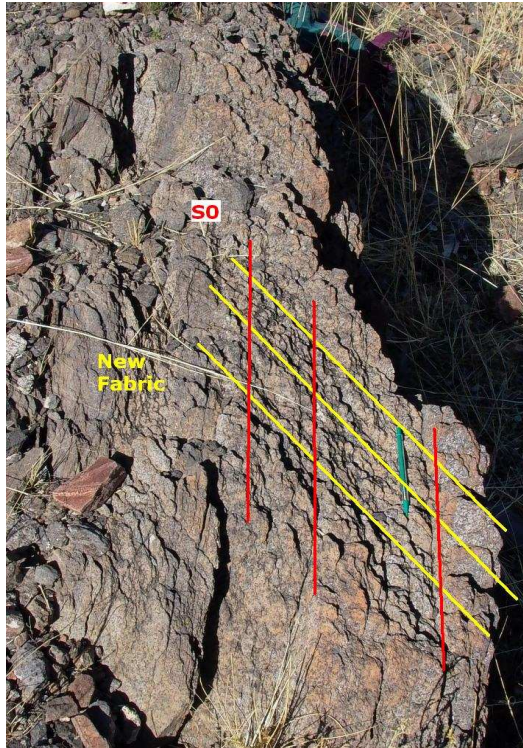


Figure 5.27: A spaced fracture cleavage (S3) is commonly observed in proximity to dykes in Unit 1 along the overturned limb and in the hinge domain. S0 indicated in image with red lines and the new fabric is indicated by yellow lines. The fracture cleavage is parallel to dyke margins.

5.4 DEFORMATION OF PEGMATITES

The degree of post-emplacment deformation of pegmatites was one of the distinguishing factors for the subdivision of pegmatites into four main, successively emplaced generations. In order to complete the description of pegmatites of the Kranzberg syncline, this chapter briefly outlines the post-emplacment deformation of the different pegmatite generations.

5.4.1 Deformation of 1st-Generation Pegmatites

First-generation pegmatites show the largest degree of deformation and are commonly deformed into close- to isoclinal, parallel folds with half wavelengths ranging from less than one metre to tens of metres. In cases where pegmatites are isoclinally folded, the sheets close on themselves without any intervening wall

rocks, forming what appears to be a single unit with bedding enveloping the folded pegmatite sheet (Fig. 5.28). In places, slickenside lineations are developed along their contacts. The folding, partial transposition and/or boudinage of 1st-generation pegmatites suggests that their original orientations have been modified to such an extent that their emplacement geometries are likely no longer preserved.

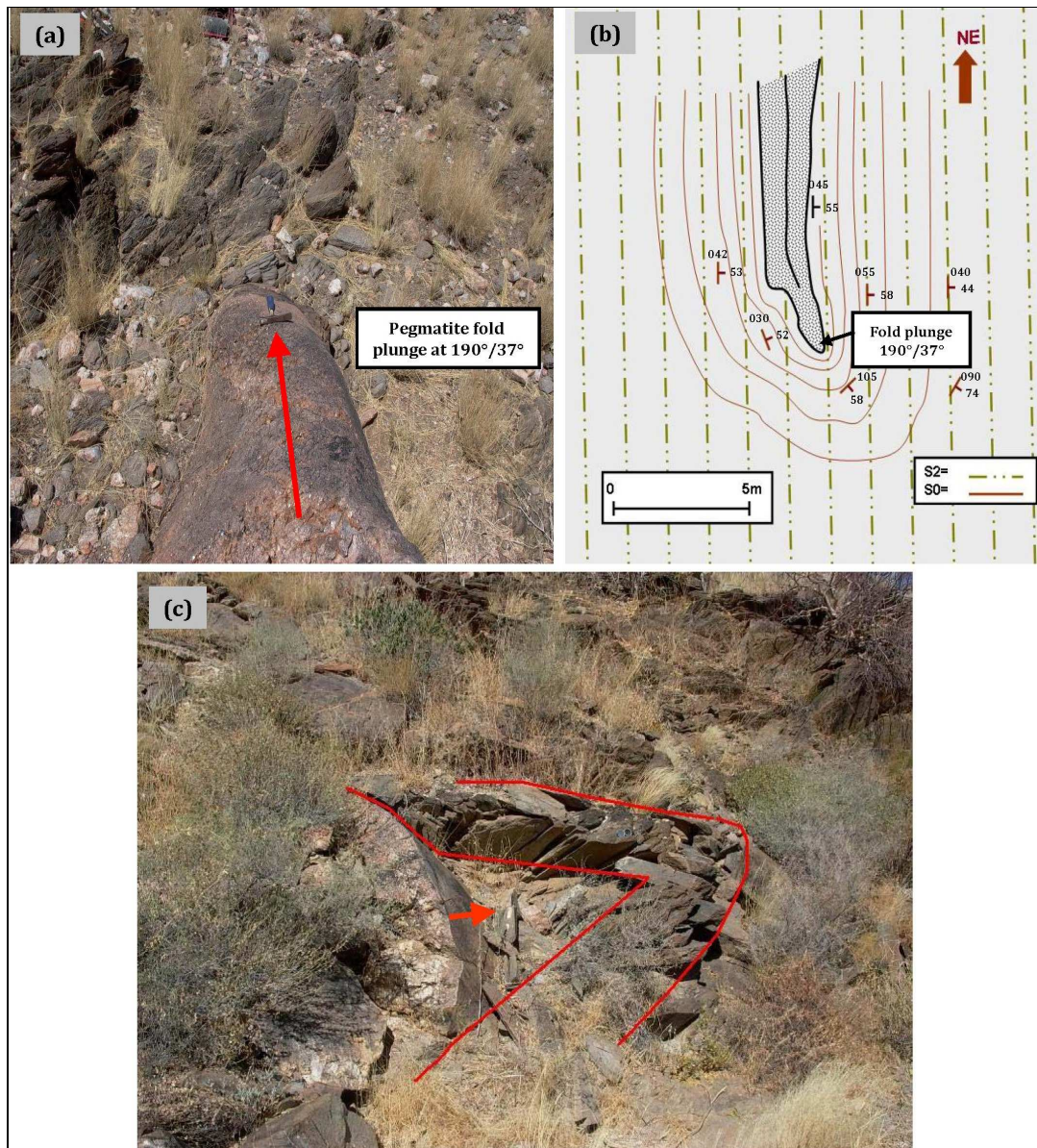


Figure 5.28: (a) Folded 1st-generation dyke plunging 190° (red arrow) with an axial-planar S2 foliation; the fold plunge is parallel to the hammer handle; (b) Line drawing of pegmatite with structural measurements; (c) First-generation pegmatite with S2 axial planar foliation, and S0 (outlined in red) wrapped around the fold axis of the pegmatite. The plunge of the fold axis is annotated by the red arrow. Compass is sitting on wall rock fold hinge for scale

The plunge of folded 1st-generation pegmatites along the normal limb is predominantly towards the S and SSE, plunging at ca. 35-40°. Interestingly, both the fold plunge of these pegmatites (ca. 190°) and the regional fold plunge of the Kranzberg syncline (ca. 098/37°) are situated on the great circle for the Kranzberg syncline (Fig. 5.29).

First-generation sills in the area have commonly undergone boudinage in the S2 plane. Boudins are typically linear rather than chocolate-tablet in shape, suggesting extension perpendicular to the regional NW-SE shortening strain (Chapter 4). Boudins range in shape and size, but generally have aspect ratios between 1:1 and 1:4. Locally, sigmoidal, Z-shaped boudins are observed, indicating that layer-parallel stretch was followed by layer-parallel shortening comprising a dextral component of shear (Chapter 4.6.3). The commonly tightly folded and/or boudinaged nature of 1st-generation pegmatites, suggest they were emplaced during D1 or early D2 deformation, and were subject to the majority if not all of the D2 deformation.

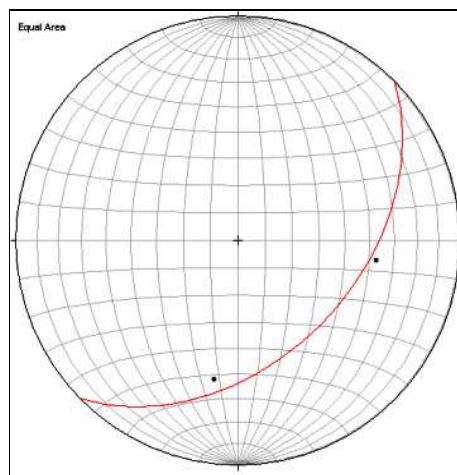


Figure 5.29: Mean S2 for the Kranzberg syncline indicated by red great circle, containing both the regional fold plunge (approx. 098/37°) and average fold axis plunges of 1st-generation pegmatites (190/37°).

5.4.2 Deformation of 2nd-Generation Pegmatites

Second-generation pegmatites are, in places, deformed into open- to tight folds with wavelengths from less than a metre (Fig. 5.30) to tens of metres. Fold axial planes are parallel to the regional S2 foliation (Fig. 5.31). In vertical sections, the folds show

a pronounced asymmetry and NW vergence. The intersection of S2 with pegmatite margins may, in places, result in a very prominent intersection lineation along pegmatite wall-rock contacts (Fig. 5.5c). Second-generation sills commonly display pinch and swell deformation and have undergone layer-parallel stretch in the S2 plane. Together with their emplacement geometries and orientations (discussed in the following Chapter 6) these features suggest a syn-D2 emplacement of pegmatites.

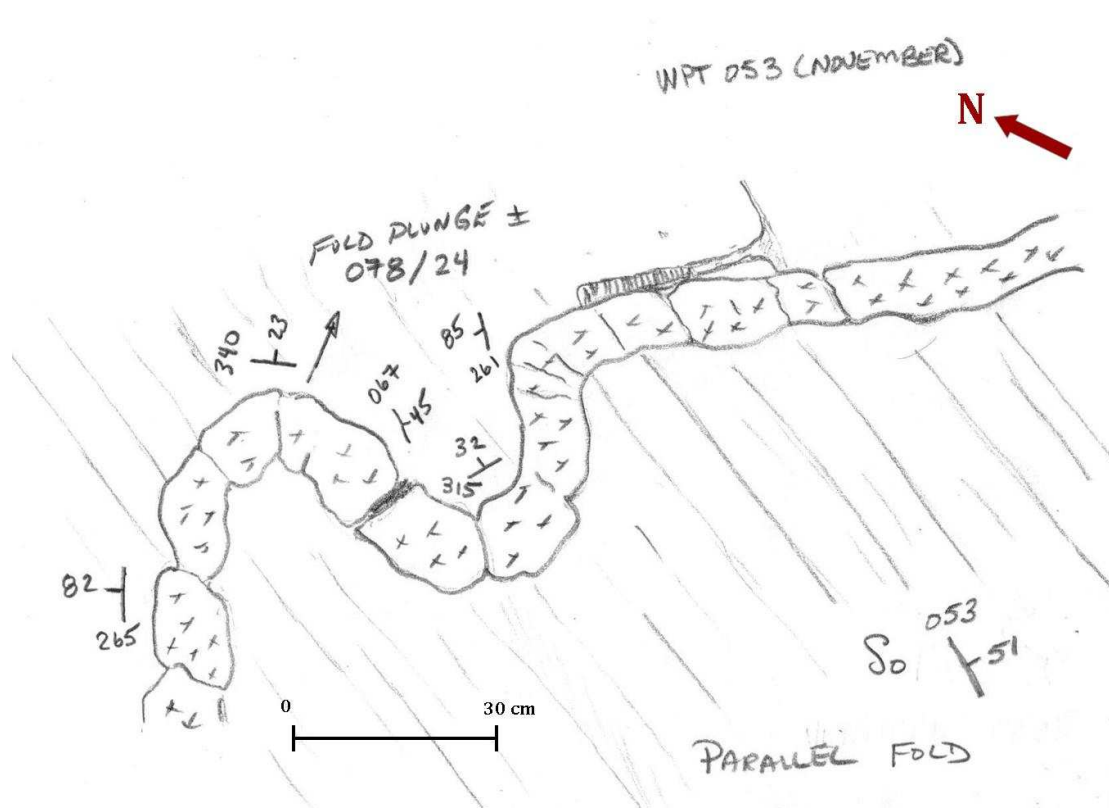


Figure 5.30: Second-generation pegmatite located in the hinge domain. The pegmatite displays close to tight fold shapes.



Figure 5.31: Normal view to hinge of 2nd-generation pegmatite with rock hammer at centre of photo illustrating S2 fabric (yellow line) from top right to bottom left of photo and dipping ca. 45° to the E .

5.4.3 Deformation of 3rd- and 4th-Generation Granites/Pegmatites

Folding has not been recorded in 3rd-generation granites, but the presence of pinch and swell structures in dykes indicate the effect of D2 deformation on the granites. The thinner fourth-generation pegmatite dykes in contrast often display gentle to open fold patterns and the sills display slight post-emplacement pinch- and- swell structures along strike. Deformational effects are very gentle, suggesting a late-D2 emplacement.

5.5 SUMMARY

Pegmatites in the Kranzberg syncline were emplaced over a protracted period of time. The timing of emplacement relative to the regional deformation (D1 and D2) forms the basis for the subdivision of pegmatites into four generations. Emplacement ranges from early- D2 (and D1?), via syn- to late D2 (2nd- and 3rd- generation pegmatites) to very late tectonic (3rd- and 4th generation pegmatites). Second-generation pegmatites are by far the most common and have been emplaced during folding (F2) and associated fold tightening and amplification.

Geometrically, sills can be distinguished from dykes. Sill-like geometries are favoured in lithologically heterogeneous sequences so that sills predominantly occur at the contacts between rheologically stratified successions. This includes Unit 1 at the base of the Kuiseb Formation that regionally correlates with the mixed carbonate-schist sequence of the Ongwati Member and the contact between the Karibib and Kuiseb Formation. Dyke formation is favoured in compositionally relatively homogeneous units, such as Unit 2 of the Kuiseb Formation. In these units, dyke formation appears to be controlled by regional strains, i.e. favouring an emplacement at high angles to the regional stretch and normal to the E plunging F2 fold axes. Importantly, within each pegmatite generation, sills and dykes form at least in part, an intersecting network of different pegmatite geometries.

Intrusive and cross-cutting relationships point to the largely contemporaneous emplacement of dykes and sills, rather than the successive and cross-cutting emplacement of the two. Despite the different stratigraphic and structural locations of pegmatite sills and dykes in various parts of the Kranzberg syncline, pegmatite sheets show similar intersecting relationships of commonly narrow and laterally continuous sills interconnected by steep, but short and thicker dykes, that breach the stratigraphy. The consequences and implications of these relationships for melt transfer and emplacement will be discussed in the following Chapter 6.

Chapter 6 - DISCUSSION

In order to constrain the controls of pegmatite emplacement in the Usakos pegmatite field, a more regional approach was adopted. This included the mapping of the lithological inventory of the host structure of the Kranzberg syncline, and the structural geology and geometry of the first-order structure. In the following, this discussion chapter addresses (1) the lithostratigraphy of the Kuiseb Formation in the Kranzberg syncline (Chapter 6.1), followed by (2) the structural geology of the syncline (Chapter 6.2), which, taken in conjunction, are used to discuss (3) the emplacement controls of pegmatites in the Usakos pegmatite field (Chapter 6.3).

6.1 LITHOSTRATIGRAPHY OF THE KUISEB FORMATION

The lithostratigraphy of the Kranzberg syncline and the Kuiseb Formation, in particular, was mapped in order to guide the structural mapping and to identify marker horizons and/or lithological packages that could be used for a correlation of units throughout the structure. This regional mapping has identified a lithostratigraphic sequence and subdivision within the Kuiseb Formation that has, hitherto, largely evaded a lithological subdivision in the CZ. A detailed sedimentological discussion of results is beyond the scope of this project and not intended in the following, but there are several aspects that seem to be at variance with the present models of e.g. the depositional environment of the Kuiseb Formation in this part of the sCZ. These aspects will be briefly discussed in the following.

According to SACS (1980), the Kuiseb Formation is defined as the uppermost unit of the Swakop Group, extending from the Southern Zone (SZ) in the S, well into the Northern Margin Zone (NMZ) in the N and across the Damara belt. Miller (2008) recently summarized the applicability of the term Kuiseb Formation, highlighting

lithological similarities, but also the evidently different depositional environments that, in fact, transgress terrane boundaries. Most detailed descriptions of the Kuiseb Formation are from the SZ (e.g. Kasch, 1988; de Kock, 1992, Kukla, 1992). Here, the Kuiseb Formation attains a thickness of > 10.000 m, although the structural duplication of the sequence complicates thickness estimates. In the SZ, De Kock (1992) distinguishes the Hureb Formation from the underlying Kuiseb Formation (*sensu stricto*). The former is interpreted to have been deposited during the convergence stage between the Kalahari and Congo Cratons, whereas the Kuiseb Formation (*sensu stricto*) is thought to have been deposited during the preceding spreading stage (Miller, 2008). The lithological similarities render a distinction between the two formations difficult in the field. In general, however, the turbiditic character of the sediments, the deformational style of the SE-vergent fold-and-thrust belt, the high-P, medium-T metamorphism of the metaturbidites, together with the occurrence of the imbricated MORB-type metabasalts and gabbros preserved as the Matchless Amphibolite Belt, signify the incorporation of the Kuiseb Formation of the SZ into the accretionary wedge that formed during convergence above the downgoing Kalahari Plate (Kukla and Stanistreet, 1991).

North of the Okahandja Lineament and on the Congo Craton, Miller (2008) suggests deposition of the Kuiseb Formation to be exclusively related to the spreading stages of the Damara belt. The maximum thickness of close to 10,000 m is reached in the NZ. The thinner development of the Kuiseb Formation in the sCZ is related to the paleo high of the Abbabis Basement Complex which was evident since the early rift stages and deposition of the basal Etusis Formation.

In this study, the Kuiseb Formation in the Kranzberg syncline has been subdivided into four distinct lithostratigraphic units (Fig. 3.6). The stratigraphic thickness of 750-800 m is a minimum thickness since the upper parts of the Kuiseb Formation are not exposed. The greatly reduced thickness is, however, consistent with the deposition of the rocks on or close to the regional Abbabis high. The mixed carbonate-schist succession of the lowermost Unit 1 is in the same stratigraphic

position as the Onguati Member, situated between the Karibib and Kuiseb Formations. Badenhorst (1992) introduced the Onguati Member to describe a transitional facies between the schist-dominated, almost exclusively siliciclastic Kuiseb Formation and the underlying marble-dominated succession of the Karibib Formation. He placed the up to 850 m thick Onguati Member at the top of the Karibib Formation. In a recent revision of the Damara Supergroup, Miller (2008) defined the Onguati Member as an unusual facies that describes the interfingering of the basal Kuiseb Formation with the upper Karibib Formation, i.e. to be located between the two formations. He defines the lower and upper boundaries of the Onguati Member as '*... the base of the first marble layer above the first Kuiseb schist layer or the base of the first schist layers with interbedded calc-silicate layers. The top of the member is the top of the last metre-thick marble layer, but thin lensoid marble layers of limited lateral extent occur above this*' (Miller, 2008, p. 13-160). This stratigraphic placing and lithological subdivision proves to be impracticable when mapping the rocks of the Kranzberg syncline. Instead, it is suggested here that the base of the Kuiseb Formation coincides with the occurrence of the first schist layer above the uppermost dark, nearly black ca. 80 m thick marble horizon of the Karibib Formation. In other words, the interlayered schist-marble succession of Unit 1 is here regarded as the basal parts of the Kuiseb Formation (Fig. 3.6), as it forms a much better defined lithological boundary in the field, which also clearly distinguishes the two major formations at the top of the Damara Supergroup.

On a regional scale, this transitional facies highlights the paleogeographic position of the area, being located between the marble-dominated Karibib shelf to the immediate north and the more pelagic, schist-dominated deposits of the very thick Kuiseb Formation further S and towards the Okahandja Lineament (Miller, 2008). The depositional environment may correspond to an upper continental slope (Miller, 2008). In this scenario, the Abbabis high and, hence, reduced thicknesses possibly indicate the presence of an inherited rift shoulder and, in general, a strongly segmented basement topography.

Units 2 to 4 correspond to the sequence of metapelites and metapsammites commonly described for the broadly turbiditic sequence of the Kuiseb Formation (e.g. Badenhorst, 1992; Miller, 1979, 2008). The succession exposed in the Kranzberg syncline shows a clear coarsening- and thickening upward trend, i.e. the predominantly metapelitic rocks of Unit 2 are succeeded by thickly-bedded, massive metapsammites of Units 3 and 4 (Fig. 3.6). This change occurs over a stratigraphic thickness of ca. 500-600 m. Such coarsening- and thickening- upward sequences are characteristic for e.g. the progradation of deltaic or even distal braided alluvial plain sediments over marine sediments (e.g. Fernández and Guerra-Merchán, 1996). The input of thick sandstone or graywacke units into the basin suggests a more proximal source of terrigenous sediments. This may rather be indicative of the progressive closure of the basin during crustal convergence. The sedimentological evolution of the Kuiseb Formation in the Kranzberg syncline may, thus, track the transition from spreading to crustal convergence, rather than deposition of the Kuiseb Formation being during the spreading stages only, as suggested by Miller (2008). This would correspond to the transition between the Kuiseb and Hureb Formations in the SZ (de Kock, 1992).

Radiometric ages for the Kuiseb Formation in the sCZ that could constrain the timing of this transition are, to date, not available. Deposition of the rocks are bracketed between the age of the Ghaub Formation (635 ± 1 Ma, Hoffmann et al., 2004), the uppermost unit of the Damara Supergroup for which a radiometric age is available and the ages of the oldest diorites and granodiorites that intrude during regional convergence (D1) at ca. 585 Ma (Gray et. al, 2006; Miller, 2008).

6.2 STRUCTURE OF THE KRANZBERG SYNCLINE IN THE USAKOS TOWN AREA

Previous structural work in the sCZ has almost exclusively focused on the prominent D2/3 antiformal dome structures (e.g. Coward, 1983; Kröner, 1984; Oliver, 1994; Poli and Oliver, 2001; Kisters et al., 2004; Johnson, 2005). The geometry and

structural evolution of the intervening synforms, in contrast, have received little attention. The synformal structures are commonly interpreted to have been moulded around and in between neighbouring dome structures (e.g. Poli and Oliver, 2001), implying a forced fold origin.

D1: evidence for early, convergence-related strains

The early, bedding-parallel S1 fabric has also been identified elsewhere in this region (e.g. Smith, 1965; Jacob, 1974; Miller, 1983; Johnson, 2005) and is commonly correlated with the convergence-related D1 deformation. However, regional scale nappes and recumbent folds reported in some of these works (e.g. Miller, 1983) to be associated with S1 cannot be identified in the Kranzberg syncline. S1 is particularly well developed in mica-dominated, schistose units, but absent from e.g. massive metapsammities. This signifies either a very pronounced strain partitioning or merely very low strain intensities in which only the micaceous units show evidence of D1 strains. Given the seemingly intact lithostratigraphy of the Kuiseb Formation, D1 strain intensities are assumed to be relatively low in this stratigraphically higher section of the Damara Supergroup.

D2: formation of regional-scale domes and synforms

The regional-scale fold structures in the Karibib and Usakos area are mainly (E)NE-trending, NW-verging, doubly-plunging folds (Kisters et al., 2004; Johnson et al., 2006). The folds are closely associated with regional-scale thrusts that record top-to-the-NW kinematics. The most prominent of these thrusts is the Mon Repos Thrust Zone (MRTZ, Fig. 6.1, Kisters et al., 2004) that juxtaposes rocks of the Abbabis basement and Etusis Formation onto the upper parts of the Damara Supergroup, mainly marbles of the Karibib Formation. Together, they are interpreted to form part of an upper- to mid-crustal, foreland- (NW-) verging fold-and-thrust belt, recording bulk NW-SE subhorizontal shortening in response to the main collisional phase of the Damara belt (D2/3) between ca. 545-510Ma. Further to the SW and towards Usakos, Johnson (2005) described the localized SW extrusion of rocks in response to regional-scale NW-SE shortening. The close spatial and temporal

relationship between the sheet-like Klein Aukas granite and the refolding of the SW hinge of the Usakos Dome led Johnson (2005) to propose that sheath-fold formation and lateral extrusion of the rocks was triggered by the gravitational collapse and lateral extrusion of the rocks above the underlying melt sheet of the Klein Aukas granite. The Klein Aukas granite can be seen to be assembled from a multitude of successively emplaced sheets, which may explain the compatibility of tectonic strain rates (i.e. refolding) with the much faster rates of granite emplacement. This orogen-parallel extrusion of rocks and refolding of earlier F2 folds into SW-closing sheath folds agrees with the findings of e.g. Coward (1983), Oliver (1994) and Poli and Oliver (2001) from dome structures and intervening synforms to the SW in the sCZ. The switch from NW- and foreland-directed transport to SW- and orogen-parallel transport corresponds to successively deeper crustal levels exposed in the sCZ (Kisters et al., 2004). These mid- and deep-crustal levels are characterized by the presence of partial melts, i.e. widespread migmatization (e.g. Jacob, 1974; Miller, 1983; Jung and Mezger, 2003; Ward et al., 2008), which may explain the rheological weakening of these deeper levels.

6.2.1 Formation of the Kranzberg syncline

The NE-trending, NW-verging Kranzberg syncline of the study area forms part of this pattern of regional-scale F2 folds. The first-order fold verges to the NW and fold plunges are commonly at moderate angles to the E and SE. The relatively consistent fold plunge of folds in the Kranzberg syncline does not correspond to or follow those of the adjacent Usakos dome. In the Usakos dome, shallow NE- and SW- doubly-plunging folds dominate in the central parts of the dome that are refolded and (over-) steepened to result in the sheath-fold geometry of the SW hinge of the dome (Johnson, 2005) (Fig. 6.1). This suggests that the Kranzberg syncline is not a forced fold that owes its shape to the adjacent Usakos dome. It also implies the presence of a shear zone between the two adjacent folds that, in effect, detaches the structural evolution of the dome from that of the syncline. Johnson (2005) tentatively placed this shear zone into the highly transposed thick marble units of the Karibib Formation. She proposed the presence of this detachment so that strain

compatibility was maintained between the extruding dome and the adjoining wall rocks of e.g. the Kranzberg syncline. Her suggestion of a bounding shear zone between the two first-order folds corresponds very well with field evidence collected in this study.

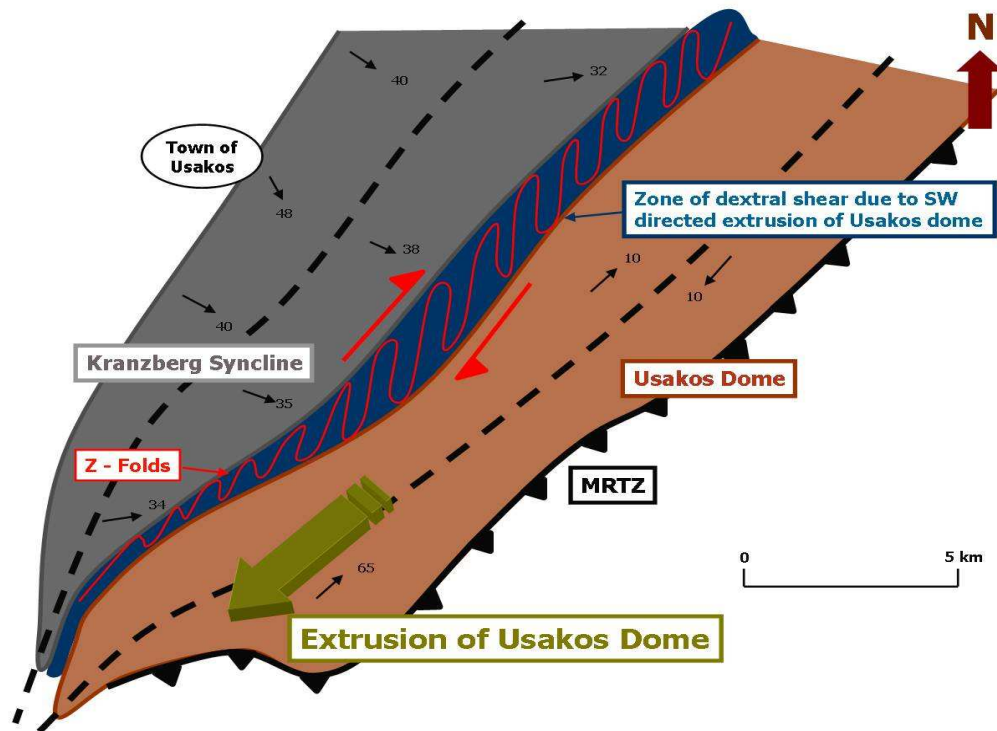


Figure 6.1: Extrusion of the Usakos dome (thick green arrow at bottom of illustration) and, as a result, the dextral shear component particularly in the marbles (dark blue) where the Usakos dome borders against the Kranzberg syncline. Note the variable fold plunge directions for adjacent synforms and antiforms within the Usakos Dome

Most importantly, it explains the distinct asymmetry and steep- to vertical plunge of the near ubiquitous Z-shaped folds that are only developed on the steep SE limb of the syncline and, in particular, in the Karibib Formation (Chapter 4.6.3, Fig. 4.26). Neither the fold asymmetry nor the fold plunge can be reconciled with an origin of the folds as lower-order parasitic folds to either the Usakos dome or the Kranzberg syncline. Both the consistent Z-shape asymmetry of folds as well as steep fold plunges are, however, consistent with their origin as drag folds, formed during a component of dextral shear resolved along the marble units. The dextral kinematics

are the result of the SW-directed extrusion of the Usakos dome relative to the adjoining Kranzberg syncline to the immediate NW (Fig. 6.1). The non-coaxial component of shear is localized into the highly ductile marble units, as testified by the, for the most part, highly transposed textures (see also Johnson, 2005).

Bedding-cleavage (S2) relationships have been used throughout the Kranzberg syncline in determining younging directions and fold plunges of lower-order folds (Chapter 4.2). As previously stated, this assumes an ideally axial planar relationship between S2 and F2 folds. While this is mostly true on an outcrop scale, the regional compilation of S0/S2 orientations shows a systematic anticlockwise rotation of S2 against S0 for both limbs of the syncline (Fig. 6.2). S2 is rotated, on average, by 14° on the normal NW limb (Chapter 4.5.1) (Fig. 4.10d) and by 25° on the overturned SE limb (Chapter 4.5.2) (Fig. 4.12d) with respect to the axial plane of the syncline.

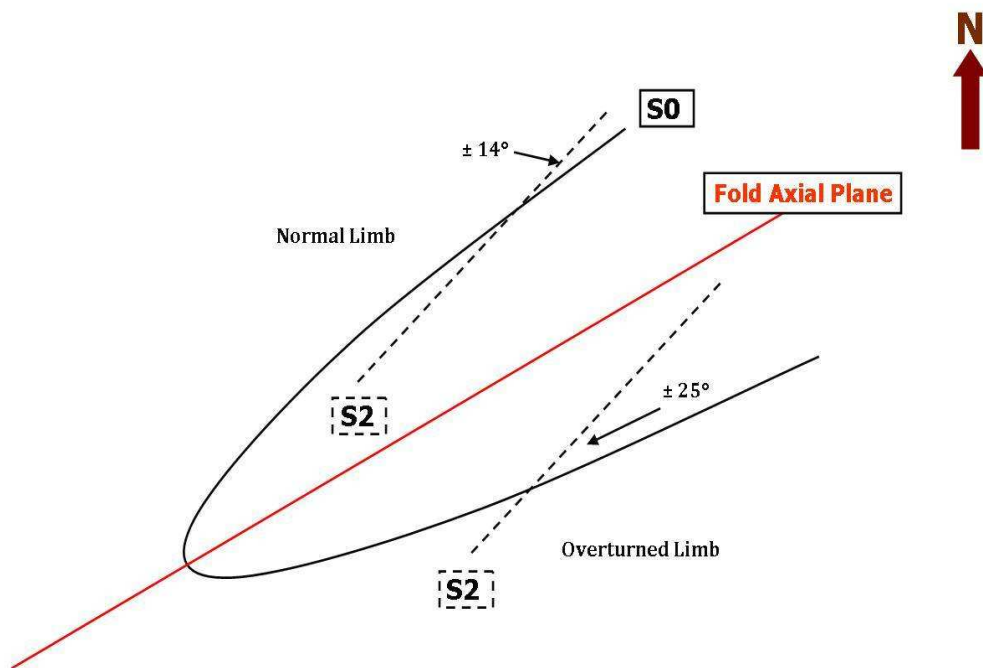


Figure 6.2: S0/S2 orientations show an anticlockwise rotation of S2 against S0, with S2 rotated on average by 14° along the normal NW limb and by 25° on the overturned SE limb

The origin of transecting cleavages in folds is controversial, but is most commonly interpreted to record folding in response to transpression. During transpression, the transcurrent component induces a clockwise rotation of the cleavage with respect to the fold axial plane in response to sinistral shear, or an anticlockwise component, signifying dextral shear to accompany the pure-shear shortening (e.g. Soper, 1986). This relationship between folds and transecting cleavages has, however, been questioned. Transecting cleavages have also been suggested to form during either successive episodes of fold superimposition (e.g. v.d Pluijm, 1990), or recording changing strain regimes during progressive deformation, in which earlier stages of pure-shear dominated shortening are followed by transcurrent shear, or vice versa (e.g. Treagus and Treagus, 1992).

The transecting nature of cleavages in the regional scale fold structures has, to date, not been described in any of the previous structural studies in the region (e.g. Smith, 1965; Jacob, 1974, Miller, 1983; Oliver, 1994; Poli and Oliver, 2001; Kisters et al., 2004; Johnson, 2005; Kitt, 2008). This raises the question as to whether it is localized and confined to the Kranzberg syncline or a more regional feature, but merely overlooked. Non-coaxial fabrics that would indicate transcurrent kinematics in the Kranzberg syncline, as a whole, are rare or absent. As discussed above, evidence for a component of non-coaxial dextral shear is, however, recorded on the steep, overturned SE limb of the syncline and localized in the marble units of the Karibib Formation and Unit 1 of the Kuiseb Formation. Hence, rather than representing a regional feature, the transcurrent component of deformation seems to be related to the more localized deformation and the differential movement between rocks of the Usakos dome and the Kranzberg syncline.

6.2.2 Structural variations in the Kranzberg syncline

The studied part of the Kranzberg syncline only covers the central parts of the much larger, NE-trending first-order structure that extends for nearly 100 km in strike length (Fig. 6.3). The NE extent of the syncline is largely hidden by Cenozoic cover, whereas the SW extent is intruded by the Stinkbank Granite.

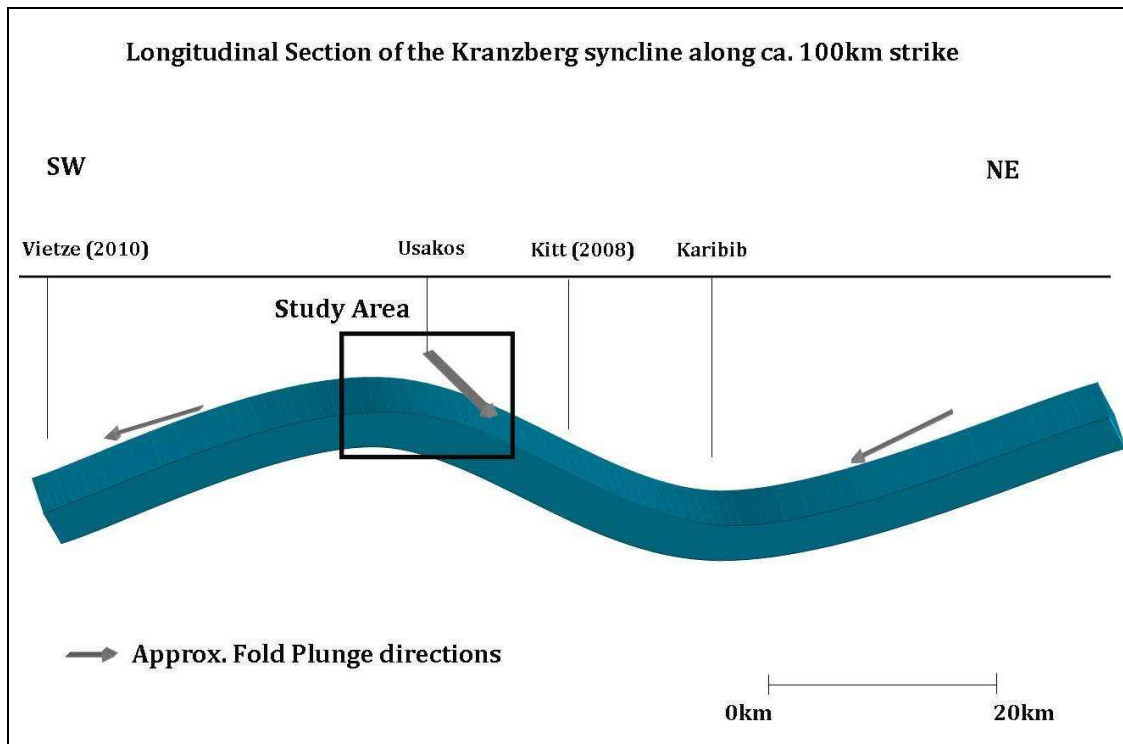


Figure 6.3: Schematic longitudinal section of the Kranzberg syncline. The black box marks the location of the study area. Grey arrows indicate a SE fold hinge plunge towards the NE, and a SW fold hinge plunge towards the SW. The youngest stratigraphic area exposed is likely to be within the Karibib area.

While fold plunges of the syncline are relatively uniform to the E and SE around the town of Usakos and in the study area, a regional compilation of fold plunges (Fig. 6.3) illustrates that the syncline is a highly non-cylindrical fold despite its consistent NE trend. This results in axial culminations and axial depressions, which, as a consequence, also determine the degree of preservation of the Kuiseb Formation in the syncline. The Kuiseb Formation is expected to be most complete in areas of axial depressions, located e.g. to the NW of Karibib (here largely under younger cover) (Fig. 6.3). In contrast, the upper parts of the Kuiseb are likely to be eroded in axial culminations, as is the case S of Usakos, in the SW parts of the study area, where Units 1 and 2 are exposed in the hinge of the first-order synform.

In the study area, mineral and mineral stretching lineations (L2m) are parallel to F2 fold axes, indicating a fold-axis parallel, moderate- to steep (35-50°) W- to NW-stretch during F2 folding (Fig. 4.10c, 4.12c, 4.16c). Previous structural studies by e.g.

Poli and Oliver, (2001) and Kisters et al., (2004) have indicated an orogen-parallel SW-stretch, but in mainly gently-plunging domes (e.g. Karibib and Usakos domes (Kisters et al., 2004); Vergenoeg and Namibfontein domes; (Poli and Oliver, 2001)). This seems to indicate, that the regional stretch is not uniform, varying from subhorizontal to steep over the scale of several kilometres between adjacent areas.

6.2.3 Deviations from the D2 structural grain

a) Stratigraphic and structural variations on the limbs of the syncline

The regional mapping has identified some drastic changes in the thicknesses of lithologies on the NW compared to the SE limb of the Kranzberg syncline. It has also delineated a several hundred metres wide, > 10 km long, trending corridor on the normal limb of the syncline in which regional F2 fold plunges, L2 lineations and bedding (S0) orientations deviate from regional D2 trends.

The most obvious difference between the two limbs of the Kranzberg syncline is the thickness of strata (eg. Fig. 4.8), with apparent thickening of units on the SE limb compared to the NW limb. In the Karibib Formation and Unit 1 of the Kuiseb Formation, the thickening is due to the pervasive bedding transposition. In e.g. Unit 1 of the Kuiseb Formation, bedding transposition is estimated to account for up to 50-100 % of the thickening due to third- order and lower fold structures (Chapter 4.5.2).

The Spes Bona Member shows the most dramatic thickness variation from the SE to the NW limb, being reduced to less than 100 m thickness, compared to > 600 m in the Usakos dome (Johnson, 2005; Kitt, 2008). The thinning of not only the Spes Bona Member, but also other formations of the Damara Supergroup on the NW limb of the syncline occurs in and along a NE trending corridor. A number of features indicate the presence of a high-strain zone to be underlying this corridor.

This includes the complete omission of e.g. the prominent graphitic marbles of the Karibib Formation and the only patchy and sporadic development of all units,

including that of the Spes Bona Member in this zone. High-strain fabrics are common (e.g. in rocks of the Chuos Formation, Fig. 3.3), but strain is very heterogeneous, indicated by the preservation of low-strain domains in e.g. the Spes Bona Member, where sedimentary structures are well preserved. Moreover, mesoscopic folds show SE and S plunges, at high angles to the regional E fold plunges. The fold geometries range from nearly recumbent, with tight- to isoclinal interlimb angles at the Kuiseb/Karibib contact (Fig. 4.24), to upright and close- to tight interlimb angles within the Spes Bona Member only 600 m to the NW. Similarly, L2m mineral lineations are rotated to S plunges, parallel to fold axes, in this zone.

The location of this structural corridor as well as its ENE trend can be correlated with a number of similarly orientated structures that correspond to either aeromagnetically defined lineaments (Miller, 2008), distinct breaks in stratigraphy (e.g. Badenhorst, 1987), or thrust zones (e.g. Kisters et al., 2004) in this area. For example, this structural zone between Usakos town and the Rooiberg structure forms the SW extension of the Onguati Lineament that finds its main expression N of Karibib (Miller, 2008). The Onguati Lineament is interpreted to represent a splay of the first-order Omaruru Lineament to the N. The latter separates the sCZ from the nCZ and coincides with dramatic thickness and facies variations within rocks of the Damara Supergroup on either side. However, the structural nature of the evidently long lived Omaruru and Onguati Lineaments are not clear. Similarly, this zone is parallel to the mainly lithostratigraphic subdivisions of the nCZ into subzones suggested by Badenhorst (1987) to the immediate N. The subzones are bounded by either faults or abrupt facies and thickness variations, following an overall NE, slightly anastomosing trend. The corridor is also parallel to e.g. the MRTZ, that can be traced for over 50 km from SE of Karibib and past Usakos in the SW (Fig. 6.4).

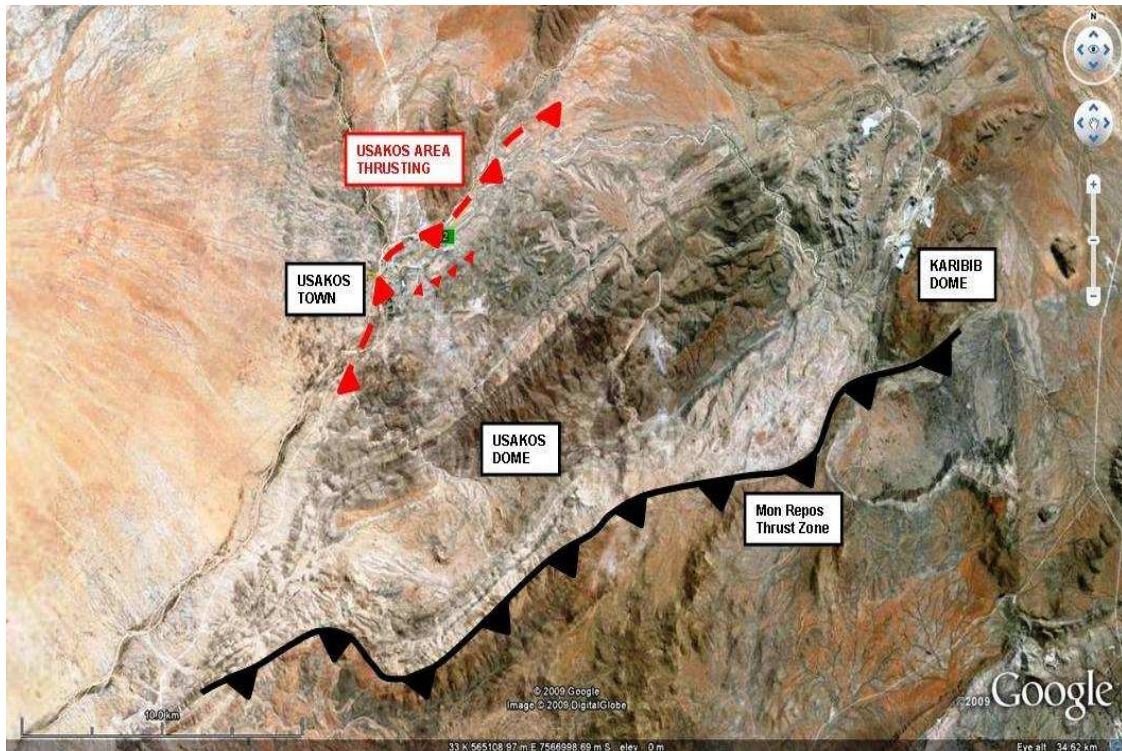


Figure 6.4: Google Earth image with the location of the MRTZ (black) shown in relation to the proposed thrusting along the synclines NW limb (red). The structure can be traced for the most part along the NW boundary of the study area, situated in the hanging wall of the massively developed Etusis Formation of the Rooiberg structure.

The presence of heterogeneous, shallow S- to SE-dipping high-strain fabrics, the rotation of e.g. fold hinges and lineations (L2m) into a down-dip orientation and the partial omission of units all seem to be consistent with an origin of this structural zone as a foreland-verging thrust. This also agrees with the NW vergence of the syncline and the location of the thrust on the shallow SE dipping limb, that is ideally orientated for the formation of a low angle thrust (Fig. 6.5).

Deformation seems to be localized below the Kuiseb Formation and into the marble units of e.g. the Karibib Formation, Okawayo Member or Rössing Formation and above the massively developed Etusis Formation in the footwall. The strain localization into highly ductile marble units is common in this part of the sCZ (e.g. Kisters et al., 2004; Anthonissen, 2009).

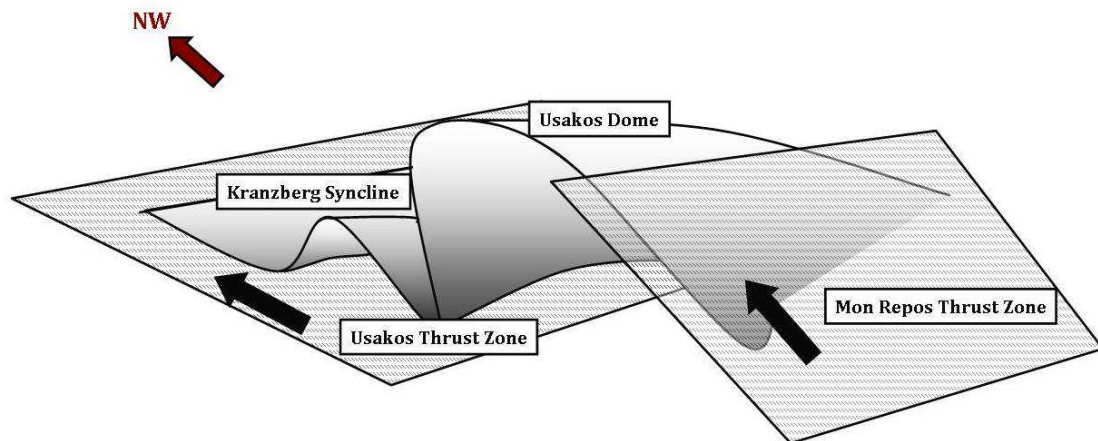


Figure 6.5: Simplified diagram illustrating the spatial relationship of the Usakos dome and Kranzberg syncline with the underlying Usakos thrust and the MRTZ.

6.2.4 Structural synopsis of the Kranzberg syncline

In summary, the Kranzberg syncline is interpreted to be a regional-scale, NW-verging F2 fold that formed during NW-SE shortening and associated thrusting. A component of dextral shear along its SE limb is responsible for the transecting and not exactly axial planar nature of the S2 foliation. The localized shear along the steep SE limb is induced by the relative SW-ward movement of rocks in the adjoining Usakos dome. A moderately-plunging, W- to NW-trending fold-axis parallel stretch of rocks in the Kranzberg syncline is indicated by the boudinage of competent layers and the presence of fold-axis (F2) parallel mineral and mineral stretching lineations (L2m). Despite its regional NE trend, parallel to the regional structural grain of the sCZ, the syncline is a highly non-cylindrical fold. Variations in fold plunge, however, do not coincide with fold plunge variations in e.g. adjacent dome structures. Overall, these features do not indicate the Kranzberg syncline to be a forced fold around adjacent dome structures but that it rather forms part of the regional pattern of NW-verging F2 folds in the Karibib district.

6.3 PEGMATITE EMPLACEMENT

The emplacement of sheet-like intrusions is likely to be controlled by the interplay of three main factors (e.g. Anderson, 1936, 1951; Brisbin, 1986; Gudmundsson,

2009). These include (1) the presence and orientation of pre-existing anisotropies, mainly bedding, (2) the orientation and magnitude of the regional and/or local stress fields, and (3) the melt/volatile pressure that drives fracture and, as such, sheet propagation. Here and throughout the discussion chapter the term 'melt' is used to denote the melt-volatile mixture that the pegmatites have most likely represented during their emplacement.

Concepts and models for the emplacement mechanisms and controls of sheet-like intrusions have mainly been developed and discussed for mafic dykes and dyke swarms (e.g. Nicholson and Pollard, 1985; Gudmundson, 2003, 2006), with the exception of e.g. Brisbin (1986) who focused on the mechanics of pegmatite emplacement. The role of granitic sheet-like intrusions for the emplacement and growth of larger plutons and laccoliths has recently been recognized and highlighted (e.g. Coleman et al., 2004; Glazner et al., 2004; Horsman et al., 2005; Morgan et al., 2008) but these works mainly focus on the processes of progressive pluton growth and the incremental construction of larger igneous bodies rather than the mechanics of sheet intrusions. Most models are broadly based on an Andersonian (Anderson, 1936, 1951) approach to fracturing and dyking, relating fracture formation to regional and/or local stresses and stress variations in the crust (Brisbin, 1986; Clemens and Mawer, 1992).

Models of sill formation, in contrast, highlight the role of mechanical anisotropies and the interplay between rock anisotropies, driving pressures (within the melt-filled fracture) and resistive pressures (fracture resistance of the wall rocks). Field (e.g. Goultly and Schofield, 2008; Gudmundsson, 2009) and experimental studies (e.g. Kavanagh et al., 2006; Menand, 2008) have shed important insights into the controls of sill-like intrusions. These studies indicate that sill formation is favoured when a feeder dyke intersects an interface, i.e. lithological contact, between an upper, more rigid and stronger layer underlain by a less rigid and weaker layer (e.g. Fig. 6.6). The deflection of the feeder dykes into a sill is interpreted to be the result of a local stress reorientation at that interface (Burchardt, 2008). Subsequent feeder

dykes are likely to be deflected along the earlier emplaced sills that, upon full crystallization, commonly represent prominent rheological interfaces and competent lithologies in sedimentary piles. This repeated sill-in-sill emplacement has, in many recent studies, been invoked to be a significant process for the progressive growth of laccolithic plutons (e.g. Morgan et al., 2005; De Saint-Blanquat et al., 2006).

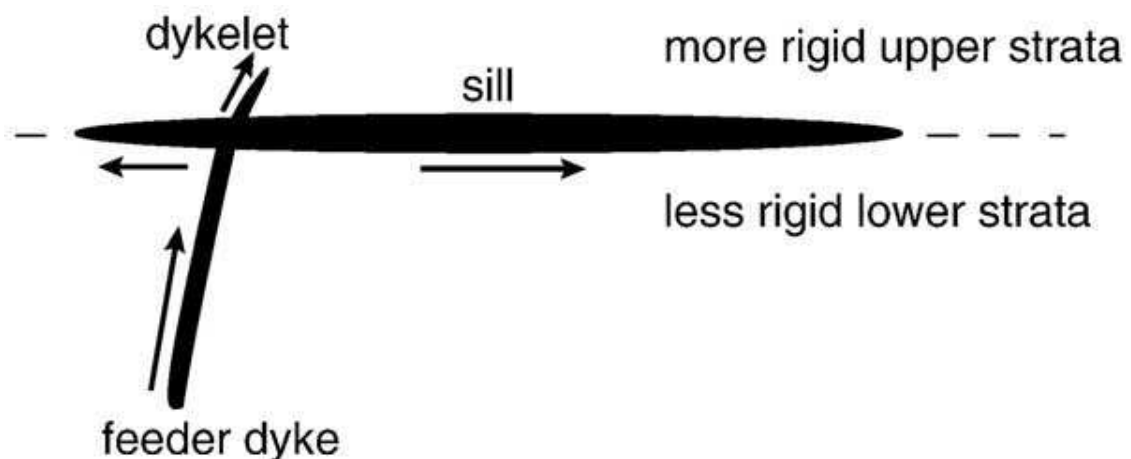


Figure 6.6: Simplified sketch of a dyke-sill transition at the horizontal interface between layers of differing competencies (Young's Moduli); from Menand (2008). The deflection of a steep feeder dyke into a sill occurs below the more competent layer. Dyke-sill hybrids form when the rigidities of the hanging and footwall layers are similar.

A hybrid dyke/sill (Fig. 6.6) forms if the rigidity ratio between the two layers is close to unity and if the ratio between driving pressure in the propagating pegmatite to the resistive pressure of the wall rocks to fracture propagation is also close to one (e.g. Kavanagh et al., 2006). In this case, both dyke- and sill-like geometries can be expected to form. There is an important consequence of this relationship between wall-rock rigidities and driving pressures, particularly for dyke-sill formation at mid-crustal levels. Given that rigidities (Young's Moduli) of crustal rocks are rather similar, particularly under high-grade metamorphic conditions (e.g. Turcotte and Schubert, 1982), hybrid sill-dyke geometries must be expected to be common in the crust. In other words, rather than forming dykes or sills, as would be expected if a purely Andersonian behaviour is assumed, dykes and sills form at the same time and in the same crustal section (e.g. Menand, 2008).

6.3.1 The role of pre-existing anisotropies

Most models of sill formation emphasize the role of horizontal interfaces and lithological contacts (Kavanagh et al., 2006; Menand, 2008). In the case of the Kranzberg syncline, both dykes and, over large parts also sills show steep attitudes and, hence, differ from commonly discussed cases of dyke-sill relationships in mainly horizontal strata. However, the significance of shallow- to moderately dipping bedding for pegmatite emplacement and sill formation, in particular, is prominent in two regions within the Kranzberg syncline, namely (1) in tightly folded rocks of particularly Unit 1 on the steep SE limb, and (2) along much of the shallow- to moderately dipping normal NW limb of the first-order fold.

On the steep SE limb, large and multiple sheeted pegmatites and granites occur in the core of moderately E plunging, second-order F2 anticlines capped by marble horizons of Unit 1. This preferential emplacement of pegmatites underlines: (1) the significance of shallowly-dipping anisotropies for the arrest of the felsic melts, as well as (2) the role of especially marbles for the ponding of melts. The ponding of granites in the core of antiforms capped by thick marble units of e.g. the Karibib Formation is a widely documented feature in the Damara belt (e.g. Jacob, 1974; Miller, 1983, 2008). Calcareous marbles, in particular, represented highly ductile lithologies during deformation and high-grade metamorphism, evidenced by the pervasive bedding transposition and recrystallization of fabrics. Hence, rather than forming rigid units that would deflect dykes into sills along bedding interfaces, marbles represented rheologically weak horizons with lower Young's Moduli compared to e.g. metapelites or metapsammities. The role of marbles for the arrest of fractures is, thus, more likely to be the result of a fracture blunting of melt-filled fractures as they intersect the low-viscosity marbles. Fracture dilation, i.e. elastic failure and wall-rock displacement is inhibited by the ductility of the wall rocks that leads to a collapse of the fracture. In the Kranzberg syncline, it is particularly the large, 3rd generation granite dykes cross-cutting the Kuiseb Formation that show the effect marbles have on fracture propagation. The up to 50 m wide dykes maintain a constant thickness along their entire extent, but show a marked pinch to a fraction

of their thickness and to only 1 m where they intersect marble horizons of Unit 1 (Fig. 5.16).

The significance of shallowly-dipping strata for sill formation is also illustrated by the predominance of bedding-parallel sills on the normal NW limb (Fig. 5.12b) compared to the steep SE limb of the Kranzberg syncline (Fig. 5.12h). The comparison of pegmatite emplacement geometries (Fig. 5.12) in the respective units (e.g. units 2 and 3) on the NW and SE limb is particularly instructive. For example, Unit 2 on the SE limb is only intruded by high-angle dykes, whereas sill-like geometries predominate in the same unit on the NW limb. The same relationship is true for Unit 3 on the NW and SE limb of the fold, leading to the overall predominance of sills over dykes on the NW limb of the syncline (Fig. 5.12b and h). Given that all other factors such as driving pressures, lithological heterogeneity, confining pressures, and regional strain are equal, it is the attitude of the bedding that appears to have determined this switch of intrusion geometries on the limbs of the synform.

In both cases, bedding anisotropies tend to arrest the ascent of pegmatite melts. This leads to the formation of stacked sill complexes in moderately- to shallowly-dipping strata (dips ca. 45°), exemplified by the closely spaced sills on the NW limb of the Kranzberg syncline. However, even pegmatite and granite sheeting over a protracted period of time, exemplified by the multiple pegmatite generations in the Kranzberg syncline, has not led to the formation of a larger, pluton-like body. Large, composite granite plutons are found, for instance, to the immediate SW in the Kranzberg syncline, where the Salem-type Stinkbank granite has intruded the Kuiseb Formation at an identical stratigraphic level. The coarse-grained, often pegmatitic Klein Aukas granite is located to the immediate S of the Usakos pegmatite field, situated in the core of the Usakos dome (Fig. 2.2). The Klein Aukas granite is made up of a multitude of subhorizontal, coarse-grained to pegmatitic sheets (Johnson, 2005). The main difference between these composite granite plutons and the Usakos pegmatite field is that the latter intrudes a moderately plunging part of a

regional-scale F2/3 fold. As a result, wall rocks show predominantly moderate (35-50°) dips, even in the hinges of the first- and second-order folds. Buoyancy-driven melt ascent may, in this case, still be guided and assisted by the inclined wall-rock strata. In contrast, both the Stinkbank and Klein Aukas granites are capped by subhorizontal strata in the hinges of horizontal or only shallowly-plunging folds, which evidently resulted in a far more efficient arrest of the melts. Hence, the formation of granites, demonstrably assembled through multiple sheeting (Miller, 1983, 2008; Johnson, 2005; Kisters et al., 2009; Vietze, 2009) seems to depend critically on the attitude of regional wall-rocks. This, in turn, depends on the plunge of first-order F2 fold structures in the CZ of the Damara belt. Horizontal or very shallow fold plunges may lead to the arrest of melts, whereas moderate fold plunges and, thus, bedding dips allow for the escape of the buoyancy-driven melts.

6.3.2 Dyke emplacement

Cross-cutting dykes are an equally important intrusive geometry in addition to bedding-parallel sills. Their cross-cutting nature illustrates that wall-rock heterogeneities must have played an only subordinate role. However, systematic variations in dyke abundance and spacing as well as dyke orientation with respect to lithological units again suggest the significance of lithologies also for dyke emplacement. These features are discussed below.

Overall, dyke orientations cluster around N- trends (NW to NE; Figs. 5.12-5.14), which is particularly evident on the steep SE limb of the Kranzberg syncline, where the majority of dykes occurs. This orientation reflects dyke emplacement normal or at high-angles to the regional stretch of rocks and parallel to F2 fold axes. Hence, the regional strain seems to represent the first-order control of dyke emplacement. This may seem at variance with the overall NW-SE, subhorizontal shortening strain and the SW-directed, subhorizontal and orogen-parallel extrusion of rocks, suggested by e.g. Poli and Oliver (2001) and Kisters et al. (2004) for this part of the sCZ. However, fold-axes parallel extension and oblique extrusion of rocks is also documented for other nearby F2 folds in the sCZ such as the Blauer Heinrich Syncline (e.g. Ward et

al., 2008), documenting the evidently more complex orogenic ductile flow pattern of rocks in the SCZ.

In addition to the controls by regional strains, pegmatite dykes show a number of characteristics that document the lithological controls on dyke emplacement, particularly on the SE limb of the Kranzberg syncline (Figs. 5.13 and 5.14). The variations relate to (1) the orientation of dykes and systematic changes thereof, and (2) the abundance and spacing of dykes. North-trending dykes have a relatively wide scatter and change abruptly in strike by as much as 30° between the lithological Units 1-4 of the Kuiseb Formation and by 10°-20° within individual units. The abrupt and systematic dyke reorientations are interpreted to reflect strain refraction in units with different competencies (Figs. 5.13 and 5.14). In all of these considerations, it is assumed that post-emplacement strains (e.g. deformation and rotation) had a minimal effect on the majority of second generation and younger dykes. However, dyke orientations on the SE limb describe a systematic rotation from NW-trending dykes in Units 3 and 4, via mainly N-trending dykes in Unit 2 to NNE-trending dykes in Unit 1 (eg. Fig. 5.14). This clockwise rotation is consistent with the dextral component of shear along the steep SE limb of the syncline and, in particular, along the marble units of the Karibib Formation and Unit 1 of the Kuiseb Formation. Hence, the passive rotation of dykes from their original orientation during dextral shearing cannot be ruled out. The abrupt changes in dyke trends between different units remain, however, and testify to the role of wall-rock rigidities for differing dyke orientations and spacing (see below).

The role of different wall-rock competencies (rigidities) for dyke emplacement is also indicated by systematic variations in dyke densities and spacing. For example, the metapelite-dominated Unit 2 of the Kuiseb Formation contains significantly more dykes compared to e.g. Units 3 and 4, whereas Unit 1 shows the composite sill-dyke relationships related to the pronounced compositional layering in this unit. Moreover, most dykes in particularly Unit 2 (Fig. 5.13) show multiple intrusive relationships, documenting the successive emplacement of melt batches along the

same or a similar site. Interacting relationships are common and dykes are closely spaced (2-10m), resembling dyke clusters. The spacing of these dyke clusters is relatively constant and, on average, around 100 m, ranging between 80-150 m in Unit 2 (Figs. 5.13d, and 514 a, b). The intervening areas show very few thin dykes or none at all. The lower abundance of pegmatite dykes in the stratigraphically higher units relates to the much wider spacing and somewhat more sporadic occurrence of dykes, which occur only every 100 to 500 m along the strike of Units 3 and 4. These changes in pegmatite dyke abundance are again abrupt and controlled by the lithological packages. For instance, the dykes of Unit 2 show a gradual thinning with pointed tips at the contact of the marbles and calc-silicates of underlying Unit 1 and the massive metapsammites of Units 3 and 4 (Fig. 5.24).

A number of observations can be deduced from this. Multiple intrusive relationships and clustering of dykes rather than even distribution point to the repeated use of already established dyke pathways by subsequent dykes. This indicates that fracture propagation and dyking is facilitated by existing dyke emplacement sites, either along the dyke-parallel foliation (Fig. 5.27, and see below) or by existing dyke-wallrock contacts that represented planes of weakness compared to the intact wall rock. Given that the melt-filled fracture and its propagation can be treated as a brittle fracture, dyke spacing in rocks undergoing shortening and concomitant extension is mainly related to (1) the width of the unit, (2) the Young's Moduli, i.e. the rigidity of the different wall-rocks, and (3) the amount of finite stretch experienced by different units in a layered sequence.

The width of the wall-rock sequence determines the extent of the strain shadow around a fracture and, as such, the area in which new fracture formation is inhibited by an originally formed fracture (e.g. Gross and Engelder, 1995). The thicker the unit, the longer the fracture and, as a result, the wider the strain shadow around which no renewed fracturing will occur. This determines the spacing of dykes. Given that the layer-parallel stretch is equal for units with different Young's Moduli,

competent units with higher Young's Moduli will fracture at an earlier stage and show higher fracture densities compared to less competent units.

For the rocks of the Kuiseb Formation, the sheer abundance and closer spacing of dykes in Unit 2 would imply the metapelites to have been more competent compared to e.g. metapsammities of Units 3 and 4. This is clearly at variance with the much stronger fabrics developed in the metapelites compared to e.g. massive metapsammities that lack internal fabrics. Moreover, and as shown above, ductile units such as marbles lead to a fracture blunting, delaying or completely inhibiting fracture formation. Hence, the relation of intense dyking confined to Unit 2 is difficult to explain. Pervasive fabrics indicate that Unit 2 was less competent to rocks of Units 3 and 4, while the larger component of layer-parallel stretch along Unit 2 should not result in increased facturing, i.e. dyke densities.

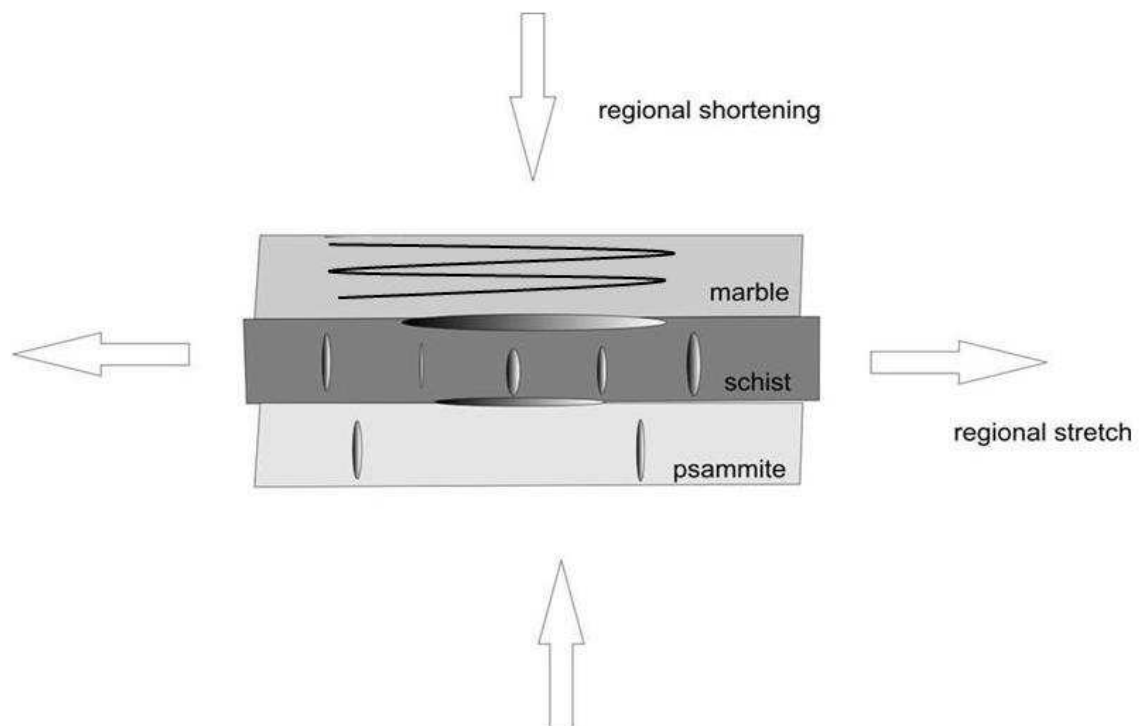


Figure 6.7: Simplified two-dimensional sketch illustrating the effects of different finite extensions (layer-parallel stretch) on the emplacement of pegmatite dykes. Layer-normal shortening during folding results in layer-parallel extension. Ductile flow in less competent units (e.g. schists) results in a larger stretch compared to more competent units (e.g. metapsammities). Schists of Unit 2 may undergo a higher layer-parallel stretch, but the ductility of the rocks should prevent fracture formation, as is observed along e.g. marble units

6.3.3 Dyke and sills in the Kranzberg syncline - relationships between regional strains, anisotropies and driving pressure

Throughout the Kranzberg syncline, length-to-width ratios (in plan view) of pegmatite sills are consistently larger compared to those of dykes (eg. Figs. 5.19, 5.20). Sheet dilation is driven by the internal melt pressure within the propagating melt-filled fracture that has to overcome the regional confining pressure plus the tensile strength of the rock ($P_m \geq \sigma_3 + T$). The latter is likely to be small for the high-grade rocks and in the order of $< 1\text{-}5$ MPa (e.g. Mecklenburg and Rutter, 2003; Brown, 2007). Larger aspect ratios of sills suggest that dilation normal to the pegmatite sheets was more difficult for sills than dykes. This is despite the fact that sills exploit bedding planes, in which the tensile strength of rocks and, thus, fracture resistance to sheet propagation, should be lower compared to that across the bedding anisotropy (e.g. Lucas and St. Onge, 1995). Given that driving pressures in the melt-filled pegmatite sills and dykes are the same, this must reflect the different orientation of sills and dykes to the regional strain. Larger length-to-width ratios of sills correspond to the emplacement of sills at high angles or normal to the regional shortening strain. This is particularly true for NE-trending sills on the steep, overturned SE limb of the Kranzberg syncline. The mainly N and NE trending dykes, in contrast, were emplaced at high angles to the regional stretch (Chapters 5.2.2 and 6.3.2). In this orientation, sheet dilation driven by the melt pressure was facilitated, which, in turn, accounts for the shorter aspect ratios of dykes.

The terminations of dykes and sills are well exposed in numerous examples (Figs. 5.19 – 5.26) and it is these locations where the actual relationship between dykes and sills can be examined. There are numerous occurrences, where sharply discordant dykes can be seen to rotate into bedding to form bedding-parallel sills (eg. Fig. 5.19). The sills may either taper and completely pinch out after only a few metres (Figs. 5.21, 5.24) or thin sills can be seen to link the stubby, en-echelon dyke segments (Figs. 5.21, 5.23). The variability of these dyke-sill relationships is illustrated by the detailed maps presented in figures 5.19 – 5.26. The complete pinching of sills indicates the collapse and closure of the melt filled-fracture. This

also signifies the balance between the driving melt pressure, able to sustain an open fracture, and the regional strain that, in the case of sills, tends to close the fracture. In the case of dykes, the dyke-normal stretch tends to stabilize the melt-filled fracture, i.e. facilitate dyke dilation. The deciding factor that determines whether a sill connecting dyke segments collapses or continues to propagate, albeit much thinner, is most likely determined by the melt supply, i.e. the volume of melt and thus melt pressure, that acts against the closure of the fracture.

Dykes are commonly interpreted to represent melt ascent pathways, mainly because of the vertical orientation that facilitates the buoyancy-driven melt ascent. In the mainly steep sequence of the Kranzberg syncline, cross-cutting dykes and bedding-concordant sills co-exist and both show steep attitudes. This raises questions as to (1) whether sills or dykes and/or both were preferential ascent conduits for pegmatites, and (2) whether steep sills are the feeders of dykes or vice versa, or whether both geometries coexist as ascent conduits. The considerations with regard to melt pressures and orientations of melt sheets to regional strains made above may provide clues.

If the melt volume in a fracture, not connected to an overpressured melt reservoir, is emplaced into a dilational site, the melt pressure in the fracture will be reduced. Given that the confining pressure and fracture resistance of the wall rocks remain constant at the emplacement site, the reduction of the melt pressure will result in the arrest of the fracture. This may account for the multiple intrusive relationships particularly displayed by the composite dykes in e.g. Unit 2 (Fig. 5.24), indicating the arrest of successively emplaced melt batches at these sites. The bedding-parallel sills, in contrast, intrude into contractional sites. The melt volume in the pegmatite sills has to compete with and, in fact, create the space available during regional deformation. As a result, the melts are constantly pressurized in sills. If there is too little melt available to maintain an open fracture against the regional shortening, i.e. melt is not replenished from an outside and distant source, the fracture will close and collapse (Fig. 5.27). If the melt pressure is able to sustain an open fracture, sills

may accommodate the mainly vertical melt ascent and lateral melt transfer created by hydraulic head into the dilational dyke site. This implies that dykes rather represent emplacement sites or, at least, transient melt reservoirs. It also implies that sills feed into dykes in the steeply-dipping strata rather than dykes providing melt for sills.

The dyke-sill relationships in the Kranzberg syncline illustrate the interplay between melt compaction and melt discharge, i.e. transport, from contractional sites (sills) following hydraulic gradients and into dilational sites (dykes) that acted as temporary melt sinks (Fig. 6.8). This occurs on a scale of metres and tens of metres to several hundred metres (Figs. 5.18 – 5.26) and appears to be a fundamental feature of pegmatite propagation in the Kranzberg syncline. It also demonstrates that relatively small hydraulic gradients, probably in the order of only several MPa, are likely to determine the geometry of the melt transfer zones. While the regional, km-scale melt transfer is determined by the buoyancy of the melt-volatile mixture, the outcrop-scale complexity recorded by the Usakos pegmatites is the result of the interplay between (1) local hydraulic heads (i.e. dilational or contractional sites as a result of regional deformation), (2) the presence and orientation of pre-existing anisotropies, and (3) the driving melt pressure that is able (or not) to support an open fracture and thereby melt transport. The resulting sheet geometries closely resemble those described for the initial small-scale segregation of melts from migmatites described by e.g. Brown and Rushmer (1997) and Brown (2007). This may suggest that this spatial relationship between contractional and dilational melt-bearing structures may represent a very stable arrangement that also accounts for the far-field melt transfer in the crust, rather than e.g. dyke swarms (e.g. Clemens and Mawer, 1992). In all of these considerations, it must be highlighted that regional strains, tensile strengths parallel and across bedding planes, melt pressures and pressure variations, and progressive dilation or contraction during deformation must describe a very fine balance.

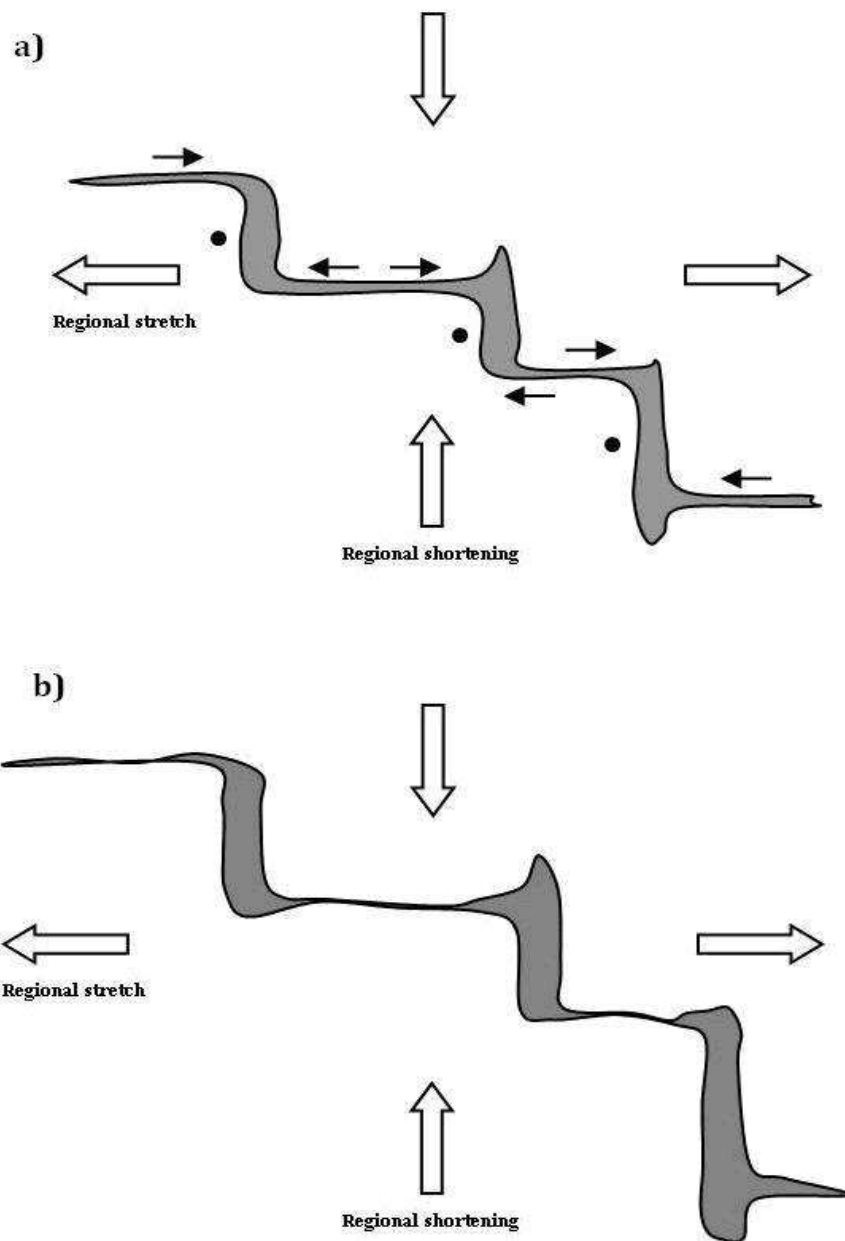


Figure 6.8: Schematic sketch illustrating the relationship between dykes and sills in steeply-dipping strata. Narrow sills undergo shortening along their extent being emplaced at high angles to the regional shortening. (a) Vertical melt ascent (indicated by solid circles) is associated by the lateral flow of melt (small, solid arrows) into dilational sites, orientated at high angles to the regional stretch, corresponding to the emplacement sites of shorter, stubby dyke segments. Dykes and sills form an interconnected melt network. Field examples of this connectivity are presented in figures 5.19 - 5.26; more complex geometries are the result of e.g. multiple intersections of sills with dykes (e.g. Figs. 5.25 and 5.26), but the overall pattern follows the schematic outline given here. (b) Illustrates an intermediate scenario, where sills have collapsed due to e.g. a drop in driving pressure. This results in only partly connected dykes and sills, or, eventually, isolated dyke segments (compare Figs. 5.20, 5.22, 5.24).

For instance, differences in tensile strengths along and across bedding anisotropies or differential stress in this mid-crustal section can only be in the order a few MPa. This may explain the variety of emplacement modes and seemingly differing controls of pegmatite emplacement that, at first sight, appear to describe a rather random stockwork.

6.3.4 Inferences about the mode of sheet propagation

In plan view, both dykes and sills commonly show well defined terminations. The majority of pegmatites show a rather lens-like geometry, in plan view, and although vertical exposure is limited, there is no indication that pegmatites are connected to a larger granitic body or melt source. Hence, pegmatites resemble isolated or only partly interconnected melt pockets of finite extent that are not driven by an external melt source. This corresponds to melt transport in hydrofractures where melt transport is determined by the buoyancy of the melt and the pressure differential between the tip and tail steeply-inclined melt pockets (see e.g. Bons et al., 2001; Brown, 2007; Kisters et al., 2009 for a more detailed discussion of this process). The melt overpressure at the fracture tip causes the wall rocks to fracture and subsequent dilation of the fracture. The tail of the fracture is underpressured, with respect to the surrounding lithostatic pressure and the melt-filled fracture closes from behind as it ascends through the wall-rock column. Ascent rates of hydrofractures are likely to be fast to prevent the melts from freezing and maintain a melt overpressure at the fracture tip and in the order of cm(s) per second (e.g. Bons et al., 2001). From their lensoid shapes, there are features that suggest that pegmatites of the Kranzberg syncline propagated as hydrofractures. Cross-cutting dykes along the overturned limb and hinge domain of the Kranzberg syncline are associated with a dyke-parallel fabric (Figs. 5.26 – 5.28). The fabric is not a mineral fabric, but rather a closely-paced fracture cleavage. This is not a regional foliation and the intensity (spacing) of the fracture cleavage decreases with distance from the pegmatite dykes. However, the localized fabric is also found in areas without pegmatite dykes. The localized nature of this dyke-parallel fabric may be explained by the elastic deformation associated with a propagating hydrofracture. Given that

ascent rates of hydrofractures are fast (cm/s; Clemens and Mawer, 1992; Bons et al., 2001), fracturing and fracture dilation in the high-grade wall rocks will most likely be accommodated by elastic failure, i.e. brittle parting along the fracture trace and elastic wall-rock displacement rather than e.g. folding. This elastic energy is stored in the wall rocks once the hydrofracture has passed and only released following the uplift of the rocks and a reduction of the lithostatic pressure. This resembles, in many aspects, the formation of joints in e.g. folds. This effect arises when the elastic component of the strain during folding, i.e. a ductile process, is stored and only released when the rocks are exhumed and confining pressures are reduced, thus explaining the systematic geometry of joints, i.e. brittle fractures, around folds and ductily deformed rocks (eg. Engelder and Geiser, 1980; Gross and Engelder, 1991; Evans, 1994). This would also explain the presence of the oblique foliation in areas without dykes, merely signifying the passing of a dyke segment (Figs. 5.27 and 6.9 below).

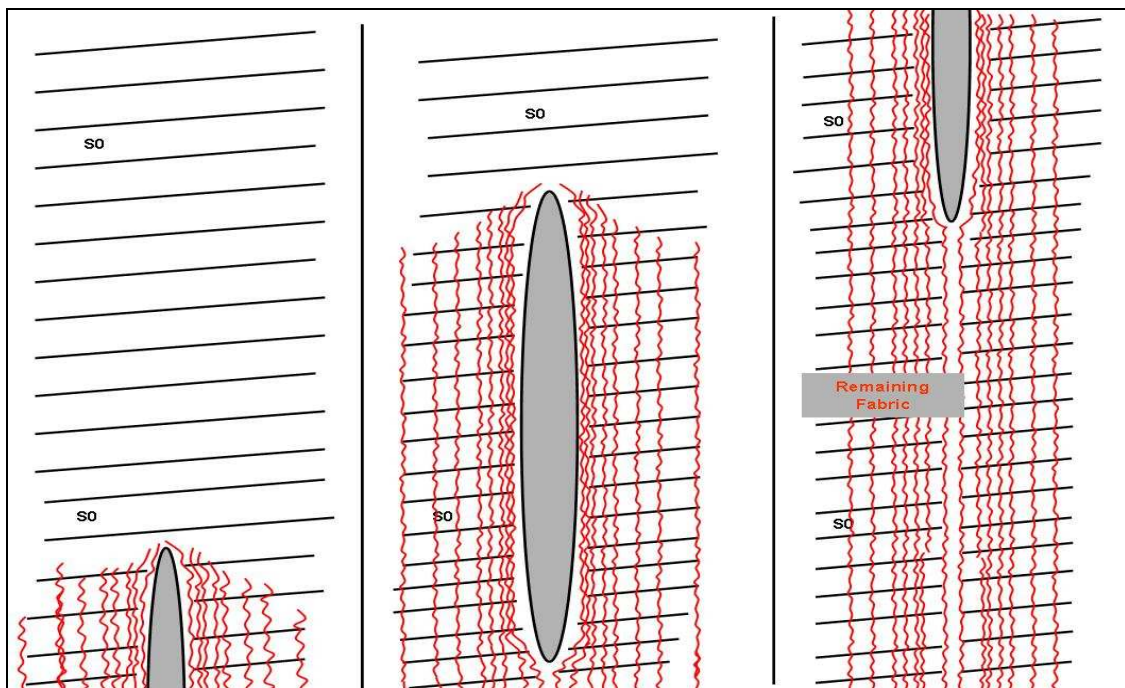


Figure 6.9: Suggested formation of new fabric often observed in proximity to dykes within Unit 1 of the overturned limb and in the hinge domain. Red lines indicate fractures in the wall rocks as the pegmatites intrude and force their way through. The fabric is most highly fractured closest to the pegmatite margins, and dissipates with distance moving away from the margin.

Sheet propagation and the subsequent collapse of the fracture is also indicated by either thin and/or only sporadically preserved pegmatite pods that align along a fracture (Fig. 6.10). Figure 6.10 illustrates the displacement of the layering along a steeply-inclined (not vertical!) fracture in a finely interbedded sequence of calc-silicate felses (red) and gray marbles in Unit 1. The fracture surface is lined by small pods of pegmatite material. This is interpreted to indicate the sheet-normal dilation of the inclined fracture and subsequent horizontal collapse of the fracture once melt had been evacuated in the propagating hydrofracture, causing the apparent displacement of the wall rock strata. This type of feature is easy to overlook in the field, unless wall rocks provide detailed markers across the fracture that help identify the displacement.



Figure 6.10: Displacement of layering along a steeply-inclined fracture in a finely interbedded sequence of calc-silicate felses (red) and gray marbles in Unit 1. The fracture surface is lined by small pods of pegmatite material. Wall rock strata displacement is interpreted to have been caused by dilation (melt infill) and subsequent collapse (melt evacuating) during hydrofracture propagation.

6.3.5 Summary

Emplacement features associated with pegmatites in the Usakos pegmatite field and the Kranzberg syncline indicate the interplay of four main factors that are important for melt transfer and ascent. This includes (1) the regional strain that favours e.g. the emplacement of dykes at high angles or normal to the regional stretch; (2) variations in wall rock rheologies that determine (a) variations in finite stretch and extension in different and adjacent lithologies, and (b) the resistance of units for fracture propagation, resulting in fracture blunting and arrest in units of low Young's Moduli, but fracture dilation in units with high rigidities; (3) the orientation of anisotropies, mainly bedding, and the attitude of larger lithological packages in first- and second-order structures, where horizontal structures, in particular, promote the formation of shallowly-dipping sills and, potentially, melt arrest; and (4) the driving melt pressures that determine as to whether melt-filled fractures remain open, and able to continue the buoyancy-driven ascent, or whether the fracture collapses, leading to the pinching and termination of the sheet-like pegmatites.

The resulting ascent and emplacement geometries are complex and characterized by the coexistence of different, commonly interconnected high-angle sheet geometries, mainly bedding-concordant sills and cross-cutting dykes. Switches in sheet orientation or variations in the emplacement mode between sill- and -dyke-like geometries are indicative of a very fine balance between these four main controlling factors. The formation and existence of localized hydraulic heads, variations in wall-rock rigidities, melt pressures and deviatoric stresses cannot have exceeded a few MPa. These complex melt transfer geometries exemplified by the pegmatite sheets are to be expected in other mid-crustal and lithologically layered and deformed terrains where, moreover, deviatoric stresses are low and wall-rock heterogeneities occur on all scales. Despite the seemingly random appearance, controls by e.g. wall-rock lithologies, regional strains and melt pressures are likely to determine the stockwork-like emplacement.

Chapter 7 - CONCLUSION

The aims of this field-based study were to map the geology of the Kranzberg syncline, its lithological inventory, structural geology, and pegmatite intrusions in order to understand the controls of pegmatite emplacement of the Usakos pegmatite field. The following conclusions can be drawn:

1. Lithological mapping that focused on the Kuiseb Formation in the core of the Kranzberg syncline has identified an up to 800 m thick succession of metaturbidites in which four main units can be distinguished. These four units describe an overall coarsening upward trend, possibly indicating sedimentation of, at least, the upper parts of the Kuiseb Formation during crustal convergence and basin closure. Different degrees of preservation and thicknesses of the rocks are related to their location with respect to axial culminations and depressions of the first-order syncline.
2. The Kranzberg syncline is a regional-scale D₂, NE-SW trending synclinal structure. It consists of a moderately SE dipping, normal NW limb and a steep- to overturned SE limb. The first- and lower-order folds show relatively consistent E plunges at moderate angles. Stretching lineations and boudinage of competent layers point to a fold (F₂)-axis parallel stretch during folding. On a regional scale, variable plunges of the first-order fold to the E and (S)W indicate the strongly non-cylindrical, doubly-plunging nature of the fold.
3. The occurrence of high-strain fabrics, rotation of structural elements such as fold axes and lineations to SE and S plunges and the omission of strata point to the presence of a NE trending structural corridor from the town of Usakos parallel to the Khan River bed along the NW boundary of the study area. This structural zone is tentatively related to a NW-verging thrust, consistent with rotation of linear elements into a down-dip direction, the omission of strata and the overall NW vergence of the syncline.

4. F2 folding is associated with an approximately axial planar, moderate- to steeply SE dipping foliation S2, consistent with the overall NW vergence of the syncline. In detail, S2 is a transecting cleavage showing a consistently anticlockwise rotation with respect to the axial plane of the fold. This suggests a dextral component of shear during or after folding. The dextral component of shear is consistent with the asymmetry and orientation of folds (F2b) on the steep SE limb of the syncline. Dextral shearing is tentatively related to the lateral, SW-directed extrusion of the adjacent Usakos dome during regional NW-SE directed shortening.
5. The structural evolution and inventory of the Kranzberg syncline suggest that the syncline is not a forced fold, i.e. formed during and in response to the formation of the regional-scale dome structures (e.g. the Usakos dome). In fact, markedly different plunges and vergence directions of the syncline with respect to the adjoining Usakos dome indicate that the structural evolution of the two was detached from each other. Structural compatibility between the two adjacent first-order structures is maintained along the thick and ductile marble units of the Karibib Formation that acted as a detachment horizon (see also point 4).
6. Based on cross-cutting relationships and deformation, four main generations of pegmatites can be identified in the Usakos pegmatite field. The majority of pegmatites were emplaced during deformation, ranging from: i) pre- to early D2 first-generation pegmatites; ii) syn-D2 pegmatites, forming the largest group in the Kranzberg syncline; iii) late-D2, third-generation granites and; iv) late- to post-D2 fourth-generation pegmatites.
7. The sheet-like pegmatites can broadly be categorized into bedding-concordant sills and bedding-discordant dykes. Both geometries show generally steep dips. Shallowly-dipping sills are largely confined to the basal,

lithologically heterogeneous Unit 1 of the Kuiseb Formation on the shallowly-dipping normal limb of the Kranzberg syncline. Larger, composite sills and/or plutons are also confined to antiformal hinges of second-order folds. The occurrence of shallowly-dipping sills highlights the significance of shallowly-dipping bedding anisotropies for sheet propagation and sill formation.

8. In steeply-dipping strata, sill- and dyke geometries coexist and can be seen to form an interconnected network. Here, pegmatite emplacement is determined by at least four interrelated factors, namely: (1) the regional strain, (2) rheological contrasts between wall-rock lithologies, (3) the orientation of pre-existing anisotropies, and (4) the driving melt pressure.
9. The underlying principle of melt migration illustrated by the Usakos pegmatite field is given by the connectivity of dykes and sills. The former are emplaced in dilational sites, at high angles to the regional stretch and in suitable lithologies, i.e. lithologies that allowed for fracture propagation. The latter are mainly emplaced at high angles to the regional shortening strain and in contractional sites. Dyke-sill interactions suggest melt transfer from contractional sites into dilational sites. This process caused the very prominent stepped propagation paths described by sills and dykes, resulting in the stockwork-like structures. Melt ascent can be accomplished in this network as long as the driving pressure is sufficiently high to maintain and/or propagate the melt-filled fractures. A drop of the melt pressure below a critical value results in the arrest of pegmatites and/or collapse of the pegmatite sheets and, hence, preserves their ascent pathways in the Kranzberg syncline.
10. Near identical melt-propagation structures are described from migmatite terrains where they are interpreted to account for the small-scale segregation of melt from the molten protoliths (e.g. Brown, 2007). Results of

this study indicate that these intersecting melt geometries occupying contractional and dilational sites may represent far more stable melt networks in the continental crust than hitherto suggested. It certainly may account for the commonly stockwork-like structures described from e.g. pegmatite fields elsewhere in mid-crustal environments.

REFERENCES

- Anderson, E.M. (1936) The dynamics of the formation cone-sheets, ring dykes, and caldron-subsidences. *Royal Society of Edinburgh, Proceedings*, 56, 128-163 pp
- Anderson, E.M. (1951) The dynamics of faulting and dyke formation with applications to Britain. *Oliver and Boyd*, Edinburgh.
- Anderson, H. and Nash, C. (1997). Integrated lithostructural mapping of the Rössing area, Namibia, utilising remotely sensed data. *World Geoscience Corporation Limited*, pp. 1-5.
- Anthonissen, C.J. (2009). The mid-crustal architecture of a continental arc - a transect through the south Central Zone of the Pan-African Damara Belt, Namibia. *Unpubl. MSc-thesis, University of Stellenbosch*, 138pp.
- Badenhorst, F.P. (1987) Lithostratigraphy of the Damara Sequence in the Omaruru Area of the northern Central Zone of the Damaran Orogen and a proposed correlation across the Omaruru Lineament. *Communications of the Geological Survey of South West Africa*, 3, 3-8 pp
- Badenhorst, F.P. (1988a) A note on stratiform tourmalinites in Late Precambrian Kuiseb Formation, Damara Sequence. *Communications of the Geological Survey of South West Africa*, 4, 67-70 pp
- Badenhorst, F.P. (1988b) The lithostratigraphy of the Chuos mixtite in part of the southern Central Zone of the Damara Orogen, South West Africa. *Communications of the Geol. Survey of S.W.A./ Namibia*, 4, 103-110 pp
- Badenhorst, F.P. (1992) The Lithostratigraphy of area 2115B and D in the Central Zone of the Damara Orogen in Namibia: with emphasis on facies changes and correlation. *Unpublished MSc thesis, University of Port Elisabeth*, 124 pp
- Baldwin, J.R. (1993). Lithium and tantalum mineralization in rare-element pegmatites from southern Africa. *Unpublished Ph.D. thesis, Univ. St. Andrews*, 314 pp
- Behr, H.J., Ahrendt, H., Martin, H., Porada, H., Rohrs, J., Weber, K., (1983). Sedimentology and mineralogy of upper Proterozoic playa-lake deposits in the Damara orogen. In: *Martin, H., Eder, F.W. Eds, Intracontinental fold belts. Berli, Springer-Verlag*, 577–610 pp
- Blewett, R. S., and Pickering, K. T., (1988) Sinistral shear during Acadian deformation in north-central Newfoundland, based on transected cleavage: *Journal of Structural Geology*, v. 10, 125-128 pp.
- Bons, P.D., Dougherty-Page, J. and Elburg, M.A., (2001). Stepwise accumulation and ascent of magmas. *Journal of Metamorphic Geology* 19, 627–633 pp

- Brandt, R. (1985). Preliminary report on the stratigraphy of the Damara Sequence and the geology and geochemistry of Damaran granites in an area between Walvis Bay and Karibib. *Communications of the Geological Survey of Namibia*, 1, 31-43 pp
- Brisbin, W.C. (1986). Mechanics of pegmatite intrusion. *American Mineralogist*, Vol 71, 644-651 pp
- Brown, M. and Rushmer, T. (1997). Consequences of deformation-assisted melt segregation: New views from the field and the laboratory. Chapter 5 of Deformation-enhanced melt segregation and metamorphic fluid transport. *Mineralogical Society Series*; Chapman & Hall Publishers. 111-139 pp
- Brown, M. (2007). Crustal melting and melt extraction, ascent and emplacement in orogens: mechanisms and consequences. *Journal of the Geological Society London* 164, 1-22 pp
- Burchardt, S. (2008). New insights into the mechanics of sill emplacement provided by field observations of the Njardvik Sill, Northeast Iceland. *Journal of Volcanology and Geothermal Research* 173, 280-288 pp
- Cameron, E.N. (1955). Concepts of the internal structure of granitic pegmatites and their applications to certain pegmatites of South West Africa. *Trans. Geol. Soc. S. Afr.*, 58, 46-70 pp
- Černý, P. (1991). Rare-element granite pegmatites: Part 1. Anatomy and internal evolution of pegmatite deposits. *Geosci. Can.* 18, 49-67 pp
- Clemens, J.D. and Mawer, C.K. (1992). Granitic magma transport by fracture propagation. *Tectonophysics*, 204: 339-360 pp
- Coleman, D.S., Gray, W. and Glazner, A.F. (2004). Rethinking the emplacement and evolution of zoned plutons; geochronologic evidence for incremental assembly of the Tuolumne Intrusive Suite. *California. Geology* 32, 433-436 pp
- Corner, B. (1982) An Interpretation of the Aeromagnetic data covering a portion of the Damara Orogenic Belt, with Special Reference to the Occurrence of Uraniferous Granite. *Unpublished. D. Sc. thesis, University of the Witwatersrand*, 108 pp
- Corner, B. (2000). Crustal framework of Namibia derived from magnetic and gravity data. *Communications of the Geological Survey of Namibia*, 12, 13-20 pp
- Coward, M.P. (1983). The tectonic history of the Damaran Belt. In: Miller, R.McG. (Ed), Evolution of the Damara Orogen of South West Africa. *Special Publication of the Geological Society of South Africa*, 11, 409-421 pp
- De Kock, W.P. (1932). The lepidolite deposits of South-West Africa. *Trans. Geol. Soc. S. Afr.*, 35, 97-113 pp
- De Kock, G.S., (1992). Forearc basin evolution in the Pan-African Damara Belt, central Namibia: the Hureb Formation of the Khomas Zone. *Precambrian Res.*, 57: 169-194 pp

De Kock, G.S., Eglinton B., Armstrong R.A., Harmer, R.E. and Walraven, F. (2000). U-Pb and Pb-Pb ages on the Naaupoort rhyolite, Kawakeup leptite and Okangava Diorite: implication for the onset of rifting and orogenesis in the Damara belt Namibia. *Communications of the Geological Survey of Namibia*, 12, 81-88 pp

De Saint-Blanquat, M., Guillaume, H., Horsman, E., Morgan, S.S., Tikoff, B., Launeau, P., Gleizes, G. (2006). Mechanisms and duration of non-tectonically assisted magma emplacement in the upper crust: The Black Mesa pluton, Henry Mountains, Utah. *Tectonophysics* 428, 1–31 pp

Diehl, B.J.M. (1986). Preliminary report of the Cape Cross-Uis pegmatite field. *Communs geol. Surv. S.W. Afr./Namibia*, 3, 39-45 pp

Diehl, B.J.M. (1993). Rare metal pegmatites of the Cape Cross-Uis pegmatite belt, Namibia: geology, mineralisation, rubidium-strontium characteristics and petrogenesis, *J.Afr. Earth Sci.* 17:167-181.

Dingwell, D.B., Hess, K.-U. and Knoche, R., (1996). Granite and granitic pegmatite melts: volumes and viscosities. *Trans. Royal Soc. Edinb.: Earth Sci.* 87, 65-72 pp

Engelder, T. and Geiser, P. (1980). On the use of regional joint sets as trajectories of paleostress fields during the development of the Appalachian plateau, New York, *J. Geophys. Res.*, 85, 6319-6341 pp

Evans, M. A. (1994). Joints and decollement zones in Middle Devonian shales; evidence for multiple deformation events in the central Appalachian Plateau: *Geological Society of America Bulletin*, vol. 106, 447–460 pp

Fernandez, J and Guerra-Merchan, A. (1996). A coarsening-upward megasequence generated by a Gilbert-type fan-delta in a tectonically controlled context (Upper Miocene, Guadix-Baza Basin, Betic Cordillera, southern Spain) *Sedimentary Geology* 105 191-202 pp

Frommurze, H.F., Gevers, T.W., Rossouw, P.J. (1942). The geology and mineral deposits of the Karibib area, South West Africa. *Expl. Sheet 79 Karibib, S.W.A. . Geol. Surv. S. Afr.*, 172 pp

Gevers, T.W. and Frommurze H.F. (1929). The tin-bearing pegmatites of the Erongo Area, South-West Africa. *Trans. Geol. Soc., S. Afr.*, vol xxxii, 111-150 pp

Gevers, T.W. (1931). Fundamental Complex of Western Damaraland, South West Africa. *Unpublished. Doctor of Science thesis, University of Cape Town*, 163 pp

Gevers, T.W. (1936). Phases of Mineralization in Namaqualand pegmatites. *Geological Society of South Africa*, vol xxxix, 331-376 pp

Glazner, A.F., Bartley, J.M., Coleman, D.S., Gray, W. and Taylor, R.Z. (2004). Are plutons assembled over millions of years by amalgamation from small magma chambers? *GSA Today* 14, 4-11 pp

Goult, N.R. and Schofield, N. (2008). Implications of simple flexure theory for the formation of saucer-shaped sills. *Journal of Structural Geology* 30, 812–817 pp

- Gray, D.R., Foster, D.A., Goscombe, B., Passchier, C.W. and Trouw, R.A.J. (2006). $^{40}\text{Ar}/^{39}\text{Ar}$ thermochronology of the Pan-African Damara Orogen, Namibia, with implications for tectonothermal and geodynamic evolution. *Precambrian Research*, 150, 49–72 pp
- Gross, M.R. and Engelder, T. (1991). A case for neotectonic joints along the Niagara Escarpment: *Tectonics* vol 10, 631-641 pp
- Gross, M.R. and Engelder, T. (1995). Strain accommodated by brittle failure in adjacent units of the Monterey Formation, U.S.A.: scale effects and evidence for uniform displacement boundary conditions. *Journal of Structural Geology*, Vol. 17, No. 9, 1303-1318 pp
- Gudmundsson, A. (2003). Surface stresses associated with arrested dykes in rift zones. *Bull. Volcanol.* 65, 606–619 pp
- Gudmundsson, A. (2006). How local stresses control magma-chamber ruptures, dyke injections, and eruptions in composite volcanoes. *Earth Sci. Rev.* 79, 1–31 pp
- Gudmundsson, A. (2009). Deflection of dykes into sills at discontinuities and magma-chamber formation, *Tectonophysics*
- Gürich, G. (1891). Deutsch Südwest-Afrika. Reisebilder und Skizzen aus den Jahren 1888 und 1889 mit einer Original-Routenkarte. *Mitt. Geogr. Ges. Hamb.*, 2, 1-216 pp
- Haack, U., Gohn, E. and Klein, J.A. (1980). Rb/Sr ages of granitic rocks along the middle reaches of the Omaruru River and the timing of orogenic events in the Damara Belt (Namibia). *Contrib. Miner. Petrol.*, 74, 349-360 pp
- Haack, U., Hoefs, J. and Gohn, E. (1982). Constraints on the origin of Damaran granites by Rb/Sr and O data. *Contrib. Mineral. Petrol.*, 79, 279-289 pp
- Haack, U., Hoefs, J. and Gohn, E. (1983). Constraints on the origin of Damaran granites by Rb/Sr and 18O data. *Contrib. Mineral. Petrol.* 79, 279–289 pp
- Haack, U. and Gohn, E. (1988). Rb–Sr data on some pegmatites in the Damara orogen Namibia. *Communs. Geol. Surv. S. W. Africa Namibia* 4, 13–17 pp
- Hartnady, C.J.H., Joubert, P. and Stowe, C.W. (1985). Proterozoic crustal evolution in South West Africa. *Episodes*, 8, 236-244 pp
- Hawkesworth, C. J., Gledhill, A., Roddick, J.C., Miller, R. McG., and Kröner, A. (1983). Rb-Sr geochronology and its bearing on models for the thermal evolution of the Damara orogenic belt, Namibia. *Spec. Publ. geol. Soc. S. Afr.*, 11, 397-407 pp
- Henderson, I.H.C. and Ihlen, P.M. (2004). Emplacement of polygeneration pegmatites in relation to Sveco-Norwegian contractional tectonics: examples from southern Norway, *Precambrian Research*, 133, 207-222 pp
- Henry, G., Stanistreet I.G. and Maiden, K.J. (1986). Preliminary results of a sedimentological study of the Chuos Formation in the Central Zone of the Damara Orogen: Evidence for mass

flow processes and glacial activity. *Communications of the Geological Survey of South West Africa*, 2, 75-92 pp

Henry, G., Stanistreet, I.G. and Maiden, K.J. (1988). Timing of continental breakup in the Damara Orogen: A review and discussion. Extended Abstracts. *Geocongress 88, Geological Society of South Africa, Durban*, 267-270 pp

Henry, G. (1992). The sedimentary evolution of the Damara Sequence in the Lower Khan River Valle, Namibia. *Unpublished Ph.D. thesis, Univ. Witwatersrand, Johannesburg*, 217 pp

Hoffmann, K.-H. (1990). Sedimentary depositional history of the Damara Belt related to continental breakup, passive margin to active margin transition and foreland basin development. Extended Abstracts. *Geocongress 90, Geological Society of South Africa, Cape Town*, 250-253 pp

Hoffman, P.F., Hawkins, D.P., Isachsen, C.E. and Bowring, S.A. (1996). Precise U-Pb zircon ages for early Damaran magmatism in the Summas Mountains and Welwitschia inlier, northern Damara belt, Namibia. *Communications of the Geological Survey of Namibia*, 11, 47-52 pp

Hoffmann, K.-H., Condon, D.J., Bowring, S.A. and Crowley, J.L. (2004). U-Pb zircon date from the Neoproterozoic Ghaub Formation, Namibia: Constraints on Marinoan glaciation. *Geological Society of America*, (Data Repository Item)

Horsman, E., Tikoff, B. and Morgan, S.S. (2005). Emplacement-related fabric in a sill and multiple sheets in the Maiden Creek sill, Henry Mountains, Utah. *Journal of Structural Geology* 27, 1426-1444 pp

Jacob, R.E. (1974). Geology and metamorphic petrology of part of the Damaran Orogen along the lower Swakop River, South West Africa. *Bulletin of the Precambrian Research Unit, University of Cape Town*, 17, 201 pp

Jacob, R.E., Kröner, A. and Burger, A.J. (1978). Areal extent and first U-Pb age of Pre-Damara Abbabis Complex in the Central Damara belt of South West Africa. *Geologische Rundschau*, 67, 706-718 pp

Jacob, R.E., Moore, J.M. and Armstrong, R.A. (2000). Zircon and titanite age determinations from igneous rocks in the Karibib District, Namibia: implications for Navachab vein-style gold mineralization. *Communications of the Geological Survey of Namibia*, 12, 157-166 pp

Jahns, R.H. and Tuttle, O.F. (1963). Layered pegmatite-aplite intrusives. *Spec. pap. Miner. Soc. Am.* 1, 78-92 pp

Jahns, R.H. and Burnham, C.W. (1969). Experimental studies of pegmatite genesis: I. A model for the derivation and crystallization of granitic pegmatites. *Econ. Geol.* 64. 843-864 pp

Johnson, S.D. (2005) Structural geology of the Usakos dome, Damara Belt, central Namibia. *Unpublished MSc thesis, University of Stellenbosch*, 159 pp

Johnson, S.D., Poujol, M. and Kisters, A.F.M. (2006) Constraining the timing and migration of collisional tectonics in the Damara Belt, Namibia: U-Pb zircon ages for the syntectonic Salem-type Stinkbank granite. *South African Journal of Geology*, 109, 427-440 pp

Jung, S., Hoffer, E., Masberg, P. and Hoernes, S. (1995). Geochemistry of granitic in-situ low-melt fractions — an example from the Central Damara orogen, Namibia. *Spec. Pub. Geol. Soc. South Africa*, 10, 21–31 pp

Jung, S., Mezger, K., Masberg, P., Hoffer, E. and Hoernes, S. (1998). Petrology of an intrusion-related high-grade migmatite implications for partial melting of metasedimentary rocks and leucosome-forming processes. *J. Metam. Geol.* 16, 425–445 pp

Jung, S., Hoernes, S. and Mezger, K. (2000). Geochronology and petrogenesis of Pan-African, syn-tectonic S-type and post-tectonic A-type granite Namibia : products of melting of crustal sources, fractional crystallization and wall rock entrainment. *Lithos*, 50, 259-287 pp

Jung, S., Hoernes, S. and Mezger, K. (2001). Trace element and isotopic (Sr, Nd, Pb, O) arguments for a mid-crustal origin of Pan-African garnet-bearing S-type granites from the Damara orogen (Namibia). *Precambrian Research*, 110, 325-355 pp

Jung, S. and Mezger, K. (2003). Petrology of basement-dominated terranes: I Regional metamorphic T-t path from U-Pb monazite and Sm-Nd garnet geochronology (Central Damara Orogen, Namibia). *Chemical Geology*, 198, 223-247 pp

Jung, S. (2005). Isotopic equilibrium/disequilibrium in granites, metasedimentary rocks and migmatites (Damara orogen, Namibia) – a consequence of polymetamorphism and melting. *Lithos*, 84, 169-184 pp

Kavanagh, J.L., Menand, T., Stephen, R. and Sparks, J. (2006). An experimental investigation of sill formation and propagation in layered elastic media. *Earth and Planetary Science Letters* 245, 799–813 pp

Kasch, K.W. (1988). Lithostratigraphic and structural geology of the Upper Swakop River area east of Okahandja, SWA/Namibia. *Geol. Surv. South West Africa/Namibia Commun.*, 4: 59-66 pp

Keller, P., (1991). The occurrence of Li–Fe–Mn phosphate minerals in granitic pegmatites of Namibia. *Communs. Geol. Surv. Namibia*, 7, 21–34 pp

Keller, P., Encarnación, R.R., Alfonso, P.P. and François, F. (1999). Chemistry, paragenesis and significance of tourmaline in pegmatites of the Southern Tin Belt, central Namibia. *Chemical Geology*, 158, 203-225 pp

Kisters, A.F.M., Smith Jordaan, L. and Neumaier, K. (2004). Thrust-related dome structures in the Karibib district and the origin of orthogonal fabric domains in the south Central Zone of the Pan-African Damara belt, Namibia. *Precambrian Research*, 133, 283-303 pp

Kisters, A.F.M., Ward, R.A., Anthonissen C.J., Vietze, M.E. (2009).

Melt segregation and far-field melt transfer in the mid-crust. *Journal of the Geological Society* vol 166; 905-918 pp

Kitt, S., (2008). Structural controls of auriferous quartz veins in the Karibib area, southern central zone of the pan-African Damara belt, Namibia. *Unpublished MSc thesis, University of Stellenbosch*, 1-133 pp

Klein, J. (1980). Evolution of first generation of folds in a marble unit (Damara Orogenic Belt, Namibia). *Geol. Rdsch.*, 69, 770-800 pp

Klemens, W. and Schwerdtner, W. (1997). Emplacement and deformation of granite pegmatite dykes in a mid-crustal regime of late-orogenic extension, southwest Grenville Province, Ontario, Canada. *Geological Magazine*, 134:3:287-295 pp

Kröner, A. (1982). Rb/Sr geochronology and tectonic evolution of the Pan-African Damara Belt of Namibia, Southwestern Africa. *Am. J. Sci.* 282, 1472-1507 pp

Kröner, A. (1984). Dome structures and basement reactivation in the Pan-African Damara belt of Namibia. In: Kröner, A. and Greiling, R. (Eds.), *Precambrian Tectonics Illustrated. E. Schweizerbart'sche Verlagbuchhandlung, Stuttgart, Germany*, 191-206 pp

Kukla, P.A. and Stanistreet, I.G. (1991). Record of the Damaran Khomas Hochland accretionary prism in central Namibia: refutation of an ensialic origin of the late Proterozoic orogenic belt. *Geology* 19, 473-476 pp

Kukla, P.A. (1992). Tectonics and sedimentation of a late Proterozoic Damaran convergent continental margin, Khomas Hochland, Central Namibia. *South African Journal of Geology*; v. 104; no. 1; 1-12 pp

Küster, D., Romer, R.L., Tolessa, D., Zerihun, D., Bheemalingeswara, K., Melcher, F., and Oberthür, T. (2009). The Kenticha rare-element pegmatite, Ethiopia: internal differentiation, U-Pb age and Ta mineralization. *Mineralium Deposita, Springer Berling/Heidelberg*, Vol 44, 7 pp

Landes, K.K. (1933). Origin and classification of pegmatites. *Amer. Mineralogist*, vol. 18, 33-56, 95-103 pp

Lehtonen, M.I., Manninen, T.E.T. and Schreiber, U.M. (1995). Geological map sheet 2214 – Walvis Bay, 1:250 000. *Geol. Surv. Namibia*

Lehtonen, M.I., Manninen, T.E.T. and Schreiber, U.M. (1996). Lithostratigraphy of the area between the Swakop, Khan and lower Omaruru Rivers, Namib Desert. *Communications of the Geological Survey of Namibia*, 11, 65-75 pp

London, D. (1986). Formations of tourmaline-rich gem pockets in maiflogitic pegmatites. *Am. Mineral*, 71, 396-405 pp

London, D. (1996). Granitic pegmatites. *Trans. Royal Soc. Edinb.: Earth Sci.*, 87, 305-319 pp

- Lucas, S.B. and St-Orge, M.R. (1995). Syn-tectonic magmatism and the development of compositional layering, Ungava Orogen (northern Quebec, Canada). *Journal of Structural Geology*. Vol 17, 4, 475-491 pp
- MacDonald, J., Burton, C., Lapidus, D.F., Coates, D.R. and Winstanley, I. (2003). Collins Geology dictionary. *Harper Collins Publishers, Glasgow*, 333-334 pp
- Martin, H. (1965). The Precambrian geology of South West Africa and Namaqualand. *Precambrian Research Unit, University of Cape Town*, 159 pp
- Martin, H. and Porada, H. (1977). The Intracratonic branch of the Damara Orogen in South West Africa: Discussion of Geodynamic models. *Precambrian Research*, 5, 311-338 pp
- Masberg, H.P., Hoffer, E. and Hoernes, S. (1992). Microfabrics indicating granulite-facies metamorphism in the low-pressure central Damara Orogen, Namibia. *Precambrian Research*, 55, 243-257 pp
- McDermott, F., Harris, N.B.W. and Hawkesworth, C.J. (1996). Geochemical constraints on crustal anatexis: a case study from the Pan-African Damara granitoids of Namibia. *Contrib. Mineral. Petrol.*, 123, 406-423 pp
- Mecklenburgh J. and Rutter E. H. (2003) On the rheology of partially molten synthetic granite. *Journal of Structural Geology* 25, 1575-1585 pp
- Menand, T. (2008). The mechanics and dynamics of sills in layered elastic rocks and their implications for the growth of laccoliths and other igneous complexes. *Earth and Planetary Science Letters* 267, 93-99 pp
- Miller, R.McG. (1974). The stratigraphic significance of the Naauwpoort Formation of east central Damaraland, South West Africa. *Trans. Geol. Soc. S. Afr.*, 77, 363-368 pp
- Miller, R.McG. (1979). The Okahanja Lineament. A fundamental tectonic boundary in the Damara Orogen of South West Africa/Namibia. *Trans. Geol. Soc. S.Afr.*, 82, 349-361 pp
- Miller, R.McG. (1980). Geology of a portion of central Damaraland, South West Africa/Namibia. *Mem. Geol. Surv. S. Afr., S.W. Afr., Sev.*, 6, 78 pp
- Miller, H. and Hoffman, K.H. (1981). Guide to the excursion through the Damara Orogen. *Geocongress 81, Geological Society of Southern Africa, Windhoek, South West Africa*, 103 pp
- Miller, R. McG. (1983). The Pan-African Damara Orogen of South West Africa/ Namibia. In: Miller, R.McG. (Ed.), Evolution of the Damara Orogen of South West Africa. *Geological Society of South Africa, Special Publication*, 11, 431-515 pp
- Miller, R. McG. (2008). The Geology of Namibia: Neoproterozoic to lower Paleozoic. *Ministry of Mines and Energy Geological Survey*, vol 2, 13-136-178, 13-291-302, 13-336-344, 13-357-410 pp
- Morgan, S.S., Horsman, E., Tikoff, B., de Saint Blanquat, M., Nugent, A. and Habert, G. (2005). Sheet-like emplacement of satellite laccoliths, sills, and bysmaliths of the Henry Mountains,

southern Utah. In: Pederson, J., Dehler, C.M. (Eds.), Interior Western United States Field Guide 6. *Geological Society of America*, 283-309 pp

Morgan, S., Stanik, A., Horsman, E., Tikoff, B., de Saint Blanquat, M. and Habert, G. (2008). Emplacement of multiple magma sheets and wall rock deformation: Trachyte Mesa intrusion, Henry Mountains, Utah. *Journal of Structural Geology* 30, 491-512 pp

Morris, G.A., Kamada, M., and Martinez, V. (2008). Emplacement of the Etive Dyke Swarm, Scotland: implications of dyke morphology and AMS data. In: Thomson, K and Petford, N., Structure and Emplacement of High-level Magmatic Systems. *Geological Society of London*, 150-158 pp

Nash, C.R. (1971). Metamorphic petrology of the S.J. area. Swakopmund District. South West Africa. *Bull. Precambrian. Res. Unit. Univ. Cape Town*, 9, 77 pp

Nicholson, R. and Pollard, D.D. (1985). Dilation and linkage of échelon cracks. *Journal of Structural Geology*, vol 7, 5, 583-590 pp

Novak, M., Selway, J.B., Černý, P., Hawthorne, F.C. and Ottolini, L. (1999). Tourmaline of the elbaite-dravite series from an elbaite-subtype pegmatite at Bližná, southern Bohemia, Czech Republic. *Eur. J. Mineral*, 11, 557-568 pp

Oliver, G.J.H. (1994). Mid-crustal detachment and domes in the central zone of the Damaran orogen Namibia. *Journal of African Earth Sciences*, 19, 331-344 pp

Passchier, C.W. (1998). Monoclinic model shear zones. *Journal Structural Geology*, 20, 1121-1137 pp

Poli, L.C. and Oliver, G.J.H. (2001). Constrictional deformation in the Central Zone of the Damara Orogen, Namibia. *Journal of African Earth Sciences*, 33, 303-321 pp

Porada, H. (1989). Pan-African rifting and orogenesis in southern to equatorial Africa and eastern Brazil. *Precambrian Research*, 44, 103-138 pp

Puhan, D. (1983). Temperature and pressure of metamorphism in the Central Damara orogen. *Geological Society of South Africa. Special Publication*, 11, 219-223 pp

Prave, A.R. (1996). Tale of three cratons: Tectonostratigraphic anatomy of the Damara orogen in northwestern Namibia and the assembly of Gondwana. *Geology*, 24, 1115-1118 pp

Raymond, L.A., (2002). The study of igneous sedimentary and metamorphic rocks, second edition, *McGraw Hill*, 193-227 pp

Rogers, G., Hyslop, E.K., Strachan, R.A., Paterson, B.A. and Holdsworth, R.E. (1998). The structural setting and U-Pb geochronology of Knoydartian pegmatites in W Inverness-shire: evidence for Neoproterozoic tectonothermal events in the Moine of NW Scotland. *Journal of the Geological Society*, 1998, vol 155, issue. 4, 685-696 pp

Roering, C. (1961). The mode of emplacement of certain Li- and Be-bearing pegmatites in the Karibib District, South West Africa. *Inf. Circ. Econ. Geol. Res. Unit, Univ. Witwatersrand*, 4, 37 pp

SACS (1980) Stratigraphy of South Africa by the South African Committee for Stratigraphy (SACS). Published 1980 by [Republic of South Africa, Dept. of Mineral and Energy Affairs, Geological Survey in \[Pretoria\]](#) . Written in [English](#).

Sawyer, E.W. (1981). Damaran structural and metamorphic geology of an area southeast of Walvis Bay, South West Africa. *Memoirs for the Geological Survey of South West Africa*, 7, 94 pp

Smith, D.A.M. (1965). The Geology of the Area Around the Khan and Swakop Rivers in South West Africa. *Memoirs of the Geological Survey of South West Africa*, 3, 113 pp

Smith, D.A.M. (1966). Geological Map of area 2215B-Usakos. *Geological Survey, Windhoek, South West Africa*

Soper, N. J. (1986). Geometry of transecting, anastomosing solution cleavage in transpression zones. *Journal of Structural Geology*, Vol. 8, No. 8, 937-940 pp

Stanistreet, I.G., Kukla, P.A. and Henry, G. (1991). Sedimentary basinal responses to a Late Precambrian Wilson Cycle: The Damara Orogen and Nama Foreland, Namibia. *Journal of African Earth Science*, 13, 141-156 pp

Steven, N.M. (1993). A study of Epigenetic Mineralization in the Central Zone of the Damara Orogen, Namibia, with special reference to gold, tungsten, tin and rare elements. *Memoirs of the Geological Survey of Namibia*, 16, 166 pp

Tack, L. and Bowden, P. (1999). Post-collisional granite magmatism in the Central Damara (Pan-African) Orogenic belt, western Namibia. *Journal of African Earth Sciences*, 28, 653-674 pp

Thomas, R., Webster, J.D. and Heinrich, W. (2000). Melt inclusions in pegmatite quartz: complete miscibility between silicate melts and hydrous fluids at low pressure. *Contrib. Mineral. Petrol.* 139, 394-401 pp

Treagus, S.H. and Treagus, J.E. (1992). Transected folds and transpression: how are they associated? *Journal of Structural Geology*, Vol. 14, No. 3, 361-367 pp

Trompette, R. (1997). Neoproterozoic (□600 Ma) aggregation of western Gondwana: a tentative scenario. *Precambrian Research*. 82, 101-112 pp

Trueman, D.L. and Černý, P. (1982). Exploration for rare-element granitic pegmaties. In: Černý, P. (Ed.), *Granitic Pegmatites in Science and Industry. Mineral Association of Canada Short Course Handbook*, vol. 8, 463-494 pp

Turcotte, D. L. and Schubert, G. (1982). *Geodynamics. John Wiley & Sons, New York*, 450 pp

Van Der Pluijm, B.A. (1990). Synchronicity of folding and crosscutting cleavage in the Newfoundland Appalachians? *Journal of Structural Geology*, Vol. 12, No. 8, pp. 1073 to 1076 pp

Von Knorring, O. (1985). Some mineralogical, geochemical and economic aspects of lithium pegmatites from the Karibib – Cape Cross pegmatite field in South West Africa/Namibia. *Communs geol. Surv. S.W. Afr./Namibia*, 1, 79-84 pp

Vietze, M.E. (2009). Geology and emplacement controls of the Stinkbank granite in the south Central Zone of the Pan-African Damara Belt, Namibia. *Unpubl. MSc-thesis, University of Stellenbosch*, 109 pp.

Von Knorring, O. and Condliffe, E. (1985). Nigerite from the Omaruru River tin deposits, Namibia. *Abstr. 13th Colloquium Afr. Geol., St. Andrews, Scotland*, 333 pp

Wagener, G.F. (1989). Systematic variation in the tin content of pegmatites in western central Namibia. *J. geochem. Explor.* 34, 1-19 pp

Ward, R., Stevens, G. and Kisters, A. (2008). Fluid and deformation induced partial melting and melt volumes in low-temperature granulite-facies metasediments, Damara Belt, Namibia. *Lithos*, 105, 253-271 pp

Wang, T., Tong, Y., Jahn, B., Zou, T., Wang, Y., Hong, D. and Han, B. (2007). SHRIMP, U–Pb Zircon geochronology of the Altai No. 3 Pegmatite, NW China, and its implications for the origin and tectonic setting of the pegmatite. *Ore Geology Reviews*, Vol. 32, Issues 1-2, 325-336 pp